DISSERTATIONES
INFORMATICAE
UNIVERSITATIS
TARTUENSIS
70

ZHIGANG YIN

Computing and Sensing in a Smart Ring



DISSERTATIONES INFORMATICAE UNIVERSITATIS TARTUENSIS
70

DISSERTATIONES INFORMATICAE UNIVERSITATIS TARTUENSIS
70

ZHIGANG YIN

Computing and Sensing in a Smart Ring

UNIVERSITY OF TARTU
Press
1632

Institute of Computer Science, Faculty of Science and Technology, University of Tartu, Estonia.

Dissertation has been accepted for the commencement of the degree of Doctor of Philosophy (PhD) in Computer Science on August 21, 2025 by the Council of the Institute of Computer Science, University of Tartu.

Supervisor

Associate Prof. PhD.	Huber Raul Flores Macario Institute of Computer Science, University of Tartu, Estonia

Opponents

Associate Prof. PhD.	Marco Antonio Zúñiga Zamalloa Computer Science Department, Delft University of Technology, the Netherlands
Prof. PhD.	Stephan Sigg Department of Information and Communications Engineering, Aalto University, Finland

The public defense will take place on September 19, 2025 at 10:15 in Narva Rd. 18-1006.

The publication of this dissertation was financed by the Institute of Computer Science, University of Tartu.

ISSN 2613-5906 (print) ISSN 2806-2345 (pdf)
ISBN 978-9916-27-985-4 (print) ISBN 978-9916-27-986-1 (pdf)

Copyright © 2025 by Zhigang Yin

University of Tartu Press
`http://www.tyk.ee/`

ABSTRACT

Pervasive computing envisions computation seamlessly embedded into daily environments, offering continuous and context-aware services. As part of this vision, wearable computing places sensing and processing capabilities directly on the body. Among wearable devices, smart rings have emerged as a promising platform due to their discreet size, constant skin contact, and increasingly advanced sensing technologies. This thesis investigates how smart rings can be repurposed to support meaningful real-world applications through natural hand interactions, focusing on healthcare, personal safety, and sustainability.

Driven by the need for unobtrusive sensing in everyday settings, we explore how compact smart rings can harness everyday hand gestures such as gripping, holding, and touching to extract physiological, contextual, or environmental information. Given that current smart rings are limited to basic applications, the core research question of this thesis is: *Can we exploit current smart rings' limited capabilities to dynamically support multipurpose functionality?* To explore this, two main challenges are addressed: sensor design and placement, and sensor data repurposing. Based on these principles, we propose three sensing systems that each tackle distinct technical challenges and application domains.

First, HIPPO estimates hand grip strength by repurposing optical sensors in smart rings to detect subtle surface deformations during natural interactions, such as squeezing a plastic cup. It achieves up to 86% accuracy, performing comparably to clinical devices without the need for specialized equipment. Second, SpikEy detects drink spiking in social settings by analyzing light reflectance while a user naturally holds a drink. It constructs generalized spiking profiles using latent representation learning and motion calibration, enabling robust detection of contaminated drinks across various liquid types and conditions. With up to 86% accuracy, SpikEy demonstrates the potential of smart rings as discreet personal safety tools. Third, SNAKE estimates produce quality based on thermal dissipation following human touch. While implemented using a thermal camera, this work extends the application space of smart rings into food quality sensing with miniaturized thermal sensors. SNAKE achieves 83% accuracy in quality classification and offers a practical, low-cost approach to reducing food waste through natural interaction.

Together, these contributions demonstrate how opportunistic sensing and behavior-driven design can expand the capabilities of smart rings. This work positions smart rings as a versatile and practical platform for pervasive computing, enabling low-effort sensing solutions that integrate naturally into everyday life.

CONTENTS

List of original publications **15**

1. Introduction **19**
1.1. Pervasive computing and sensing 19
1.2. Wearable devices 21
1.3. Smart rings 22
1.3.1. Smart rings: State-of-the-art in a nutshell 22
1.3.2. Sensor design and placement 23
1.3.3. Sensor data repurposing 25
1.4. Contributions 26
1.4.1. HIPPO 26
1.4.2. SpikEy 27
1.4.3. SNAKE 27

2. HIPPO: Pervasive hand-grip estimation from everyday interactions **28**
2.1. Introduction 28
2.2. Related work 30
2.3. Motivation 31
2.4. Pervasive hand-grip strength monitoring 32
2.5. Prototype design and baselines 35
2.5.1. HIPPO prototype design 36
2.5.2. Baselines 37
2.6. Smart glove experiments: Robustness of hand-grip strength estimation 38
2.6.1. Experimental design 38
2.6.2. Analysis and results 40
2.7. Practicality: Smart ring experiments 47
2.7.1. Experimental design 48
2.7.2. Results 50
2.7.3. Impact of design and environmental factors on HIPPO . . . 53
2.8. Discussion 60
2.9. Summary 62

3. SpikEy: Preventing drink spiking using wearables **63**
3.1. Introduction 63
3.2. Related work 65
3.3. SpikEy design 67
3.3.1. Latent modeling of optical signals 68
3.3.2. Motion and ambient light compensation 71
3.4. Experimental setup 73
3.4.1. Controlled static experiment 73
3.4.2. Dynamic experiment 75

3.4.3. Baselines . . . 76
3.5. Results . . . 78
3.5.1. Light values as proxy for drink spiking . . . 78
3.5.2. Overall performance . . . 82
3.5.3. Comparison with baselines . . . 84
3.5.4. Drink spiking generalization . . . 85
3.6. Results for dynamic nightclub scenario . . . 86
3.7. Discussion . . . 89
3.8. Summary . . . 91

4. SNAKE: Harnessing human touch for produce quality estimation to foster sustainable retail practices 92
4.1. Introduction . . . 92
4.2. Related work . . . 94
4.3. Limitations of current solutions . . . 96
4.3.1. Manual inspection . . . 97
4.3.2. Estimation using computer vision . . . 98
4.4. SNAKE design and methodology . . . 99
4.4.1. SNAKE overview . . . 100
4.4.2. Robust and accurate parameter extraction against touch variations . . . 101
4.4.3. Theoretical background . . . 103
4.5. Experimental setup . . . 104
4.5.1. Experimental design . . . 104
4.5.2. Baselines . . . 106
4.6. Results . . . 107
4.6.1. Thermal dissipation time as a proxy for decomposition . . . 107
4.6.2. SNAKE performance . . . 110
4.6.3. Comparison to baselines . . . 112
4.6.4. SNAKE and interactions with different duration . . . 114
4.6.5. Capturing internal produce quality . . . 116
4.6.6. Generality and further considerations . . . 117
4.6.7. Other factors . . . 118
4.7. Reducing palm temperature fluctuations . . . 124
4.8. Reducing environment temperature fluctuations . . . 127
4.9. User study . . . 128
4.10. Discussion . . . 132
4.11. Summary . . . 135

5. Conclusions and future directions 136
5.1. Conclusions . . . 136
5.2. Limitation reflections . . . 137
5.3. Future directions . . . 137

Bibliography **141**

Appendix A. The Evolution of Wearables: A Survey on Trends, Challenges, and the Emerging Impact of Smart Rings **189**
A.1. Introduction 189
A.2. Survey scope 190
A.2.1. Related surveys 191
A.2.2. Selection of articles 193
A.3. Wearable computing and applications areas 194
A.3.1. Core functional areas 195
A.3.2. Domain-specific applications 197
A.4. Wearable usage and sensors 201
A.4.1. Wearable usage 201
A.4.2. Sensors 202
A.5. Wearable devices 205
A.5.1. Head-mounted wearables 206
A.5.2. Neck wearables 210
A.5.3. Trunk-worn wearables 210
A.5.4. Upper-limb wearables 210
A.5.5. Lower-limb wearables 213
A.5.6. Wearables across whole body 214
A.5.7. Wearable fusion 215
A.6. Wearable sensing pipeline 215
A.6.1. Overview 215
A.6.2. Data collection 217
A.6.3. Data cleaning and preprocessing 217
A.6.4. Feature engineering 220
A.6.5. Modeling and evaluation 221
A.6.6. End-user usage and perception 228
A.7. Wearable smart ring: emerging applications and challenges 228
A.7.1. Smart ring wearable emergence 229
A.7.2. Hand-driven interfaces for smart rings 231
A.7.3. New emerging applications with smart rings 232
A.7.4. Challenges for smart ring design and development 236
A.8. Conclusion 240

Acknowledgements **241**

Sisukokkuvõte (Summary in Estonian) **242**

Curriculum Vitae **243**

Elulookirjeldus (Curriculum Vitae in Estonian) **244**

LIST OF FIGURES

1. Human-centered interaction in IoT-driven pervasive sensing environments. 21
2. Potential sensor placement and design in smart rings. 24
3. Different hand behaviors and patterns. 25
4. Contributions in the thesis, a) HIPPO in Chapter 2, b) SpikEy in Chapter 3, c) SNAKE in Chapter 4 26
5. Pervasive hand-grip strength analysis, a) Light reflectivity pattern of the object in different states, b) Available positions in hand for light sensing deployment, c) Hand-grip relax state, d) Hand-grip applied strength state. 33
6. Sensing pipeline for processing sampling of hand-grip strength. . . 35
7. Prototypes used to measure hand-grip strength: (a) HIPPO prototype integrated onto a wearable (glove); (b) Dynamometer baseline; (c) Wood ball baseline; and (d) Pressure plate baseline. 37
8. Capturing hand grip strength, a) Light characterization of different positions (in the relaxed state), b) the variation of light value across all participants in different positions (in the relaxed state). 40
9. Comparison of different baselines in hand-grip strength assessments, a) normalized comparison, b) and (c) with their respective physical units. 41
10. Hand-grip strength captured by different light sensors in different positions (All the participants). 42
11. Hand-grip analysis divided per group using the best sensor per group, a) and b) with normalization, c) and d) with physical units. 44
12. Estimated pressure on the object (DYNA-hand) captured by the light sensor in position-1. 45
13. Ranking of 4 devices in use (the most comfortable–4, the least comfortable–1). 46
14. Hand-grip strength estimation performance in different positions. . 48
15. Common house hold objects used in the wild experiment: a) optimized HIPPO wearable that consists in a wristband and a ring; b) (1) first set: A) disposable cup, B) plastic cup, C) kitchen sponge; b) (2) second set: D) paper-sheet, E) fleece jacket, F) face mask, G) plastic bag, H) beer can, I) metallic scrubbers. 49
16. Capturing hand-grip strength, a) Variations in light values of the objects across all participants (in the relaxed state), b) Light characterization of the objects (in the relaxed state), c) Quantification of hand-grip strength in different objects across all participants. . . . 50
17. Estimated pressure on the object (DYNA-hand) captured by the light sensor in different objects. 51
18. Hand-grip strength estimation performance of different objects. . . 53

19. a) The changes in light intensity values for the additional household objects, b) evaluation of other factors on HIPPO: (1) Laser vs LED, (2) Unseen (new) object and (3) Sensing without objects 53
20. Light intensity (LUX) in different experimental environments (IAL: indoor ambient light, Dark: indoor dark, OAL: outdoor ambient light). 54
21. Estimated pressure (DYNA-hand) captured by light reflectivity changes through 7-day measurements in different environments: IAL-indoor ambient light, Dark-indoor dark, OAL-outdoor ambient light. . . . 56
22. Hand-grip strength estimation performance by 10-fold cross validation across 7-day measurements in different environments. 57
23. Evaluations on hand-grip strength estimation (RMSE) and strength type classification(%) across 7-day measurements in different environments. 58
24. Estimated pressure (DYNA-hand) captured by light reflectivity changes on unseen (new) object through 7-day measurements in different environments. 58
25. Light values of hand with different states in different environments: profile - light profile of the whole hand in the flat state, gripped - light values in the hand-grip applied strength state, relaxed - light values in the flat state where the sampling area is based on the area of the sensing point in gripped state. The same OAL-gripped values shown with both IAL and Dark environments. 59
26. a) Wireless baseline, b)-f) SpikEy design: (b) Prototype, (c) Sensor positions, (d) Drinks, (e) Pipeline, (f)Application 67
27. SpikEy prototype 68
28. Profiles of different drinks identified by SpikEy: no spiked (NS), spiked (S), and their differences (D), with sensor positioned on the side. 70
29. a)-b) Factors affected the light values, Hand motion, A0: bartender area, A1: dance area, A2: relaxing area, A3: cross the 3 areas. c)-d) Distribution of each motion axis. e) ECDF. 71
30. Calibration Pipeline 72
31. Common drinks in the experiment 74
32. Light values of 12 hours monitoring. I-aspirin, II-ibuprofen, III-cetirizine. 79
33. The changes in light values with time, (a-f) side view, (g-l) top view. 81
34. Train performance and test confusion matrices for side view, 0: non-spiking, 1-spiking. 83
35. a) Confusion matrix of multi-class classification (no-spike, drug I, drug II, drug III) using leave- one-drink-out approach, b) Spiking detection without the latent representation features. AE-Autoencoders. 83
36. Effects of window sizes on drink spiking detection. above row: side sensor, bottom row: top sensor. 84

37. (a-b) Temperature effect, (c-d) Other generalizations 86
38. Light values after calibration 86
39. Light values across all participants in different interactions. Lbeer_I: light beer spiked by aspirin. 87
40. Light values of cup samples 88
41. SNAKE produce quality estimation. 93
42. a) Thermal imaging modelling pipeline; a, b, m, n are the frame timestamps during the thermal dissipation, $0<a<b<m<n<T$, b) Testbed. 101
43. Evaluation results in long interactions (1-min touch). (a) Thermal dissipation time of each produce. (b) Firmness value for each produce as given by the durometer. (c) Thermal dissipation time of different produce across the $14-$ day period. (d) Relationship between thermal properties and the mean dissipation time, k, α and C_p as mentioned before. 108
44. SNAKE performance by considering the thermal dissipation and produce type, (a)-(b) classification, (c)-(d) regression. Long touch/interactions (1min); Long touch/interactions (10sec). 111
45. Fruit firmness estimation performance considering sensing information and produce type. 113
46. a) STD from 3 samples per fruit, b) MAD of light values, e) MAD of wireless amplitude. 113
47. a) Fruit mass decreases over days, b) Linear slope with 95% CI for all items when considering the first 40s from the thermal dissipation, c) Linear slope with 95% CI for all items when considering the first 5s from the thermal dissipation 115
48. a) Average linear slope (scaled) in different time intervals of the thermal dissipation, b) Target slope over 14 days, c) Average target slope for all fruits. 116
49. Thermal performance with different touch interaction duration. . . 117
50. Short interactions: a) Relationship between thermal properties and the linear slope, thermal conductivity k, thermal diffusivity α, and specific heat capacity C_p. b) SNAKE performance, target slope calculated from the first 5 seconds of thermal dissipation. 118
51. Target slope of each produce in short interactions 119
52. Average target slope for all fruits in short interactions 119
53. Target slope: a) Different participants; b) Genders; c) The main experiment and user studies. 120
54. Target slope for different conditions. S: Sample; S1 (5°C+no film), S2(5°C + film), S3 (23°C+film), and S4 (23°C+no film). 122
55. a) Target slope for different conditions. 1 (5°C+no film), 2(5°C + film), 3 (23°C+film), and 4 (23°C+no film). b) Thermal dissipation time in different background. 122

56. Dissipation time of melon in different parts of the hand. Total: thermal fingerprints of the whole hand, i.e., palm and fingers. . . . 124
57. Temperature compensation (max, min, avg). T_o: original dissipation time, T_r: reference dissipation time, TS_o: original target slope, TS_r: reference target slope. 125
58. SNAKE performance boosting by palm temperature, (a)-(b) classification, (c)-(d) regression. Long interactions (1min); Short interactions (10s) 126
59. Environmental compensation, TS_o: original target slope, $TS_o^{'}$: compensated target slope, TS_r: reference target slope. 128
60. SNAKE augmenting common scale appliances. a) Integration using a 3D-printed design prototype, b) User interface and application usage. 129
61. Wearable applications on different body parts 195
62. Wearable usage with smartphones 202
63. Wearable sensing pipeline 216
64. Hand-driven interfaces for smart rings. two main functions: active interaction and passive sensing 232

LIST OF TABLES

1. Comparison of distributed, mobile, pervasive computing. 20
2. Comparison of wearable devices. Energy consumption/ Computing power: *High* means intensive processing needs. Usage time: *Long* means suitability for all-day monitoring. Obtrusiveness: *High* means a greater level of user disturbance or visibility. 24
3. Hand-grip measurements from participants across different days. *DH: Dominant Hand*, *R: Right*, *L: Left*. 32
4. Data similarity between different sampling devices. Red colours indicate there is significant differences ($p<0.05$). The positions refer to different fingers: little finger (1), middle finger (2), index finger (3). 42
5. Correlation (Kendall) coefficient (τ) analysis for all devices (Divided by group) 43
6. Correlation (Kendall) coefficient (τ) analysis for all devices. . . . 44
7. Statistical analysis between light reflectivity changes in different positions and DYNA-hand (value of dividing the dynamometer value with the hand size): red colour indicates lack of statistical significance in similarity or correlation. 45
8. Root mean square error RMSE (unit kg) and R^2 score of predicting hand-grip strength (HS) in different experimental conditions. Model data $\rightarrow$ Predicted. Regression Method: Automatic Relevance Determination Regression (ARD), Ridge Regression (Ridge). Features: light reflectivity change (L), gender (G) and hand size (S), age (A). 48
9. Data similarity ($p-$value) between light reflectivity changes in the object and two measures: DYNA (dynamometer value), DYNA-hand (estimated pressure on the object, calculated by dividing the dynamometer reading (force) with the hand size). 51
10. Evaluation on regression (RMSE kg, R^2 score) of predicting hand-grip strength (HS) and classification accuracy(%) of predicting hand-grip strength type (ST) in different conditions. Features: light reflectivity change (L), gender (G), hand size (S), age (A) and object (O). 52
11. Root mean square error RMSE (kg) and R^2 score of predicting hand-grip strength (HS) in different environments. Features: light reflectivity change (L), gender (G) and hand size (S), age (A), object (O), light conditions LUX (C). 55
12. Unseen object evaluations in different environments. 58
13. Light values (ADC) without objects in different environments: profile - light profile of the whole hand in the flat state, gripped - light values in the hand-grip applied strength state, relaxed - light values in the flat state where the sampling area is based on the area of the sensing point in gripped state. 59

14. State-of-the-art of liquids with different sensing modalities. slight: vibro-motor is used to generate small vibrations for liquid. na: not applicable. The classification accuracy for all related liquid assessments is above 80%. 66
15. Spiking observations of main appearance changes. 78
16. Detection of drink spiking (no-spiked vs. spiked) on the samples of the drink that was left out from training the CNN model. TP – True Positive, FN – False Negative, FP – False Positive, TN – True Negative. 82
17. Statistical rank of the fruit quality evaluation: 5-strongly agree and 1-strongly disagree. 98
18. Regression predicting firmness (F); Features: Thermal dissipation time (T), Target dissipation slope (TS), Produce type (PU). –: misinterpretation 111
19. Regression predicting firmness (F) and classification performance for baselines; Features: light value (L), CSI amplitude (A), Produce type (PU), –: misinterpretation. 112
20. Weight of variables to fit linear slope (LS) in long interactions. Variables: produce mass (M). Total means the thermal dissipation time. 115
21. Weight of variables to fit linear slope (LS) in short interactions. Variables: produce mass (M). Total means the thermal dissipation time. 115
22. Regression predicting firmness (F) for HIPPO; Features: Thermal dissipation time (T), Target dissipation slope (TS), Palm temperature (P), Produce type (PU). 126
23. Comparison between related surveys and this survey, focusing on sensing pipeline, sensor details, wearable device coverage, and depth in smart rings. 191
24. Keyword descriptions 194
25. Common sensor in wearables: unit, data type and functionality . . 203
26. Existing works of wearables: main areas, body parts, purposes and sensors 207
27. Comparison of common wearables: advantages and disadvanges. Number means body parts. Energy consumption/ Computing power: *High* means intensive processing needs. Usage time: *Long* means suitability for all-day monitoring. Obtrusiveness: *High* means a greater level of user disturbance or visibility. 230

LIST OF ORIGINAL PUBLICATIONS

Publications included in the thesis

1. **Yin, Zhigang**, Mohan Liyanage, Abdul-Rasheed Ottun, Souvik Paul, Agustin Zuniga, Petteri Nurmi, and Huber Flores. "HIPPO: Pervasive hand-grip estimation from everyday interactions." In Proceedings of the ACM on Interactive, Mobile, Wearable and Ubiquitous Technologies 6, no. 4 (2023): 1-30. DOI: 10.1145/3570344
2. **Yin, Zhigang**, Mohan Liyanage, Abdul-Rasheed Ottun, Farooq Dar, Mayowa Olapade, and Huber Flores. "Demo Abstract: A Smart Ring Monitoring Your Health using Hand-grip Strength." In Proceedings of the 21st ACM Conference on Embedded Networked Sensor Systems, pp. 486-487. 2023. DOI: 10.1145/3625687.3628395
3. **Yin, Zhigang**, Mohan Liyanage, Agustin Zuniga, Petteri Nurmi, and Huber Flores. "Hedgehog: Detecting drink spiking on wearables." In Proceedings of the 24th ACM International Workshop on Mobile Computing Systems and Applications, pp. 61-67. 2023. DOI: 10.1145/3572864.3580336
4. **Yin, Zhigang**, Ngoc Thi Nguyen, Agustin Zuniga, Mohan Liyanage, Petteri Nurmi, and Huber Flores. "SpikEy: Preventing Drink Spiking using Wearables." In Proceedings of the 27th SIGCHI ACM International Conference on Multimodal Interaction. 2025. DOI: 10.1145/3716553.3750782 - **Best Paper Award Nomination**
5. **Yin, Zhigang**, Mohan Liyanage, and Huber Flores. "Protecting Yourself Against Drink Spiking Using Wearables." In Proceedings of the 24th ACM International Workshop on Mobile Computing Systems and Applications, pp. 135-135. 2023. DOI: 10.1145/3572864.3581582 - **Best Demo Runner-Up Award**
6. **Yin, Zhigang**, Marko Radeta, Mohan Liyanage, Mayowa Olapade, Abdul-Rasheed Ottun, Agustin Zuniga, Pan Hui, Petteri Nurmi, and Huber Flores. "SNAKE: Harnessing Human Touch for Produce Quality Estimation to Foster Sustainable Retail Practices.", ACM Transactions on Sensor Networks, 2025, DOI: 10.1145/3733720

Publications not included in the thesis

7. **Yin, Zhigang** and Huber Flores. "The Evolution of Wearables: A Survey on Trends, Challenges, and the Emerging Impact of Smart Rings." (under review)
   - The full version of this survey paper is included in Appendix to further reflect the scope and depth of the author's contribution beyond the main chapters.

Other published work of the author

8. **Yin, Zhigang**, Mayowa Olapade, Mohan Liyanage, Farooq Dar, Agustin Zuniga, Naser Hossein Motlagh, Xiang Su et al. "Toward city-scale litter monitoring using autonomous ground vehicles." IEEE Pervasive Computing 21, no. 3 (2022): 74-83. DOI: 10.1109/MPRV.2022.3152926
9. Mayowa Olapade, Adeyinka Akintola, **Zhigang Yin**, Reo Kuchida, Marko Radeta, and Huber Flores. 2025. Tiny but Mighty: When Smart Rings Meet Large Language Models. In Companion of the the 2025 ACM International Joint Conference on Pervasive and Ubiquitous Computing (UbiComp Companion '25). DOI: 10.1145/3714394.3756295
10. Dar, F. A., Olapade, M., Ottun, A. R., **Yin, Z.**, Liyanage, M., Norbisrath, U., ... & Flores, H. (2025). TOAD: Profiling and Evaluating 3D Printed IoT Rapid Prototype Designs. ACM Transactions on Internet of Things. DOI: 10.1145/3724128
11. Post, Kevin, Reo Kuchida, Mayowa Olapade, **Zhigang Yin**, and Huber Flores. "Making Sensing Interactive and Descriptive with LLMs: Context Reasoning from Multi-Sensor Data." In Proceedings of the 26th International Workshop on Mobile Computing Systems and Applications, pp. 130-130. 2025. DOI: 10.1145/3708468.3715686
12. Kevin Post, Reo Kuchida, Mayowa Olapade, **Zhigang Yin**, Petteri Nurmi, and Huber Flores. 2025. ContextLLM: Meaningful Context Reasoning from Multi-Sensor and Multi-Device Data Using LLMs. In Proceedings of the 26th International Workshop on Mobile Computing Systems and Applications. Association for Computing Machinery, New York, NY, USA, 13–18. DOI: 10.1145/3708468.3711892
13. Ngoy, P., Dar, F., Liyanage, M., **Yin, Z.**, Norbisrath, U., Zuniga, A., ... & Flores, H. (2025). Supporting Sustainable Computing by Repurposing E-waste Smartphones as Tiny Data Centres. IEEE Pervasive Computing. DOI: 10.1109/MPRV.2025.3541558
14. Zuniga, A., Olapade, M., Motlagh, N.H., Liyanage, M., **Yin, Z.**, Dar, F., Nguyen, N.T., Akintola, A., Radeta, M., Tarkoma, S. and Flores, H., 2024. Low-Cost Sensing for Environmental Sustainability. IEEE Pervasive Computing. DOI: 10.1109/MPRV.2024.3448199
15. Flores, Huber, Agustin Zuniga, Marko Radeta, **Zhigang Yin**, Mohan Liyanage, Naser Hossein Motlagh, Ngoc Thi Nguyen, Sasu Tarkoma, Moustafa Youssef, and Petteri Nurmi. "SEAGULL: Low-cost pervasive sensing for monitoring and analysing underwater plastics." In 2024 IEEE/ACM Ninth International Conference on Internet-of-Things Design and Implementation, pp. 49-60. IEEE, 2024. DOI: 10.1109/IoTDI61053.2024.00009
16. Dar, Farooq, Mohan Liyanage, Mayowa Olapade, **Zhigang Yin**, Abdul-Rasheed Ottun, Adeyinka Akintola, Francisco Airton Silva, and Huber

Flores. "Demo Abstract: PRINCE: Device Energy Estimation with a Single Photo." In 2024 IEEE/ACM Ninth International Conference on Internet-of-Things Design and Implementation , pp. 231-232. IEEE, 2024. DOI: 10.1109/IoTDI61053.2024.00031

17. Dar, Farooq, Mayowa Olapade, Abdul-Rasheed Ottun, **Zhigang Yin**, Mohan Liyanage, Agustin Zuniga, Monica Passanantti, Sasu Tarkoma, Petteri Nurmi, and Huber Flores. "LIZARD: Pervasive sensing for autonomous plastic litter monitoring." In 2024 IEEE/ACM Ninth International Conference on Internet-of-Things Design and Implementation, pp. 37-48. IEEE, 2024. DOI: 10.1109/IoTDI61053.2024.00008
18. Olapade, Mayowa, Abdul-Rasheed Ottun, **Zhigang Yin**, Mohan Liyanage, Adeyinka Akintola, and Huber Flores. "Seamless Integration of Nano-Drones and Sensors for Agriculture Monitoring at Scale." In Proceedings of the 13th International Conference on the Internet of Things, pp. 189-192. 2023. DOI: 10.1145/3627050.3630733
19. Olapade, Mayowa, Abdul-Rasheed Ottun, **Zhigang Yin**, Mohan Liyanage, Aleksandr Makarov, and Huber Flores. "Low-cost produce quality monitoring at scale: A practical re-purposing framework for pervasive agriculture." In Proceedings of the 13th International Conference on the Internet of Things, pp. 129-137. 2023. DOI: 10.1145/3627050.3627055
20. Dar, Farooq, Mohan Liyanage, Marko Radeta, **Zhigang Yin**, Agustin Zuniga, Sokol Kosta, Sasu Tarkoma, Petteri Nurmi, and Huber Flores. "Upscaling fog computing in oceans for underwater pervasive data science using low-cost micro-clouds." ACM Transactions on Internet of Things 4, no. 2 (2023): 1-29. DOI: 10.1145/3575801
21. Ottun, Abdul-Rasheed, Pramod C. Mane, **Zhigang Yin**, Souvik Paul, Mohan Liyanage, Jason Pridmore, Aaron Yi Ding, Rajesh Sharma, Petteri Nurmi, and Huber Flores. "Social-aware federated learning: Challenges and opportunities in collaborative data training." IEEE Internet Computing, 27, no. 2 (2022): 36-44. DOI: 10.1109/MIC.2022.3219263
22. Dar, Farooq, Hilary Emenike, **Zhigang Yin**, Mohan Liyanage, Rajesh Sharma, Agustin Zuniga, Mohammad A. Hoque, Marko Radeta, Petteri Nurmi, and Huber Flores. "The MIDAS touch: Thermal dissipation resulting from everyday interactions as a sensing modality." Pervasive and Mobile Computing, 84 (2022): 101625. DOI: 10.1016/j.pmcj.2022.101625

Patents

- Flores, Huber, **Zhigang, Yin** and Mohan Liyanage. "A system and method for sensing drinks, 2023" (Patent-pending)
  - Filed and under examination.

Author's Contribution to the Publications

- **HIPPO (Publications 1 and 2)**: As the lead author, he was responsible for the conceptual design, theoretical framework, user study planning, data collection, analysis, and interpretation. He also took the lead in drafting the final manuscripts.
- **SpikEy (Publications 3, 4 and 5)**: The author initiated the conceptual design and conducted preliminary research to demonstrate the feasibility of drink spiking detection using smart rings under controlled settings. Building on this, he extended the work beyond the published Hedgehog system by developing new sensing methodologies, including motion and ambient light calibration. He also led the experimental design and data collection under diverse conditions, performed in-depth analysis, and contributed substantially to writing and refining the manuscripts.
- **SNAKE (Publication 6)**: The author led the development of the conceptual framework and sensing pipeline, contributed to the theoretical grounding, and designed and conducted user studies over independent periods. He analyzed the data and was responsible for preparing and finalizing the manuscript.

1. INTRODUCTION

For many years, people relied on large and complex machines to collect physiological signals or environmental information. These tools were often used in hospitals, research labs, or industrial settings, far from everyday life. Even measuring something basic like heart rate or movement required wires, screens, and trained professionals. Today, that landscape has drastically changed (see Appendix A for a systematic review on wearables). With the rapid growth of wearable technology, sensing and computing have shrunk in size and grown in capability, embedding themselves seamlessly into daily routines. A smart ring, worn effortlessly on a finger, can now perform tasks once reserved for entire machines, such as tracking health signals, managing secure authentication, and interacting with surrounding contexts in real-time. This shift is part of a broader movement toward pervasive computing, where intelligence no longer sits in distant systems but is present in the objects we carry and wear. In this context, smart rings represent a step toward more personal, continuous, and integrated technology.

1.1. Pervasive computing and sensing

Over the past few decades, computing systems have progressed through several significant phases, shifting from isolated, centralized systems to more distributed, mobile, and context-aware environments [2, 367]. During the 1970s and 1980s, computing was largely centralized, relying on mainframe systems that provided computational resources from a single location. In the 1990s, the emergence of distributed computing introduced client-server architectures that improved access to shared resources, supported data processing across multiple nodes, and enhanced system flexibility. In the early 2000s, the expansion of internet infrastructure and web-based technologies brought global connectivity, followed by the rapid growth of mobile computing. This paradigm introduced portable devices that could stay connected in a wide range of environments while also presenting new challenges, such as variable network performance, limited energy resources, and the need for adaptive support. Building upon these earlier developments, pervasive computing has emerged as a more integrated approach by embedding computational and sensing capabilities into everyday surroundings. It emphasizes context awareness, seamless operation, and minimal user intervention. As a result, pervasive computing presents more complex challenges than its predecessors, as it emphasizes continuous, context-sensitive interaction between users and the surrounding digital infrastructure. Table 1 presents a comparison of distributed, mobile, and pervasive computing. Overall, distributed computing laid the foundation for shared resources across networks, mobile computing extended this by introducing portability and real-time access, and pervasive computing further advanced the model by bringing context awareness and seamless integration into daily life.

Pervasive computing (also known as ubiquitous computing) refers to the inte-

Table 1: Comparison of distributed, mobile, pervasive computing.

Aspect	Distributed Computing	Mobile Computing	Pervasive Computing
Key goal	Resource sharing across networked systems	Access to computing while in motion	Seamless integration of computing into daily environments
Typical devices	Servers, desktop clients	Smartphones, tablets	Embedded devices, wearables, smart environments
Connectivity	Networked but mostly fixed	Wireless and portable	Constant, often automatic and background-based
User interaction	Explicit and task-oriented	Interactive and screen-based	Minimal and often implicit
Context awareness	Limited	Partial (e.g., location awareness)	High (location, activity, environment)
Design focus	Scalability, communication protocols	Mobility support, energy efficiency	Context sensitivity, ambient intelligence

gration of computing capabilities such as processors and sensors into everyday objects and environments, allowing them to operate in the background and provide context-aware services [46, 367, 141]. These systems are typically networked and embedded in objects such as cars, clothing, furniture, or household appliances. Unlike traditional computing models that require user attention and direct input, pervasive computing aims for unobtrusive operation and natural interaction without user distraction, making computing less visible. It brings digital systems into close connection with daily routines while reducing the need for active control. By leveraging machine learning, data analysis, and context-awareness, pervasive computing systems can adapt to changing conditions in real time and support applications such as health monitoring, smart homes, and ambient intelligence environments. It focuses on supporting users through seamless, adaptive, and human-centered experiences in both personal and shared environments.

The Internet of Things (IoT) and pervasive computing are closely related fields that together drive the transformation of physical environments into intelligent, adaptive systems [31, 141]. IoT refers to a network of interconnected physical devices such as sensors, mobile phones, wearables, appliances, vehicles, and buildings that collect and exchange data through communication networks. These devices are typically equipped with communication and computational capabilities to support real-time data acquisition and interaction. While IoT lays the groundwork for connectivity and data exchange, pervasive computing builds on this foundation by embedding computational intelligence into both devices and their surrounding environments. It emphasizes context awareness, unobtrusive

operation, and user-centered interaction, allowing systems to adapt to contextual changes and deliver intelligent, seamless services across diverse and large-scale environments. As illustrated in Figure 1, pervasive computing places the human at the center, with various IoT sensors and modalities continuously monitoring contextual information such as motion, heart rate, and environmental conditions. These systems work subtly in the background, adapting to user behavior and integrating naturally into everyday life.



Figure 1: Human-centered interaction in IoT-driven pervasive sensing environments.

1.2. Wearable devices

As pervasive computing moves closer to everyday human experiences, wearable computing rises as a natural progression that brings computational systems into continuous and direct contact with the body [171, 20]. These devices form a unique branch of the Internet of Things (IoT), marked by their close physical placement and their capacity to gather and transmit physiological, behavioral, and contextual information. Wearables combine sensing, processing, and communication functions in compact forms that support constant interaction. Designed to be lightweight, discreet, and comfortable, they fit easily into daily routines while offering personalized insights and services. Their growing importance in areas such as health tracking, activity recognition, authentication, and environmental awareness highlights their role in advancing human focused computing across both personal and professional domains.

Wearable devices can be grouped according to their location on the human body [171]. This classification includes six primary regions: head, neck, trunk, upper limb, lower limb, and full-body wearables. Head-mounted devices such as glasses, headphones, hats, and masks support applications like visual interaction, cognitive monitoring, and immersive experiences. Neck-based wearables, including smart necklaces and assistive collars, focus on posture support, motion tracking, and rehabilitation. Trunk wearables such as smart belts and sensor-integrated garments collect vital signs related to respiration and heart activity. Devices worn on the upper limbs like watches, gloves, and rings, are used for activity recognition, hand gestures, finger motion, and physiological data collection. Wearables placed on the lower limbs, including shoes, insoles, and socks, contribute to movement analysis, physical therapy, and daily monitoring. Full-body devices, such as smart textiles and flexible patches, provide widespread sensing and are used in both research and real-life applications. This body-based structure reflects how physical placement shapes the interaction, sensing, and overall function of wearable technologies across different areas of daily use.

Wearable devices often operate in coordination with smartphones due to their limited processing power and energy storage. Most of them rely on smartphones for tasks such as data visualization, signal analysis, and long-term storage. Acting as a central hub, the smartphone manages communication and delivers feedback through companion apps, allowing wearables to stay compact while supporting real-time interaction and daily use.

1.3. Smart rings

Among wearable devices, smart rings stand out for their very low energy consumption, long usage time, very small size, and minimal obtrusiveness, as shown in Table 2. Unlike bulkier options like smartwatches, glasses, or gloves, smart rings offer a discreet, culturally accepted, and comfortable form factor suitable for long-term use in daily life. Positioned on the finger, a site rich in nerve endings and blood vessels, they are effective for capturing physiological signals such as heart rate and blood oxygen levels. Although limited in computing power, smart rings can work alongside smartphones or edge devices to support applications in health, authentication, and user interaction.

1.3.1. Smart rings: State-of-the-art in a nutshell

Wearable technology has undergone significant advancements in recent decades, as detailed in our survey (Appendix A). Smart rings are not new; they have existed for several years and have gained popularity since around 2015, with notable examples such as the OmniRing and Oura Ring [492, 434, 317]. Despite this growth, their core designs and structures have changed little. Most rely on the same set of components: battery, microcontroller, communication module and a narrow range

of sensing modalities such as PPG and IMU (motion) sensors. The main limitations of current designs are:

- **Limited sensing diversity**: most rely on motion and PPG sensors.
- **Minimal design evolution**: core hardware layout has remained largely unchanged.
- **Under-utilization of the hand**: its rich nerve distribution and flexibility remain unexplored for sensing.

As a result, current smart rings are primarily limited to basic applications: activity recognition (e.g., step counting, walking) via IMU, and sleep tracking (e.g., heart rate, blood oxygen) via PPG. These capabilities are often adapted from other wearables, such as smartwatches, rather than designed specifically for the ring form factor. Incorporating new sensing modalities could extend functionality, but miniaturization challenges restrict the integration of diverse sensor types into a ring form factor; otherwise, the market would already be saturated with multifunctional designs. Beyond these constraints, the unique sensing opportunities offered by the hand's anatomy, such as the dense network of nerves, fine motor control, and flexible joints, remain largely unexplored in smart ring design. These features can be utilized to enable richer interactions and broader sensing capabilities than current sensors alone.

These limitations motivate the following **research question**: ***"Can we exploit current smart rings' limited capabilities to dynamically support multipurpose functionality?"*** Addressing this question requires tackling two main challenges: **sensor design and placement** to enable new forms of hand interactions, and **sensor data repurposing** so that the same data can serve multiple functions. This approach can enable new possibilities for smart rings using off-the-shelf components without adding complexity.

1.3.2. Sensor design and placement

The full potential of smart rings remains underexplored, particularly in relation to sensor placement and structural design strategies. Figure 2 illustrates the potential of different sensor configurations in smart rings. Sensors can be placed on the inner surface to maintain contact with the skin for physiological measurements such as heart rate or temperature, or on the outer surface to support object interaction and environmental sensing. Some designs use multiple sensors around the ring to enhance robustness or capture multiple modalities simultaneously. For example, combining internal physiological sensing with external ambient monitoring can help infer emotional states or risks. Ring rotation can also be used intentionally to switch between sensing tasks, allowing users to align specific sensors for targeted activities, such as drone control. Additionally, finger-touch interfaces (e.g., tapping or swiping) enable natural and unobtrusive interaction in applications like virtual and augmented reality.

Table 2: Comparison of wearable devices. Energy consumption/ Computing power: *High* means intensive processing needs. Usage time: *Long* means suitability for all-day monitoring. Obtrusiveness: *High* means a greater level of user disturbance or visibility.

Wearables	Energy Consumption	Computing Power	Usage Time	Size	Obtrusiveness
Glasses	High	High	Short	Medium	Medium
Earphones	Low to Moderate	Low	Medium	Small	Low
Neck-worn	Low to Moderate	Low	Medium	Small to Medium	Low to Medium
Trunk-worn	Low to Moderate	Low to Moderate	Variable	Medium	Low
Watches	Moderate	Moderate	Medium	Small	Medium
Wristbands	Low	Low	Long	Small	Low
Gloves	High	High	Short	Large	High
Shoes (Socks/Insoles)	Moderate	Low to Moderate	Medium	Small to Medium	Low
Textiles	Low to Moderate	Low	Long	Variable	Very Low
Patches	Low to Moderate	Low	Short to Medium	Small	Very Low
Rings	Very Low	Low	Long	Very Small	Very Low

These strategies highlight a key advantage of sensor relocation: expanding functionality without increasing hardware complexity. For instance, while most existing smart rings use an inner-mounted PPG sensor for heart rate measurement, relocating the PPG to the outer surface could allow it to monitor surrounding contexts instead. Such redesigns open new capabilities but also require adapting how the collected data is interpreted, linking sensor placement innovation directly to the challenge of **data repurposing**. However, these choices inevitably reflect trade-offs in sensing accuracy, interaction style, and usability, which must be balanced to maintain the versatility of smart rings in everyday use.

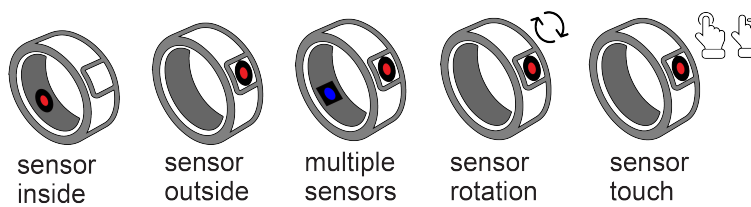


Figure 2: Potential sensor placement and design in smart rings.

1.3.3. Sensor data repurposing

Although smart rings are equipped with compact sensing hardware, their true potential lies in repurposing sensor data for multiple functions. This approach leverages different interpretations of the same sensor signals to support diverse applications without adding new hardware. The hand, with its naturally flexible palm and fingers, presents unique opportunities for such data reuse, enabling detection of a wide range of activities and events. However, realizing this potential poses significant challenges. Unlike the relatively stable wrist, the fingers are in constant motion, introducing high variability and signal noise. This makes sensor data from smart rings more complex to interpret reliably. Repurposing strategies must therefore be carefully designed to account for the fine-grained dynamics and individuality of hand and finger movements. In some cases, more stable wearables like smartwatches may remain better suited for continuous monitoring tasks that demand minimal motion artifacts or broader sensing surfaces.

Despite these challenges, smart rings can still extract meaningful information by utilizing hand behavior and gesture patterns, as illustrated in Figure 3. For example, during grip behavior, sensor data in smart rings can be repurposed to estimate hand grip strength for healthcare. In a pointing posture, motion or orientation sensors can be used for direction-based input or contextual awareness. When the user holds or touches objects, temperature or pressure data can inform material sensing, stress detection, and food quality. Pinch gestures may be used for interaction tasks such as zooming or object selection, while clap patterns, although less frequent, could serve as triggers for event detection or interaction cues such as social engagements.

For instance, beyond common activity recognition, IMU sensors in current smart rings can be repurposed for applications such as hand-washing hygiene monitoring [453], where the sensor data can capture fine-grained hand movements more effectively than smartwatches. While there has been some progress in sensor data repurposing for smart rings, it remains limited, with many studies still at preliminary stages and lacking systematic evaluations. Overall, these examples demonstrate **how new sensor designs and data repurposing, tailored to natural hand interactions, can significantly expand the functionality of smart rings**. All of the contributions in this thesis build on these principles to address real-world challenges in healthcare, social safety, and food waste reduction, which are reflected in Chapters 2, 3, and 4, respectively.

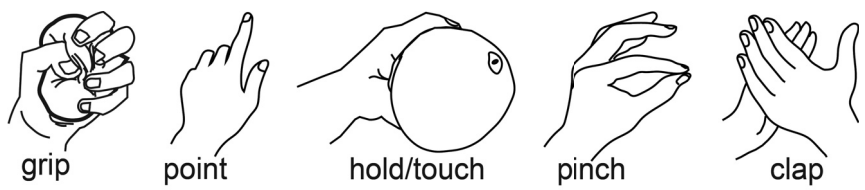


Figure 3: Different hand behaviors and patterns.

1.4. Contributions

As part of this thesis, we have authored several publications that explore the growing role of smart rings in wearable computing through **innovative sensor repurposing and design**. Chapters 2, 3, and 4 present our key findings, and Figure 4 summarizes the contributions made in each chapter. These three contributions are structured to achieve the objectives described in Section 1.3:

- Proposing and prototyping innovative sensor designs in smart rings.
- Demonstrating sensor data repurposing to enable unique interactions through innovative sensing pipelines and methodologies.
- Conducting rigorous and systematic evaluations to validate feasibility and effectiveness, especially in real-world use cases.

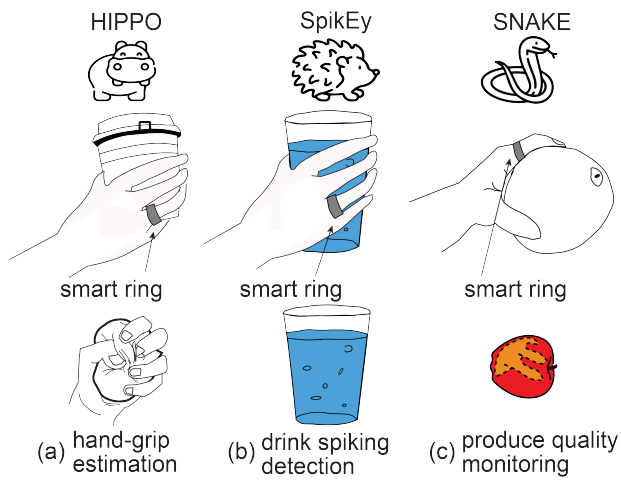


Figure 4: Contributions in the thesis, a) HIPPO in Chapter 2, b) SpikEy in Chapter 3, c) SNAKE in Chapter 4

1.4.1. HIPPO

In Chapter 2, we design and develop HIPPO, a novel sensing approach that estimates hand grip strength opportunistically through everyday interactions using light reflectance. Traditional methods, such as clinical dynamometers or pressure-sensing devices, typically depend on dedicated equipment and are restricted to clinical settings, limiting their feasibility for continuous or daily monitoring. HIPPO repurposes light sensors integrated onto the exterior of smart rings in a new design to capture subtle changes in surface reflectivity when users interact with common objects like plastic cups or kitchen sponges. Our results demonstrate that HIPPO can estimate grip strength with up to 86% accuracy, performs comparably to clinical baselines, and offers a low-cost, unobtrusive solution for continuous grip strength assessment in real-life contexts.

1.4.2. SpikEy

In Chapter 3, we address the limitations of traditional drink spiking detection methods, which often rely on single-use chemical tests or dedicated devices that are substance-specific, costly, and impractical in dynamic social environments. To overcome these challenges, we design SpikEy, a smart ring system that repurposes optical sensors to opportunistically detect spiked drinks during natural interactions. SpikEy captures subtle changes in light reflectance and refraction, and enhances robustness through latent modeling of optical signals using autoencoders, combined with motion and ambient light calibration via inertial sensing. This approach enables generalization across diverse drink types, drug substances, and real-world settings. SpikEy achieves up to 86% detection accuracy, significantly outperforming both visual inspection and existing sensing baselines, including our prior system, Hedgehog. This work highlights the potential of smart rings as discreet, low-cost tools for enhancing personal safety in everyday social contexts.

1.4.3. SNAKE

In Chapter 4, we develop SNAKE, a thermal sensing approach that estimates produce quality by analyzing heat transfer from a user's hand during natural touch interactions. This method repurposes compact thermal sensors, potentially embeddable in smart rings, to capture the thermal dissipation profile left on fruit surfaces, which reflects internal quality and spoilage patterns. Unlike traditional methods such as manual inspection or camera-based systems, often inaccurate, labor-intensive, or dependent on costly, specialized equipment, SNAKE offers a low-cost, contact-driven solution that aligns with real-world consumer behaviors. Experimental results show that SNAKE achieves up to 83% accuracy, outperforming optical and wireless sensing baselines while maintaining robustness across various produce types, environments, and touch durations. This work extends the application space of smart rings into food quality sensing and sustainable retail decision-making.

2. HIPPO: PERVASIVE HAND-GRIP ESTIMATION FROM EVERYDAY INTERACTIONS

As discussed in the previous Chapter, the flexibility of the hand and fingers, along with their natural interactions, can be harnessed to monitor a wide range of user activities and enhance situational awareness. One such interaction *grip* is particularly important, not only for object manipulation but also as a potential indicator of health. However, current methods for estimating hand grip strength rely on dedicated clinical tools such as dynamometers or pressure-based devices, which are cumbersome to use, limited to specific contexts, and require interaction with specialized objects. To overcome these limitations, this chapter introduces HIPPO, a light-sensing method that repurposes compact optical sensors in smart rings to estimate grip strength through everyday interactions. By observing changes in surface reflectance as users squeeze familiar objects such as plastic cups and kitchen sponge, HIPPO supports unobtrusive and accurate grip strength estimation, validated through rigorous experiments involving diverse users, object types, and wearable configurations.

2.1. Introduction

The human hand is exceptional. Besides allowing us to interact with everyday objects and perform numerous activities [497, 107], it can also be used as an indicator of human health. Indeed, the force that a person generates through grip, can indicate not just the strength of the hand, but also serve as an early indicator of a wide range of health conditions [291, 292]. Among others, hand-grip strength has been linked to muscle loss [403], a decline of mental cognition [3] and onset of diabetes [232]. Besides serving as a direct indicator of health, hand-grip strength also has other clinical uses. For example, stroke rehabilitation can use hand-grip strength to assess the performance of the upper motor system [120, 19].

Limitations of state-of-the-art. Current solutions for estimating an individual's hand-grip strength are cumbersome to use as they are restricted to specific contexts and require interacting with a dedicated object. For example, the most common approach for estimating hand-grip strength is to rely on a dynamometer, which is a clinically certified measurement device. The dynamometer produces a score (unit kg or lb) which is then converted into a categorical grip strength assessment (e.g., weak, normal, strong) according to normative reference tables obtained from large-scale clinical studies [286, 355]. While easy-to-use and accurate, its usage is restricted to medical environments and is mostly only used as part of health checks as a separate measurement device is required. Dynamometers also are laborious to use as they require periodic re-calibration and as the measurements must be taken following a stringent test protocol. While some efforts have been made to provide easier access to hand-grip estimates, e.g., through dynamometers

connected to smartphones [108], these similarly require interactions with a dedicated measurement device and are prone to inaccuracies in the measurements. The main alternative is to rely on an object that embeds pressure sensors (i.e., force resistors), but these similarly require interactions with dedicated objects or wearing a device that integrates the sensors at grip contact points and are mostly tailored to specific application scenarios, such as remote surgery [287].

Contributions. This paper contributes HIPPO as a novel light sensing based approach for estimating the hand-grip strength category of an individual. Humans touch many different objects every day, ranging from personal possessions to home appliances, food items, clothing and so forth [497]. HIPPO exploits these interactions to opportunistically estimate hand grip information from interactions with such everyday objects. The intuition is to re-purpose light sensors that are readily available – or that can be easily integrated – on smart rings, gloves, and other wearables to monitor changes in light reflections from the surface of an object as the individual interacts with the object by gripping and squeezing it. This makes it possible to use a wide range of everyday objects, such as, clothes, disposable cardboard cups, and food packaging to piggyback hand-grip information. We develop two proof-of-concept prototypes that harness this principle. Our first and earlier prototype takes advantage of light sensors integrated into an outdoor glove, and our second prototype further optimizes the form-factor and integrates the sensors onto a ring that is combined with a smartwatch type of device that is responsible for controlling the sensor. We also describe the design of the underlying sensing pipeline.

We validate and demonstrate the benefits of HIPPO through rigorous experiments that consider hand-grip measurements from 44 participants (smart glove: 24 and smart ring: 20). As part of the experiments, we compare our approach against several baselines, including a clinical dynamometer and custom objects that integrate pressure sensors. The results demonstrate up to 86% accuracy in determining the hand-grip strength category of an individual and a close correspondence between changes in light intensity values and the pressure exerted by the individual on an object (RMSE 2.57 - 9.89 depending on the extent of side information that is available). HIPPO significantly improves on a pressure sensor based baseline and produces hand-grip estimates that are comparable to a clinical dynamometer used as the gold-standard. We also show that HIPPO operates robustly across a wide range of everyday objects and participants with different characteristics. Taken together, our results demonstrate that using light reflectance resulting from everyday interactions is a promising solution for opportunistic capture of hand-grip characteristics and for achieving unobtrusive monitoring of an important health parameter.

Summary of Contributions:

- **Novel method and sensing modality** for capturing hand grip strength opportunistically using light reflectance measurements resulting from everyday interactions with objects.

- **Novel insights** into light sensing by demonstrating that the changes in the surface of objects captured by light measurements correlate with hand-grip strength measurements, as given by a clinical baseline.
- **Extensive benchmarks** demonstrate that light sensing provides better performance than pressure sensors and is comparable to a clinical dynamometer.

2.2. Related work

Hand patterns and activity recognition: Human activity recognition have been studied extensively from simple activities, such as walking, to more fine-grained activities, such as folding clothes [25]. Hand posture and pressure are relevant to analyze situational impairment that can hamper interactions with mobile applications [140]. Motion sensors along with gesture interactions with screens have been studied to identify hand patterns [220]. Electromyography sensing also has been proposed to detect holding patterns of objects [112]. Squeeze gestures have been studied to understand the human grip for holding smartphones [339]. Pressure information from hand-grip and fingers have been analyzed for interactive interfaces [382, 369]. New wearable devices also have been studied to capture information from the human hand [221]. Unlike these works, we focus on hand-grip strength as it simultaneously provides health information.

Hand-grip and health: Hand-grip strength has been shown to be a good indicator for diagnosing multiple health conditions. The most evident condition that can be monitored is the loss (or gain) of muscle strength over time [411]. Typically, loss of muscles occurs as individuals age or get drastically ill [49, 38]. Hand-grip strength can also provide insights into the cognitive function of individuals as they get older. More severe conditions can also be predicted through the monitoring of hand-grip strength [291]. For instance, it has been studied that obesity changes the structure of the hand, and thus it can influence hand-grip strength [403]. Likewise, cardiac disorders have been linked to low hand-grip strength in individuals [291, 327]. Other studies also have demonstrated the importance of hand-grip strength by using it as a predictor to identify diabetes, respiratory diseases and even cancer [59, 232, 398]. Due to the simplicity of measuring hand-grip strength, it is a test that can be used to easily monitor the health of a population [286]. In our work, we design and develop an approach that can be embedded in wearable devices, such as smart rings and gloves, such that hand-grip strength can be monitored continuously.

Pervasive digital health: Research in pervasive health has steadily evolved [26, 278]. As smart devices have become pervasive tools to collect personal data from individuals continuously, numerous sensors have been piggybacked and re-purposed to monitor several health aspects of individuals. For instance, light sensors can be used to collect heart rate measurements and analyze blood stream and glucose of individuals [149, 178]. A camera also has been shown to be useful to obtain sample measurements to estimate heart rate [191]. With this information

collected over time, several conditions that affect human health have been studied. For instance, heart rate measurements can be easily collected by hand wrists and smart watches to diagnose sleep deprivation and stress [352, 165]. Heart rate also has been estimated solely by grabbing a smartphones [206]. Respiratory information has been collected through the microphone of smartphones to diagnose respiratory diseases [163, 162], e.g., COVID-19. Motion sensor information from smartphones has been analyzed to diagnose Parkinson's disease [233]. Passive thermal imaging have been also investigated to extract temperature from objects touched by humans [90, 107]. Other smartphone solutions have been designed to capture the physical conditions of individuals, e.g., eating activities [478]. Unlike previous work, our work focuses on measuring hand-grip strength using light sensors.

2.3. Motivation

Previous research suggests that hand-grip characteristics may be dependent on the context where they are taken, with particularly the posture of the user, the time-of-day, and prior activity being factors that can affect hand-grip characteristics [365]. On the other hand, there is evidence to suggest that hand-grip strength is generally consistent over time, as long as the context remains sufficiently similar [50]. We first demonstrate that robust hand-grip assessments are possible by carrying a small-scale study that shows hand-grip assessments to be consistent also when taken outside of a medical environment, even when taking in different days, using different postures, or different times-of-day. We next detail our experiment and results.

Setup: We recruited 10 participants and measured their hand-grip strength 8 times during a two-week period. The mean age of the participants was 29.6 (standard deviation 7.78). The time-of-day for the measurements was varied to ensure any variations resulting from daily fluctuations would be captured. During each measurement period, hand-grip was assessed six times in total, three times each for left and right hands. All measurements were taken using a dynamometer. The dynamometer requires the participants to follow a simple but precise procedure (See Subsection 2.5 and 2.6 for a description about the apparatus and procedure). At the beginning of each measurement period, the dynamometer was configured according to the gender and age of each participant. The grip area of the dynamometer was also adjusted for each participant until the second joint of the index finger was at a 90 degree of the handle. After this, each participant performs the dynamometer procedure and measurements were recorded. The grip measurements were also classified into one of three categories following the common methodology for assessing the physical status of a person [286, 346]: *weak, normal and strong*. This is accomplished by configuring the dynamometer with the relevant user characteristics, and mapping the score produced by a dynamometer to a category through a normative reference table that accounts for variations in user characteristics.

Table 3: Hand-grip measurements from participants across different days. *DH: Dominant Hand*, *R: Right*, *L: Left*.

Participants		day1		day2		day3		day4		day5		day6		day7		day8	
id	DH	L	R	L	R	L	R	L	R	L	R	L	R	L	R	L	R
1	Right	weak	weak	weak	normal	weak	normal	weak	normal	weak	normal	weak	normal	weak	normal	weak	normal
2	Right	normal	normal	normal	normal	normal	normal	normal	normal	normal	normal	normal	normal	normal	normal	normal	normal
3	Right	weak	weak	weak	normal	weak	weak	weak	weak	weak	weak	weak	weak	weak	weak	weak	weak
4	Right	weak	normal	weak	normal	normal	normal	normal	normal	weak	normal	normal	normal	normal	normal	weak	normal
5	Right	weak	weak	normal	normal	weak	normal	weak	normal	weak	normal	weak	normal	weak	normal	weak	normal
6	Right	weak	weak	normal	normal	normal	normal	normal	normal	weak	normal	weak	weak	normal	normal	weak	weak
7	Right	weak	weak	weak	weak	weak	weak	weak	weak	weak	normal	weak	normal	weak	weak	weak	weak
8	Right	weak	weak	weak	weak	weak	normal	weak	weak	weak	normal	weak	normal	weak	normal	weak	normal
9	Right	weak	weak	weak	weak	weak	weak	weak	weak	weak	weak	weak	weak	weak	weak	weak	weak
10	Right	normal	normal	normal	normal	normal	normal	normal	normal	normal	normal	normal	normal	normal	normal	normal	normal

Results: Table 3 shows the results and separately includes information about the dominant hand (DH) of the participant and grip strength measurements for the left (L) and the right hand (R). The dominant hand generally outperforms the weaker hand, which shows the measurements process to be accurate. In line with results in medical studies [50], the measurements are highly consistent across different days despite being taken at different-times-of-day. The only variations we observe are shifts between adjacent categories, e.g., there are some cases where we can observe a shift from weak to normal or vice-versa. These findings suggest that hand-grip is generally consistent and that the variations caused by different contexts are generally small. However, the results also suggest that hand-grip strength should be sampled multiple times in different contexts to minimize the influence of any situational factors. Our approach is well-suited for this purpose as it opportunistically harnesses everyday interactions which take place in wide range of contexts, thus offering ample data to overcome situational influences in the measurements.

2.4. Pervasive hand-grip strength monitoring

The proposed method for hand-grip strength estimations takes advantage of the fact that interactions with certain objects result in topological transformations in the shape of the object and that these changes can be captured through light reflectance [498]. The amount of force that is applied on the object influences the extent of change in the shape, and this in turn affects the amount of light that is reflected by the surface of the object (Figure 5(a)). Examples of this kind of interactions include crumpling, squeezing and pressing down objects such as packaging or clothes. In the rest of this subsection, we briefly explain the theoretical foundation of our solution, and present the algorithmic pipeline that we use for mapping light reflectance values into hand-grip strength estimates.

Overview: The general principle behind HIPPO is illustrated in Figure 5. A light sensor (light source + photoresistor) worn on the user's hand, e.g., integrated onto the exterior of a smart glove or a smart ring, is used to measure changes in light reflectance as the user interacts with (malleable) objects. When the object is held in hand normally, the surface of the object covers the light sensor and the intensity

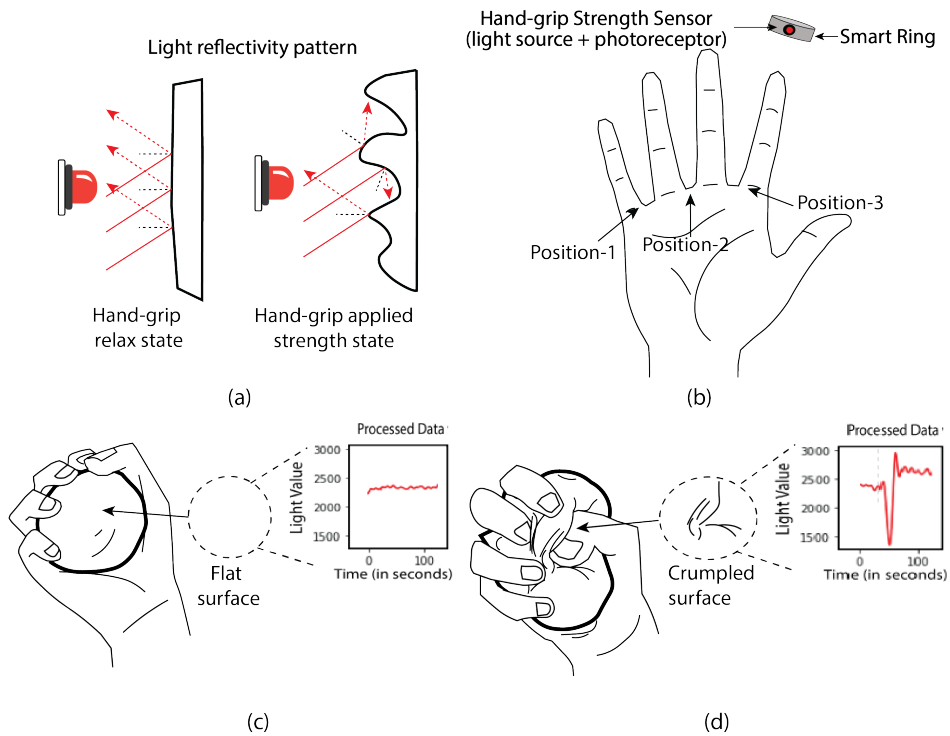


Figure 5: Pervasive hand-grip strength analysis, a) Light reflectivity pattern of the object in different states, b) Available positions in hand for light sensing deployment, c) Hand-grip relax state, d) Hand-grip applied strength state.

of the reflected light is (approximately) constant and this value is used as reference value for estimating overall hand grip strength. As the user grips the object, the surface of the object changes. The extent of these changes depends on the force that is applied on the object, as well as the material of the object. Changes in the surface of the object affect the intensity of the reflected light as the sensor is in closer contact to the object and as the refraction and reflection patterns from the object's surface change. As the pressure on the object is maintained, the changes in the surface and consequently also the intensity of the reflected light become (approximately) constant. HIPPO monitors for these changes in light reflectance, and estimates the hand grip strength opportunistically using differences between the intensity at initial and maximal strength.

When users grab an object, the overall force exerted on the object is distributed among the different fingers grasping an object and the distribution of force along the different fingers further depends on the nature of the interaction as well as the surface material of the object [223, 262]. Optimally the measurements would be taken from all fingers, or from the thumb since that tends to have the highest overall contribution. In practice, the sensors need to be integrated with a device that is easy to wear with a smart ring or a wearable glove being the most practical approaches. As part of our experiments, we separately consider measurements from three different fingers to demonstrate the practicality of our approach. Specifically, we consider measurements from the index, middle and little finger as these are the three most important fingers (referred to as position-1 to position-3) in Figure 5(b) for hand grip. The index finger typically serves as the first point of contact with the object, but it tends to have the smallest overall contribution. The middle finger tends to have the most consistent contribution to grip strength, whereas the contribution of the little finger depends on the nature of the task with the contribution being largest in tasks that require careful finger coordination.

Theoretical foundation: HIPPO estimates hand-grip strength from changes in light reflectivity induced on the surface of an object [116]. As a beam (source) of light is pointed to a surface, the light is reflected back from the surface. When an individual interacts with an object, e.g., by squeezing it, the interaction results in a pressure (P) being applied to the object. The grip exerts a force (F) over the surface area of the object (S), which in turn results in a deformation of the surface area S of the object. The extent of this deformation is indicative of the force that is being applied. Formally, this relation is given by $P = \frac{F}{S}$. Deriving an exact estimate of F would require knowing the surface area that is being measured. Instead, HIPPO uses the changes in light intensity as input to machine learning algorithms to estimate the hand-grip strength and the appropriate category (weak, normal, strong) of the individual's hand-grip strength.

Sensing pipeline: Figure 6 illustrates the sensing pipeline from data collection to signal processing and eventual estimation of hand-grip strength. The pipeline operates using light sensors that comprise of a light source and a photoreceptor. As

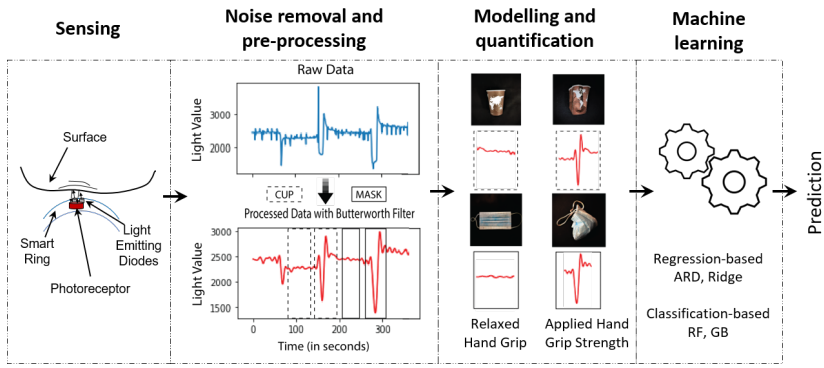


Figure 6: Sensing pipeline for processing sampling of hand-grip strength.

we measure reflections from objects that the user interacts with, the sensor needs to be on the exterior of the device, integrating them and facing outward from the user's hand. In practice, also a proximity sensor should be integrated on the device to minimize unnecessary sampling.

Our implementation of the sensing pipeline detects interactions with malleable everyday objects from the light intensity measurements and processes these to estimate hand-grip strength. First, interactions can be detected from peaks in the intensity measurements. We then find a rest point where the hand is holding the object, but not yet squeezing or applying pressure on it (Figure 5(c)). This forms a reference point for analysing the overall force that is exerted. Once the individual exerts a force on the object, the shape of the object starts to deform and this results in changes in the reflected values (Figure 5(d)). These changes comprise the input to the sensing pipeline. Since hand-grip strength measurements are provided by a quick grip (following certified dynamometer procedure), only measurements that are provided below the 2-3 seconds range are considered as valid measurements that depict hand-grip strength. In line with established practices [251], the light measurements are first cleaned using Butterworth and Chebyshev filters. Next, light patterns that depict hand-grip strength are labelled as relaxed hand-grip or applied hand-grip. This data is then used to construct standard machine learning regressors for estimating hand-grip strength: Automatic Relevance Determination Regression (ARD), and Ridge Regression (Ridge). This data is also used to classify hand-grip strength categories using two common classifiers: Random Forest (RF) and Gradient Boosting (GB). Note that while the intensity measurements are dependent on the location of the sensor, the pipeline itself is agnostic of the sensor location and can operate using measurements from multiple different positions.

2.5. Prototype design and baselines

The possible design space for our solution is immense as the only requirement is having a light sensor (i.e., light source and photoreceptor) relatively close to the surface of the object that is being interacted with. Our contribution focuses

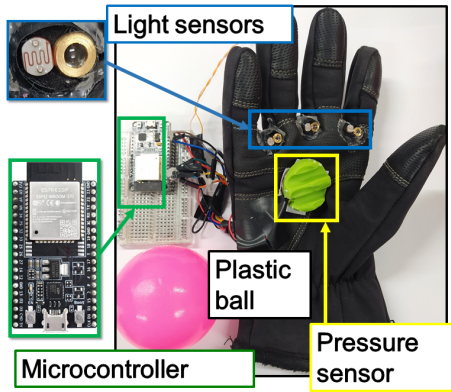
on demonstrating the principle of using light reflections for estimating hand-grip strength, and for conducting our experiments we implemented a proof-of-concept prototype that integrates three light sensors on a smart glove. The glove allowed us to place multiple sensors simultaneously on the object and evaluate the impact of sensor orientation relative to the object on the estimation performance. In practical use we would expect our solution to be integrated to a smart ring or other hand worn wearable and the sensors in our prototype have been placed on different fingers to emulate how rings would be worn – as well as to evaluate the robustness of our approach against changes in hand position. We next describe the prototype and the baselines our system is compared against in the experiments.

2.5.1. HIPPO prototype design

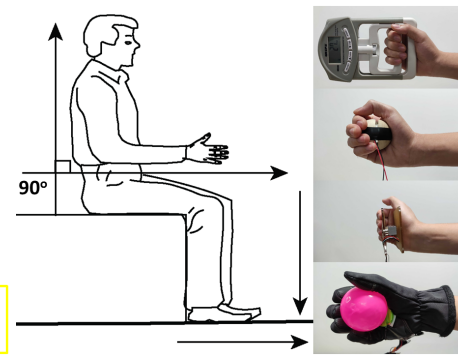
The prototype shown in Figure 7(a), consists of a glove that integrates three light sensors connected to an ESP32 development board. The key reason for using a glove is that it can be easily extended with multiple sensors to provide measurements simultaneously from different angles. The board controls the sampling frequency and uploads the collected data to a web server in real-time. Each light sensor consists of a red laser diode (650nm, 5mW, $3-5$V) and a GM5539 photo-resistor (5MΩ). The light sensor is easy to deploy, and the components are also low cost, which makes our solution affordable and easy to scale, e.g., a pack of 10 lasers and 20 photo resistors costs around 10 US dollars. We use the ESP32 development board as a microcontroller because of its inbuilt Wi-Fi connection facility and it provides multiple inputs to connect multiple sensors at the same time. Each photo resistor changes its resistance according to light intensity, and we use this to measure reflected light. The ESP32 reads photo resistors' values and forwards the values to a web server together with a timestamp. By default, the photo resistor captures analog voltage measurements, which are then changed to digital voltage representations. We use the output value of the ADC (analog to digital conversion, with a resolution of 12 bits, i.e., the voltage is discretized to 4096 levels) as the physical unit to represent the intensity of reflected light. The glove is also equipped with a piezoelectric sensor located on the palm. Data from the sensor is collected using a Multimeter PeakTech 3430 that measures real time voltage with a timestamp. Collected data from the pressure sensor and light sensors are synchronized to analyze hand-grip strength from different sensing angles. The sampling rate of the sensor is 5Hz, and we found that about 50 samples on average are necessary to characterize the strength applied on an object with 97.5% confidence.

In our main controlled experiment, the glove is used alongside a plastic ball that is partially inflated. When the plastic ball is held in hand without any exertion, this provides a reference point that can be used to quantify hand-grip strength. Once a force is exerted, the surface of the object changes, and this can be simultaneously measured by changes in the internal air pressure and changes in the reflected light.

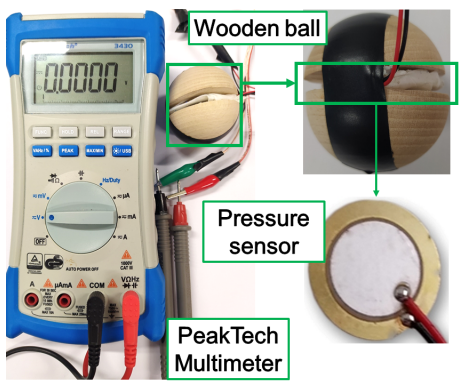
Internal air pressure is measured using a pressure gauge tool (Kixre Digital Tire Pressure Gauge). The device measured 0 PSI units when the ball was held, and up to 9.9 PSI when it was squeezed. Later we also conduct separate experiments where we consider a wide set of everyday objects instead of an inflatable ball.



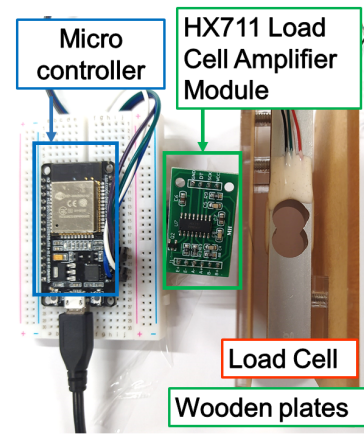
(a) Light sensing



(b) Body position and baselines (Baseline 1 on the top)



(c) Baseline 2



(d) Baseline 3

Figure 7: Prototypes used to measure hand-grip strength: (a) HIPPO prototype integrated onto a wearable (glove); (b) Dynamometer baseline; (c) Wood ball baseline; and (d) Pressure plate baseline.

2.5.2. Baselines

Dynamometer (Baseline 1). To verify the performance of HIPPO, an off-the-shelf commercial dynamometer is used to obtain valid reference measurements that depict hand grip strength (gold standard). We used the GRIPX EH101 dynamometer[1] that is shown in Figure 7(b). The dynamometer measures hand-grip strength

[1] https://gripx.net/

in kilograms (kg) and has a measuring capacity of 198lbs (90kgs). The device is certified to produce highly accurate measurements. The dynamometer maps the grip strength into one of three categories for grip strength (weak, normal, and strong) based on normative grip-strength tables. Since these tables are dependent on age and gender, the dynamometer needs to be configured separately for each individual prior to using it.

Wooden ball (Baseline 2). The second baseline is a squeezable stress-ball type of design shown in Figure 7(c). The object is designed using wood, resulting in an even distribution of pressure along the surface. Indeed, many other materials absorb some of the pressure and can mislead the pressure readings. Note that this only affects the baseline that uses pressure sensors, and not the use of light reflectance measurements. The wooden ball was cut into halves and a piezoelectric pressure sensor was placed in between them. The piezoelectric sensor exploits mechanical stresses by measuring the voltage across a piezoelectric element generated by the applied force. We record the induced voltage, measured in millivolts (mV), using a Multimeter that connects to a computer with one mega ohm resistor in between to get a real time log of voltage readings with its respective timestamp.

Pressure plates (Baseline 3). Our final baseline consists of wooden pressure plates. The prototype is shown in Figure 7(d) and uses the dual-channel 24 Bit HX711 load cell amplifier module, and a Bending Beam Load Cell (straight bar load cell). A load cell is a transducer device, which converts mechanical force into a measurable electrical output in response to, and proportional to, the force applied to it. We mounted the load cell in between two wooden plates so that when pressure is applied to the wooden plates, it will pass to the load cell. Since the load cell output is very small, we use the HX711 load cell amplifier that helps the microcontroller read the changes in the resistance of the load cell and get very accurate load measurements. Once the pressure is applied to the load cell, the microprocessor can read the corresponding discrete-valued voltage (as given by the ADC output) and upload this value to the Web server with a timestamp.

2.6. Smart glove experiments: Robustness of hand-grip strength estimation

We first conduct experiments with $N = 24$ participants that focuses on assessing the robustness and accuracy of using light reflection measurements to estimate hand-grip strength. These experiments are conducted using a smart glove prototype integrating HIPPO. We later further explore a smaller and more practical prototype that integrates HIPPO into a smart ring, and we evaluate how the ring prototype can be used to estimate grip strength from everyday interactions.

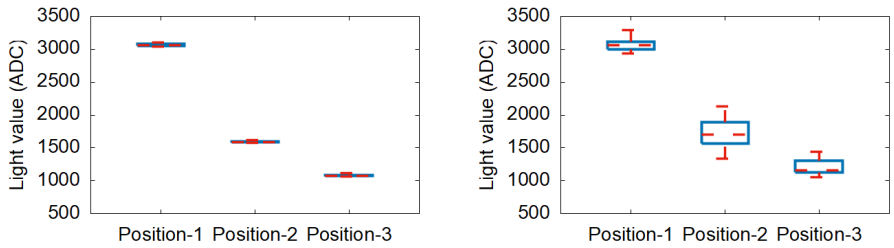
2.6.1. Experimental design

Study design. The experiment is designed as a within-subject design where participants perform hand-grip force measurements with four different devices

at two different times-of-day and days. We encode the data as a 1×2 factorial design with device type and trial as independent variables as this allows us to evaluate the effect of different devices, times-of-day, as well as to identify potential order effects. The device type variable has four levels, corresponding to our prototype and the three baselines: Smart glove (GLOVE), Dynamometer (DYNA), Wooden ball (W-BALL) and Pressure plates (PLATES). The trial variable has two levels, corresponding to the first and second time that the experiment was conducted. To eliminate order effect and biases, whilst keeping the number of trials manageable, trial number was counterbalanced following a Latin Square design, resulting in eight experimental conditions: (1) Trial1-GLOVE, (2) Trial2-GLOVE, (3) Trial1-DYNA, (4) Trial2-DYNA, (5) Trial1-W-BALL, (6) Trial2-W-BALL, (7) Trial1-PLATES and (8) Trial2-PLATES. The trial number was limited to two as the intensity of the hand-grip strength tends to decrease with multiple attempts. We also provide a three minute break between successive tests to change the device and let the muscles relax. For this experiment, $N = 24$ participants were recruited (Males=12, Females=12). The participants were university students and staff from different fields and nationalities. Their average age was 28.5 ± 3.58 and all of them were right-handed.

Procedure. Before starting the study, the researcher who conducted the experiment demonstrated to the participant how to perform the task and provided a detailed description about how to grab each device. Each participant also signed an informed consent form, following local IRB regulations. Prior to starting the experiment, we used a ruler to measure the hand dimensions (breadth and length) of each participant as this allows us to estimate the total surface area of the hand. Once the participant was ready to start the experiment, the different experimental conditions were presented to participants and the participants carried them out one by one. Each experimental task was carried out similarly to our dynamometer experiments in Subsection 2.3 and illustrated in Figure 7(b). Specifically, the participants were asked to sit with feet on the floor and the back touching the chair. The elbow of the (right) hand holding the device measuring hand-grip strength is placed at the participant side at a 90 degree angle. We followed a rapid exchange grip REG test which requires the participant to apply the maximum grip force on each device for 2 to 3 seconds without holding their breath, and then release the grip and relax. The force applied on each device was recorded. This REG test is a commonly used clinical method to assess the sincerity of effort during grip strength evaluation. None of these values were reported to the participants in between the experiments to avoid any potential compensation effects. After the experiment concluded, a brief interview with the participant was conducted to analyze the user experience and overall perception of the devices. Upon concluding the experiment, the scores were revealed to the participant (if they were interested in knowing them). The evaluation took place in one university room across one week in time slots between 11:00 and to 07:00 pm. For each participant, the overall experiment lasted 35 min to 40 min.

2.6.2. Analysis and results



(a) (b)

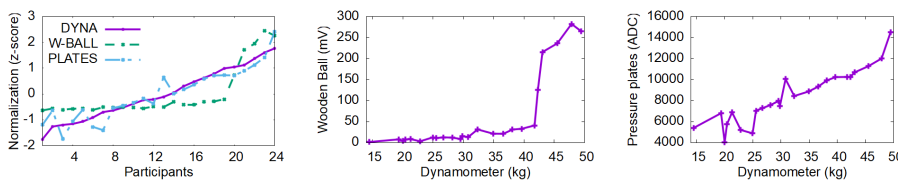
Figure 8: Capturing hand grip strength, a) Light characterization of different positions (in the relaxed state), b) the variation of light value across all participants in different positions (in the relaxed state).

Stability of steady-state estimates. The capability to estimate force grip strength depends on the potential to obtain an accurate reference measurement when the object is held normally without exerting any additional force. Figure 8(a) and (b) visualize the distribution and variation in light sensor values obtained from the three fingers when the object was held in a relaxed state (i.e., no force exerted). The former focuses on a specific point on the object, whereas the latter depicts different points when hold by different participants. In both figures (a and b), we can observe the variance of the measurements to be low across all fingers but the mean value depends on the finger from which the measurements are. The specific values of the fingers (shown in Figure 8a) are as follows: little finger (position-1, mean=3063.59, SD=27.79), middle finger (position-2, mean=1588.81, SD=22.98) and index finger (position-3, mean=1090.01, SD=34.45). Likewise, we also estimate the light reflectivity values at the different positions as objects are held by different individuals in a relaxed state. Figure 8b shows the results. From the figure, we can observe that there are small variations in light values: Position-1: Mean = 3073.99, SD=103.52; Position-2: Mean = 1712.61, SD=215.67; Position-3: Mean = 1205.75, SD=110.92, indicating that stable light values can be captured to derive hand grip strength.

The index and the middle finger have similar patterns, with the index finger resulting in slightly lower intensity as the sensor is better covered by the object when no force is exerted. In contrast, the little finger has highest intensity indicating that less light is blocked by the object. Note that the difference between fingers does not affect the final estimates as the overall force is estimated from changes in intensity of reflected light between maximum and minimum grip force. These results are in line with existing studies on grip distribution [287, 223]. The low variance of the measurements across all fingers shows that the reference point can be estimated robustly, whereas variations across fingers simply highlight how the distribution of force along different fingers is captured by the light intensity

values. This indicates that the changes in object surface can be captured accurately irrespective of position, but that the absolute values are sensitive to contact position. As we next demonstrate, the relative values are robust across locations, and hence it is sufficient to have a calibration reference point for a specific position.

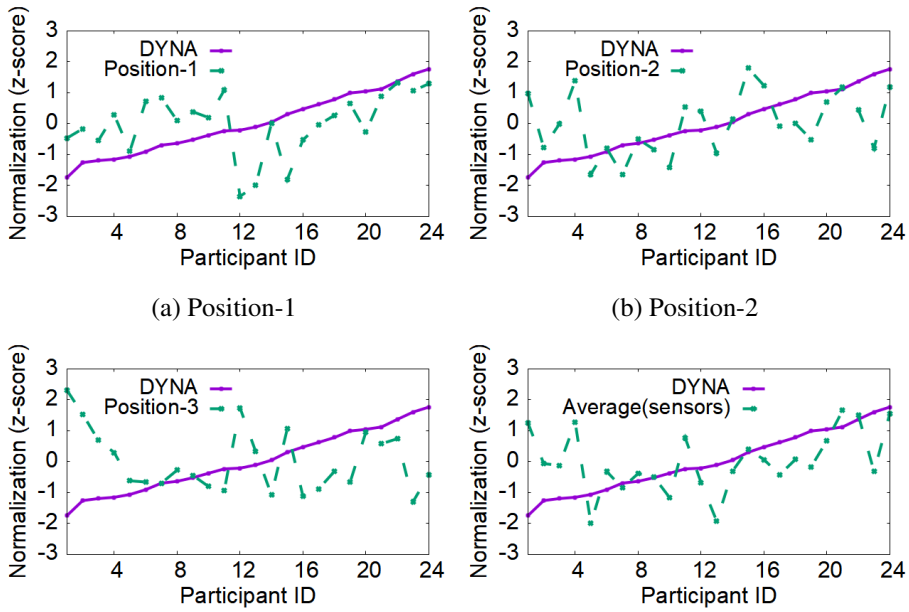
Baseline and experiment validity. Figure 9(a) shows the hand-grip strength assessments for the baselines and compares them against the dynamometer which serves as the gold standard. As the measurements the devices produce are on different scales, we normalize the data using z-score scaling to make it comparable. We can observe that both the wooden ball and the pressure plates follow the same trend as the dynamometer reference values. As the order of devices was randomized across the trials, the high correspondence between the different devices indicates that the hand-grip values were consistent throughout the experiment and validates our experimental design. In addition, Figures 9(b) and (c) also show the level of linear relation between the default units of dynamometer (kg) and, wood ball (mV) and plates (ADC), respectively. In our experiments, participants scored between normal and weak types of hand-grip strength.



(a) (b) (c)

Figure 9: Comparison of different baselines in hand-grip strength assessments, a) normalized comparison, b) and (c) with their respective physical units.

Light measurement quality. Next we demonstrate that the light intensity measurements reflect the same differences as what the baselines capture. We use a Kolmogorov-Smirnov test to compare the measurements from HIPPO against each of the baselines, where the null hypothesis (H_0) states that the two samples come from the same distribution, while the alternative hypothesis (H_1) states that they come from different distributions. To analyze the effect of different finger positions, we perform the analysis separately for each of the three finger positions considered in our study. The results of the analysis are shown in Table 4. With a single exception (little finger cf. wooden ball), no statistical differences can be observed with the measurements, i.e., they come from a similar distribution. The measurements from different finger positions have high similarity with the dynamometer. The finger positions also have similarity across each other, suggesting that HIPPO can operate well at different finger positions, even if the distribution of force that is captured differs across fingers. The sole exception in the results is the wooden ball, which overall results in lowest similarities. This is due to the hard surface of the wooden ball. Moreover, a key factor for the lower similarity is that the sensors are inside the ball and the surface absorbs some of the force that is exerted on it.



(a) Position-1 (b) Position-2

(c) Position-3 (d) Average (all sensors)

Figure 10: Hand-grip strength captured by different light sensors in different positions (All the participants).

Indeed, the wooden ball also has low similarity with the other baselines, including the clinical dynamometer (gold standard).

Table 4: Data similarity between different sampling devices. Red colours indicate there is significant differences ($p<0.05$). The positions refer to different fingers: little finger (1), middle finger (2), index finger (3).

Devices		DYNA	W-BALL	PLATES	GLOVE Sensors		
					Position-1	Position-2	Position-3
DYNA		1	0.139	0.994	0.902	0.994	0.902
W-BALL		0.139	1	0.139	0.011	0.067	0.067
PLATES		0.994	0.139	1	0.902	0.994	0.902
GLOVE Sensors	Position-1	0.902	0.011	0.902	1	0.902	0.262
	Position-2	0.994	0.067	0.994	0.902	1	0.902
	Position-3	0.902	0.067	0.902	0.262	0.902	1

Sensor position. Figure 10 shows the results for the different participants for the different fingers and compares the results against the dynamometer reference. The relative patterns align with the dynamometer for most participants, but there are also some deviations from the reference. The best alignment results from using all three positions simultaneously as the optimal finger from which to sample measurements varies across the participants. This is to be expected as the contribution of each finger on the overall force that is applied varies across individuals [223, 223, 287]. Note also that the patterns for the little finger (position-1) and index finger (position-3) are often reversed and the patterns often offset each other. This is due

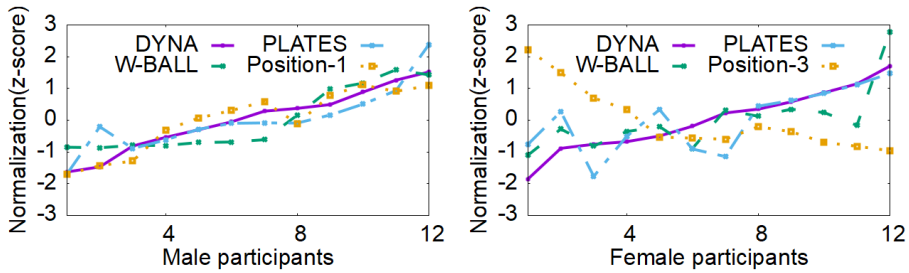
to higher pressure on the index finger resulting in a loosening of the grip at the little finger, and conversely higher force on the little finger indicating a smaller contribution of the index finger. The middle finger is expected to result in the most consistent pattern, but this depends also on the characteristics of the object and the force that is applied on the object. Malleable objects with a soft surface can result in significant changes in the surface of the object and this can decrease the contact of individual fingers. For example, the experiments consider a squeezable ball whose shape undergoes significant changes and this can result in the grip of the middle finger loosening. Nevertheless, as the results indicate, these variations can most of the time be overcome by simply using multiple contact points. Further stability can be achieved by analysing the reflection patterns in more detail and filtering out periods where the reflection characteristics undergo changes.

Individual differences. To better understand variations across individuals, we next split the participants into two groups based on gender (Figure 11). Figure 11(a) and (b) compares (on a normalized scale) the hand-grip data captured by all the devices. In parallel to this, Figure 11(c) and (d) show the level of linearization between the dynamometer and the light reflectivity values with their actual physical units. This group (male and female) division is motivated by the fact that hand size and physical strength are governed by gender characteristics [420]. Table 5 shows the Kendall correlation of the measurements when the participants are grouped and Table 6 shows the results without grouping. Here, the null hypothesis (H_0) states that there is no association between the two variables, while the alternative hypothesis (H_1) states that there is an association between the two variables. The results show that the correlations for index (position-3) and little finger (position-1) are significantly higher when the participants are grouped by gender. Note also that the sign of the correlation changes (for both genders) depending on the finger. A negative correlation indicates a reduction in light intensity as force is applied, which indicates a closer contact between the sensor and the surface of the object. Positive correlation, in turn, means the contact is not as tight which results in higher amount of light reflecting back to the receptor – as well as small amounts of ambient light being able to enter the sensor. This also further explains why the variations in the index and little finger measurements, as discussed above, tend to offset each other.

Table 5: Correlation (Kendall) coefficient (τ) analysis for all devices (Divided by group)

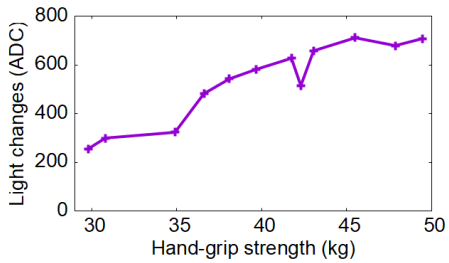
Devices	GLOVE Sensors (Male)			GLOVE Sensors (Female)		
	Position1-M	Position2-M	Position3-M	Position1-F	Position2-F	Position3-F
DYNA	0.85	0.03	-0.21	0.33	-0.12	-0.82
W-BALL	0.76	0.06	-0.18	0.18	-0.48	-0.58
PLATES	0.79	-0.09	-0.21	0.09	0.06	-0.45

To further understand the differences, we next calculate the DYNA-hand which briefly estimates the pressure on the objects based on the hand size. DYNA-hand is the value of dividing the dynamometer reading (force) with the hand size

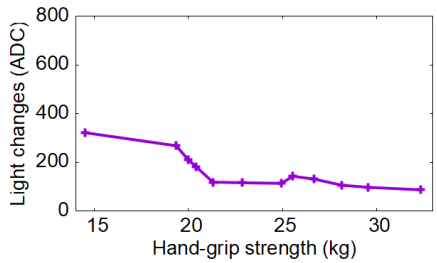


(a) Male in position-1

(b) Female in position-3



(c) Male in position-1



(d) Female in position-3

Figure 11: Hand-grip analysis divided per group using the best sensor per group, a) and b) with normalization, c) and d) with physical units.

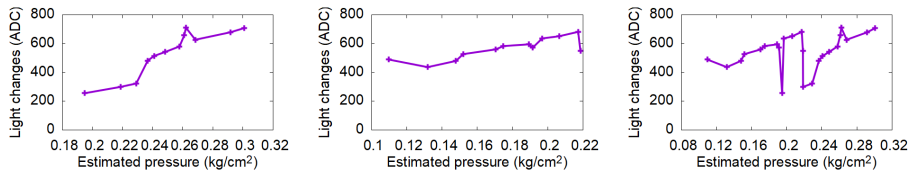
Table 6: Correlation (Kendall) coefficient (τ) analysis for all devices.

Devices	**DYNA**	**W-BALL**	**PLATES**	**GLOVE Sensors**		
				Position-1	**Position-2**	**Position-3**
DYNA	1	0.86	0.86	0.29	0.19	-0.21
W-BALL	0.86	1	0.80	0.25	0.15	-0.13
PLATES	0.86	0.80	1	0.22	0.20	-0.13

which is calculated from the hand dimensions collected prior to the study (hand-size $\approx$ hand-length $\times$ hand-breadth, DYNA-hand = $\frac{DYNA}{hand-size}$). Table 7 shows the similarity values (from a Kolmogorov-Smirnov test) and also the correlation analysis (Kendall). The similarities are high for all finger positions and both genders, highlighting that the general principle of using light intensity variations is viable means of estimating changes in grip force. The extent of changes depends on the surface area of the hand, and using the gender of the participant tends to serve as a proxy to these changes. Naturally estimating the surface area of the hand is infeasible on a simple wearable sensor. The most practical way to overcome this limitation is to (i) select sensor position based on hand-size or (ii) collect measurements from multiple positions simultaneously and (iii) adapt the analysis according to variations in the light intensity values. For people with smaller hand, the increase in grip at index finger seems to be best indicative of grip force, whereas for people with larger hand size the grip force can be reliably

Table 7: Statistical analysis between light reflectivity changes in different positions and DYNA-hand (value of dividing the dynamometer value with the hand size): red colour indicates lack of statistical significance in similarity or correlation.

Statistical Analysis	Position-1			Position-2			Position-3		
	Male	Female	All	Male	Female	All	Male	Female	All
Similarity	0.998	0.998	0.994	0.998	0.998	0.902	0.998	0.536	0.902
Correlation	0.88	0.67	0.39	-0.12	-0.09	0.14	-0.36	-0.73	-0.23



(a) Male participants (b) Female participants (c) All participants

Figure 12: Estimated pressure on the object (DYNA-hand) captured by the light sensor in position-1.

estimated from the loosened grip at the little finger. In addition, we can observe the significant correlation between the light sensor in position-1 and DYNA-hand. Figure 12 also shows the strong relation in position-1 especially when the gender is considered. However, there is no significant correlation for other positions, except the female participants in position-3. Therefore, we can conclude that the position-1 can achieve the best hand-grip strength estimation, which will be further proved in the following.

Comfort in Capturing Hand-grip Strength. Besides individual differences of participants, we explored the user experience by measuring the comfort (or discomfort) of performing the hand-grip strength experiments with the different devices. As a dynamometer has a flexible ergonomic design to adapt easily to any individual, it is important then to analyze the perception of participants when using the devices. To do this, after the experiment finalized, we ask all the participants to assign ranking values (on a 4-point Likert scale) based on their comfort when using the devices. The scale is anchored at 1 (very uncomfortable) and 4 (very comfortable). Figure 13 shows the results. Overall, the participants ranked the glove as the most comfortable, especially male participants. P3 mentioned that *"squeezing everyday objects is a very non-intrusive way because it is not noticeable"*. Another participant P12 also mentioned that *"the glove is very a lightweight solution"*. In contrast, there were also participants that disliked the glove, specifically female participants. P7 mentioned that *"it is difficult to squeeze the plastic ball as its too big for my hands"*. Another participant P20 said that *"I cannot apply proper hand-grip strength as the plastic ball is slippery"*. P18 also said that *"the plastic ball is too soft and it is difficult to assess whether I am applying my maximum hand-grip strength or not"*. In the case of the other devices, W-BALL was ranked as the second most preferable option, especially from female participants. Indeed,

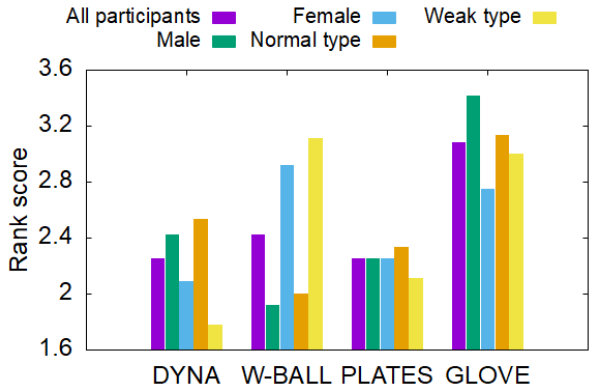


Figure 13: Ranking of 4 devices in use (the most comfortable–4, the least comfortable–1).

P9 mentioned that *"the wooden ball is small enough and provides better control when squeezing the object"*. Several participants also mentioned that *"the wooden ball is painful and hurts the hand as the material is too rigid"*. PLATES and DYNA received almost the same scores. The main comments about PLATES were that *"it is not easy to press and the shape square design hurts the hand"*. Likewise, the main comments about DYNA were that *"it is too heavy, it seems that the design is not balanced (the frontal part is more heavy than the back one) and it is difficult to provide hand-grip strength as it is too rigid"*. Overall, HIPPO provides the least intrusive and easiest-to-use solution and is preferred by the user compared to the baseline approaches.

Hand-Grip Strength Estimation (Classification). Hand grip strength is typically reported using discrete categories that offer a standardized and normative point for comparison. We next demonstrate how HIPPO can support coarse-grained classification of hand grip strength into different grip categories. We use four parameters for prediction: light values (L), gender (G), hand size (S), age (A), and three sensor positions: little finger, middle finger and index finger. Gender and age are well-known to affect hand-grip strength with normative reference tables typically considering these two variables to characterize the hand grip values [286]. Normative values also typically separate values depending on height, and potentially also weight. Height correlates strongly with hand size and thus the use of hand size indicator is equivalent to the use of height as part of dynamometer procedures [151]. We consider two simple machine learning classifiers: Random Forest and Gradient Boosting to guarantee that models can be deployed in low-power environments and 5-fold cross validation to evaluate the generalization of the models. When we train a L-G-S specific model, the average performance for the different fingers is 80% (little finger: 86%, middle finger: 70.5%, index finger: 84%). Once we train a model that considers the relationship between the strength and the age given by the dynamometer norm, L-G-S-A model, the average performance increases to 83% (little finger: 86%, middle finger: 79%,

index finger: 84%), indicating the importance of age in strength type classification. In terms of gender, the average classification performance for male participants results in 86.1% (little finger: 91.7%, middle finger: 75%, index finger: 91.7%) and for females 79.2%, (little finger: 79.2%, middle finger: 83.3%, index finger: 75%). These results confirm not only the influence of sensor positions, but also the information that gender can provide into the model. Naturally, other context issues might affect the estimates (e.g., object size, fit of the glove). Overall, the results demonstrate that hand-grip strength can be accurately estimated using HIPPO and especially when the sensor is worn in the little finger.

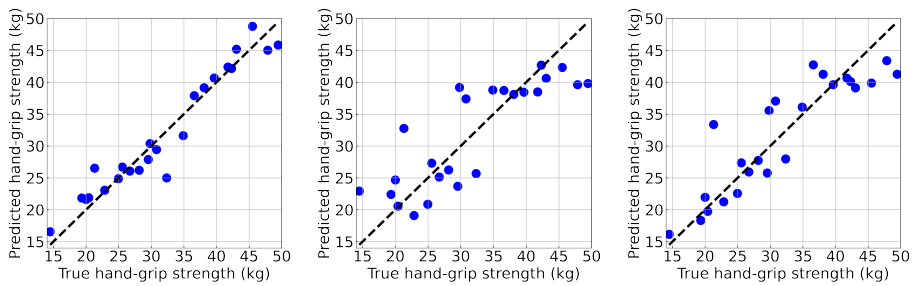
Hand-Grip Strength Estimation (Regression). We next demonstrate the potential of using machine learning to estimate the *exact* hand-grip strength based on light measurements and information about the characteristics of the participants. We considered two common regression models (ARDRegression and Ridge) to predict hand-grip strength by 10-fold cross validation across participants (i.e., both trials from each participant were always kept in the same fold to minimize correlations in the test and training sets). We also normalize the input parameters (hand size and lighting values) for more robust regression performance. The regression model effectively provides a mapping that can be used to convert the light reflectivity values captured by the sensor to a physical unit through a correspondence with another measurement device. The root mean square error RMSE (unit kg) and R^2 score of the regression experiments are shown in Table 8. When only the light reflectivity changes are considered, the average RMSE is 9.72 kg and the R^2 score is 0.01 across all regressors in different positions. This depicts a simple model that estimates hand-grip strength with minimal information about the individuals. Once an additional parameter gender or hand size is considered in the model, the average of RMSE decreases significantly for all positions (gender: RMSE = 4.72 kg, hand size: RMSE = 5.96 kg) with higher model relevance (gender: R^2 score = 0.75, hand size: R^2 score = 0.63). This supports the insight that individual physical characteristics may improve the regression model further. The best regression performance is achieved in all positions by including more than two factors, being light reflectivity changes (L), gender (G) and hand size (S) and the performance can be further improved when more measurements are taken. The best results are obtained for the little finger: RMSE 2.57 kg and R^2 score 0.93 across both regressors. Since different finger positions influence the hand-grip strength estimates, we also evaluate regression performance for measurements collected from different fingers. The results in Figure 14 show that the true values and predicted values are mostly distributed along a linear line for all positions, especially in position-1 (little finger), indicating accurate hand-grip strength estimation for HIPPO.

2.7. Practicality: Smart ring experiments

The results thus far have demonstrated that light sensors located on fingers can be used to estimate hand-grip strength. We also showed that the results vary across

Table 8: Root mean square error RMSE (unit kg) and R^2 score of predicting hand-grip strength (HS) in different experimental conditions. Model data $\rightarrow$ Predicted. Regression Method: Automatic Relevance Determination Regression (ARD), Ridge Regression (Ridge). Features: light reflectivity change (L), gender (G) and hand size (S), age (A).

Test conditions	Position-1						Position-2						Position-3						Overall
	ARD		Ridge		Average		ARD		Ridge		Average		ARD		Ridge		Average		Average
	RMSE	R^2	RMSE	R^2	RMSE	R^2	RMSE	R^2	RMSE	R^2	RMSE	R^2	RMSE	R^2	RMSE	R^2	RMSE	R^2	RMSE R^2
(L) $\rightarrow$ HS	9.63	0.02	9.49	0.05	9.56	0.04	10.08	-0.07	9.70	0.01	9.89	-0.03	9.84	-0.02	9.59	0.03	9.72	0.01	9.72 0.01
(L,S) $\rightarrow$ HS	5.42	0.69	5.38	0.70	5.40	0.70	6.45	0.56	6.49	0.56	6.47	0.56	6.10	0.61	5.90	0.63	6.00	0.62	5.96 0.63
(L,G) $\rightarrow$ HS	3.33	0.88	3.32	0.88	3.33	0.88	5.98	0.62	6.14	0.60	6.06	0.61	4.80	0.76	4.75	0.76	4.78	0.76	4.72 0.75
(L,S,G) $\rightarrow$ HS	2.58	0.93	2.56	0.93	2.57	0.93	5.42	0.69	5.42	0.69	5.42	0.69	4.51	0.79	4.29	0.81	4.40	0.80	4.13 0.81
(L,S,G,A) $\rightarrow$ HS	2.55	0.93	2.68	0.93	2.62	0.93	5.42	0.69	5.62	0.67	5.52	0.68	4.44	0.79	4.50	0.79	4.47	0.79	4.20 0.80



(a) Position-1 (b) Position-2 (c) Position-3

Figure 14: Hand-grip strength estimation performance in different positions.

different fingers and individuals, with the best results requiring to use multiple contact points and background information about the user's gender. As the smart glove can constrain the hand-grip of some participants, we next demonstrate that our solution is feasible also in more practical scenarios by presenting an optimized design of the HIPPO wearable, and carrying out further experiments using everyday household objects and $N = 14$ participants. These experiments were designed to show that HIPPO can indeed piggyback interactions with everyday objects to obtain continuous estimates of grip strength. We also consider a wider variety of experimental conditions and new situations that can influence the estimations of hand-grip strength though HIPPO.

2.7.1. Experimental design

Everyday objects. As household objects used in our experiments, we rely on a (A) disposable cup (Poly-Coated paper), (B) plastic cup (PET), (C) kitchen sponge (Microfiber), (D) Paper-sheet (Wood fibres), (E) Fleece jacket (Polyester), (F) Face mask (Polypropylene - PP), (G) Plastic bag (HDPE), (H) Beer can (Aluminum) and (I) Metallic scrubbers (Stainless steel) (see Figure 15(b)). The first three objects were evaluated by all participants, whereas objects (D) - (I) were only sampled by a single participant (6 trials per object). Limiting the number of objects that were interacted with was necessary to maintain the length of the study feasible for participants.

Participants. 14 participants were recruited (Males=7, Females=7). The participants were university students, staff and also the researcher's social circle from different fields and nationalities. Their average age was 23.93 ± 5.01 and all of them were right-handed.

Wearable prototype. We built an optimized smart ring prototype that embeds the light sensors to a ring and connects to a computing board for carrying out the analysis of values. Figure 15(a) shows the prototype which is worn by an individual in the right hand and located in the ring finger (light sensor in position-1). The prototype uses a wireless M5StickC PLUS ESP32 development board that controls the sampling frequency of the light sensor and uploads the samples to a centralized server. The M5StickC Plus contains an inbuilt Wi-Fi connection facility, battery supplies (120 mAh @ 3.7V) and LCD screen to externalize the activities of the board. Moreover, it is lightweight (21g) and portable, such that it can be placed in a wristband ($65 * 25 * 15$mm). The M5StickC PLUS reads photo resistor's values through G36 pin and can show the light reflectivity values on its screen in real time. The board externalizes a light sensor through a dedicated and isolated wire that is attached to a plastic ring. The ring is a ready-made manufactured product, whose shape is flexible as its core is made from an elastic wire. We used the same type of red laser diode (650nm 5mW $3-5$V) and a photo-resistor (5MΩ) as in our smart glove prototype. Since the shape of ring is flexible, it is easy to adjust to different finger characteristics.

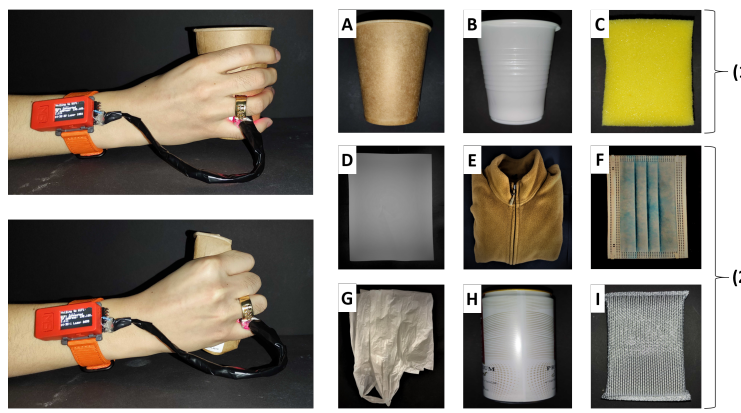


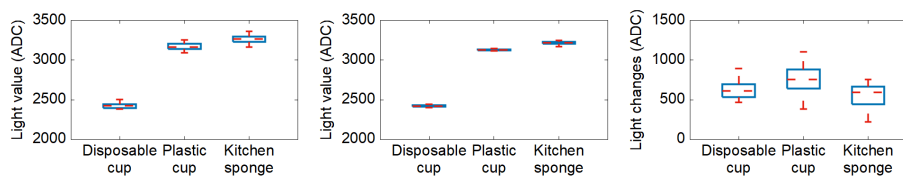
Figure 15: Common house hold objects used in the wild experiment: a) optimized HIPPO wearable that consists in a wristband and a ring; b) (1) first set: A) disposable cup, B) plastic cup, C) kitchen sponge; b) (2) second set: D) paper-sheet, E) fleece jacket, F) face mask, G) plastic bag, H) beer can, I) metallic scrubbers.

Procedure. Experiments we carried follow the same standard procedure as when using the dynamometer (See details in Subsection 2.6). As in previous experiments, the researcher conducting the experiment explained the overall procedure and collected a signed informed consent form from every participant. The

experiment was encoded into a 1×2 factorial design with the object type and trial as independent variables, following the design of our controlled experiment. To eliminate order effect and biases, whilst keeping the number of trials manageable, trial number was counterbalanced following a Latin Square design, resulting in eight experimental conditions: (1) Trial1-DYNA, (2) Trial2-DYNA, (3) Trial1-A, (4) Trial2-A, (5) Trial1-B, (6) Trial2-B, (7) Trial1-C and (8) Trial2-C (A, B and C are the 3 objects for the experiment). The duration of the experiment was around 25 minutes. In addition to this, the researcher collected 6 trials worth of measurements for the other objects (D)-(I). The evaluation took place in the same university room as the other experiments (see Subsection 2.6).

2.7.2. Results

Characteristics of light intensity. Figure 16(a) shows a characterization of the light reflectivity values for the different objects across all participants. The mean light values vary across different objects and the variance in the light measurements for each object is low: disposable cup (Mean=2431.18, SD=59.26), plastic cup (Mean=3172.54, SD=45.94) and kitchen sponge (Mean=3266.34, SD=59.09). The variation in the measurements is mostly caused by small motions, but overall the effect is negligible. The effect of these motions can be mitigated by integrating a motion sensor that detects periods where the hand is stable and only considering those periods. Figure 16(b) illustrates this point, showing how the variance in measurements is significantly reduced when only stable periods are considered for measurements. Finally, Figure 16(c) compares the light values across different objects and across all the participants. The values vary across objects, which simply shows that the changes in intensity depend on the surface characteristics of the objects. As HIPPO uses relative changes in light intensity between minimum and maximum grip force, this does not affect the hand-grip strength estimates. However, the result shows that interactions with *different* objects can be identified from the light intensity values.



(a) (b) (c)

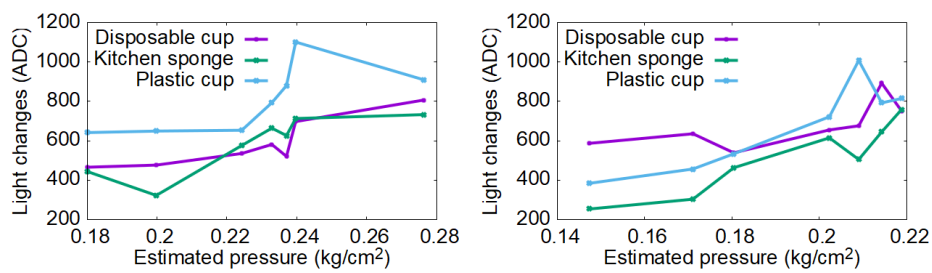
Figure 16: Capturing hand-grip strength, a) Variations in light values of the objects across all participants (in the relaxed state), b) Light characterization of the objects (in the relaxed state), c) Quantification of hand-grip strength in different objects across all participants.

Validity. We verified that our new wearable design captures representative data of hand grip strength by comparing the collected light measurements against the

gold standard (dynamometer). Table 9 shows the results of Kolmogorov-Smirnov test on pairs of data. No statistically significant differences are found (p>0.05), i.e., the *changes* in light intensity values reflect the actual force-grip strength. We also separately compare the similarity of the changes in light intensity values with the estimated pressure applied on the object, i.e., the force given by the dynamometer divided by the approximate hand surface area size. The similarity with pressure values is slightly higher than with the dynamometer values, especially for female participants. Thus, similarly to the controlled experiments, the fit between the sensor and the object have slight influence on the intensity values but overall the results are sufficiently stable across participants to estimate hand grip strength. Figure 17 also indicates that there is a strong correlation between the light reflectivity changes and DYNA-hand in different objects for males and females. From Table 9, we can also observe that despite the different mechanical properties of the objects, the generality of our approach across different objects is well-suited for different participants. We also performed a Spearman correlation analysis between the light changes and the estimated pressure. Here, the null hypothesis (H_0) states that there is no monotonic correlation between the two variables, while the alternative hypothesis (H_1) states that a monotonic correlation exists. A strong and statistically significant correlation ($p < 0.05$) was observed between the light changes and the hand-grip values across all paired measurements, consistent with the similarity indicated by the K–S test.

Table 9: Data similarity ($p-$value) between light reflectivity changes in the object and two measures: DYNA (dynamometer value), DYNA-hand (estimated pressure on the object, calculated by dividing the dynamometer reading (force) with the hand size).

Similarity	**Disposable cup**			**Plastic cup**			**Kitchen sponge**		
Analysis	**Male**	**Female**	**All**	**Male**	**Female**	**All**	**Male**	**Female**	**All**
DYNA	0.962	0.937	0.904	0.962	0.937	0.998	0.962	0.937	0.904
DYNA-hand	0.962	0.962	0.920	0.962	0.962	0.999	0.962	1	0.999



(a) Male participants

(b) Female participants

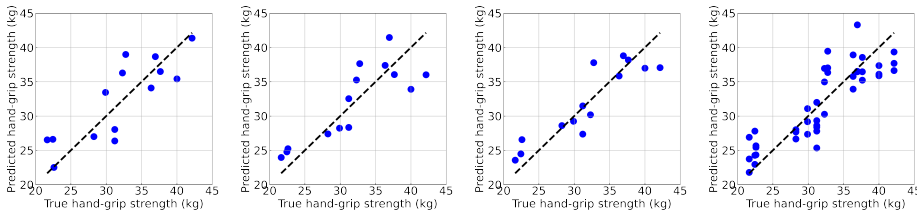
Figure 17: Estimated pressure on the object (DYNA-hand) captured by the light sensor in different objects.

Table 10: Evaluation on regression (RMSE kg, R^2 score) of predicting hand-grip strength (HS) and classification accuracy(%) of predicting hand-grip strength type (ST) in different conditions. Features: light reflectivity change (L), gender (G), hand size (S), age (A) and object (O).

Test conditions	Object	Regression		Classification(%)
		RMSE	R^2	
(L,S,G,A)	Disposable cup	3.54	0.68	71.7
	Plastic cup	3.44	0.70	73.3
	Kitchen Sponge	2.96	0.78	73.3
	All objects	3.20	0.75	90.6
(L,S,G,A,O)	All objects	3.22	0.74	91.9

Performance. We evaluate HIPPO performance by using the same regression and classification models as before to predict exact hand-grip strength (10-fold cross validation) and strength category (5-fold cross validation). We report the average accuracy across all tests. In this experiment, participants scored all types (weak, normal and strong) of hand-grip strength. We also trained the model on individual objects to test the classification sensitivity of different objects. From the smart glove experiment, the best performance of estimated hand-grip strength is achieved by the combination of the light change, hand size and gender. Therefore, we consider this combination for our field (i.e., in the wild) evaluation. We still consider age as an input parameter due to the relevance between age and strength type according to the dynamometer norm table. Table 10 shows the classification accuracy of HIPPO on the individual object as well as all objects in different conditions. We can observe that plastic cup and kitchen sponge (both 73.3%) performed better than a disposable cup (71.7%). Since squeezing the disposable cup is harder than squeezing the plastic cup and sponge, the variation in light changes using the disposable cup across the participants is lower, which might lead to a low accuracy. The performance of the individual object can be further improved if more samples are obtained from each object since most hand grips are of the normal category in the experiment. The accuracy increased greatly up to 90.6% when training the models on all objects. Therefore, a better hand-grip strength type estimation can be achieved with the combined measurements from different daily objects. Moreover, when we consider the object type as one of the parameters and train the model on all objects, The best performance can be achieved with the accuracy 91.9% (RF 90.6% and GB 93.1%), a slight increase compared to the performance on all objects without considering object types. This further proves that although different mechanical properties of the objects might result in different patterns of light reflectivity, their performance of strength type estimation is almost consistent. Figure 18 also shows that accuracy is good since the predicted and true values closely align with a straight line centered in the origin.

Other household objects. Figure 19(a) shows the light sensor values of the additional household objects (i.e., (D) - (I)) that were sampled six times by the



(a) Disposable cup (b) Plastic cup (c) Kitchen sponge (d) All objects

Figure 18: Hand-grip strength estimation performance of different objects.

researcher. In line with the other results, each individual object has a unique light fingerprint despite the force being (approximately) constant. The fingerprints also have low overall variance: paper sheet (Mean=1298.21, SD=302.60), fleece jacket (Mean=2452.42, SD=47.92), face mask (Mean=1731.34, SD=211.65), plastic bag (Mean=1621.75, SD=352.26), beer can (Mean=645.63, SD=185.85), metallic scrubbers (Mean=2145.54, SD=17.62). Overall the variance is somewhat higher for some of the objects. This mainly concerns objects that are hard to grab (paper sheet) or that have a shiny (beer can) or translucent surface (plastic bag). Taken together, the results show that HIPPO is practical and can operate robustly across users and everyday household objects. Some objects are better suited for HIPPO than others, but these can be identified by examining the distribution and changes in light intensity values.

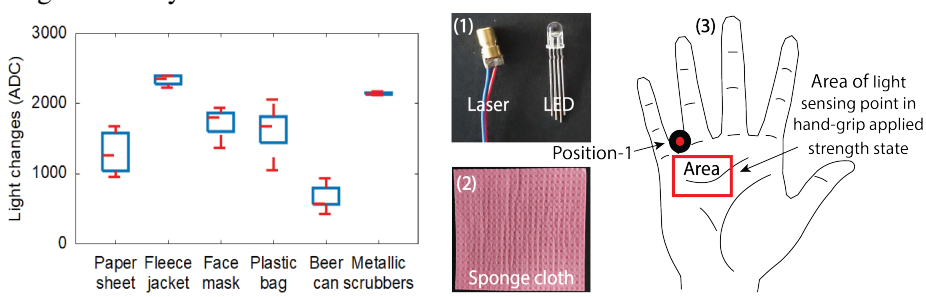


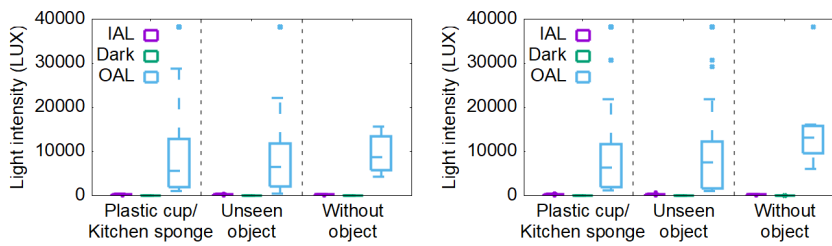
Figure 19: a) The changes in light intensity values for the additional household objects, b) evaluation of other factors on HIPPO: (1) Laser vs LED, (2) Unseen (new) object and (3) Sensing without objects

2.7.3. Impact of design and environmental factors on HIPPO

HIPPO has been designed as a solution that can operate as part of everyday interactions instead of requiring a dedicated measurement protocol, unlike existing solutions. We next briefly assess the effects of different environmental and other design factors on the performance of HIPPO to demonstrate that the hand-grip estimates are robust across a wide range of factors. These tests were carried out through separate experiments conducted independently and in a small scale setting

with additional participants. The main reason for this is to avoid having longer experiments, which are not engaging to participants and can potentially be noisy, and also to avoid the experiments from becoming a burden for participants. Moreover, it is not possible to obtain consistent hand-grip measurements from consecutive measurements that require applying heavy force. We recruited 6 participants (age 31.83 ± 9.70), three males and three females, to have a balanced distribution (participants 1-3 are females). The procedure to collect hand-grip measurements remains the same as in previous experiments (see details in Subsection 2.6). The duration of the experiment was on average 30 minutes. These experiments are conducted using the same smart ring prototype as described previously (laser as the light source).

Effect of the luminosity. Since environmental conditions can influence light values, we have also evaluated the impact of environmental luminosity considering three conditions: indoor dark (Dark), indoor ambient light (IAL) and outdoor ambient light (OAL). The indoor ambient light condition is the same as in the previous experiment. Measurements were collected for 7-days for laser and LED independently. Plastic cup and kitchen sponge (See B and C in Figure 15(b)) were used as the household objects in this experiment. Figure 20 shows the luminosity (LUX) of the measurements in the different environments. The luminosity is stable in the two indoor environments, whereas the ambient light contains more variations in the outdoor case. Luminosity shows to be constant during both laser and LED experiments.



(a) Laser (b) LED

Figure 20: Light intensity (LUX) in different experimental environments (IAL: indoor ambient light, Dark: indoor dark, OAL: outdoor ambient light).

Figure 21(a-d) shows the results of estimated pressure (DYNA-hand) and their respective light values in the different luminosity environments. We also separated the results by gender as hand size and finger positions play an important role, as we showed previously. From the figure, we can observe that light changes can estimate relatively similar pressure in all the environments. We also repeat the regression experiments by re-training our models using the measurements from the 7-days. Training and testing are carried out using leave-one-day-out cross validation. Table 11 shows the laser results of HIPPO using RMSE and R^2 values. The accuracy is consistently high, with the two indoor environments resulting in the

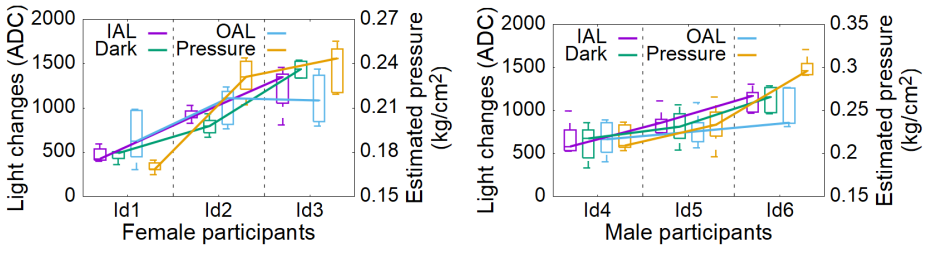
Table 11: Root mean square error RMSE (kg) and R^2 score of predicting hand-grip strength (HS) in different environments. Features: light reflectivity change (L), gender (G) and hand size (S), age (A), object (O), light conditions LUX (C).

Sensors	Test conditons	Measure-1		Measure-2		Measure-3		Measure-4		Measure-5		Measure-6		Measure-7		10-CV	
		RMSE	R^2	RMSE	R^2	RMSE	R^2	RMSE	R^2	RMSE	R^2	RMSE	R^2	RMSE	R^2	RMSE	R^2
Laser	**IAL (L,S,G,A,O)**	2.64	0.87	3.47	0.80	3.60	0.79	2.59	0.89	2.62	0.89	3.19	0.87	3.03	0.89	3.13	0.85
	(L,S,G,A,O,C)	2.64	0.87	3.47	0.80	3.60	0.79	2.59	0.89	2.62	0.89	3.19	0.87	3.03	0.89	3.14	0.85
	Dark (L,S,G,A,O)	3.60	0.76	2.66	0.88	3.73	0.78	2.85	0.86	3.33	0.81	3.52	0.85	3.74	0.82	3.47	0.82
	(L,S,G,A,O,C)	3.60	0.76	2.66	0.88	3.73	0.78	2.85	0.86	3.33	0.81	3.52	0.85	3.74	0.82	3.47	0.82
	OAL (L,S,G,A,O)	4.77	0.59	4.42	0.68	4.08	0.73	3.70	0.77	3.40	0.80	4.42	0.76	4.04	0.79	4.19	0.74
	(L,S,G,A,O,C)	4.78	0.58	4.46	0.67	4.08	0.73	3.70	0.77	3.45	0.80	4.68	0.73	4.04	0.79	4.23	0.73
	All (L,S,G,A,O)	3.70	0.75	3.51	0.80	3.78	0.77	3.16	0.83	3.28	0.82	3.93	0.81	3.58	0.84	3.54	0.81
	(L,S,G,A,O,C)	3.70	0.75	3.51	0.80	3.78	0.77	3.16	0.83	3.28	0.82	3.99	0.80	3.58	0.84	3.56	0.81
LED	**IAL (L,S,G,A,O)**	5.38	0.36	4.28	0.74	6.15	0.56	4.48	0.63	4.92	0.54	5.35	0.69	4.32	0.77	5.24	0.61
	(L,S,G,A,O,C)	5.34	0.37	4.53	0.70	6.08	0.57	4.40	0.64	4.85	0.55	5.56	0.67	4.38	0.77	5.24	0.61
	Dark (L,S,G,A,O)	5.48	0.34	4.40	0.72	5.61	0.63	3.50	0.77	4.01	0.69	5.08	0.72	5.04	0.69	4.94	0.65
	(L,S,G,A,O,C)	5.50	0.33	4.39	0.72	5.61	0.63	3.69	0.75	4.03	0.69	5.11	0.72	5.10	0.68	4.94	0.65
	OAL (L,S,G,A,O)	5.82	0.25	4.55	0.70	6.11	0.56	4.88	0.56	5.15	0.49	5.55	0.67	4.54	0.75	5.39	0.59
	(L,S,G,A,O,C)	5.83	0.25	4.54	0.70	6.19	0.55	4.86	0.56	5.16	0.49	5.88	0.63	4.53	0.75	5.41	0.59
	All (L,S,G,A,O)	5.69	0.28	4.42	0.72	5.94	0.59	4.25	0.67	4.94	0.54	5.30	0.70	4.54	0.75	4.98	0.65
	(L,S,G,A,O,C)	5.69	0.28	4.42	0.72	5.95	0.59	4.25	0.67	4.95	0.53	5.35	0.69	4.54	0.75	4.99	0.65

best performance. Thus, luminosity impacts the results due to largest variations in ambient sunlight, but this is generally negligible. The regression results in Figure 22 (a-d) similarly show high accuracy, and the average classification performance for strength type is 90.87% (IAL: average 93.44%, Dark: average 92.26%, OAL: average 88.69% and All: average 90.87%) as shown in Figure 23(c).

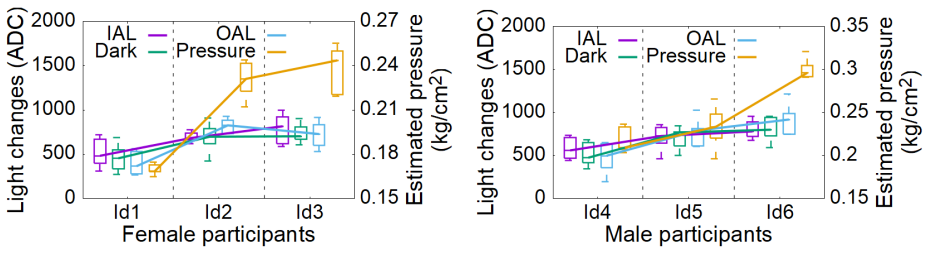
Effect of light source. We also assessed whether the laser could be replaced by a LED (red-color, 5 mm in size, 0.06W power draw, and luminous intensity of 1500 mcd at a 30° angle) shown in Figure 19(b)(1). The laser produces monochromatic and heavily directed light, whereas the spectrum of light produced by the LED contains more variation. The results in Figure 21(e-h) show that no clear relationship can be established between light changes and the estimated pressure (DYNA-hand) as given by the dynamometer. This is a direct consequence of the variations in the light spectrum of the LED and in practice this mostly affects the regression estimates and cases where the strength values are close to the border between two categories. Indeed, the laser consistently outperforms the LED source, even if the LED can also be used to obtain insights about hand-grip strength. Specifically, HIPPO combined with laser performs better than LED in regression from Table 11 (laser: average RMSE= 3.56 kg, and LED: average RMSE=5.01 kg), as well as in classifying the hand-grip strength category (IAL: average 91.66%, Dark: average 89.82%, OAL: average 80.85% and All: average 85.31%). We also notice from Figure 23 (d) that the performance of LED is not consistent during different days (OAL) and the accuracy is below 80% for 3 out of 7-day measurements. Figure 22 (e-h) also show estimation performance by 10-fold cross validation, which we find to be less accurate along $y = x$ with LED, especially in outdoor environments.

Unseen household objects. Ultimately HIPPO should operate on any everyday interactions without having to rely on models tailored for specific objects. We tested performance for a previously unseen object by introducing an object made of sponge cloth (cellulose with cotton) shown in Figure 19(b)(2). We train the models



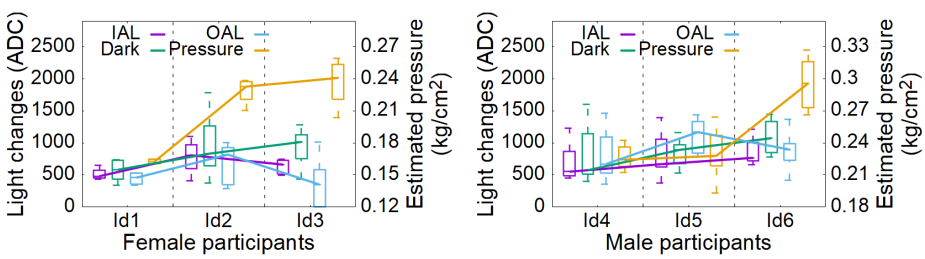
(a) Laser: plastic cup

(b) Laser: plastic cup



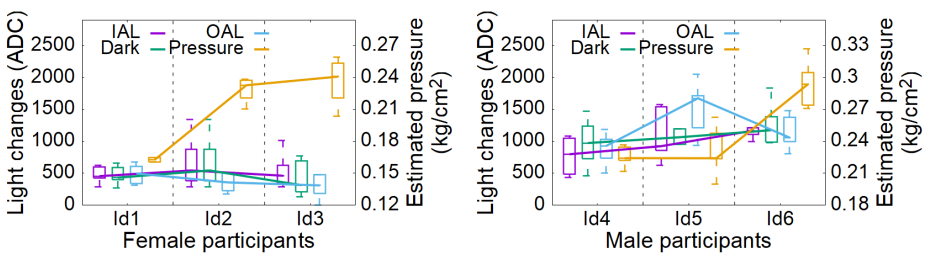
(c) Laser: sponge

(d) Laser: sponge



(e) LED: plastic cup

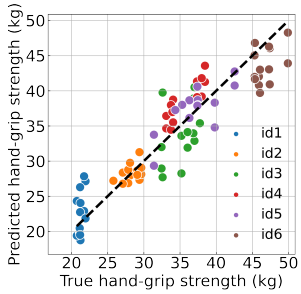
(f) LED: plastic cup



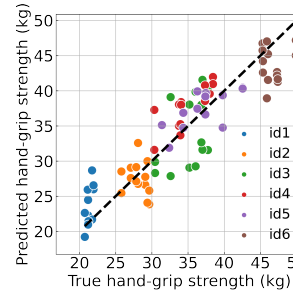
(g) LED: sponge

(h) LED: sponge

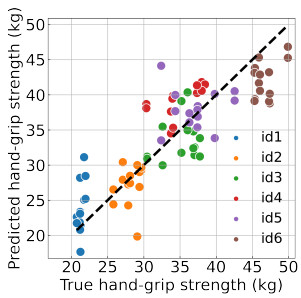
Figure 21: Estimated pressure (DYNA-hand) captured by light reflectivity changes through 7-day measurements in different environments: IAL-indoor ambient light, Dark-indoor dark, OAL-outdoor ambient light.



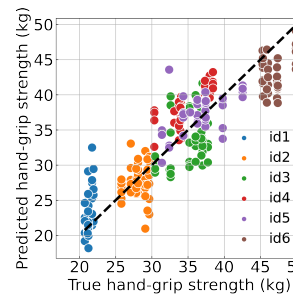
(a) Laser: IAL



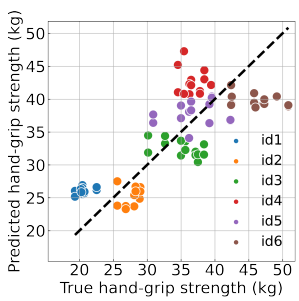
(b) Laser: Dark



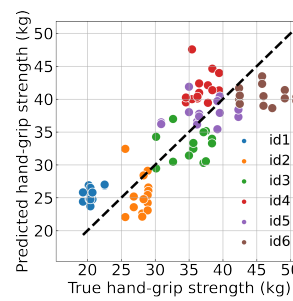
(c) Laser: OAL



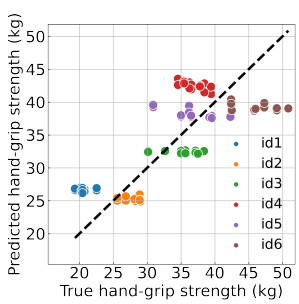
(d) Laser: All



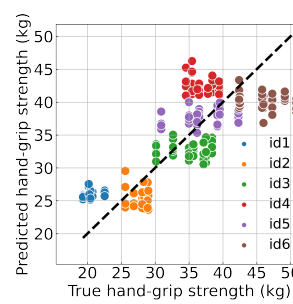
(e) LED: IAL



(f) LED: Dark

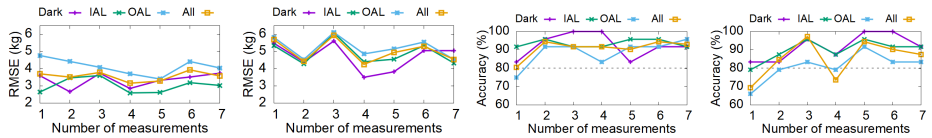


(g) LED: OAL



(h) LED: All

Figure 22: Hand-grip strength estimation performance by 10-fold cross validation across 7-day measurements in different environments.



(a) Laser (b) LED (c) Laser (d) LED

Figure 23: Evaluations on hand-grip strength estimation (RMSE) and strength type classification(%) across 7-day measurements in different environments.

Table 12: Unseen object evaluations in different environments.

Test conditions	Regression	Classification(%)						
	RMSE	Id1	Id2	Id3	Id4	Id5	Id6	All Ids
IAL	5.45	71.43	85.71	100	71.43	78.57	100	**83.33**
Dark	4.91	71.43	100	100	71.43	100	100	**90.47**
OAL	4.84	85.71	85.71	100	85.71	100	100	**92.86**
All	5.05	85.71	90.48	100	69.04	100	100	**90.88**

with the data from the two objects described above (plastic cup and kitchen sponge) and test against the data from the cloth. The data of the cloth was also collected across 7-day measurements from the same 6 participants as the plastic cup and kitchen sponge. The results in Figure 24 show the trend between light changes and estimated pressure to be similar, and robust across gender, and environment. Table 12 shows the regression and classification performance, which remain reasonably high despite variations across individuals (IAL 83.33%, Dark 90.47 and OAL 92.86% and All 90.88%). For two users (1 and 4, female and male), the drop in performance was more significant (1: 71.43%, 4: 71.43%), which resulted from low similarity between the light values considered for training and testing. The sponge cloth is easiest to squeeze and thus it should result in highest variation and deformations. The two users whose estimates were least accurate both had low pressure grips, resulting in a small number of deformations and making the light intensity values relatively stable. Thus, the performance with unseen objects depends on the characteristics of the object and may also depend on the grip-strength category of the individual as the presence or absence of deformations may impact how well prior data fits the user.

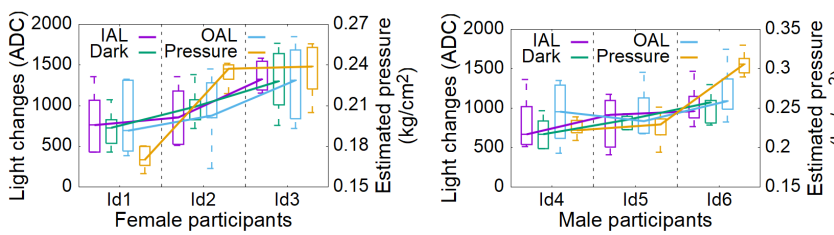
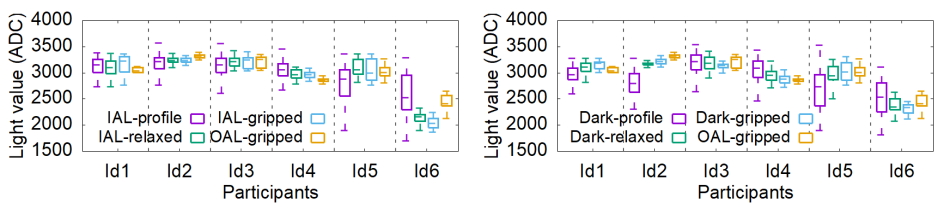


Figure 24: Estimated pressure (DYNA-hand) captured by light reflectivity changes on unseen (new) object through 7-day measurements in different environments.

Table 13: Light values (ADC) without objects in different environments: profile - light profile of the whole hand in the flat state, gripped - light values in the hand-grip applied strength state, relaxed - light values in the flat state where the sampling area is based on the area of the sensing point in gripped state.

Participants	IAL			Dark			OAL
	Profile	Relaxed	Gripped	Profile	Relaxed	Gripped	Gripped
Id1	3124.66±160.07	**3098.57±160.16**	**3160.73±169.46**	2967.15±161.50	**3099.02±105.23**	**3152.84±77.16**	**3050.94±42.99**
Id2	3166.21±185.28	**3232.78±54.23**	**3239.79±45.64**	2823.02±267.93	**3168.97±44.06**	**3322.69±40.39**	**3322.69±40.39**
Id3	3132.75±188.94	**3212.64±96.54**	**3217.71±109.55**	3169.31±201.13	**3186.00±133.89**	**3128.87±67.21**	**3217.70±109.55**
Id4	3055.49±155.59	**2972.56±81.71**	**2960.00±61.37**	3064.16±119.11	**2944.32±104.08**	**2873.54±82.57**	**2877.44±66.09**
Id5	2792.64±362.54	**3086.82±153.19**	**3058.77±204.64**	2697.65±394.11	**2982.57±172.06**	**3020.08±181.59**	**3015.21±105.84**
Id6	2607.17±395.79	**2121.34±117.20**	**2042.92±110.74**	2521.258±325.29	**2383.64±156.06**	**2308.92±105.36**	**2431.00±150.99**

Performance without object. Hand-grip strength estimates should only be calculated when the user is interacting with an object, and thus there is a risk of false positives if the user clenches their fist or keeps the hand open without exerting a pressure. As final step, we investigate whether these cases can be reliably detected and omitted from analysis. We perform this from the same participants by examining the light intensity values when the user's hand is clenched (or gripped) or open without interacting with an object. Figure 25 shows the resulting light values and the light values in the flat (or relaxed) state are from the area shown in Figure 19(b)(3). The light values are similar for the same individual, and we can observe similarities between the relaxed and clenched (gripped) states. This indicates that when there is a hand-grip, the sensors read the same information no matter the environment. Table 13 shows the mean and standard deviation of the light intensity values, showing small variations between the relaxed and the clenched states. These values are significantly different from those when the user interacts with an object, and thus interactions with objects can be detected by identifying sudden significant changes in the light intensity values. This suggests that false positives can be significantly mitigated. Another implication of this result is that it offers potential for resource savings by helping to identify when measurements need to be processed.



(a) IAL+OAL (b) Dark+OAL

Figure 25: Light values of hand with different states in different environments: profile - light profile of the whole hand in the flat state, gripped - light values in the hand-grip applied strength state, relaxed - light values in the flat state where the sampling area is based on the area of the sensing point in gripped state. The same OAL-gripped values shown with both IAL and Dark environments.

2.8. Discussion

Factors that influence hand-grip strength: Age and gender are factors that influence hand-grip measurements, and there are very well defined index values associated with them. The average grip strength is 46kg for men and 29kg for women [286]. In our work, we demonstrated that our light sensing approach can also capture this strength as the results preserve the relative patterns measured by a certified dynamometer.

Room for improvement: We demonstrated in our work that hand-grip strength can be estimated using light sensors located in a smart glove prototype. As software and hardware of light sensors are already miniaturized, e.g., smartwatches, the deployment of our approach can be optimally envisioned within smart rings. Indeed, existing commercial solutions either implement light sensors (that can be re-purposed) or could be easily extended with light sensors to introduce our approach transparently into daily routines of users. The performance of HIPPO showed highly promising performance, correlating well with a clinical baseline (dynamometer), but naturally there is further work to improve the robustness of the estimates and to support interactions with a wider range of household objects. We are also interested in generalizing our approach into a larger spectrum of interactions with household objects, and different body positions.

Threats to validity: In CHI standards, a sample size of around 12 participants is common for user studies [56], making our sample size reasonable for a systematic evaluation of the proposed methods. However, this limited sample size does not cover all age groups and lacks a balanced distribution across grip strength types, particularly strong grip, which is more common among athletes. This can pose potential threats to validity. Therefore, we are interested in exploring a wider range of demographics to further generalize HIPPO and improve model accuracy.

Daily hand-grip monitoring: Previous work has reported that the body position that is used for measuring hand-grip strength can influence the results of the overall measurements [365]. However, it is also noticed by these studies that to overcome this problem, the strength values just have to be adjusted based on the body position, such that those can be interpreted fairly. In addition, it has also been found that just 4 kg of hand-grip strength is required to perform 90% of daily living activities (ADL) [190]. Thus, there are opportunities to measure hand-grip strength directly from interactions or indirectly by asking the user. As part of the post questionnaire for each participant in our main experiment, we asked whether they have used dynamometer before to measure their hand-grip strength. Overall 62% of the participants mentioned that they did not use it before. We also asked whether they would be interested on acquiring a dynamometer in the future to measure their hand-grip continuously at home. Overall 83.3% of participants mentioned that they are not interested. All in all, this highlights further the need of non-intrusive approaches for measuring health based on hand-grip indicators.

Other light spectrum: We demonstrated that light sensing in the red spectrum can

be used to capture hand-grip strength measurements. By looking at the reflective patterns of the changing surface of the object as the hand squeezes the object, it is possible to extrapolate the intensity of the hand-grip. Other spectrum of light can also be re-purposed to achieve this, e.g., blue and green, we are interested in investigating its performance as some spectrums are preferable over others based on the context of the user. For instance, red light would be suitable underwater when compared with blue light.

Comparison to other sensing modalities: While pressure sensors can be used as an alternative sensing modality to measure hand-grip strength, its deployment is rather difficult as its placement within the hand plays an important role to obtain accurate measurements. Thus, it is difficult to introduce it in a transparent manner to users. In our work, an additional pressure sensor is located in the (hand) palm and we found high variance in the results when measuring hand-grip of squeezing objects. One reason of this is that soft materials tend to absorb the grip force so that the sensor is not able to detect and distinguish it. For instance, a rubber ball will absorb most of the force from the hand-grip.

End-user adoption: The results demonstrate that a simple light sensor embedded in a ring can be used to estimate the hand grip strength of an individual, and to provide insights into changes in the user's health. Naturally further optimizations would be required in practice. Firstly, most wearable devices are combined with a compendium application that runs on a smartphone. HIPPO could similarly benefit from such design, offloading the analysis of the light intensity values onto the smartphone instead of performing them on the ring. The smartphone application can also be used to obtain information that supports the analysis, e.g., hand size parameters could potentially be estimated on the smartphone from touch screen interaction patterns. The sampling on the ring can also be further optimized using a proximity sensor to detect when the user is interacting with objects. Moreover, a well-designed smart ring tailored to individual users is also important for accurate estimation.

Inherent object characteristics : Surface deformations are dependent on inherent characteristics of the material of the object being interacted with and these variations can affect the light intensity measurements captured by HIPPO. For example, hard surfaces (such as the wooden ball used as the baseline) might not alter their shape, whereas malleable objects can undergo significant surface changes. In both cases, the light intensity values change as force is applied, but the patterns of changes vary depending on the surface of the object. Further improving the robustness of the estimates may require averaging estimates from multiple interactions and potentially from different objects. Alternatively, it may be possible to suggest activities to create opportunistic moments for hand-grip estimation, e.g., by inducing interactions on a smartphone by providing recommendations. Then the object type can be identified either through computer vision or via manual input in the app. As object color can indeed affect light reflectivity, we are also interested

in exploring its effect on light reflectivity changes during grip.

Application scenarios: HIPPO presents an important first step toward harnessing everyday interactions for deriving health related information. While the main focus in this paper has been on interactions with everyday objects, HIPPO is also beneficial to more specialized domains. For example, hospitals or care homes could give medical rings to patients and use HIPPO to continuously estimate hand grip instead of requiring separate test assessments.

Practicability: Optimally, we envision HIPPO to be integrated into smart rings, which already contain the required sensor, re-purposing these devices for hand-grip estimation. The light sensors used by HIPPO are low-cost, low-power, and small in size, making it reasonably easy to integrate HIPPO with diverse wearables. Indeed, wearables already use light sensors for measuring heart rate and other physiological parameters, and HIPPO uses similar technology but is placed on the exterior of the wearable to derive hand grip information. Our experiments showed that it is possible to detect when objects are held and this information can be used to optimize resource consumption.

2.9. Summary

We contributed HIPPO, an innovative sensing solution and a new sensing modality for assessing hand-grip strength from opportunistic interactions with everyday objects. HIPPO captures hand-grip estimations by looking at changes in the surface of objects using light sensors. Through extensive experiments that considered a wide range of everyday objects and 44 participants, we demonstrated that HIPPO can capture hand-grip estimations that align with a clinically certified dynamometer. We also compared our proposed method against other state-of-the-art baselines, demonstrating that HIPPO can capture pressure-based estimations through light and provide an easy-to-use and natural alternative that harnesses everyday interactions. The best results are obtained when there are multiple measurement points per individual, i.e., when multiple interactions with different objects are piggybacked. The results also showed some interactions being better for estimation as others as the contact between the light sensor and the object needs to be sufficiently good to capture the changes in shape. The HIPPO workflow is straightforward. First, the system requires the input of the object type (either manually or via computer vision), along with user information (age, gender, hand size) and background adaptation to ambient light conditions. Once this setup is complete, HIPPO proceeds with grip-strength measurement during the user's interaction with the object. Our demo work [465] also demonstrate how HIPPO works in practice. Our method paves the way toward non-intrusive solutions for capturing individual's hand-grip strength – an important health-related parameter – continuously and pervasively.

3. SPIKEY: PREVENTING DRINK SPIKING USING WEARABLES

As covered previously, we investigated how smart rings can estimate grip strength through everyday interactions, showcasing the potential of repurposing hand behavior for health sensing. In this Chapter, we explore another common hand interaction *hold* as an opportunity to address a growing safety concern: drink spiking. Drink spiking is difficult to detect, often occurring in crowded social environments using substances that leave no visible trace. Existing solutions are either substance-specific, require costly or intrusive equipment, or fail to operate in real-world settings due to fixed properties. To overcome these challenges, we introduce SpikEy, a smart ring–based sensing system that uses light reflectance and motion calibration to identify the presence of foreign substances in drinks. Rather than detecting specific drugs, SpikEy constructs generalizable *spiking profiles* from latent optical signals, achieving robust performance across various drink types, concentrations, and environments. Through technical innovations in signal modeling and practical validation in real-world scenarios, SpikEy demonstrates the feasibility of using smart rings for personal safety through unobtrusive and everyday interactions.

3.1. Introduction

Drink spiking, the deliberate act of adding substances to drinks without the knowledge or consent of the person consuming them, is a worrisome and increasingly prevalent trend that is being fueled by easier access to substances. Perpetrated with the intention of making a victim more vulnerable to physical assault or other harm, drink spiking is a serious threat to individuals. Drink spiking is also not just limited to alcoholic drinks, but can target non-alcoholic drinks, such as water, soda, soft drinks, or juices and take place in any social occasion. While the prevalence of spiking is difficult to estimate reliably, academic surveys and official polls suggest that between 5% and 15% of people have reported experiencing spiking at some point [401, 144, 40]. These reports likely underestimate the situation as they also state that people can feel ashamed or stigmatize to seek medical attention or to discuss the matter [47]. Experiencing spiking often results in depression and can lead to physical danger or harm [385, 53]. This underscores the seriousness of drink spiking, highlighting how it poses a significant and a real threat to people. Detecting drink spiking is unfortunately difficult as the spiking typically happens in crowded social occasions where it is impossible to consistently observe the drink container and its contents. Common spiking substances also are not directly visible, making it difficult to realize when the drink has been tampered with. To safeguard individuals against spiking, there is thus a need for solutions that can identify whether drinks are spiked. At the same time, these methods need to be

unobtrusive to ensure they are acceptable in social contexts.

Limitations of state-of-the-art. Currently, limited support exists for safeguarding against drink spiking. While drug manufacturers are starting to take steps to reduce the possibility of spiking, e.g., by incorporating a colorant that reacts heavily with water [94], this is not universally applicable. Single-use chemical tests are another potential countermeasure [441]. These can be standalone or be integrated with bracelets, straws, or even drink containers [448, 103]. These primarily focus on specific substances, or class of substances, making them unsuitable as a universal solution. They also tend to be costly and depend on the liquid that is being tested. While there have been pervasive sensing solutions for analyzing liquids, these usually focus on identifying the type of liquid or extracting specific characteristics from it, such as sugar or alcohol content [460, 187, 189, 350, 98, 188, 289]. These are easier to detect as they rely on fixed properties and usually can rely on static measurement setups whereas spiking needs to be detected in uncontrolled social settings. Moreover, current solutions often rely on specialized setups, limiting their practicality.

Contributions. This paper contributes SpikEy as an accurate, robust, and inconspicuous solution for identifying drugs and extracting their characteristics in drinks. Rather than concentrating on specific drug types, SpikEy establishes *spiking profiles* that provide insights into the chemical characteristics of substances added to drinks. These profiles are categorized by drug and compound types, as well as the types of liquids involved, offering greater generality than existing approaches. SpikEy constructs these profiles from light reflectance measurements obtained using low-cost optical sensors. The principle of optical sensing for liquid analysis has been demonstrated in previous research [466, 308], but there are significant challenges to convert these signals into generic profiles that enable robust and accurate characterization of drinks. The key challenge is that light reflectance measurements are sensitive to various factors, including differing concentrations, motion, and ambient conditions. For example, the detection performance of existing optical solutions varies when the concentration of the drink is halved [466]. The measurements can also be contaminated by motion-induced noise, making robust estimation challenging. Indeed, as we demonstrate, motion-induced noise can decrease performance significantly unless addressed. SpikEy incorporates two key technical innovations to overcome these challenges. First, SpikEy represents spiking profiles using latent representations of optical signals. These are captured through a lightweight autoencoder structure specifically designed for devices with limited memory and processing capabilities. This approach allows for integration into compact wearables, such as the smart ring prototype used in our experiments. Second, SpikEy employs motion sensors (accelerometers and/or gyroscopes) to perform *motion calibration* on the optical signals. This calibration process reduces noise in the measurements and facilitates the separation of ambient light from the reflectance data obtained from the drink.

Through extensive experiments involving various drug profiles, concentrations,

and liquids, we demonstrate the effectiveness of SpikEy in detecting spiking. SpikEy achieves high detection accuracy of up to 86%, significantly outperforming wireless sensing and optical baselines ($\approx$ 10-20% lower detection performance). Results from an ablation study highlight that the autoencoder representation is crucial for maintaining robust and consistent performance, enabling accurate detection in previously unseen drinks and generalizing across different users ($\approx$ 30% improvement in performance). We also conducted a small-scale user study in an emulated nightclub environment, which validated that our motion compensation technique, combined with the autoencoder model, allows for accurate detection in practical scenarios where light measurements may be contaminated by motion-induced noise. The results from this scenario demonstrate over 20% improvements over manual visual inspection, significantly improving user safety. Taken together, SpikEy offers a novel approach for harnessing wearable technology to enhance personal safety and paves the way for utilizing wearables to support everyday interactions. SpikEy also represents a significant advancement in the fight against drink spiking, providing a practical and effective solution for safeguarding individuals in social settings.

3.2. Related work

Optical sensing has been widely used in many domains [60, 498, 193, 249, 474, 248, 78, 308, 464]. It can be utilized for heart rate estimate, hand-grip strength estimation. micro-plastic detection in food and drinks, produce quality estimation, human-activity tracking, user-mobile interaction enhancement, communication and localization. Recent studies have explored the repurposing of sensors from smart devices to identify various liquids and materials, including alcoholic beverages, sugar content, liquid density, surface tension, viscosity [473, 98, 187, 460, 188, 189, 381, 400, 380, 252, 250, 435, 63, 115, 290]. Table 14 shows the exisiting work of liquid identification with different sensing techniques. Wireless sensing has been explored mostly for liquid identification, e.g., common drinks in stores and alcoholic concentration. However, all these works need a specialized measurement setup and most of testbed deployments are static or partial, e.g., only transmitter antenna up and down by motor. Besides, they are mainly limited to static or stable liquid identification without movement. Thus, deploying these methods can be challenging and complex in everyday scenarios, especially in dynamic contexts. For example, drink spiking can occur at any time in public spaces where containers held by pedestrians in motion are not stationary, which makes the deployment of such solutions impractical for detection. Similarly, smartphones also mainly foucs on the stable liquid identification and have specific requirements in deployment, e.g., container types. Thus, although smartphones can be used for every scenarios, they are still limited to dynamic contexts in social life.

The detection of drink spiking has traditionally focused on the chemical composition of liquids. For instance, rapid capillary zone electrophoresis (CZE) has

Table 14: State-of-the-art of liquids with different sensing modalities. slight: vibro-motor is used to generate small vibrations for liquid. na: not applicable. The classification accuracy for all related liquid assessments is above 80%.

Ref	Device integration	Sensing	Liquid	Noise resilience			Deployment
				ambient light	liquid movement	everyday scenario	
[381]	specialized devices and deployment for wireless (transmitter TX and recevier RX)	RF-based	identification	na	no	no	partial (TX up/down)
[379]		RF-based	identification	na	no	no	partial (TX up/down)
[380]		Wi-Fi	identification	na	no	no	static
[115]		Wi-Fi	identification	na	no	no	static
[252]		mmWave	identification	na	no	no	static
[435]		mmWave	identification	na	no	no	partial (up/down)
[98]		ultra-wideband (UWB)	identification	na	no	no	static
[426]		RFID	identification	na	no	no	dynamic
[460]	specialized devices	acoustic	fraud detection	na	no	no	static
[188]	specialized devices	optical	liquor quality monitoring	yes	slight	no	static
[290]	specialized devices	optical	alcohol concentration	partial	no	no	static
[63]	smartphone	LiDAR	identification	partial	no	yes	static
[400]		acoustic	identification	na	no	yes	static
[189]		accelerometer	identification	na	slight	yes	static
[473]		camera	identification	na	slight	yes	static
[250]	earphone	acoustic	identification	na	no	yes	static
[466]	smart ring	optical	spiking detection	no	no	yes	static
Our work	smart ring	optical	spiking detection	yes	yes	yes	dynamic

been employed to identify benzodiazepines (benzos) in spiked beverages such as Coca-Cola, orange juice, beer,and Bacardi [438]. Spectroscopic techniques have also been utilized, with fluorescence spectroscopy being investigated to detect flunitrazepam (Rohypnol) in colorless alcoholic liquids like vodka and tequila [241]. Gas chromatography-mass spectrometry GC-MS methods are also used to detect the stability of benzodiazepines in spiked drinks for drug facilitated sexual assault cases [131]. Additionally, ultraviolet and electrochemical methods have been examined for the detection of benzodiazepines in liquids [366]. Although these techniques have proven effective in identifying spiked drinks, they often require specialized and expensive equipment (e.g., capillary electrophoresis instrument up to 150000 dollar) in laboratory settings, limiting their integration into wearable devices and large-scale deployment.

Recently, industrial manufacturers, such as DrinkSavvy, have developed specialized cups, glasses, and straws that change color instantly upon detecting a spiked drink. While this method offers continuous monitoring, it can be easily circumvented by using similar-looking utensils and is limited to detecting only specific drugs. Drug test kits (test papers) are also widely used for detecting drink spiking due to their lightweight, user-friendly, and cost-effective nature. However, many are still designed to detect only specific drugs and can be influenced by certain beverages, such as red wine or dark cola. Additionally, subtle or unclear color changes along with hard-to-interpret results may make these products challenging to use effectively in real-world settings such as crowded or low-light environments.

Besides, these approaches could be also social awkward to some extent. Unlike these approaches, we have developed a novel sensing method and a smart ring wearable device designed to identify drink spiking. Our method leverages the advances in light reflectivity and wearable technology to provide a more accessible and scalable solution for drink spiking detection.

Closest to our work, Hedgehog [466], employs a smart ring for drink spiking detection but has only been tested in controlled environments with steady drinks. Although it also uses optical reflectance, it struggles with motion and ambient light interference, resulting in low accuracy in uncontrolled settings. SpikEy builds on this sensing modality but addresses these challenges for dynamic and real-world conditions, presenting the first practical wearable system for accurate drink spiking detection. Moreover, Hedgehog relies solely on hand-crafted features (e.g., averaging light values), which may overlook complex temporal or spectral patterns. In contrast, SpikEy extracts spiking profiles using autoencoders that capture the chemical characteristics of added substances and can generalize across different drinks, drugs, and contexts, offering greater robustness and flexibility.

3.3. SpikEy design

SpikEy has been designed to deliver an accurate, robust, and inconspicuous solution for the analysis and identification of drugs in various drinks. The primary technical challenges arise from the need to maintain a consistent and coherent signal representation amidst the myriad of variations encountered during measurements. These variations can originate from factors such as the ambient environment, the specific type of drink, the container used, the drugs involved, and the differing behaviors of users. The following subsections outline the overall design of SpikEy and emphasize the key technical contributions that enable it to effectively tackle these challenges. SpikEy incorporates advanced signal processing techniques, adaptive algorithms, and machine learning models that are specifically tuned to account for the diverse conditions under which the system operates. Additionally, motion compensation techniques are used to mitigate the effects of motion-induced noise. By leveraging these innovations, SpikEy ensures reliable performance and high accuracy in spiking detection.

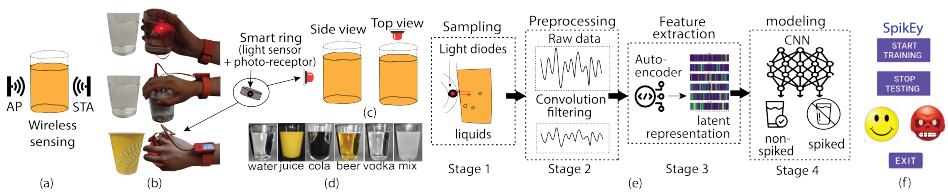


Figure 26: a) Wireless baseline, b)-f) SpikEy design: (b) Prototype, (c) Sensor positions, (d) Drinks, (e) Pipeline, (f)Application

SpikEy leverages light reflectance measurements of drinks to estimate whether a drink has been spiked. This process is executed through a four-stage pipeline,

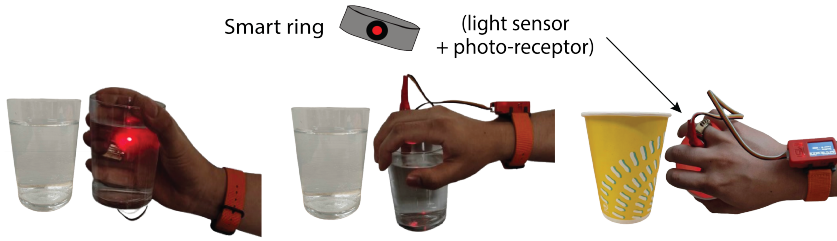


Figure 27: SpikEy prototype

illustrated in Figure 26(e). The first stage, *sampling*, involves capturing the light reflected from drinks using an optical sensing device. The current SpikEy prototype integrates a red-laser light emitter and a photo-receptor within a smart ring. Figure 27 demonstrate the functionality of SpikEy when integrated into a smart ring operates, allowing inconspicuous analysis of drinks. In the second stage, *pre-processing*, noise is filtered from the collected measurements using convolution filtering. Concurrently, accelerometer signals are employed to compensate for noise introduced by hand movements and fluctuations in ambient light conditions, introduced by wearing the ring in dynamic real-world conditions (Figure 26(b)). The third stage, *feature extraction*, utilizes deep learning autoencoders to derive latent representations from the pre-processed measurements. This process results in a lower-dimensional space that encapsulates the distinguishing features of spiked and uncontaminated drinks, and is key to achieving robust and efficient recognition performance. Finally, the *modeling* stage employs convolutional neural networks (CNNs) to assess the spiked status of drinks using the latent features extracted by the autoencoders as inputs. This multi-stage approach has been designed to ensure accurate and robust detection of potential drink tampering, and to help enhance user safety and confidence.

3.3.1. Latent modeling of optical signals

SpikEy centers on the robust and accurate extraction of features from reflected light measurements, aiming to reliably detect drink spiking. This task presents significant challenges due to the inherent variability in fluid dynamics of different types of drinks and the potential presence of various substances, including medications. To navigate these complexities, we employ a systematic methodology that integrates autoencoders for latent feature extraction and convolutional neural networks (CNNs) for classification.

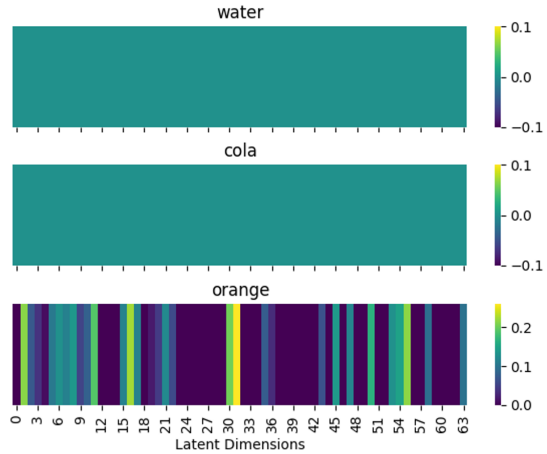
Feature extraction with autoencoders: To effectively manage the diverse characteristics of drinks and drugs, SpikEy utilizes autoencoders to learn a compressed representations of the optical measurements. SpikEy's autoencoder features three dense layers in both encoder and decoder, with a lightweight structure that includes an encoding dimension of 16 units to capture essential features from the input data while minimizing parameter count and complexity for efficient processing on resource-constrained devices. This representation captures essential features

in a latent space and many sensor applications have shown autoenconders to be powerful at processing sensor measurements [143, 488]. This capability is highly relevant for detecting drink spiking as any variations in light characteristics show up as anomalies in the latent representation. We extract the latent space from the preprocessed data, specifically targeting the time window where drink spiking is suspected, referred to as the Region of Interest (ROI). The latent space corresponds to the feature space representing significant deviations in the variance. Figure 28 shows profiles for six different drinks without (left) and with spiking (middle), as well as the difference in representations (right) to highlight how changes in the drink composition result in large variations in the latent profiles, helping to distinguish drinks that are spiked from uncontaminated ones.

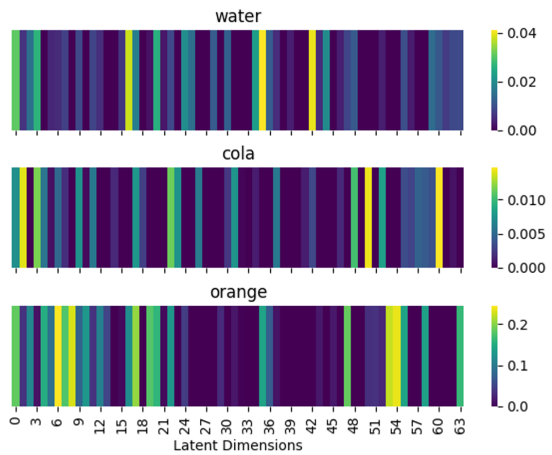
After preprocessing, our system extracts feature vectors from the ROI using the encoder part of the autoencoder. This process reduces the dimensionality of the data while capturing essential features. Min-max normalization is applied to ensure that these values are comparable across different drinks and drugs on a consistent scale. We employ one-second sliding windows with a 50% overlap to measure the variance of consecutive measurements. We also evaluate the robustness of our approach across different window sizes, incrementing from 1 to 5 seconds.

Classification with convolutional neural networks: Once the latent representations are obtained, we leverage these feature vectors to train a Convolutional Neural Network (CNN) for both binary (spike vs. non-spike) and multi-class (different drug types) classification tasks. CNNs are particularly well-suited for this task, as they can effectively learn spatial hierarchies and patterns from the latent features. To ensure the model is suitable for resource constrained wearables such as smart rings, we use a shallow model with a small number of filters. Specifically, the model we use comprises an input layer, a convolutional layer with 64 filters, a kernel size of 3, and a ReLU activation function to capture local patterns in the data, a max pooling layer to reduce dimensionality while retaining important features, and a fully connected layer that produces the final output. The output layer uses a sigmoid activation function for binary classification or a softmax activation function for multi-class classification. As the loss functions, we utilize binary cross-entropy for binary classification and categorical cross-entropy for multi-class classification.

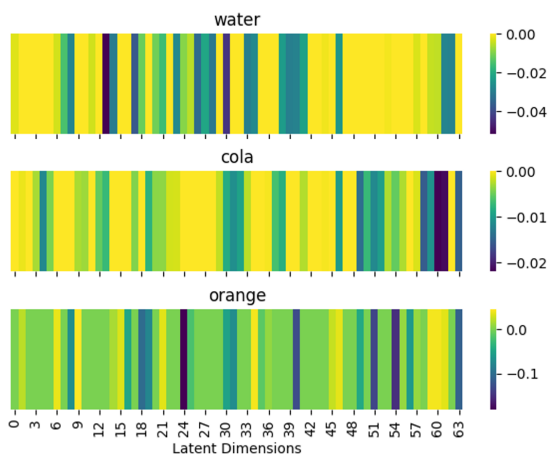
Model training and validation is performed using leave-one-drink-out cross-validation. Accordingly, the models are trained and validated on all but one drink, with the left-out drink serving as the test set. This ensures the model is robust and generalizes well to unseen data. The folds are constructed using stratification, which helps mitigate biases in the training and validation process. Model evaluation employs standard classification metrics, such as precision and recall, with a particular focus on true positive values to demonstrate the model's ability to accurately detect spiking.



(a) Side-NS

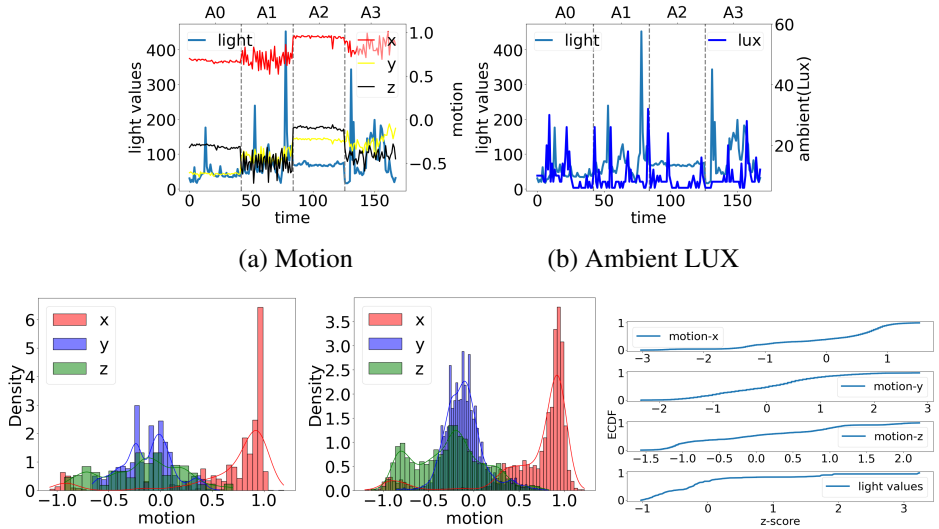


(b) Side-S



(c) Side-D

Figure 28: Profiles of different drinks identified by SpikEy: no spiked (NS), spiked (S), and their differences (D), with sensor positioned on the side.



(a) Motion (b) Ambient LUX

(c) A0: bartender (d) A1: dance area (e) ECDF

Figure 29: a)-b) Factors affected the light values, Hand motion, A0: bartender area, A1: dance area, A2: relaxing area, A3: cross the 3 areas. c)-d) Distribution of each motion axis. e) ECDF.

3.3.2. Motion and ambient light compensation

In everyday settings, people's hand movements and varying environments contaminate optical signals with motion-induced noise. Figure 29(a-b) illustrates these variations using data from a simulated nightclub (see Subsection 3.4.2). To address this noise, the second technical contribution of SpikEy is a calibration pipeline that integrates accelerometers (and potentially other motion sensors) with ambient light sensors to compensate for light reflectance measurements. We now describe this calibration process (see Figure 30).

Motion distribution: Before calibration, we analyze motion behavior in various areas to understand its influence on light reflectivity. As shown in Figure 29(a), light reflectivity is significantly affected by users' movements. For instance, in social scenes, individuals sway more in the dance area than in the relaxing area, leading to greater fluctuations in measured light values. Given the variability in user behavior across different environments, it is crucial to examine motion distributions specific to each area. Figures 29(c-d) depict the motion distributions for two areas, A0 (standing) and A1 (dancing), revealing significant differences along the x and y axes. To account for these variations, we calibrate light reflectance measurements based on area-specific motion characteristics, improving the reliability of SpikEy in detecting spiked drinks. We automatically detect different areas by identifying periods of consistent motion, reinitializing the motion profile once the variance of accelerometer values stabilizes.

Motion calibration: To calibrate light values in each area, we analyze the distribu-

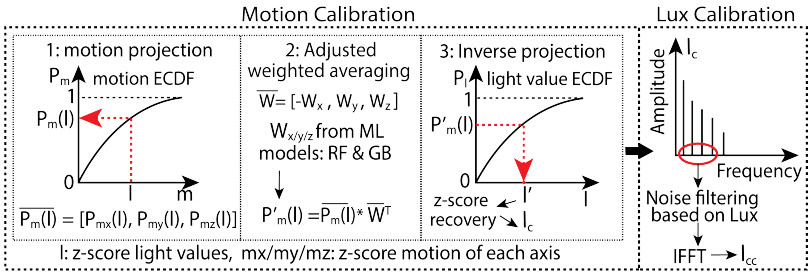


Figure 30: Calibration Pipeline

tion of values specific to that environment using the empirical cumulative distribution function (ECDF), which effectively represents accelerometer values [161]. The calibration process involves three key steps.

First, we normalize each motion axis using z-score normalization, as shown in Figure 29(e). This standardization facilitates accurate comparisons across axes. Next, we derive the ECDF for each motion axis, yielding cumulative probability distributions P_{mx}, P_{my}, P_{mz} for the x, y, and z axes, respectively. We project the light values l onto each axis's ECDF to evaluate their individual impact on light reflectivity, resulting in a cumulative probability distribution vector $\overline{P_m(l)} = [P_{mx}(l), P_{my}(l), P_{mz}(l)]$, quantifying each motion axis's influence on light value distributions.

In the second step, we combine the effects of each motion axis using an ensemble classifier that integrates Random Forest (RF) and Gradient Boosting (GB) models. These classifiers capture the relationships between motion axes and light values, allowing us to obtain average weights W_x, W_y, W_z. It is important to note that a simple weighted average is inadequate for calibrating light value distributions due to variations in sensor orientation. Estimating the sensor's orientation and realigning the motion axes can introduce inaccuracies; thus, we focus on a smart ring that captures measurements while the user grips the drink container, constraining possible motion patterns.

As shown in Figure 29(e), the ECDFs of light values and the y and z motion axes exhibit a similar concave-down pattern, while the x-axis diverges. When light values are input into the x-axis ECDF, they generate larger cumulative probabilities, introducing significant noise when projected back using the inverse ECDF. This explains the numerous outliers in the original data, see Subsection 3.6. To mitigate the impact of x-axis motion, we adjust the weighted average using a subtraction method, resulting in a calibrated cumulative probability representation $P'_m(l)$ for the light values. Finally, we input the calibrated probability $P'_m(l)$ into the inverse ECDF of the original light values to obtain the calibrated light values l'. By transforming l' back to the original scale using the mean and standard deviation of the original light values, we recover the calibrated value l_c.

Ambient light calibration: In addition to motion, we observe similar situations that ambient light introduces low-frequency noise with high amplitude, distorting

readings [188]. To mitigate these effects, we utilize frequency-domain techniques. We first extract the 100 dominant frequency components based on ambient light amplitude. The choice of dominant frequencies depends on sample size; while more components may enhance filtering, they also risk overfitting.

To remove specific frequency components from the light-reflectivity signal, we employ a digital notch filter that targets and eliminates identified frequencies while preserving the remaining signal's integrity. We also eliminate any phase distortion that may arise during filtering to ensure accurate timing of the signal. After filtering, we perform an inverse Fast Fourier Transform on the modified light signal, converting it back into the time domain for a cleaner representation of the light values l_{cc}. Then latent representations of these calibrated light values are extracted in the sensing pipeline for drink spiking detection.

3.4. Experimental setup

SpikEy is designed for real-world settings, but we also test if it is compatible in stationary settings, as most state-of-the-arts of liquid sensing are in static deployments, see Subsection 3.2. Thus, we conducted two studies to validate SpikEy: (1) a 12-hour controlled static experiment to monitor spiking patterns with different drinks and drugs over time, and (2) a dynamic experiment in an emulated nightlife environment to assess SpikEy in practical and realistic settings.

3.4.1. Controlled static experiment

Design: Our first experiment estimates drink spiking across three experimental variables: (i) drink type, (ii) drug type, and (iii) sensor position. We also conducted user experiments to assess the generality of our method and enhance preprocessing through motion and light sensors for signal calibration (see Subsection 3.3.2). We selected six common acidic drinks (pH < 7) for testing (Figure 31): a) *water* (pH 6.5), b) *100% orange juice* (pH 3.5), c) *dark cola* (pH 2.5), d) *light beer* (pH 3.5), e) *vodka* (pH 4), and f) *mixed long drink* (pH 3.5). Selection considered factors affecting spiking detection: (1) drug solubility influenced by solvent properties (e.g., pH, alcohol content) [37, 213], (2) dark or dense drinks obscure light signals, and (3) bubbly or mixed drinks introduce variability similar to cocktails. All these drinks were purchased in the local markets except for tap water. We also found that most drinks are acidic on markets. The main ingredients of mixed drink are gin, grapefruit soda and carbonated water.

We selected three over-the-counter drugs that represent the three most important categories of chemical reactions within the Biopharmaceutics Classification System (BCS) [293, 211, 100]: (a) aspirin powder (500 mg, Class I), (b) ibuprofen powder (500 mg, Class II), and (c) cetirizine tablet (10 mg, Class III). Class IV drugs were intentionally excluded from our study due to their low solubility and high detectability. Indeed, drugs within this class are typically formulated for topical use as ointments or lotions, rendering them unlikely candidates for drink spiking.

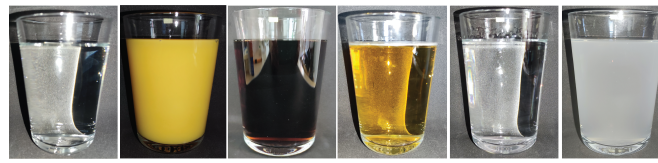


Figure 31: Common drinks in the experiment

Sensing was performed at two distinct positions, as illustrated in Figure 26(c): (1) side—located midway on the container's surface, and (2) top—positioned approximately 1 cm above the liquid. Side sampling facilitates natural data collection during regular use, while top sampling enhances spike detection, particularly in opaque containers. This dual-position sensing approach ensures comprehensive coverage and improves the accuracy of drug identification in various drinking scenarios.

Drug solubility is a critical factor in detecting drink spiking, with adequate solubility defined as at least 100 mg/L [392]. In our study, we selected aspirin, ibuprofen, and cetirizine to simulate the behavior of spiking drugs based on their physicochemical properties. Although the selected drugs do not possess psychoactive effects, they serve as effective models for understanding dissolution rates and absorption profiles pertinent to restricted substances. These drugs encompass all possible chemical interactions. Substances specifically designed for spiking may exhibit better solubility, but otherwise they have the same reactions and changes in liquid composition. This choice is crucial, as the Biopharmaceutics Classification System (BCS) categorizes drugs based on their chemical reactions and solubility characteristics, allowing us to draw meaningful comparisons. By encompassing all BCS classes—except Class IV, which is easily identifiable due to its low solubility—our research provides a comprehensive understanding of various drug types and their chemical behaviors in solution. Furthermore, the drugs we employed are safe and legal, which ensures ethical experimentation while also ensuring that our findings can be applied in real-world scenarios without compromising safety. This approach allows us to gather valuable insights into the detection of spiking drugs while adhering to ethical standards.

Procedure: We used 225 mL of liquid in a transparent glass, representing a typical serving size. Drinks were brought to room temperature (23 °C), and cetirizine tablets were ground into powder to enhance solubility. Each drink was spiked by adding drug powder directly without stirring, with a 12-hour measurement period recorded for each condition. Drinks were discarded after each trial to prevent accidental ingestion. Our experiments followed a 6-3-2 design: testing six drink types and three drugs with the sensor at both positions, plus a non-spiked baseline for comparison.

Testbed: We implemented a controlled testbed to maintain precise sensor position-

ing. The setup includes a black background with position markers to minimize reflections and ensure consistent container placement. Experiments were conducted in darkness (zero LUX), with drinks in a 2 mm transparent glass container. A 650 nm red laser diode (5 mW) provides the light source, and a GM5539 photoresistor captures reflections. The sensing unit, connected to a wireless M5StickC PLUS ESP32 microcontroller, samples at 5 Hz and uploads data in real-time.

3.4.2. Dynamic experiment

Apparatus: We developed a practical prototype using the same devices and sensors as in the main experiments, incorporating a red laser emitter and a photo-receptor embedded in a smart ring (see Figure 27). The accelerometer in the microcontroller tracks hand motion, collecting light and accelerometer data (X, Y, Z axes). An app for smartphones has also been developed, which alerts users to potential spiking through vibration and sound notifications (Figure 26(f)) - app interface showing yellow face changes to red face). To simulate nightclub lighting, we used two small disco balls with RGB color mixing and variable emission angles. Ambient light intensity was measured using a LUX app, capturing data across both low and high intensity levels.

Study design: We conducted a user study with a $2 \times 2 \times 2$ factorial design involving two new cup types (transparent glass, $TCUP$; and non-transparent paper, $NCUP$), two new drink types (light beer, *Lbeer*; and dark beer, *Dbeer*), and two drug classes (Class I: aspirin, Class III: cetirizine) as previous expriements. For generalization, we used four cups of each type for each drink: two non-spiked ($TCUP$-1, $TCUP$-2) and two spiked ($TCUP$-3, $TCUP$-4), which are shuffled for participant evaluation.

Participants: We recruited 26 participants (13 males, 13 females; age 27.9 ± 4.4) from the university and nearby areas. Participants were blinded to the drink and drug contents. Due to study duration, half evaluated drinks spiked with cetirizine and half with aspirin, resulting in 16 drinks per participant. Each participant signed an informed consent form in compliance with local IRB regulations and was not permitted to taste the drink during the experiment.

Procedure: We simulated a nightclub environment with rotating disco balls and mixed lighting. Participants could play their favorite music during the experiment. The study consisted of two parts, lasting approximately one hour.

Part-1: User Perception: We first conducted a blind experiment to assess human detection of drink spiking. Participants examined all 16 cups in random order and indicated whether each drink was spiked without researcher interferences. The answer is simple with only "yes" and "no". They then completed a brief survey on their perceptions of drink spiking, e.g., *"What quality made you suspect your drink was spiked?"*

Part-2: Smart Ring Evaluation: Participants wore the smart ring on their dominant hand and simulated four nightclub scenarios: bartender area ($A0$) - moderate motion activities, dancing area ($A1$) - high intensive motion activities,

relaxing area ($A2$) - low motion activities, and moving across areas ($A3$). A separate smartphone with SpikEy was given to participants (located in their pocket). All 16 drinks started in the bartender area, where participants picked a random drink and followed typical nightclub flow. They tested drink spiking with 10-second measurements in each area, providing sufficient confidence (97.5%) for drink characterization [466]. Participants held paper cups only at the top (sensor top view) and glass cups both at the side and top. After the experiment, participants rated their experience on a five-point Likert scale (5: high, 1: not at all) for the question, *"Did this experiment feel like a similar nightclub experience?"*. Overall, most participants (80.8%) reported that the experiment provided a similar experience to that of nightclubs or bars.

3.4.3. Baselines

SpikEy has been designed to facilitate accurate, robust, and inconspicuous analysis of drink spiking in everyday environments, in contrast to existing methods that primarily focus on analyzing liquid contents in controlled settings. The closest alternatives for dynamic settings include drink bracelets, which typically target specific drugs, and visual assessments by individuals. In contrast, a wider array of options exists for performance comparison in controlled environments. Our experiments encompass both controlled static measurements and dynamic real-world assessments, allowing us to compare SpikEy against three established baseline methods that cover both scenarios. Specifically, we consider wireless sensing and optical sensing as baselines for the controlled setting, while visual inspection by humans serves as a baseline for the dynamic setting. These comparisons are detailed below.

Wireless sensing. Wireless sensing is widely employed for liquid analysis; however, it is often constrained to specialized instrumented containers and static measurement setups due to the need for precise control over the positioning of transmitters and receivers [98, 350]. This limitation makes wireless sensing less suitable for dynamic scenarios, which are the primary focus of our research. To provide insights into how our system compares with state-of-the-art liquid sensing techniques, we evaluate SpikEy against a wireless sensing baseline within our controlled static setup. It is important to emphasize that the main objective of our work is to facilitate continuous monitoring in dynamic real-world environments that can adapt to user context. Given the limitations of wireless sensing, it is impractical and infeasible to consider it as a baseline for our dynamic experiments. This comparison underscores one of the key benefits of SpikEy: its adaptability and capability to operate effectively in changing real-world environments.

We analyze wireless sensing for drink spiking identification using Channel State Information (CSI) from WiFi signals. The signal characteristics, such as amplitude and phase, are influenced by the drink's composition, allowing their use as inputs for classification. We employed two ESP32 microcontrollers: an active

access point (AP) as the transmitter and an active station (STA) as the receiver, operating at a 10 Hz sampling rate with default settings (2.4 GHz, channel 6) [175]. The AP and STA were positioned 10 cm apart, with the drink placed between them, potentially blocking the line-of-sight (LOS) of the WiFi signals. We evaluated the same set of drinks, spiking them with the same drugs as described in Subsection 3.4.1. For each drink, we collected 30-minute data (25-min training and 5-min validation) under consistent conditions.

We first eliminate non-useful CSI data, then denoise it using a moving average across each subcarrier, followed by principal component analysis (PCA) for dimensionality reduction. This method aligns with previous work using the ESP32 microcontroller for physical rehabilitation tracking [176]. The data is formatted with 100 samples per model input, incorporating a 50% overlap for augmentation.

We implemented a convolutional neural network for spiking classification, starting with an input layer followed by four 1D convolutional layers (with 128, 64, 32, and 16 filters) using batch normalization (L2) and ReLU activation. Dropout (0.2) is applied to all layers except the last to prevent overfitting. A global average pooling layer condenses features, and a dense layer with softmax activation outputs class probabilities. Training utilized a batch size of 32 and 500 epochs, with early stopping if validation accuracy stagnated for 10 epochs.

Optical sensing. This baseline is implemented using Hedgehog [466], which also employs optical sensing and machine learning to assess whether a drink has been spiked. SpikEy integrates an advanced processing pipeline and has been designed for dynamic real-world contexts, whereas Hedgehog (i) relies on controlled, static experimental conditions that do not account for motion-induced noise caused by user movements—conditions that differ significantly from the dynamic, real-world scenarios where drink spiking detection is crucial, and (ii) uses hand-crafted features, which can be suboptimal as they may overlook complex patterns in time-series data. To facilitate a fair comparison, we consider the first 30 minutes of our controlled data and extract the average light value over the same duration (1 minute) as Hedgehog. Leave-one-drink-out cross-validation is employed with simple classifier models: Random Forest (RF) and Gradient Boosting (GB), which were also utilized by Hedgehog.

Visual inspection. This baseline engages participants' visual and olfactory senses by asking them to observe and/or smell drinks to determine whether they have been spiked. The goal is to evaluate the effectiveness of human sensory perception in detecting drink spiking, serving as a baseline for comparison with technological approaches. The study procedure is described in Subsection 3.4.2 (procedure part-1) and this baseline is only considered for our measurements collected from a dynamic setting.

Table 15: Spiking observations of main appearance changes.

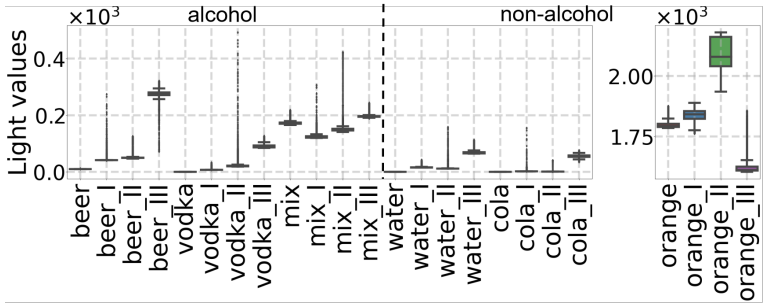
Drinks Solubility	Alcohol (%)	Aspirin(I) high	Cetirizine(III) high	Ibuprofen (III) low
beer	**4.5%**	no	foggy	surface particles
vodka	**40%**	bottom particles	bottom particles	surface+bottom particles
mix	**5.5%**	no	no	submerged+surface particles
water	**0**	no	foggy	surface particles
dark cola	**0**	no	no	surface particles
orange juice	**0**	submerged particles	no	submerged+surface particles

3.5. Results

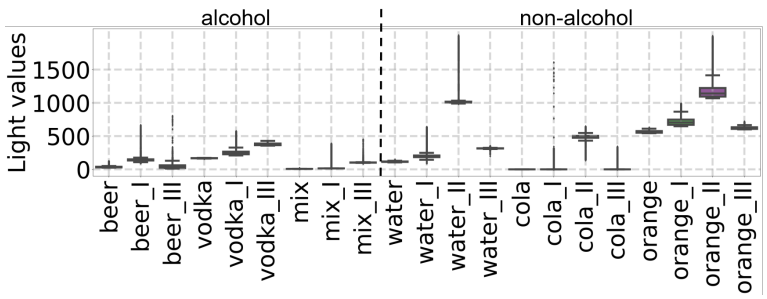
3.5.1. Light values as proxy for drink spiking

Drink characterization: We begin by demonstrating that individual drinks exhibit unique light reflectance fingerprints, allowing us to characterize the differences among drinks based on their drug content. Figure 32(a) displays the results of light values obtained from the side view. The profiles of all normal drinks remain stable, including the bubbles in cola and beer, indicating the reliability of their physical and chemical properties. Minor variations in 100% orange juice and mixed drinks are attributed to non-homogeneity, such as uneven distribution of pulp in the juice, which causes fluctuations in light detection. Prior to statistical analysis, we assessed the normality of the data using the Shapiro-Wilk test, where the null hypothesis (H_0) states that the data follows a normal distribution, while the alternative hypothesis (H_1) states that the data are not drawn from a normal distribution. It reveals that most drinks did not follow a normal distribution ($p < 0.05$). Subsequently, the non-parametric Friedman test confirmed statistically significant differences in light values across all drinks ($\chi^2 = 7.6 \times 10^6, p < 0.05$). Here, the null hypothesis (H_0) states that all related groups have the same median, while the alternative hypothesis (H_1) states that at least one group's median is different. This indicates that SpikEy can effectively distinguish between different drinks, including those that are spiked. Pairwise post-hoc comparisons (Wilcoxon-Bonferroni) further validated that the differences in light values are statistically significant for all pairs ($p < 0.05$), with the exception of water and cola, which showed similar values near zero and minimal light reflectance. Here, the null hypothesis (H_0) states that the median difference between paired observations is zero, while the alternative hypothesis (H_1) states that the median difference is not zero. While we can observe differences in drink contents, accurately identifying the specific liquid type remains challenging.

Drug difference: Table 15 summarizes the visual changes observed after spiking drinks with three different drugs. It is important to note that these observations were made under controlled laboratory conditions and may not fully represent real-world scenarios of spiking detection in complex social contexts – which is evaluated separately in Subsection 3.6. Drinks spiked with aspirin typically



(a) sensor side view



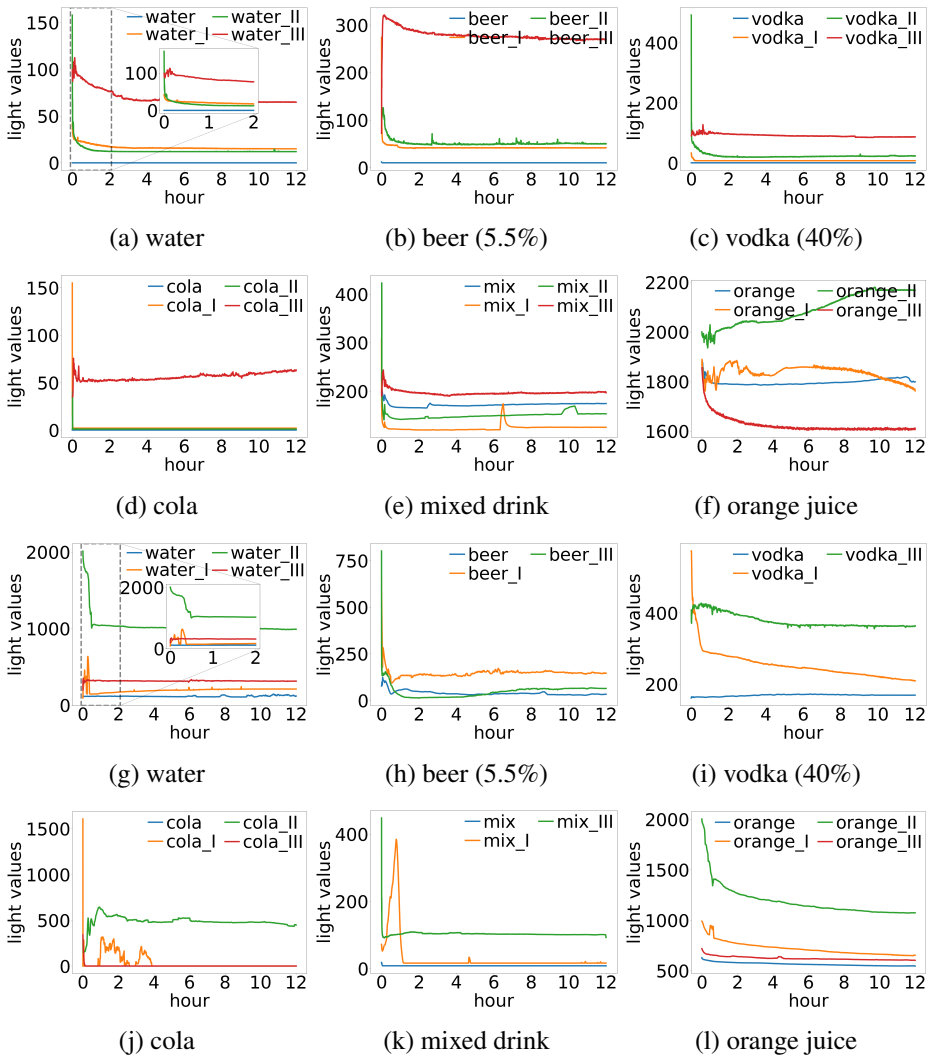
(b) sensor top view

Figure 32: Light values of 12 hours monitoring. I-aspirin, II-ibuprofen, III-cetirizine.

retain their original appearance (e.g., water, beer, and cola), resulting in minimal differences, as illustrated in Figure 32(a). High-solubility cetirizine and aspirin share similarities in appearance when no obvious changes occur. However, spiking with cetirizine can cause a foggy appearance in certain drinks (e.g., beer), enhancing its distinguishability from normal drinks (see Figure 33(a-f)). Conversely, low-solubility ibuprofen tends to float as visible particles on the liquid surface, leading to subtle differences from normal drinks, except for juice and mixed drinks where many particles become submerged. Generally, drugs from Class II are easier to detect visually, while Class I and Class III drugs are more challenging. Vodka is an exception, as many particles settle at the bottom, resulting in minimal visual differences after spiking. This suggests that higher drug concentrations do not necessarily correlate with increased solubility.

Spiking pattern over time: Continuous monitoring of light values allows us to capture changes in interactions over time, thereby improving the reliability of spiking detection. Figure 33(a-f) presents light values over time for various drinks from the side view. We observe a sharp increase in light values immediately after spiking, attributed to intense interactions between the drug compounds and the liquid. Following this initial spike, the light values gradually stabilize. The non-stable state at the beginning poses the greatest challenge for SpikEy in detecting drink spiking, characterized by random patterns and large fluctuations. In contrast, the stable state presents a clear and unique light profile, facilitating easier detection, despite minor fluctuations. We employed a rolling window approach with a fixed size to identify approximate change points in the states, finding that light reflectivity generally stabilizes for most spiked drinks within two hours. An exception is dense orange juice, which requires more time to stabilize due to its high viscosity and suspended solids that impede drug particle movement and dissolution. Our model primarily targets the first 30 minutes to address the challenges of spiking detection, as this period exhibits the most significant fluctuations.

Side view vs. top view: Figure 32(b) illustrates the results from the top view. While the baselines remain reliable, slight variations are evident compared to the side views, such as the presence of bubbles in beer. This discrepancy may arise from the direct interaction between the sensing beam and the liquid surface. We excluded ibuprofen experiments for some drinks due to similar phenomena and easy detection for both sensing and human observation, retaining only necessary drinks for generalization. Water serves as a prime example where ibuprofen particles float on the surface, leading to light values primarily reflecting the powder itself rather than the drink. Consequently, variations in light values stem from intrinsic differences between the drugs and liquids. Friedman tests reaffirm that differences in light values are statistically significant for all drinks ($\chi^2 = 6.3 \times 10^6, p < 0.05$). Pairwise post-hoc comparisons (Wilcoxon-Bonferroni) confirmed significant differences across all pairs ($p < 0.05$), enhancing drink characterization. Figure 33(g-l) reveals a similar spiking pattern as observed in the side view, with



(a) water (b) beer (5.5%) (c) vodka (40%)

(d) cola (e) mixed drink (f) orange juice

(g) water (h) beer (5.5%) (i) vodka (40%)

(j) cola (k) mixed drink (l) orange juice

Figure 33: The changes in light values with time, (a-f) side view, (g-l) top view.

light values stabilizing within two hours, except for aspirin in cola and vodka, where dynamic floating particles can lead to random values.

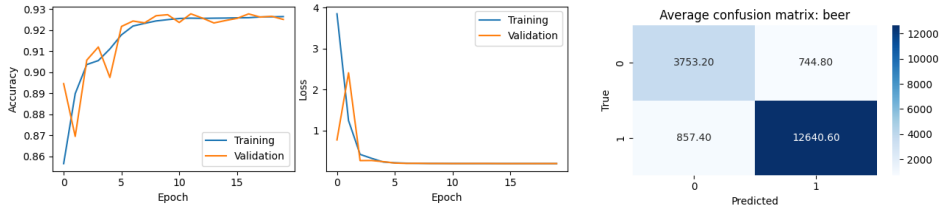
3.5.2. Overall performance

Next, we demonstrate the performance of SpikEy in predicting drink spiking. We focus on the first 30 minutes of the 12-hour monitoring period for modeling, as this timeframe exhibits the most drastic variations in light values. Latent representations were utilized to train the CNN, employing a sliding window size of 1 second. We evaluated performance using various metrics (accuracy, precision, recall, F1-score).

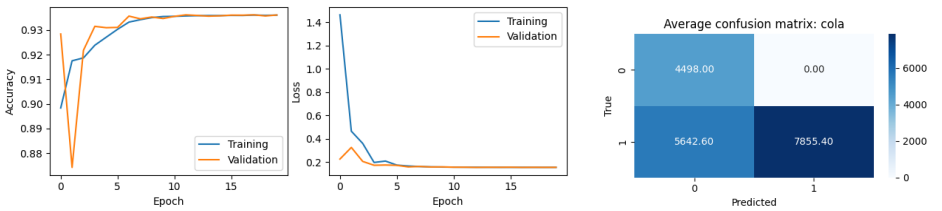
Table 16: Detection of drink spiking (no-spiked vs. spiked) on the samples of the drink that was left out from training the CNN model. TP – True Positive, FN – False Negative, FP – False Positive, TN – True Negative.

Position	Drink	Mean TP	Mean FN	Mean FP	Mean TN	Accuracy	Precision	Recall	F1-score
Side sensor	Beer	12592.20	905.80	576.00	3922.00	**91.77%**	**95.63%**	93.29%	**94.44%**
	Vodka	12347.00	1151.00	0.00	4498.00	**93.60%**	**100.00%**	**91.47%**	**95.54%**
	Mix	12056.20	1441.80	1568.00	2930.00	83.28%	88.52%	**89.32%**	88.91%
	Water	11788.00	1710.00	0.00	4498.00	90.50%	**100.00%**	87.33%	93.24%
	Cola	8167.40	5330.60	0.00	4498.00	**70.38%**	**100.00%**	**60.51%**	**75.33%**
	Orange	13393.80	104.20	2204.00	2294.00	87.17%	**85.87%**	**99.23%**	**92.07%**
Top sensor	Beer	8780.60	217.40	4303.20	194.80	66.5%	67.11%	**97.58%**	79.53%
	Vodka	6606.00	2392.00	0.00	4498.00	82.28%	**100%**	73.42%	84.54%
	Mix	7461.40	1536.60	0.00	4498.00	88.61%	**100%**	82.92%	90.66%
	Water	8464.20	533.80	0.00	4498.00	96.04%	**100%**	**94.07%**	96.94%
	Cola	3193.00	5805.00	0.00	4498.00	56.99%	**100%**	35.49%	52.38%
	Orange	8883.00	115.00	3436.20	1061.80	73.69%	72.11%	98.72%	83.34%

Performance: Table 16 presents the performance metrics for both views. The side view achieved an average accuracy of 86.11% (other metrics averaging: precision=95%, recall= 86.86%, F1-score=89.92%) in detecting spiked drinks, indicating that SpikEy can effectively identify unseen spiked drinks. This means the confidence for flagging a case as positive is high (high precision), and very few positive cases of spiked drinks are missed (reasonably high recall). However, detecting spiked cola proved to be the most challenging, with a recall of 60.51%, meaning that only approximately two out of three spiked drugs were correctly identified. This difficulty arises because ibuprofen particles typically do not dissolve significantly in cola, resulting in minimal differences from normal cola (see Figure 33(d)). Conversely, the top view shows a lower recall of 35.5% for spiked cola, indicating that only ibuprofen was detectable, while the other two drugs were not (see Figure 33(j)). The top view generally performed well for most drinks, with an average accuracy of 77.44% (precision=89.87%, recall= 80.83%, F1-score=81.84%). However, it struggled particularly with beer and cola, where overlapping light values between normal and cetirizine resulted in numerous false positives, as shown in Figure 33(h). This overlap also occurred with orange juice, where light values for most non-spiked drinks remained stable, while minor variations persisted in orange juice within the trained model. Figure 34 illustrates high accuracy and low loss in both the training and validation datasets for two drinks from the side view, indicating effective training (fitting) and generalization

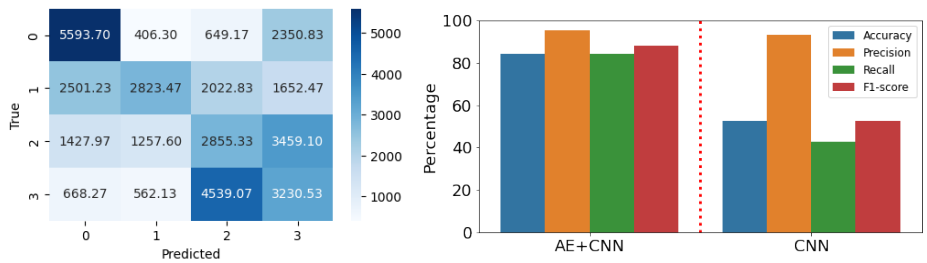


(a) Leave out: beer



(b) Leave out: cola

Figure 34: Train performance and test confusion matrices for side view, 0: non-spiking, 1-spiking.



(a) Multi-class

(b) Calibrated values

Figure 35: a) Confusion matrix of multi-class classification (no-spike, drug I, drug II, drug III) using leave- one-drink-out approach, b) Spiking detection without the latent representation features. AE-Autoencoders.

to unseen data.

We applied the same model for drug classification, but the performance was less satisfactory, with many misclassifications among the drugs, as an example shown in Figure 35(a). This is likely due to the model encountering unseen drinks, leading to unpredicted interactions during spiking. While our model accurately captures the distinction between normal drinks (stable patterns) and spiked drinks (random patterns), it struggles with precise drug identification, suggesting the need for a more generalized model in future research.

Autoencoder ablation study: To evaluate the effectiveness of latent representation features, we repeated experiments without using autoencoders and compared the results. Figure 35(b) shows a significant decrease in recall when only the CNN model was employed, with latent representations improving accuracy by

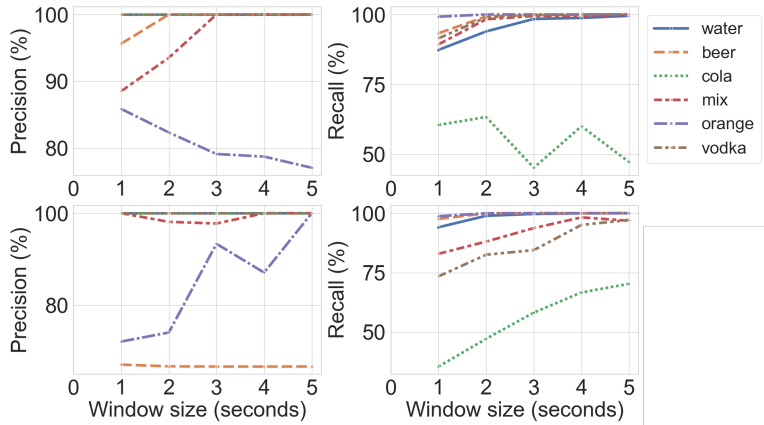


Figure 36: Effects of window sizes on drink spiking detection. above row: side sensor, bottom row: top sensor.

approximately 30%. This demonstrates that the integration of autoencoders and CNNs are key to achieving accurate detection performance. Our model improved accuracy by at lease 10% to 20% compared to baseline Hedgehog [466], see next subsection.

Window size effect: We also explored the impact of varying the window size from 1 to 5 seconds, as shown in Figure 36. Overall, increasing the window size enhances drink spiking detection, allowing for the capture of more latent details. Notably, the performance for cola and orange juice varied across both views, suggesting that sensing from multiple perspectives can improve SpikEy's performance.

3.5.3. Comparison with baselines

Wireless sensing: In the context of wireless sensing, the accuracy in classifying the normal drinks without spiking was high at 83%. This indicates that wireless sensing performs well for normal drink classification. However, when evaluating spiking performance using binary classification (non-spiked: 0, spiked: 1), accuracy dropped significantly to 54%. This suggests that wireless sensing is better suited for liquid detection but it struggles with detecting drink spiking. This is likely due to the subtlety of compound modifications. Additionally, the rapid detection required for drink spiking presents a challenge for wireless sensing, and its performance is expected to be even lower with unknown drinks.

Hedgehog comparison: The average accuracy for the Hedgehog system (side view) was 75%, lower than that of SpikEy (beer 75%, vodka 83%, mixed drink 75%, water 90%, cola 52%, and orange juice 75%). The recall for cola dropped significantly to 35%. The Hedgehog system performed even worse in the top view, achieving an average accuracy of 60.9% (beer 63%, vodka 66%, mixed drink 28%, water 84%, cola 55%, and orange juice 70%). While Hedgehog maintains high accuracy for detecting drink spiking in water, as shown in previous

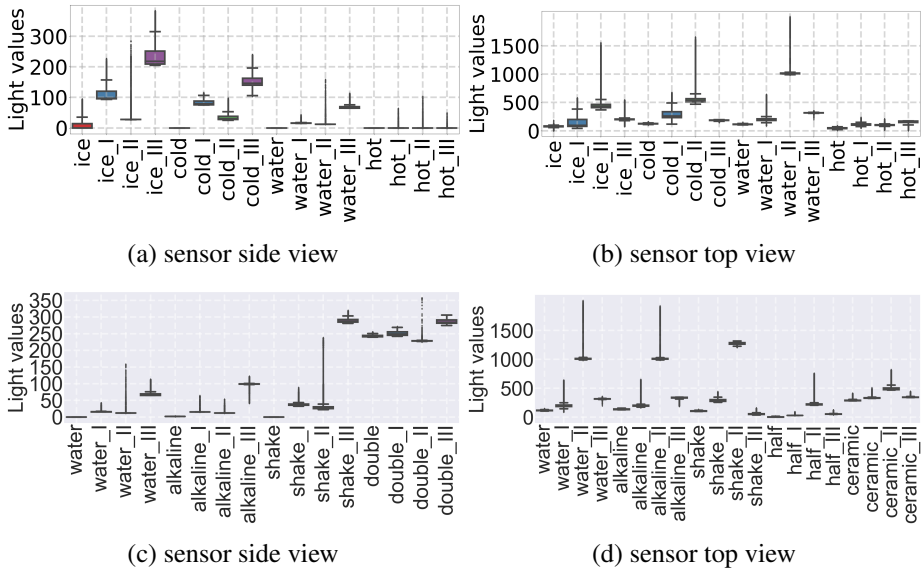
research, its performance is inconsistent across other drinks, such as beer and cola. As Hedgehog relies on simple machine learning models and optical sensing, this result demonstrates how SpikEy design is key to achieving accurate and robust performance with optical sensors. Indeed, SpikEy improved accuracy by at least 10% to 20% and maintained consistency across most drinks using latent representations.

3.5.4. Drink spiking generalization

We have demonstrated the effectiveness of SpikEy in detecting drink spiking. Additionally, we considered other factors influencing drink spiking, such as drink temperature. The testbed remained the same, with 12-hour monitoring, using previous light values of water at 23 °C as a reference.

Drink temperature: We investigated the effects of three additional temperatures on drink spiking: water with ice cubes (−18 °C), cold water (3 °C), and hot water (76 °C). All conditions were derived from the same water source. Figure 37 (a-b) shows that lower temperatures enhance the significance of spiking detection, particularly for both views. Cold drinks reduce drug solubility, resulting in more drug compounds remaining undissolved and submerged, which enhances light reflectivity. Additionally, the noise from ice cubes is minimized with average values close to the reference. Conversely, at higher temperatures, the differences between normal and spiked drinks diminish, as many drug particles quickly settle at the bottom, forming flocculent precipitates, resulting in fewer dissolved particles. The results indicate a consistent trend across drugs regardless of temperature. The light values of water at different temperatures remain similar for the side view, and Kolmogorov–Smirnov (KS) tests confirm the similarity in distribution ($p > 0.05$). However, the top view reveals some differences: ice ($Mean = 74.6$), cold ($Mean = 129.3$), room temperature ($Mean = 118.8$), and hot ($Mean = 32.6$). This discrepancy may be due to temperature-induced air effects influencing the sensor when directed at the liquid surface. Overall, our model demonstrates greater generalization across various temperatures compared to the top view due to its enhanced sensitivity.

Other considerations: We also generalized our approach to other factors, such as shaking the drink and testing alkaline drinks. We added three drinkable alkaline drops to water (pH=10). Given that most glass cups are made of silicon dioxide with a thickness of around 2mm, we mainly explored the shape of the glass cup in side views, e.g., using double-layer glass. For the top view, we considered the effect of the distance between the sensor and the liquid surface, testing half the original volume of the drink and drugs at approximately 5 cm distance. Additionally, as the top view can benefit from non-transparent cups, we tested a ceramic cup. Figure 37(c-d) illustrates consistent spiking detection across the three drugs under different conditions, with stable baseline values compared to spiked drinks. Shaking the drink increased drug solubility, resulting in greater light reflectivity, while the



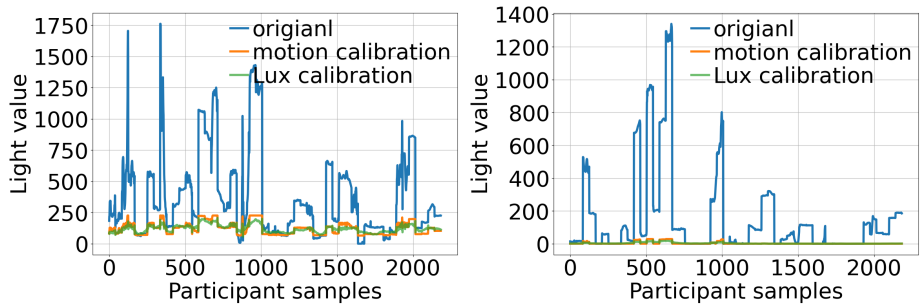
(a) sensor side view

(b) sensor top view

(c) sensor side view

(d) sensor top view

Figure 37: (a-b) Temperature effect, (c-d) Other generalizations



(a) light beer

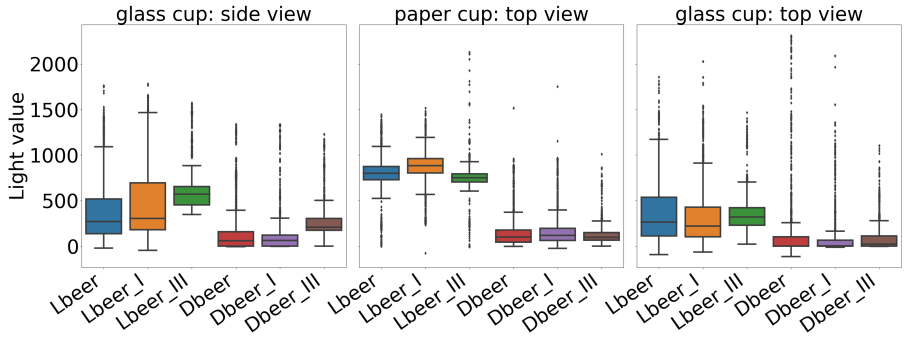
(b) dark beer

Figure 38: Light values after calibration

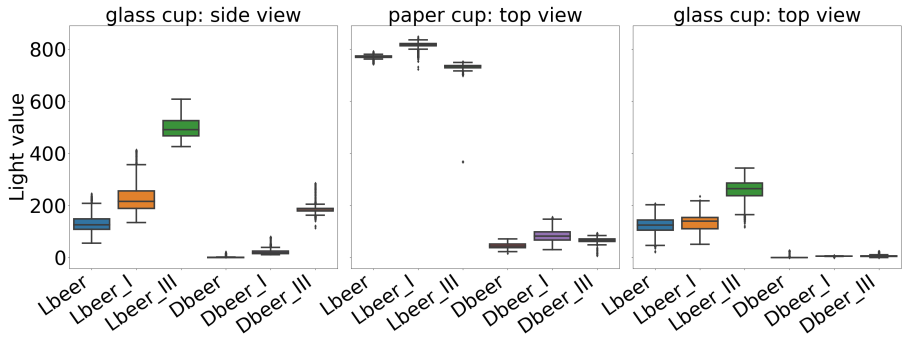
pH effect was minimized due to similar values. Overall, SpikEy shows strong generalization across varying conditions.

3.6. Results for dynamic nightclub scenario

Drink spiking: Figure 38 illustrates an example of the calibrated light values, which are notably more stable than the original values when characterizing the drinks. Our calibration model can effectively mitigate the noise induced by motion. Figure 39 presents light values for all participants, revealing significant variations in the original light values across all conditions (Figure 39(a)). This variability complicates the establishment of a reliable profile for spiking characterization, as there are considerable overlaps between non-spiked and spiked drinks. However,



(a) Original values



(b) Calibrated values

Figure 39: Light values across all participants in different interactions. Lbeer_I: light beer spiked by aspirin.

after calibration, Figure 39(b) shows clear differences in light values, aligning with trends observed in controlled experiments using transparent glass cups. Additionally, the profiles of each drink differ across the three interactions. Friedman tests conducted on the calibrated values indicate significant differences among the six drinks (for all interactions, $\chi^2 \approx 2 \times 10^4, p < 0.05$). Pairwise post-hoc comparisons (Wilcoxon-Bonferroni) further confirm statistically significant differences for all pairs ($p < 0.05$) in each interaction, demonstrating that SpikEy can accurately identify spiked drinks. Notably, variations in light values are smaller in non-transparent cups, as the paper effectively reduces ambient light noise. Although the performance of the top view in glass cups is not as strong as that of the side view due to overlaps in aspirin spiking, we explored the generalization across cup samples of the same type. Figure 40 shows light values for beer across different cup samples, revealing similarities irrespective of whether a glass or paper cup is used. Wilcoxon tests further confirm that differences between cup samples are not significant ($p > 0.05$).

Spiking performance in wild: We utilizes the best-trained models in Subsection 3.5 to test whether a drink is spiked using the wild data. When applied to non-

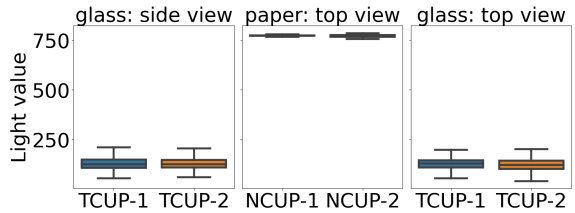


Figure 40: Light values of cup samples

calibrated data, SpikEy model yields a low average accuracy of 47.5% (42% for light beer and 53% for dark beer) in the side view. This low performance is expected due to significant noise in the raw data. However, data calibration for the side sensor markedly improves accuracy to an average of 71.3% (60.8% for light beer and 82.5% for dark beer), indicating strong generalization, particularly for dark beer. Wilcoxon Rank-Sum tests show no significant differences between stationary (A0 and A2) and moving (A1 and A3) conditions ($p > .05$), suggesting the effectiveness of our motion and light calibration approach.

While calibration enhances performance for light beer, subtle variations may not be fully captured when transferring the model from laboratory conditions to the real-world. The control model relies on variance to infer drink spiking, yielding average standard deviations for the side view (non-spiked = 4.88, spiked = 16). In the wild, dark beer spiking is accurately detected due to similar deviations (non-spiked = 2.76, spiked = 13.66) as observed in controlled conditions. However, drift persists after calibration, leading to lower accuracy for light beer, despite maintaining a similar deviation pattern (non-spiked = 31.84, spiked = 47.94) compared to the controlled setting. Dark liquids effectively mitigate ambient light effects, suggesting that further reduction of low-frequency noise in ambient light calibration for light-colored drinks could further improve accuracy while balancing the risk of overfitting.

The top view may not be ideal for detecting spiked substances, as accuracy declines from 51.5% (calibration) to 46.5% (non-calibration). Unlike the side view, where light interactions occur at a stable cross-section of the liquid, the top view is more susceptible to variations from surface dynamics (e.g., ripples or movement when held), complicating reliable differentiation between spiked and non-spiked drinks. This is supported by Figure 39(b). Additionally, some participants reported discomfort while grasping the drink, leading to unexpected noise. The average standard deviation for the top view from the controlled model is (non-spiked = 5.63, spiked = 88). However, the distance between spiked and non-spiked drinks in the wild is minimal from the top view (e.g., *Lbeer* in $TCUP$: non-spiked = 31.16, spiked = 33.58; *Dbeer* in $TCUP$: non-spiked = 3.59, spiked = 2.61). Overall, the side position proves more effective for drink spiking detection in real-world scenarios.

Comparison to visual inspection (baseline): The majority evaluated drink spiking based on appearance, bubbling and fizzing, followed by residues and smell.

However, still 50% of participants admitted to making random guesses. Overall, the performance of visual inspection for detecting drink spiking is low, with an accuracy of 52.4% (compared to 71.3% for SpikEy). We found that accuracy was slightly higher for glass cups compared to paper cups: 54.9% for glass and 50.9% for paper, as participants could inspect the glass from multiple angles.

Summary: To summarize, the results from the nightclub scenario highlight the effectiveness of SpikEy in accurately detecting drink spiking also in (close to) real-world scenarios. The calibration of light values significantly enhances detection accuracy, particularly for dark beverages, while the side view consistently outperforms the top view. Moreover, the comparison with visual inspection underscores the potential of SpikEy to provide a more reliable and objective method for drink spiking detection, addressing a critical safety concern in social settings. These insights pave the way for further advancements in drink safety technologies, ultimately contributing to enhanced public safety.

3.7. Discussion

Naturally, there is room for further work and improvements. We discuss some key points below.

Implications: The experiments consistently demonstrated accurate and robust performance, achieving over 85% accuracy in controlled settings while still reaching over 70% accuracy in dynamic scenarios. In contrast, visual inspection yielded results comparable to random guessing, and other baseline methods necessitated controlled environments to be effective—yet SpikEy outperformed them in both contexts. Our findings suggest that SpikEy could potentially prevent 7 out of 10 spiking attempts, representing a significant advancement in public safety and providing a means to protect vulnerable individuals (20% improvements compared to manual inspection). Additionally, SpikEy is applicable to a variety of drugs and can be used inconspicuously, facilitating its integration into real-world social situations.

Choice of drugs: To ensure legal and ethical compliance, our experiments focused on common drugs rather than those specifically classified as spiking substances, which are subject to strict access restrictions. The selected drugs encompass all relevant categories within the Biopharmaceutics Classification System (BCS), ensuring coverage of all possible chemical reaction types. The primary differences between common drugs and spiking substances lie in solubility relative to liquid concentration, which we also assessed separately in our experiments.

Choice of drinks: While we evaluated a broad range of drinks, there are naturally some beverages and combinations that were not covered. Different drinks and their combinations primarily affect solubility and viscosity patterns, which were varied in our experiments. Overall, the results demonstrated accurate and robust performance across a wide range of these parameters, indicating that SpikEy has

significant potential as a highly relevant real-world solution.

Sensing position: SpikEy supports flexible sensing positions, whether at the side or the top of a glass, allowing users to perform sensing with the same hand holding the glass (side-view sensing) or with the other hand (top-view sensing). We are also interested in exploring the bottom position of sensing for transparent and translucent cups, as some drug compounds may settle at the bottom in certain drinks, such as vodka. Sensing from different angles can enhance performance. While SpikEy performs well with both transparent and non-transparent cups, further exploration of materials, such as metal and plastic cups, could yield additional insights. Incorporating motion sensors into the ring could also enhance calibration accuracy.

Drug concentration: Varying drug concentrations can affect light absorption during drink spiking. In our experiments, we increased the drug dosage to two pills while keeping the water volume constant. Results showed similar trends in average light values: for the side view, one pill (class-I= 14.5, class-II =10.8, and class-III = 63.6) versus two pills (class-I= 37.2, class-II =26.5, and class-III = 100.32); for the top view, one pill (class-I= 199.3, class-II =1036.8, and class-III = 316.9) versus two pills (class-I= 148, class-II =884.4, and class-III = 270.8). Kolmogorov-Smirnov tests confirmed similar distributions between drug concentrations ($p > 0.05$), indicating that light reflectivity is functionally related to drug concentration.

Usage and adoption: Our study demonstrated how SpikEy can power a smart ring to identify drink spiking. Interestingly, only a few participants (23.1%) possessed a high level of awareness regarding drink spiking in public places. However, a significant majority (80.7%) expressed interest in using the smart ring for safety, provided the price is reasonable.

Machine learning optimization: Although SpikEy achieves good performance for drink spiking detection, the model could be further improved by explicitly analyzing the precision–recall trade-off using ROC curves with AUC or precision–recall (PR) curves with AUPRC. As the current model only applies the default threshold, adjusting the classification threshold on predicted probabilities would allow these curves to identify an operating point that optimizes the balance between recall and precision for real-life deployment. This optimization is particularly important for highly imbalanced datasets, as in real-life scenarios where the vast majority of drinks are not spiked.

Runtime performance: While our primary focus was on ensuring accurate, robust, and inconspicuous detection, practical deployments of SpikEy can benefit from performance optimizations. Modern wearables typically rely on companion applications running on smartphones, allowing for heavier computations to be offloaded to these devices. Additionally, as demonstrated by DeepSeek and other recent AI models [261], the runtime performance of CNN and autoencoder solutions can be further enhanced through quantization without sacrificing accuracy. Other

potential optimizations include utilizing proximity sensors to trigger sampling and integrating optical sensors to support motion calibration, rather than relying solely on IMUs.

Bootstrapping and growth: Integrating SpikEy with crowdsensing mechanisms could enhance the knowledge base of identifiable drinks, improving the detection and analysis of drink spiking over time. Experience Sampling Method (ESM) and opportunistic sensing could facilitate data collection, creating datasets for robust training of AI models for drink and liquid classification. Leveraging crowdsensing can also provide valuable insights regarding drink types, substances involved, and the symptomatic responses of individuals subjected to spiking.

3.8. Summary

We contributed SpikEy, an innovative sensing method that can be integrated into wearables for identifying drink spiking. Through rigorous experiments, we demonstrated that SpikEy can be used to identify different types of drinks from specific light reflectivity fingerprints, and to identify drink spiking robustly and accurately (up to 86% accuracy). SpikEy is demonstrated with a smart ring prototype, and results show it can be easily implemented with off-the-shelf smartwatches, working across various cup types, drinks, ambient light conditions and user behaviors in social scenes. The SpikEy usage is straightforward. When users hold one drink, the smart ring collects light values which are calibrated based on motion and ambient lighting conditions. This can be handled in the background via the smartphone application. Users typically hold the drink for approximately 10 seconds to ensure sufficient data collection. After that, the system performs drink spiking detection on the smartphone. SpikEy also outperformed existing solutions, offering more realistic practical usage. SpikEy contributes to creating safer social environments and empowers individuals to take control of their safety in public spaces.

4. SNAKE: HARNESSING HUMAN TOUCH FOR PRODUCE QUALITY ESTIMATION TO FOSTER SUSTAINABLE RETAIL PRACTICES

Building on the previous Chapter, where we explored how smart rings can detect spiked drinks through natural holding interactions, we now turn our attention to another everyday behavior *touch* and its potential for promoting sustainability. Food waste remains a global challenge, with organic produce frequently discarded due to visual imperfections or a lack of accurate quality information. Existing solutions for assessing produce quality are difficult to deploy to retail environments as they lack the ability to seamlessly integrate with retail practices, often requiring specialized equipment or controlled interactions. In this Chapter, we introduce SNAKE, a thermal sensing approach that estimates produce quality by analyzing heat transfer from a person's hand during natural touch. SNAKE captures thermal dissipation patterns and uses them to infer internal freshness, offering a low-cost and contact-driven solution that aligns with existing retail behaviors. Thermal sensors have been integrated into smart rings primarily to enhance gesture recognition [480]. However, their data can also be effectively repurposed for applications such as product quality monitoring. To demonstrate further the flexibility of our method, we provide an additional use case that considers the integration of SNAKE into IoT devices commonly deployed in retail stores. This opens the door for real-time, on-the-go produce evaluation through natural interactions, supporting both consumers and retailers in reducing food waste.

4.1. Introduction

The sustainability of retail processes is a critical concern, with an estimated 17% of global food intended for consumption ending up as waste [337]. Organic produce with a limited shelf life is a major contributor of this waste [93] as they are often discarded due to decay or visual imperfections, such as color concerns, irregular size, or blemishes [326]. Consumers have a strong desire to reduce food waste but often lack the information that can drive the desired behaviors [145, 314]. Pervasive computing technologies have the potential to address this concern by offering insights into produce quality to reassure consumers to minimize unnecessary disposal. This not only benefits the consumers but can also aid retailers, e.g., by minimizing storage requirements and managing waste more efficiently.

Limitations of state-of-the-art. Current solutions for produce quality estimation are difficult to deploy to retail environments as they lack the ability to seamlessly integrate with retail practices, often requiring specialized equipment or specific interactions. Instead, visual inspection by the naked eye remains the prevailing solution for both consumers and retailers [341]. While solutions for produce quality estimation exist, these primarily target other parts of the supply chain.

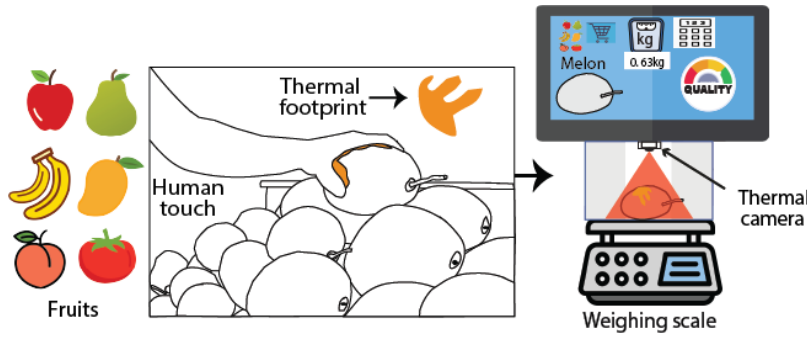


Figure 41: SNAKE produce quality estimation.

Examples of relevant technologies include automated image processing [224, 15], wireless sensing [265], spectral imaging [203, 428] or optical (light) sensing [498]. With the exception of computer vision, all of these require specialized equipment and laborious interactions, making them unsuitable for consumers. Computer vision, in turn, only captures visual irregularities and thus effectively serves as a supplement to naked eye without being able to assure consumers on the actual quality of produce. Improving the situation requires accessible and cost-effective technical solutions that integrate with retail practices while concurrently provide informative and actionable information on reducing food waste and loss.

Contributions. We contribute SNAKE, a pervasive sensing solution for produce quality estimation from natural human touch interactions. SNAKE improves on existing solutions by offering an accessible and low-cost solution that can seamlessly integrate with existing retail processes. As SNAKE harnesses natural interactions, it does not pose any interaction requirements on customers. The system is also cost-effective, only requiring a thermal camera (approx. $500) or a thermal array sensor ($10 – $500 depending on resolution) to be installed at a location where it can monitor user interactions. SNAKE can also integrate with existing retail practices, e.g., as illustrated in Figure 41, the thermal camera can be integrated with scales making SNAKE able to estimate produce quality as part of existing practices. Households can also adopt SNAKE using a smartphone with a thermal camera or a USB-attached thermal camera.

SNAKE estimates produce quality by leveraging thermal radiation transferred from touch interactions. By monitoring the dissipation rate of this transferred heat, SNAKE extracts a dissipation fingerprint that characterizes the dynamics of thermal behaviour. Internal thermal characteristics of produce govern the rate at which the produce decays [67, 119], and these internal characteristics affect how the produce exterior absorbs and reflects thermal radiation. The dissipation fingerprint extracted by SNAKE captures these changes in thermal behavior, and uses them to estimate produce quality. However, accurately estimating thermal characteristics from opportunistic human touch interactions is highly challenging as surface variations, distinct interaction patterns, and the ambient environment affect thermal transfer. Different produce types exhibit unique thermal properties that affect heat

dissipation rates and external temperature fluctuations (e.g., refrigerated vs. room environments) further complicate modeling. SNAKE overcomes these challenges by leveraging an innovative modeling pipeline that compensates against these variations, ensuring consistent and accurate produce quality estimation across diverse user interactions and ambient conditions. Specifically, SNAKE uses computer vision techniques to accommodate variations in human touch patterns, including the size of the touched region and the duration of the interaction. Additionally, compensation models are integrated to account for variability in hand temperature and the ambient temperature.

Systematic and rigorous independent evaluations conducted over time, involving multiple users, the five most prominent produce categories, and diverse interaction patterns, demonstrate that SNAKE achieves approximately 83% accuracy in estimating produce quality and outperforms state-of-the-art baselines, including optical and WiFi sensing. Independent studies conducted over repeated intervals with the same produce type validate our methods. Our evaluation demonstrates that thermal radiation induced by touch interactions is sufficient for capturing produce decomposition and that thermal dissipation values closely relate to firmness values, validating the theoretical model underpinning our approach. We also demonstrate that SNAKE can operate robustly across different ambient environments, individuals touching the produce, and touch duration patterns. We also conduct smaller-scale experiments with additional produce and conditions to demonstrate that SNAKE can be generalized to a wider range of produce and that it can operate effectively in the long term. Finally, we evaluate the practical potential of SNAKE through a user study with 100 participants that compares our method to traditional manual inspection. We developed a prototype integrating SNAKE with standard retail scale appliances. The prototype uses a 3D-printed deployment designed to simulate real-world retail scenarios. User evaluations of this new prototype solution indicate that SNAKE can enhance consumer purchasing decisions by at least 25% and reduce food waste by 10% to 15%, demonstrating significant economic benefits that warrant its adoption in retail environments. Additionally, we provide an in-depth discussion on the integration and implementation of SNAKE, addressing potential challenges for user perception and emphasizing the minimal barriers to its deployment in real-world retail settings. Taken together, our work offers a promising, effective, and innovative solution for supporting produce quality estimation by harnessing human interaction patterns.

4.2. Related work

Produce quality monitoring: Manual inspection is the most common method for produce quality estimation. While easy to implement, it is highly laborious, prone to errors, not scalable, and very inefficient [493]. Automated systems have been developed to overcome these limitations and are mostly powered by computer vision [41]. These methods, however, are sensitive to illumination and occlusions

and high-quality footage, requiring an unobstructed view of the produce's surface to be able to estimate quality. Some CV-based applications are already available on app stores to evaluate produce quality (e.g., Clarifruit and Intello Track). These apps are mainly for businesses instead of small retailers and customers. They require ongoing subscription fees, and the cost is unlimited. Besides the image quality, user factors can also affect the final results in the apps, as they need to fill up the defect. This undoubtedly requires user expertise with extra burden. In addition, Clarifruit requires the Brix values (sugar content) of produce, which can be measured by refractometer and spectrometer. However, the refractometer is destructive and can cause produce waste. The spectrometer is non-destructive but very expensive (e.g., F-750 produce quality meter around 10000 dollars). Intello Track app has region limitations at present and users in a few countries (USA, Singapore, and India) can register.

The main alternative to visual techniques is spectral imaging, such as near-infrared (NIR) sensing [203], hyperspectral imaging [428, 139], or specific light wavelength imaging [498, 318], depending on the parts of the light spectrum considered. Although these methods capture additional details about produce, they require costly, bulky, and specialized equipment, making them impractical for end-users. For example, NIR sensing is used in commercial spectrometers for non-destructive internal fruit measurements, but deploying this technology at scale is expensive. Wireless signals can also estimate the water content of the produce [184]. However, these techniques are highly sensitive to the measurement setup and dynamic environment and can only measure one item at a time. High-quality cameras are also needed to improve the accuracy of moisture and soluble solids content measurements in wireless sensing [265]. Similarly, thermal imaging has been explored in agriculture for applications such as harvesting and manufacturing [279, 104, 416, 12]. Thermal imaging typically detects bruises or diseases in produce on the basis of surface temperature. However, this analysis is not tailored to user perception or interactions. We advanced thermal imaging by developing a user-friendly solCution that assists humans in estimating produce quality in practical deployments.

Customer-center solutions: Customer-oriented solutions have been developed using smart IoT and wearable devices for end-users to assist their daily activities. For instance, users can take pictures of their food using their mobile camera to analyze calorie intake [335]. Cameras attached to the inside of a refrigerator door can monitor food inventory, plan shopping, and reduce household waste [123]. Some mobile applications are developed to reduce food waste, e.g., improving fridge storage practices [266], bridging the gap between waste instances and past user-behavior reflection [124, 472]. A smartfridge network utilizes IoT devices such as particle photons and a companion app for remote browsing and reservation of food donations, improving food distribution and addressing food insecurity [28]. Tools for online food shopping websites and in-store interactive displays or tablets are used to support sustainable food shopping for stakeholders by providing

eco-feedback visualizations and guidance on environmentally friendly products [259, 378, 372]. Other IoT devices (e.g., TV) are also used to minimize food waste, e.g., user education and awareness promotion by interactive gameplay [391]. Likewise, RFID stickers have been used to learn the quality of food via wireless [159]. Other sensors can also be utilized to support better decision making [148], for instance, when buying groceries at a shop and disposing or preserving household produce [197]. The wearable FitNibble utilizes a proximity sensor and IMU to monitor hand-to-mouth gestures and chewing, addressing challenges in automating food journaling for better dietary habits [36]. Other wearables can also be placed in different body positions (wrists, ear and neck) to monitor food intake for health suggestions by various sensors (piezoelectric, acoustic or EMG/ EGG) [170]. Other work has investigated the miniaturization and portability of spectral technologies, such that it is possible to integrate into handheld devices [471] and smartphones [92]. Unlike others, we rely on COTS thermal cameras to provide end sales solutions that support the customers through natural human touch interactions. SNAKE can be deployed in any personal (smartphone [106]), wearable (smart ring [480]) or user-assisted (scanner [235]) device.

Smart retail solutions: Smart IoT (Internet of Things) devices are enhancing retail activities and optimizing retail experiences [417]. An intelligent mobile grocery assistant is developed to support customers during grocery shopping by creating shopping lists and providing personalization [44]. Other smart applications provide information on products (e.g., expiry date, quality indicators and offers) to understand consumer preferences, enhancing the shopping experience and purchase likelihood [110]. The ThirdEye system utilizes smart glasses integrated with inertial sensors to track physical browsing in retail, which can optimize store layouts and improve the overall shopping experience [344]. Retail stores can also deploy a low-energy Bluetooth indoor positioning system to track consumers' paths efficiently and improve decision-making in retailing [396]. RFID readers integrated into smart shopping carts and smart shelving can streamline billing and enhance inventory management by attaching RFID tags to products [247, 377]. Smart shelves also use image recognition systems and sensor-based systems to analyze benefits, costs and planned developments, offering the most suitable solutions for retailers [212]. In addition, a smart shopping cart system can allow customers to scan items and view product details on the cart screen by interactive GUI, offering service assistance and minimizing shopping time [111]. Compared to others, we take a step forward in the smart capabilities of retail self-checkout systems by developing functionality to promote sustainable practices.

4.3. Limitations of current solutions

Consumer quality assessments primarily rely on visual assessment by the naked eye [341]. However, this method falls short of capturing the true quality of the produce. Computer vision can be used to automate visual assessment, but it is also

unable to evaluate the true quality of a produce. To further motivate the need for enhanced solutions for quality estimation, we first highlight the constraints of both manual and automated visual assessment techniques.

4.3.1. Manual inspection

To assess challenges in manual inspection, we conducted a two-week survey at a local university, engaging 60 participants (31 males, 29 females, age ranges: 18-57 years (28.7 ± 9.73)) across classrooms, offices, and the university canteen. Each participant examined a basket of seven organic produce items thoroughly (passion fruit, plum, apple, tomato, mandarin orange, mango, and melon) and rated their quality on a five-point Likert scale (1: strongly disagree – 5: strongly agree) in response to a closed-ended question (e.g., *"Is this tomato of good quality to eat?"*). Additionally, two open-ended questions explored shopping habits, inquiring about time from purchase to consumption (*"On average, how soon will you consume the produce that you purchase?"*) and strategies for assessing fruit quality. Completing the survey took on average 10 minutes. Participation was both anonymous and voluntary. To capture variations in internal quality, we employed the same set of produce throughout the two-week study, and restricted the number of respondents per day. Freshly procured at the start, the produce was consistently stored in the same room between the assessment days. Surveys were conducted on six evaluation days with 10 participants each, strategically aligned with key decomposition stages: day 1 (fresh), days 6, 8, 10 (active decay), and days 12, 14 (advanced decay). This approach provided insights into the accuracy and challenges in produce quality assessment. The produce items were deliberately chosen to represent commonly purchased items that pose significant challenges for manual inspection. As produce undergo decomposition, micro-bacterial proliferation ensues, leading to the softening of produce and eventually into visual alterations. The produce categories chosen for the study have thicker epicarp (skin) which delays the occurrence of visual alterations, which makes manual inspection challenging.

Results: To estimate the accuracy of manual inspection, we compared the subjective ratings given by the participants with the decomposition stage of the produce. Table 17 reveals that produce received improved scores despite the stage of advanced decay. A notable exception is the plum due to the softer skin, which exhibited clear visual alterations that participants correctly identified. In contrast, the other produce lacks such visual cues, resulting in minimal differences in quality assessments across the study period, highlighting the limitations of manual inspection. It is important to emphasize that these results were designed to shed light on the challenges inherent in manual inspection, rather than perform rigorous assessment of inspection accuracy. For example, we acknowledge that some produce may not have been fully ripe on day one despite being freshly procured from a supermarket, and hence the quality potentially is better on day 6 and 8 than on day

Table 17: Statistical rank of the fruit quality evaluation: 5-strongly agree and 1-strongly disagree.

Produce	Stage 1	Stage 2			Stage 3	
	Day-1	Day-6	Day-8	Day-10	Day-12	Day-14
Passion	2.6±0.9	2.2±1.0	2.6±1.2	2.7±1.1	2.1±1.1	2.3±0.9
Plum	3.6±1.5	2.5±0.9	2.6±1.7	1.2±0.4	1.2±0.4	1.7±1.0
Apple	**4.4±1.1**	**4.6±0.5**	**4.2±0.9**	**4.5±0.5**	**4.3±0.7**	**4.4±0.5**
Tomato	**4.0±1.1**	**4.1±0.6**	3.9±1.1	**4.1±1.2**	3.8±0.8	3.3±1.1
Mandarin	3.8±1.3	3.8±1.2	**4.0±1.3**	3.7±1.3	3.8±0.6	3.7±1.1
Mango	2.9±1.0	3.1±1.3	3.8±0.9	**4.4±0.5**	**4.5±0.5**	3.5±0.9
Melon	3.8±0.9	**4.0±0.8**	**3.8±0.6**	**4.0±0.8**	**4.1±0.9**	**4.1±0.9**

1. However, as the study spanned two weeks, this effect would not extend to the end of the second week, therefore not accounting for the observed results.

In terms of purchase habits, most participants made independent purchase decisions (80%) and consumed produce within the first five days (85%). This contrasts sharply with the quality assessments, where even the two weeks old produce items were deemed fresh. Participants prioritized appearance and color (95%) in quality assessments, followed by taste and smell (75%), texture (60%), and estimated nutritional value (33%). Several comments from participants revealed a reliance on touch and smell in the absence of visual cues. However, it became evident that subjective preconceptions often influenced the estimations rather than them being based on actual produce quality. For instance, participants associated hardness with unripeness and softness with ripeness, with some accurate and some misleading outcomes. For example, soft mango was correctly deemed ripe whereas a tomato was deemed ripe on day 14 due to its smell and softness despite already starting to rot. In summary, the survey results underscore how participants utilized simple heuristic principles for produce quality assessment, which, while sometimes accurate, could also be highly misleading. This reliance on heuristics transcends also to the retail environment, potentially resulting in consumers purchasing produce that are at the end of their life-cycle or that do not meet the consumers' expected quality assessments. Both of these issues lead to consumers discarding produce, contributing to elevated levels of food waste and loss. Offering an alternative method that accurately reflects the actual state of produce can mitigate these challenges and reduce unnecessary waste. Our work introduces an innovative technique that leverages human touch interactions to capture produce's internal state. This approach offers a more reliable and accurate solution for produce quality assessments.

4.3.2. Estimation using computer vision

Automated visual assessment using computer vision [42] is the primary automated solution for quality assessment. We next illustrate that this approach encounters the same limitations as manual inspection, rendering it inadequate for supporting customers. We evaluate computer vision using 294 images captured over the

same 14-day period as our survey (see Subsection 4.5), covering three produce items from the same seven categories. Images are labeled by decomposition stage: fresh (days 1-5), active decay (days 6-10), and advanced decay (days 11-14). It is important to note that these labels are not intended to precisely characterize produce quality but to signify the quality trends and help highlight the challenges associated with computer vision. We assessed five widely-used deep learning models: DenseNet201, InceptionV3, MobileNetV3large, ResNet50 and Xception. To enhance the generality, we replaced the top-most dense layer with three fully connected layers (1024, 1024 and 512 neurons) to capture more complex relationships. Pretrained weights from ImageNet were leveraged to configure the parameters of the convolutional layers to capture a broad set of visual cues, while separately learning the weights of the dense layers using the training data. The evaluation employed 5-fold cross validation, with images standardized to a common 300×300 resolution and augmented via random angle rotation, vertical and horizontal flips, and width and height shift changes. The augmented training dataset comprised 18 884 images (15 108 for training, 3776 for validation). Training utilized a batch size of 512 images and 100 epochs. Early stopping was utilized to stop training if validation accuracy stagnated for 10 consecutive epochs.

Despite the diversity and complexity of the model architectures, the best performing model achieved only 48% accuracy in predicting the decomposition stage. The lack of visual cues in the images, aside from plum as discussed previously, contributed to this limitation. While potential enhancements could be made to the model structure, the primary issue remains: visual cues are insufficient for accurate quality assessment. This is not to argue that computer vision techniques are not suitable - indeed, they are widely used during other produce life-cycle stages, e.g., packaging can use computer vision to identify diseases or defects [195]. However, these methods are inadequate for the retail environment as the available visual cues are insufficient for accurate quality assessment. These results further emphasize the crucial need for novel and improved solutions for accurate produce quality estimation within the retail environment.

4.4. SNAKE design and methodology

SNAKE is an innovative, accessible, and cost-effective solution for estimating produce quality. It leverages heat transferred from human touch interactions [90]. Specifically, when customers touch produce, heat is transferred from their hands to the exterior surface of the produce. Once the interaction stops, the temperature begins to *dissipate* as the produce surface seeks equilibrium with the ambient temperature. The rate at which the heat decreases is referred to as the *dissipation rate*, which is the key variable that SNAKE monitors. This dissipation rate is directly linked to the internal characteristics of the produce (see Subsection 4.4.3), which correlate with changes in overall quality. Note that even a short interaction can result in a significant amount of heat transfer due to the difference between the

produce's temperature and that of the human hand. As a result, dissipation time can differ significantly from the duration of the customer's interaction with the produce.

SNAKE employs a thermal camera to capture and monitor the rate at which thermal radiation dissipates, using these measurements to estimate produce quality. The key technical challenge addressed by SNAKE is accurately estimating produce quality from the transferred heat, as surface variations, distinct interaction patterns, and ambient conditions all affect heat transfer. Different types of produce also exhibit unique thermal properties that influence heat dissipation rates, necessitating adaptive modeling for consistent quality assessment. Additionally, external temperature fluctuations (e.g., between refrigerated and room environments) introduce further variability that must be accounted for.

SNAKE tackles these challenges with an innovative pipeline that accommodates variations in human touch patterns, including the size of the touched area and the duration of the interaction. The size is addressed by adaptively normalizing the monitored area, while the duration is managed using a two-phase approach with two linear regression models to normalize heat transfer to a consistent scale. Specifically, SNAKE incorporates a theoretical model of dissipation constructed from controlled measurements and estimates an empirical model from heat transferred during customer interactions of arbitrary durations. By correlating these models, our approach supports robust produce estimation from short (approximately 5 seconds) dissipation measurements, even when the theoretical model considers dissipation measurements collected over a longer time window. To enhance robustness further, SNAKE incorporates compensation models that account for hand temperature and environmental temperature variability, ensuring consistent performance across diverse conditions (more details in Subsections 4.7 and 4.8).

4.4.1. SNAKE overview

SNAKE leverages heat transfer from touch interactions to estimate produce quality using a four-stage pipeline summarized in Figure 42 and elaborated in Algorithm 1. The first phase, *sampling*, involves collecting video footage from a thermal camera or a thermal array sensor. The second phase, *data processing*, extracts image frames from the video data and performs preprocessing on them. This preprocessing involves converting the images to greyscale using Gaussian blur and thresholding (Lines 1 - 3) to separate the produce item from the background. As touch interactions result in the produce item having differing thermal patterns than the ambient environment, this simple approach suffices for separating the foreground and background. The third phase, *parameter extraction*, converts the thermal fingerprint into a consistent representation and estimates the dissipation rate of the produce. Finally, the *modeling* phase employs machine learning using the extracted parameters as input to assess produce quality.

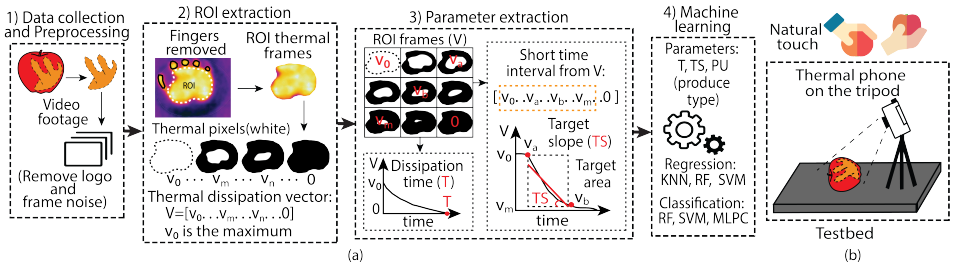


Figure 42: a) Thermal imaging modelling pipeline; a, b, m, n are the frame timestamps during the thermal dissipation, $0<a<b<m<n<T$, b) Testbed.

Algorithm 1 Calculate Vector (V) From Hand Heat

Require: Frames from thermal footage
Ensure: Thermal dissipation vector (V)

for each INPUT **do**
  image ← Conversion to Grayscale; Apply GaussianBlur, Threshold
end for
initialize V array
for each i in *images* **do**
  x, y, w, h ← cv2.boundingRect() {*heat coordinates*}
  ROI ← image[y:y+h, x:x+w] {*hand palm coordinates*}
  thermalarea ← count white pixels(255)
  Add thermal value to vector V
end for
V ← Scale V, Sliding window V

4.4.2. Robust and accurate parameter extraction against touch variations

SNAKE requires robust and accurate estimates of the thermal dissipation values to estimate produce quality reliably. However, this is highly challenging as the amount of heat that is transferred to an item depends on the area that the hand touches and the duration of the interaction. We next detail how SNAKE overcomes these challenges.

To accommodate variations in the touch area, SNAKE extracts a region of interest (ROI) from the image frames and analyzes dissipation only within this area. The ROI corresponds to the part of a produce item that the user touched. Note that interaction force has a negligible effect on SNAKE as the size of the ROI only depends on the area that the user interacts with. Greater – or weaker – interaction force affects the contact between the produce surface. This can improve or decrease overall heat conduction, but does not affect the size of the area where this heat resides [90, 119, 204]. Indeed, by capturing the ROI, SNAKE measures the thermal response directly, allowing it to capture these variations in heat transfer without relying on predefined assumptions about force.

We extract the ROI by forming a bounding box around the area where the hand touched the produce item (line 6), and using contour detection to extract this area (line 7). To further enhance robustness, we also remove noise from the image frames by eliminating areas with low-intensity thermal radiation as these can be a result of reflections from other sources [364] or caused by weak or accidental touch interactions. Specifically, we eliminate thermal values that are outside of the 90% quantile of the distribution of thermal values within the bounding box. After preprocessing, we extract a dissipation vector V by calculating the reduction in ROI area compared to the previous frame (lines 8-9). Thermal dissipation time T is calculated from the reduction of the *white* area in the thermal fingerprint until it fully disappears (all *black*), indicating that the thermal value in the vector reaches zero. To make these values comparable against variations in touch area, we scale the dissipation values to a consistent scale. As the scaling can magnify low-intensity areas at the expense of high-intensity areas, we smooth the values with a sliding window filter [237] before scaling them. The filtering is done using one-second windows and it utilizes 50% overlap.

The parameter estimation also needs to cope with variations in interaction duration as these also influence the amount of thermal radiation that is transferred onto the produce item. SNAKE achieves this using a regression approach that converts observed interactions to a consistent scale and allows estimating the current state of the produce. This is accomplished using two regression models. The first uses the available image frames to estimate the dissipation slope, denoted LS (linear slope), which allows estimating the overall dissipation time from measurements that are available at that point. Linear slope LS is calculated based on common linear regression. The regression model for the target slope is incrementally estimated by threshold and re-updated after each frame. Separately, SNAKE integrates a second regression model that provides a reference for the dissipation slope at different stages of decomposition. We refer to this as the target slope, and denote it using TS. By comparing the current estimate LS with the reference TS provided by the target slope, the state of the decomposition can be estimated. Both regression models are obtained using linear regression, but we use robust regression for the target slope to improve model fit as short duration tends to cause more variance and can otherwise result in poor model fit. As an example shown in Figure 42(a), we consider a short-time interval of m frames from the dissipation vector V, where thermal values follow the sequence $V_0 > V_a > V_b > V_m$, with corresponding timestamps $0 < a < b < m$. The linear slope LS is estimated from the interval between timestamps 0 (dissipation start) to m. However, to ensure accurate dissipation rate estimation, we filter out frames where adjacent thermal value changes are minimal by threshold, as they do not effectively represent the dissipation process. The target slope TS is then updated and derived from the interval between timestamps a to b within the m frames. As part of the experiments, we also consider models that leverage produce type (PU) as input feature to see how tailoring the analysis to specific produce category can improve performance. Most existing solutions rely

on produce category, and this information can be easily obtained either from user input or using computer vision.

4.4.3. Theoretical background

Thermal radiation is electromagnetic radiation that results from changes in the thermal state of an object. This radiation is visible in the infrared part of the light spectrum [354] and can be captured using a thermal imaging device, such as a thermal camera or a thermal array sensor. The amount of thermal radiation that can be captured from the object depends on *emissivity*, denoted as ε, which indicates the fraction of thermal radiation the object emits or absorbs [280]. The higher the emissivity, the better thermal radiation can be captured. Organic materials and water both have high emissivity, making them conducive to thermal radiation capture.

A thermal footprint, also known as a fingerprint, refers to the distinctive pattern of thermal radiation an object emits, depicting how it differs from its surroundings. SNAKE captures these footprints and analyzes the rate at which they change over time to assess produce quality. This rate of change is referred to as *thermal dissipation* [106]. According to the laws of thermodynamics, any object will seek to reach a thermal equilibrium with its environment. Consequently, any thermal radiation decays over time and the dissipation rate characterizes the speed at which this decay occurs.

Water loss is a key factor affecting produce quality, as dehydration accelerates postharvest deterioration [270, 313]. It is often referred to as weight loss, mass loss, or moisture loss, as all three terms describe its direct impact on fresh produce [39, 322]. Water loss causes wilting, shriveling, and loss of firmness, diminishing both visual appeal and nutritional value [166, 154, 338]. This reduces consumer desirability and saleable weight while accelerating spoilage by depleting stored food reserves and increasing susceptibility to pathogens. Thus, effective moisture management is essential for preserving freshness, extending shelf life, and maintaining overall produce quality.

Fresh produce has a high water content which decreases over time due to transpiration and causes the fruit pulp to lose firmness and eventually to decay. As water has high emissivity, this means that the amount of heat the produce emits from its interior to the exterior decreases as the produce decays. The pace of the transpiration process within a produce can be characterized by three thermal properties [304, 208]: thermal conductivity k, thermal diffusivity α, and specific heat capacity C_p [296, 268]. Thermal conductivity signifies the rate at which heat traverses the fruit, while thermal diffusivity quantifies the material's heat-conducting ability relative to its heat storage capacity. Heat capacity determines the amount of energy required to raise the temperature of the produce incrementally (one kilogram by one degree). As these parameters are directly linked with water loss, they are also indicative of the changes we expect to see in thermal radiation

and its dissipation. For example, high water content leads to faster thermal transfer from the produce's interior, resulting in distinct changes in the thermal fingerprints.

In parallel to the internal changes, the exterior of the produce may be softer or undergo other alterations that can affect its emissivity. Together these two behaviours change the dynamics of thermal transfer over time, and SNAKE builds on the idea of monitoring and capturing these changes. As will be shown in the evaluation, changes in the dissipation fingerprints reflect these changes and enable accurate estimation of the actual produce quality.

4.5. Experimental setup

We evaluate SNAKE through rigorous and systematic experiments that account for the decomposition of fresh produce. Due to the limited shelf life of produce, our evaluation incorporates independent studies conducted over time with the same items. In addition to an in-depth analysis of SNAKE, we compare its performance against two state-of-the-art baselines that use alternative sensing modalities. We next describe our experimental design and procedure as well as the baselines we compare against.

4.5.1. Experimental design

Procedure: Our primary experiment considers produce quality estimates measured each day over a 14− day period by two participants, referred to as P1 and P2. We additionally conducted small-scale follow-up tests which focused on assessing the generality of our approach. These measurements are described as parts of the results in Subsection 4.6.7. In our experiments. we consider seven different types of produce, corresponding to fresh produce that are commonly available and purchased from supermarkets and covering the 5 primary categories of produce [498]: pepo (melon, passion fruit), pome (apple), berry (tomato), drupe (plum, mango) and hesperidium (mandarin orange). As discussed in Subsection 4.3.1, we focus on most produce with thicker epicarp as these are the most difficult ones for visual inspection and generally result in the highest amount of misclassifications by the consumers and potentially by the retail staff. To assess variation within produce of the same category, we consider three items from each category, selecting items with different sizes and shapes, but with a similar visual appearance. Thus, in total 21 items were used.

Prior to starting the experiment, the fruits being measured were first placed into clean baskets where they were kept until they had attained thermal equilibrium with the room's temperature. Each produce was kept in a separate basket to ensure there was no thermal transfer between produce in the experiments. Both participants then interacted with each of the 21 produce by holding them for 60 seconds (long interaction) and 10 seconds (short interaction). Interaction time refers to the duration the produce is held. While longer durations were used

for feasibility analysis, the system is designed to work with brief, real-world interactions (e.g., 5–10 seconds). Once the time had elapsed, the participants placed the fruit on a testbed where different measurements were collected (see below). The participants were free to choose the produce in any order they preferred and they interacted with the produce naturally using their dominant hand. The long and short interaction duration emulate differing interaction patterns with the former corresponding to a careful examination of the produce and the latter for a brief and superficial inspection. Our prior work has shown that 10 seconds is sufficient for estimating thermal dissipation patterns [106], whereas the longer interactions offer an opportunity to assess statistical variation within the samples. To ensure consistent measurements, we used a clinically certified contactless optical thermometer (DR CHECK FC500) to verify that the skin temperature of the participants conducting the experiment was normal prior to having them interact with the produce. We also assessed the palm temperature of the participants using a thermal imaging scanner (FLIR TG267) before touching the produce. These measurements were used to assess the effect potential variations in hand temperature have on the results.

Testbed and measurements: Measurements were collected using a controlled testbed, illustrated in Figure 42, located within a single room. We used the same room throughout the experiments to minimize external variation from different environmental conditions, and to ensure the thermal measurements can be reliably compared across days and produce items. The testbed consisted of a FLIR-capable smartphone (Caterpillar CAT S61) which was placed on a tripod at approximately 30 cm distance from a table with a black background and surface. The black background allows obtaining clean video footage of the thermal footprint without influencing the thermal radiation emitted by other objects in the surrounding environment.

Once the produce item was placed on the testbed, video footage of thermal dissipation was recorded using the thermal camera of the CAT S61 smartphone. The camera has internal calibration which was triggered prior to starting the recording. Thermal dissipation time was estimated automatically from the thermal video and validated by comparing it to a ground truth obtained from manual inspection with a stopwatch. To ensure consistent ambient conditions, we recorded the ambient temperature (23°C–23.8°C) and relative humidity ($32 \pm 2.24\%$) of the room where the testbed was located. These measurements were collected using a Netatmo portable weather station. Additionally, once the thermal dissipation measurements were collected, we used our two baselines (optical sensing and wireless sensing; see below) to measure the items. Finally, a picture of the produce was taken at the end of the experiment. These images were also utilized in Subsection 4.3.

Ground truth: Ground truth for the produce was obtained using a durometer to record the firmness of each fruit. Firmness refers to the softness or hardness of the produce and it is commonly used as an indicator of produce quality [425]. Firmness

can be affected by water (mass) loss as decomposition initiates. This influences the internal thermal properties of produce, contributing to superficial changes [177, 322]. Water loss and firmness changes rates are commonly interconnected. Thus, SNAKE builds the relation between the thermal imaging and produce firmness by looking at the water loss rate. The durometer readings were taken three times per day and averaged to obtain a firmness score for each produce. As the durometer we used the commercial fruit hardness tester (Turoni 53215TP) which has a measuring capacity of 90 shore. While the durometer manufacturer states the device to be non-invasive, in practice it requires contact with the surface of the produce item. This could cause damage to the skin of the item, thus accelerating decay. To ensure this is not the case, we took firmness measurements only from two of the items (referred to as S1 and S2) and used the third item as a reference to compare potential effects on thermal dissipation across days. No statistically significant differences in thermal dissipation were observed across the three items, validating that the durometer had no impact on produce decay. We also measured the fruit mass (in grams) using a kitchen scale.

Ethics: The experiments were given ethical approval by the IRB of University of Tartu and all participants recording the measurements gave their informed consent to allow using their measurements.

4.5.2. Baselines

As part of the experiments, we compare SNAKE against two baselines, elaborated below. The measurements for the baselines were collected simultaneously as we recorded the thermal footage.

Optical sensing (Baseline 1): We compare the performance of SNAKE against a state-of-the-art optical sensing solution [498]. This approach relies on a green laser diode and a photoresistor to measure reflected light from the produce's surface. We consider reflectivity analysis of fruits using the photoresistor connected to the analog input pin of an M5StickC PLUS ESP32 development board, which integrates Wi-Fi and Bluetooth capabilities. The M5StickC PLUS controls the sampling frequency (5Hz) and uploads the samples to a Web server. The photoresistor captures light changes based on its resistance exposure to the light intensity of the reflected material and this information is stored on a Web server. The distance between the sensor and fruit is within one centimeter, and two random 1-minute measurements per fruit are taken to mitigate the potential biases.

Wireless sensing (Baseline 2): We also compare the performance of SNAKE against state-of-the-art wireless sensing solutions [265, 405]. We measure the Channel State Information (CSI) of WiFi signals (2.4GHz frequency and channel six), which carry information about the propagation characteristics of radio signals. When the radio signals traverse through the produce, the signal characteristics, e.g., amplitude, phase; are affected by the produce's interior composition, which can be used as input to estimate ripeness. We use two ESP32 microcontrollers: active

access point (AP) as the transmitter and active station (STA) as the receiver, since they are small and easy to deploy. The distance between the AP and STA was set to 20cm, so placing a fruit between them could block the line-of-sight (LOS) of the WiFi signals. Two random 1-minute measurements are also considered.

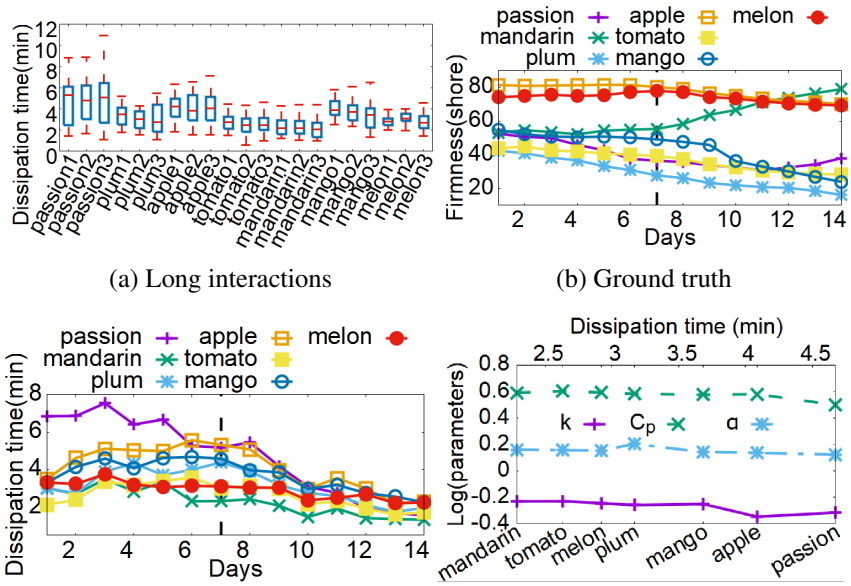
To pre-process the WiFi data, we first denoise the signals using convolution-based filtering. We then form frames from the measurements using a one second sliding window with 50% overlap. To identify the most relevant parts of the signal, we use principal component analysis (PCA) on the data and use the three top-most principal subcarrier components to represent the measurements. We opted for three principal carriers as over 90% of all information was contained by them. We then separate the low and high frequency components of the signal using Daubechies 2 discrete wavelet transform to separate the low and high frequency components for both CSI amplitude and phase. We average the low frequency components of the amplitudes and use them as the main feature as the average value of the high frequency components is close to zero. Also the phase information largely captures dynamic oscillations in the environment rather than static effects caused by the composition of the produce.

4.6. Results

4.6.1. Thermal dissipation time as a proxy for decomposition

SNAKE relies on thermal dissipation measurements to estimate produce quality. The measurements are used as a proxy for internal changes taking place inside the produce, which in turn characterize decomposition and the quality of the produce. We begin our evaluation by validating the use of thermal dissipation measurements, demonstrating that they can be used to characterize different produce and that they correlate with gold standard estimates as measured by a durometer. For details on the experimental setup we refer to Subsection 4.5.

Figure 43(a) shows the thermal dissipation distribution of different produce items, averaged across the experiment duration (i.e., 14 days). From the figure we observe that the differences between produce items are larger than differences within items of the same produce category. Krusal-Wallis tests were used to verify that the differences in thermal dissipation are significant for all the produce ($\chi^2 = 141.99$, $\eta^2 = 0.23$, $p < .05$). Here, the null hypothesis (H_0) states that all groups come from populations with the same median, while the alternative hypothesis (H_1) states that at least one group comes from a population with a different median. This implies that thermal dissipation can reliably characterize different produce categories. When comparing individual produce, the surface characteristics of the produce affect the variation in thermal dissipation. Specifically, produce that undergo clear surface changes have higher variance in thermal dissipation (e.g., mango and passion fruit) whereas those that undergo fewer surface changes are more stable over time (e.g., melon). Pairwise post-hoc comparisons (Dunn-



(a) Long interactions (b) Ground truth

(c) Long interactions (d) Thermal properties

Figure 43: Evaluation results in long interactions (1-min touch). (a) Thermal dissipation time of each produce. (b) Firmness value for each produce as given by the durometer. (c) Thermal dissipation time of different produce across the 14−day period. (d) Relationship between thermal properties and the mean dissipation time, k, α and C_p as mentioned before.

Bonferroni) of the thermal dissipation time indicated significant differences in all but two cases: plum and melon ($\chi^2 = 1.10, p > .05$) and apple-passion fruit ($\chi^2 = 0.27, p > .05$). Here, the null hypothesis (H_0) states that there is no difference in the medians of the two groups being compared, while the alternative hypothesis (H_1) states that there is a difference in their medians. This indicates that thermal dissipation time generally distinguishes between different fruits, but may struggle with specific produce that have similar surface characteristics. In these cases, additional measurements are needed to estimate fruit type robustly.

Figure 43(b) shows changes in firmness for the produce across the 14 day experiment period, indicating that most produce decompose approximately within a week at which point a significant drop in firmness can be observed. The hardness of the produce skin affects the decomposition speed with mandarin orange and passion fruit having slightly slower decomposition due to their harder epidermis. To compare the firmness values with thermal dissipation, Figure 43(c) shows the average dissipation time of all fruits for 14 days. On visual inspection, the thermal dissipation time follows the same trend as the firmness values. To verify that these patterns are meaningful, we calculated the (Kendall τ) correlation between thermal dissipation time and changes in produce firmness. The correlation is strong (92.86% of all fruits), confirming that dissipation time correlates with changes in firmness, which is a widely used indicator of produce quality [1]. We separately calculated the correlation between thermal dissipation values and produce mass, which was similarly found to be strong and very significant (95.23%). Both firmness and mass are commonly used to characterize produce decomposition processes as they capture internal changes (e.g., thermal properties) taking place within a produce [164, 304]. Finally, we calculated the correlation between thermal dissipation time and three distinct thermal properties: thermal conductivity, thermal diffusivity, and specific heat capacity (see Subsection 4.4.3). In particular, we rely on typical values of these thermal properties [164, 304, 146, 207, 122, 147]. The Kendall correlation verified a statistically significant relationship between thermal dissipation time and these three parameters (for all parameters, $\tau < -0.71, p < .05$). Hence, our results demonstrate that thermal dissipation measurements can serve as proxy for internal changes taking place inside the produce. As we consider produce from all main fruit categories, this finding also demonstrates that SNAKE generalizes across distinct decomposition patterns. Specifically, while the most common decomposition pattern is softening of the produce exterior over time, there are also produce for which the surface hardens after an initial softening phase (e.g., mandarin).

As the durometer requires contact with produce skin, we additionally compared the thermal dissipation values of the item (S3) for which durometer was not applied to the items that were measured with the durometer (S1 and S2). There were no significant differences in within-produce variation, as confirmed by Friedman tests ($p > 0.05$). This indicates that the durometer does not cause significant damage to the produce surface and that the firmness and thermal dissipation values can be

reliably compared across the entire period.

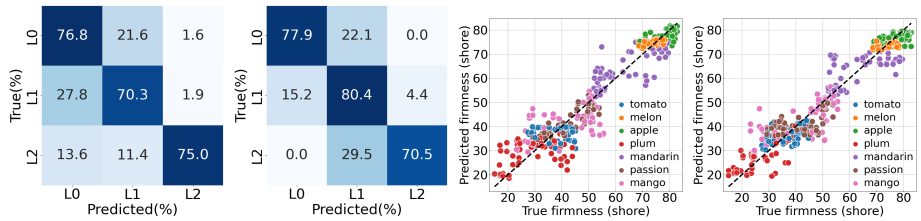
4.6.2. SNAKE performance

We next use our measurements to evaluate the overall performance of SNAKE by comparing the estimates derived from thermal dissipation values with measurements provided by the durometer. We first conduct classification experiments to obtain a coarse-grained indication of performance. We then supplement these with regression experiments that compare changes in thermal dissipation with changes in firmness, as measured by the durometer.

Classification for coarse-grained quality assessment: We first consider classification experiments where we categorize the fruits into the three common ripeness classes: fresh (L0), active decay (L1) and advanced decay (L2). These labels are intended to capture trends in produce quality and to offer a way to obtain a coarse-grained assessment of performance, not to characterize produce quality precisely. We categorized the measurements into these classes using clustering based on the firmness values. We separately consider short (10 second) and long (1 minute) interactions to assess how the measurement window affects performance. As classification techniques we consider three simple yet common machine learning techniques: Multilayer Perceptron (MLP), Support Vector Machine (SVM), and Random Forest (RF). The input features for all classifiers were the thermal dissipation time, target slope, and produce category. Features were normalized using min-max normalization, and one-hot encoding was used to assign labels for samples. As evaluation metric we use classification accuracy which was calculated using a 5-fold cross-validation.

When only thermal dissipation is considered, the average estimation accuracy is relatively low for both interactions (short: 57.15%, long: 54.86%). This corresponds to a generic model when no information about the produce is given. Once we consider the produce type, the average performance of SNAKE improves for both short (average: 73.13%) and long interactions (average: 73.65%). The differences between 10-second and 1-minute interactions were not found to be statistically significant, suggesting that SNAKE can reliably estimate quality from interactions with different duration. Figure 44(a-b) shows the confusion matrix of the SVM classifier. The misclassification mainly happens between adjacent ripeness classes, which can be mitigated by improving the granularity of the labels. Indeed, as the labels were assigned using clustering, the borders between adjacent labels are not clearly distinguishable. The results from regression experiments below further support this view, demonstrating consistently low error and good model fit.

Regression-based quality assessment: To obtain a more fine-grained estimate of SNAKE's potential for assessing produce quality, we performed regression experiments that assess the potential of thermal dissipation being able to estimate firmness, a key indicator of produce quality. As in the classification experiments,



(a) Long touch (b) Short touch (c) Long touch (d) Short touch

Figure 44: SNAKE performance by considering the thermal dissipation and produce type, (a)-(b) classification, (c)-(d) regression. Long touch/interactions (1min); Long touch/interactions (10sec)

Table 18: Regression predicting firmness (F); Features: Thermal dissipation time (T), Target dissipation slope (TS), Produce type (PU). –: misinterpretation

Sensing modality	Features	Day1/2	Day3/4	Day5/6	Day7/8	Day9/10	Day11/12	Day13/14	5-CV	
		RMSE	RMSE	RMSE	RMSE	RMSE	RMSE	RMSE	RMSE	R^2
Long interactions	**(T)**	0.263	0.285	0.274	0.304	0.321	0.330	0.344	0.293	–
	(T,PU)	0.141	0.080	0.060	0.072	0.095	0.125	0.135	0.092	0.895
Short interactions	**(TS)**	0.262	0.248	0.301	0.283	0.272	0.328	0.335	0.263	0.151
	(TS,PU)	0.085	0.098	0.089	0.091	0.090	0.085	0.141	0.084	0.913

we separately considered short and long interactions. Similarly, to the classification experiments, we focus on simple techniques as these would be easier to deploy in practical use: K-Nearest Neighbor (KNN), Support Vector Regression (SVR), and Random Forest (RF). As evaluation metrics we consider the average root mean square error (RMSE) which was calculated using two different cross-validation approaches: a 7-fold cross-validation where two successive days are combined into a fold, and a time-independent 5-fold cross-validation.

Table 18 shows the average root mean square error RMSE for each regression model and the R^2 score for each interaction. We can still observe poor performance when only considering the thermal dissipation, as the models cannot identify the characteristics of each produce. However, after adding the produce type information, SNAKE consistently performs well, capturing a high amount of variance (short interaction: RMSE=0.084, $R^2 = 0.913$). The performance between short and long interactions was similar, and no statistically significant differences were observed. Figure 44(c-d) also shows that the true values and predicted values are mostly distributed along a linear line, indicating accurate firmness estimation for SNAKE.

While the fit of the regression line is generally good, for some produce the errors remain somewhat higher which is mostly due to differences in produce surface characteristics. The most notable cases are the plum and the mandarin orange as can be seen from the variation around the diagonal. In Subsection 4.7 we demonstrate how to further improve produce estimation performance by harnessing information about palm temperature variations.

Table 19: Regression predicting firmness (F) and classification performance for baselines; Features: light value (L), CSI amplitude (A), Produce type (PU), –: misinterpretation.

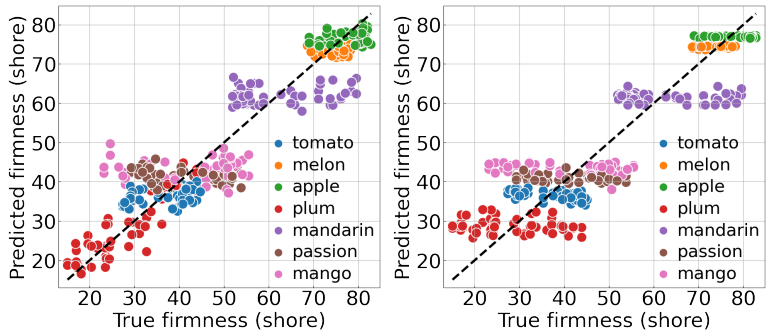
Sensing modality	Features	Day1/2 RMSE	Day3/4 RMSE	Day5/6 RMSE	Day7/8 RMSE	Day9/10 RMSE	Day11/12 RMSE	Day13/14 RMSE	5-CV RMSE	5-CV R^2	5-CV Classification
Optical sensing	**(L)**	0.282	0.230	0.260	0.268	0.286	0.295	0.334	0.262	0.155	44.72%
	(L,PU)	0.185	0.133	0.101	0.074	0.093	0.126	0.183	0.107	0.870	56.8%
Wireless sensing	**(A)**	0.245	0.240	0.277	0.286	0.309	0.327	0.352	0.294	–	47.45%
	(A,PU	0.172	0.135	0.083	0.061	0.079	0.146	0.191	0.119	0.842	52.13%

4.6.3. Comparison to baselines

We next compare SNAKE with state-of-the-art baselines leveraging optical and wireless sensing (see Subsection 4.5) and demonstrating the superior performance of SNAKE.

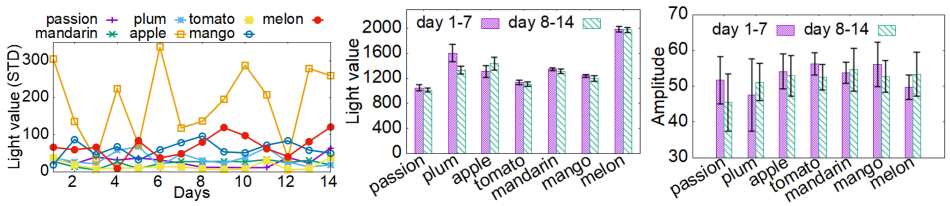
Table 19 compares optical sensing and wireless sensing against SNAKE. While all systems benefit from produce information, SNAKE consistently outperforms the baselines in both classification and regression tasks. In classification, optical sensing achieves an average accuracy of 56.8% whereas wireless sensing achieves an average accuracy of 52.13%, which is significantly lower than the $\approx 73\%$ classification accuracy achieved by SNAKE. For regression the findings are similar. Specifically, optical sensing achieves slightly better performance (RMSE = 0.107, $R^2 = 0.87$) than wireless sensing (RMSE = 0.119, $R^2 = 0.842$), but both baselines are significantly worse than SNAKE (short interactions: RMSE=0.084, $R^2 = 0.913$). When produce information is not available, the performance of SNAKE remains reasonable whereas the performance of optical sensing and wireless sensing drops considerably, explaining only $10-20\%$ of variation. This demonstrates that SNAKE achieves robust performance across different application scenarios, emphasizing the versatility and robustness of SNAKE compared to baselines. To better understand the performance of the baselines, Figure 45 shows the results of the regression experiments for both optical sensing and wireless sensing. Optical sensing performs well with produce that have clear surface changes, such as plum, whereas wireless sensing shows significant variations across all produce. In contrast, as we have shown, SNAKE operates consistently across most of the produce.

To gain deeper insights into the performance of optical sensing, Figure 46(a) illustrates the standard deviation of light reflection measurements over the 14-day data collection period. The deviation of the reflected light measurements remains relatively stable across the days, with the apple being the only exception. This variability can be attributed to significant changes occurring on the surface of the apple compared to other produce. Indeed, visual inspection of the collected images reveals substantial alterations in the surface color of the apple, with differences in pigmentation being the primary cause of variations in the light values. Figure 46(b) displays the mean absolute deviation for all produce. The measurements of the three samples of the same produce were averaged to obtain a more robust estimate



(a) Optical sensing (b) Wireless sensing

Figure 45: Fruit firmness estimation performance considering sensing information and produce type.



(a) Optical sensing (b) Optical sensing (c) Wireless sensing

Figure 46: a) STD from 3 samples per fruit, b) MAD of light values, e) MAD of wireless amplitude.

for each produce type. Subsequently, the data was divided into separate sets for the first and last seven days to estimate the average light values. The figure illustrates that the most significant changes occur for plum, whose surface softens during the decomposition process, while other produce show smaller variations in light measurements. Although optical sensing can track decomposition across different produce types, its overall performance is contingent on the sampled area of the produce. Since optical sensing utilizes a beam of light for sampling, a single sample may not sufficiently represent the overall quality. In contrast, SNAKE overcomes this limitation by sampling a larger surface area using natural human interactions.

We also conducted a similar analysis for wireless sensing. Figure 46(c) illustrates the mean absolute deviation for the low-frequency components of the CSI amplitude. The differences in the mean values between the first and last seven days can be more accurately quantified compared to optical sensing. However, we observed higher variations in the samples taken on different days. This suggests that while it is feasible to identify the produce to some extent, identifying its decomposition state and quality may be challenging. Wireless sensing requires a specialized measurement setup involving the physical deployment of transmitters and receivers, as well as stringent control of the measurement setup to ensure accurate estimations. Wireless sensing is also heavily influenced by the surrounding context, indicating impracticality for real-world deployments. In contrast, SNAKE utilizes heat transmitted from the user's hand to the produce. As the intervals of body temperature do not change considerably between individuals, SNAKE can be readily adapted for diverse contexts and interactions.

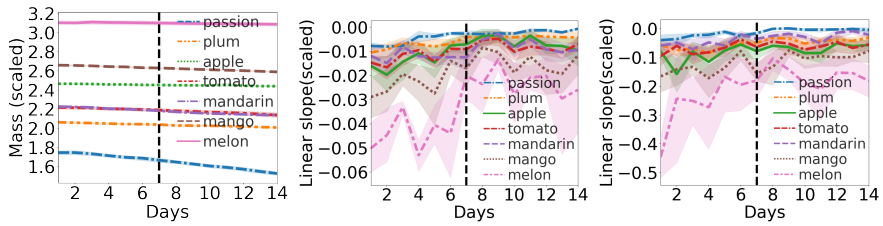
4.6.4. SNAKE and interactions with different duration

Our results thus far have demonstrated that SNAKE accurately estimates produce quality, outperforming state-of-the-art baselines. These results were obtained using interactions with a fixed duration (10 seconds or 1 minute), and generalizing to touch interactions with arbitrary duration is also essential for the practicality of SNAKE. In this subsection we further scrutinize short and long interactions, and demonstrate that using the slope of the thermal dissipation makes it possible to estimate produce quality from interactions with a different duration.

Table 20 analyzes the relation between linear slope (LS) estimate obtained from thermal dissipation measurements of long interactions and produce mass (M). In the analysis, we consider different windows for analyzing the dissipation time to understand the effect the duration of the thermal footage has on estimation. From the table, and as also illustrated in Figure 47, we observe that the longer the footage of dissipation, the stronger the relation between the linear slope and produce mass. The relationship saturates at around 40 seconds ($R^2 = 0.68$) with longer intervals resulting only in minor improvements. The weight of the regression is negative, which means that the speed of thermal dissipation (i.e., higher value of slope)

Table 20: Weight of variables to fit linear slope (LS) in long interactions. Variables: produce mass (M). Total means the thermal dissipation time.

Intervals	first 1s	first 5s	first 10s	first 20s	first 30s	first 40s	first 50s	first 60s	Total
M	-1.12	-3.85	-3.65	-3.64	-3.92	-4.08	-4.18	-4.23	-3.57
R^2	0.20	0.30	0.40	0.51	0.63	0.68	0.71	0.71	0.68



(a) All fruits (b) Long interactions (c) Short interactions

Figure 47: a) Fruit mass decreases over days, b) Linear slope with 95% CI for all items when considering the first 40s from the thermal dissipation, c) Linear slope with 95% CI for all items when considering the first 5s from the thermal dissipation

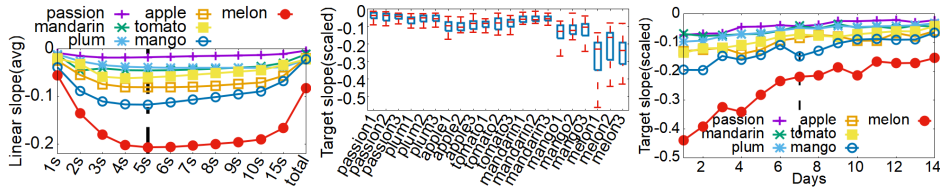
increases as produce mass decreases.

Table 21 shows the corresponding results for short interactions, considering dissipation intervals from 1 to 15s. Note that the analysis is done on the dissipation measurements induced by the interactions, which allows us to use a longer interval than what the interaction duration was (i.e., 10 seconds for short interactions). As with the long interaction data, the fit of the model improves with larger intervals. The model fit is good from around 5 second onward ($R^2 = 0.68$), improving until around 10 seconds, after which the fit starts to decline. As with the long interactions, the relationship between slope and produce mass is still negative, confirming consistency of the pattern, see Figure 47.

Interactions with short duration are easier to capture in practice, and we next analyze the 5 second dissipation intervals in more detail, see Figure 48(a). Overall, the first 5 seconds capture over 50% of the overall thermal dissipation compared to initial values. Therefore, estimates of produce quality can be obtained from thermal dissipation lasting at least 5 seconds. Despite its utility for produce quality estimation, the linear slope may exhibit local irregular oscillation for some fruits, such as melon in Figure 47(c). Figure 48(b) shows the target slope estimated from the first 5 seconds for all fruits in short interactions. We can observe that the different fruits have distinct slopes. We also verified (using Kruskal-Wallis tests) that these differences are statistically significant ($\chi^2 = 315.27$, $\eta^2 = 0.53$,

Table 21: Weight of variables to fit linear slope (LS) in short interactions. Variables: produce mass (M). Total means the thermal dissipation time.

Intervals	first 1s	first 2s	first 3s	first 4s	first 5s	first 6s	first 7s	first 8s	first 9s	first 10s	first 15s	Total
M	-7.45	-18.17	-23.67	-26.18	-26.65	-26.41	-25.93	-25.36	-24.63	-23.94	-20.47	-9.55
R^2	0.31	0.45	0.55	0.60	0.68	0.68	0.70	0.70	0.72	0.71	0.68	0.68



(a) Short interactions (b) Target slope (c) Target slope

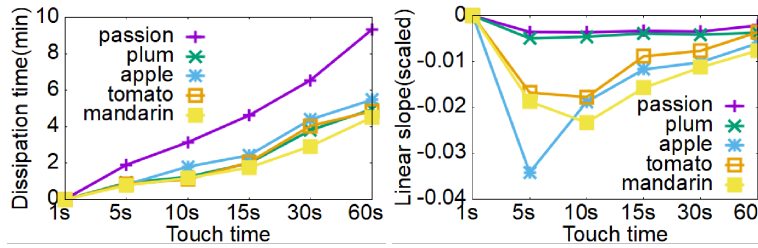
Figure 48: a) Average linear slope (scaled) in different time intervals of the thermal dissipation, b) Target slope over 14 days, c) Average target slope for all fruits.

$p < .05$). We used Friedman tests to compare samples of the same produce and with one exception the target slopes of distinct samples of the same produce were not significantly different ($p > 0.05$). The only exception is the melon, which is due to variations in palm temperature affecting the thermal transfer and consequently also dissipation patterns. We demonstrate this in Subsection 4.7 and also extend SNAKE by presenting a compensation model that overcomes this issue. Moreover, Figure 48(c) shows that the target slope follows similar trends as the firmness obtained by the durometer. The pattern of the target slope is also consistent with the linear slope analysis for all fruits. Overall, the results indicate that the target slope captures fruit decomposition accurately.

To demonstrate the use of the slope, we carry out a small-scale follow-up experiment where we consider a fresh set of produce covering the main categories (one sample per fruit type) and vary the touch time considering the following values: 1s, 5s, 10s, 15s, 30s and 1min. Figure 49(a) shows the average dissipation time with different touch periods. The differences between the fruits are consistent, and the dissipation values increase approximately linearly as touch time increases. The corresponding changes in the slope are shown in Figure 49(b). For fruits with a harder exterior, the slope is consistent across time, whereas those with a softer exterior absorb more thermal radiation and the speed of dissipation depends on the extent of radiation that is absorbed by the fruit. The saturation point comes between $5-10$ seconds, after which the magnitude of the slope consistently decreases. This effect is clearly also visible in the dissipation values and thus the slope and the dissipation values complement each other and support robust produce quality estimation with touch interactions having different durations. In Subsection 4.6.7, we demonstrate that this is sufficient also for practical scenarios, such as integration with a scale or a self-checkout kiosk.

4.6.5. Capturing internal produce quality

Tables 20 and 21 illustrate a strong relationship between the linear slope (LS) estimated from thermal dissipation and produce mass (grams) for both long and short interactions, particularly when considering a larger dissipation interval (e.g., 5 seconds in short interactions). Given that mass loss can impact produce quality, as discussed in Subsection 4.4.3, these findings demonstrate that SNAKE effec-



(a) Random touch duration (b) Random touch duration

Figure 49: Thermal performance with different touch interaction duration.

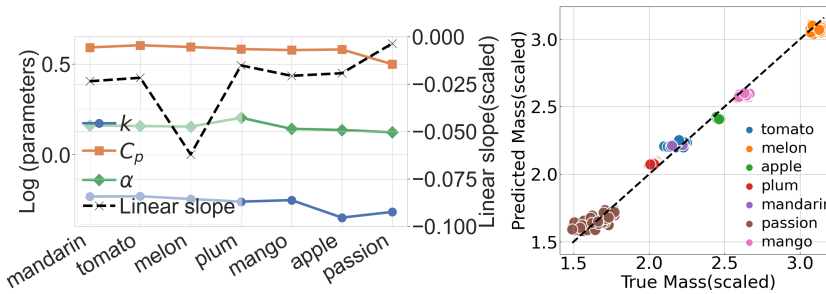
tively captures internal produce quality through LS measurements. Additionally, Figure 47 shows a clear correlation between changes in linear slope over days and variations in produce mass. As produce decomposes and loses mass, the thermal dissipation rate—indicated by the slope magnitude—declines. This decline occurs because key thermal properties, such as thermal conductivity (k), thermal diffusivity (α), and specific heat capacity (C_p), typically decrease during decay.

Figure 50(a) presents the correlation between the average linear slope and thermal properties based on typical values from the literature, as noted in Subsection 4.6.1. The linear slope, derived from the total thermal dissipation time in short interactions, consistently shows that weaker thermal properties (lower values) correspond to a lower thermal dissipation rate (smaller slope magnitude), with an average Kendall statistic of $\tau = -0.57$. While some fluctuations exist (e.g., for melon) due to variations in slope during dissipation that a single linear slope cannot fully capture, the slope is generally sufficient for estimating produce quality. Overall, these results indicate that the thermal dissipation rate (or slope) can serve as a reliable indicator of changes in internal produce characteristics and, consequently, produce quality.

We also utilized the target slope in short interactions to predict produce mass. After applying min-max scaling to the mass data, we achieved accurate predictions (RMSE = 0.044, $R^2 = 0.95$) using 5-fold cross-validated regression (Subsection 4.6.2) with target slope (TS) and produce type (PU), as shown in Figure 50(b). This performance can be further enhanced by incorporating palm temperature (RMSE = 0.037, $R^2 = 0.97$), as discussed in Subsection 4.7. These results reinforce the potential of using thermal dissipation for estimating produce quality.

4.6.6. Generality and further considerations

We next extend the analysis to a wider range of produce types to further demonstrate the generality of our results. We consider 14 produce types (7 types the same as the main study) as depicted in [498], which still covering the main 5 categories of produce: pepo (melon, watermelon, passion fruit), pome (apple, pear), berry (kiwi, tomato, banana, avocado), drupe (plum, peach, mango) and hesperidium (mandarin, lemon). Pepo and hesperidium fruits generally have a thick epicarp,



(a) Thermal properties (b) Mass prediction

Figure 50: Short interactions: a) Relationship between thermal properties and the linear slope, thermal conductivity k, thermal diffusivity α, and specific heat capacity C_p. b) SNAKE performance, target slope calculated from the first 5 seconds of thermal dissipation.

pomes have a moderately thick epicarp, while berries and most drupes have a thin epicarp. All the new fruits are initially in a fresh and edible state without signs of decomposition. For generality analysis, two samples are still considered for each produce (S1 and S2). Thus, in total 28 fruits are used in the experiment with various shapes and sizes (even the same type). The testbed and measurement remain the same as in Subsection 4.5. However, only short interactions (10sec touch) are considered. This study is conducted over a year separate from the main experiment, providing evidence of the generality of SNAKE.

The majority of fruits still exhibited a decrease in firmness over two weeks; however, passion fruit and mandarin follow the main study's trend, and the new lemon aligns with mandarin's pattern. Figure 51 shows the target slope estimated from the first 5 seconds for all fruits in short interactions. We can still observe the distinct slopes of different produce and Kruskal-Wallis tests further verify that the differences are statistically significant ($\chi^2 = 274.14$, $\eta^2 = 0.69$, $p < .05$). Besides, Wilcoxon rank-sum tests demonstrate that SNAKE exhibits no significant differences between distinct samples of the same produce ($p > 0.05$). Figure 52 shows a similar target slope trend across all fruits, with Figure 52(a) indicating consistent slopes across different study periods. Statistically, Kolmogorov-Smirnov tests confirm that there is no significant distributional differences in target slopes between the experiment and the main study ($p > 0.05$). This indicates the long-term effectiveness and reliability of SNAKE. Moreover, fruits with hard epicarps, such as pepos, tend to show greater variability in target slope during decomposition than those with thin epicarps, like berries and drupes. Overall, these results strengthen the generalization of SNAKE.

4.6.7. Other factors

As the final step, we demonstrate that SNAKE generalizes across different considerations: individuals, storage practices, backgrounds and practical usage. We select

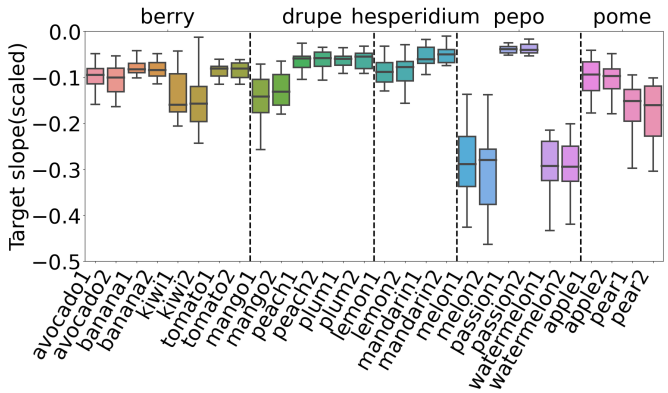
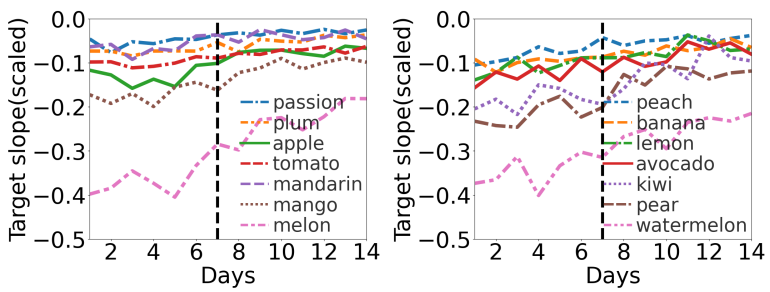
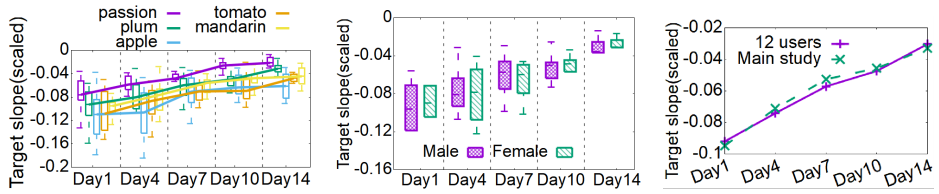


Figure 51: Target slope of each produce in short interactions



(a) (b)

Figure 52: Average target slope for all fruits in short interactions



(a) All participants (b) plum (c) plum

Figure 53: Target slope: a) Different participants; b) Genders; c) The main experiment and user studies.

a small set of representative produce (mandarin orange, plum, apple, passion fruit, and tomato) from each category to further analyze SNAKE. The testbed follows the design described in Subsection 4.5. The interaction time was set to 10 seconds.

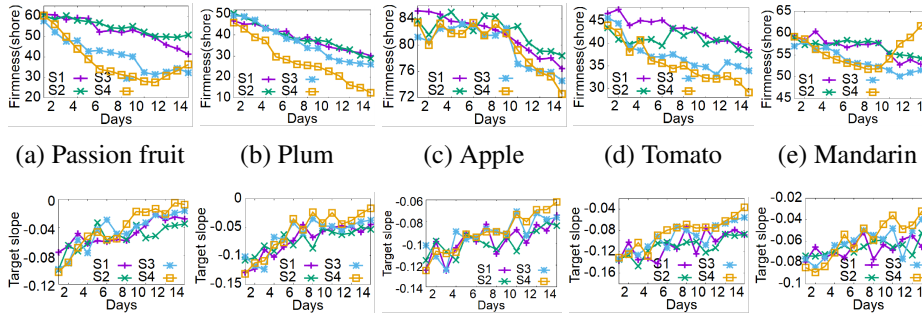
Other users: We recruited 12 participants (6 female and 6 male) to assess the generality of SNAKE across different users. Measurements were collected on 5 different days within a two-week period at days $1, 4, 7, 10$ and 14. The average palm temperatures of the participants were 32.01 ± 2.09 °C (male: 32.26 ± 1.96 °C, female: 31.78 ± 2.2 °C). Figure 53(a) shows the target slope (TS) of fruits across all participants over 14 days, and we can observe a similar trend as in our main experiments. This indicates that SNAKE can estimate fruit quality accurately across different users. Figure 53(b) shows the target slope of the plum as an example between male and female participants. We can observe the relative trend is also consistent across genders. A Wilcoxon signed rank test using genders showed no significant differences in the target slope across different days for all the fruits ($p > .05$). Kolmogorov-Smirnov tests further verify that the distribution of target slope is not statistically different ($p > .05$) between the main experiment and our case study (passion fruit: KS=0.4, plum: KS=0.2, apple: KS=0.4, tomato: KS=0.4, mandarin:KS=0.4), see Figure 53(c) with plum as an example. This verifies that the models only depend on produce category and decomposition state, demonstrating the consistency of SNAKE across different individuals.

Storage practices: The preservation time of fruits can be prolonged by wrapping them inside a protective film or keeping them refrigerated. We next assess how these practices affect SNAKE performance within two weeks. We rely on four new samples (S1, S2, S3 and S4) for each produce (see above) and use them to measure four different experiment conditions considering combinations of protective film (on/off) and storage (refrigerated, 5°C, or ambient room temperature, around 23°C): S1 (5°C+no film), S2(5°C + film), S3 (23°C+film), and S4 (23°C+no film). The relative humidity in the fridge is $48.25 \pm 2.49\%$ higher than the room humidity. 5°C is chosen as we observe that some produce types are stored in the cooling system around this temperature from the local supermarkets. Produce in the refrigerator was taken out and held by the hand for 10s at the ambient room temperature. Next, the produce was placed back in the fridge for thermal footprint measurement. The film was removed to take measurements, and then the fruit was

wrapped in a new film for each experimental instance.

Figure 54 shows the changes in firmness and target slope for the fruits over the 14 days. The pattern of target slope across days is similar between the fridge and room, although the slope increases slower when the produce is in the fridge. This indicates that SNAKE works well even in very low temperatures. In addition, the results are as expected. Specifically, the protective film and refrigeration slow down decomposition and these effects can be captured using SNAKE. Figure 55(a) further demonstrates less variation in target slope for all fruits (average standard deviation: S1=0.017, S2=0.014, S3=0.022 and S4=0.027) with film and refrigeration, which aligns with the lower variation in firmness changes (average standard deviation: S1=4.10, S2=3.19, S3=5.17 and S4=6.53) shown in Figure 54(a-e). This indicates that SNAKE can perform consistently for produce quality estimation across different conditions. Friedman tests also reveal significant differences in target slope among the four conditions ($\chi^2 = 17.74$, $W = 0.42$, $p < .05$). Even though the apple itself generally has a long shelf life, SNAKE accurately detects subtle variations in target slope under film and refrigeration (standard deviation: S1=0.013, S2=0.011, S3=0.015 and S4=0.018), comparable to the ground-truth firmness (standard deviation: S1=2.8, S2=2.2, S3=3.0 and S4=3.5) shown in Figure 54(c). Indeed, refrigeration results in higher relative humidity than room temperature. The combination of lower temperature and higher relative humidity can minimize moisture loss and preserve produce freshness longer [177]. Wilcoxon Rank-Sum tests also demonstrate the significant differences of storage temperatures ($\chi^2 = 2001$, $p < .05$), indicating better freshness preservation due to refrigeration. In addition, 55(a) reveals a greater median slope amplitude under low temperatures for all produce (refrigerator: average $median = -0.079$, room: average $median = -0.068$). This observation aligns with Newton's Law of Cooling, which states colder environments accelerate thermal dissipation.

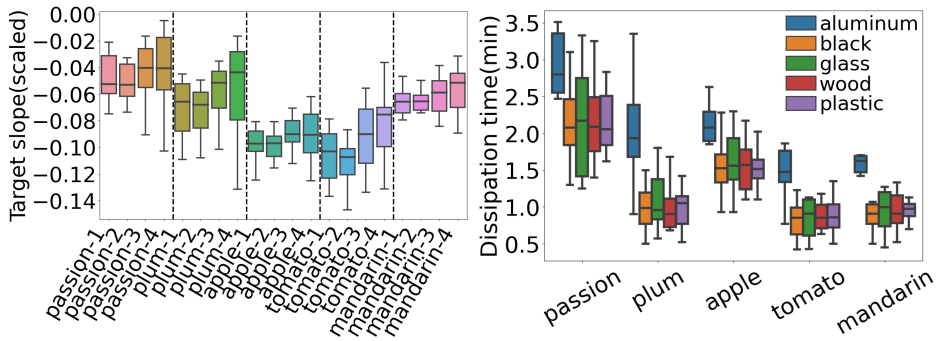
Similarly, protective films can enhance produce freshness with larger median slope amplitudes, particularly for thin-skinned fruits, e.g. plum (film = -0.052, no film =-0.043) and tomato (film =-0.052, no film =-0.043) at room temperature. These fruits are highly susceptible to moisture loss due to their permeable skins, which plastic wrap can mitigate. Consequently, plastic wrap is commonly used on cut fruits, as their exposed flesh leads to even faster moisture loss. While mandarin's thick peel offers some protection, it remains vulnerable to moisture loss and hardening at room temperature due to pores and oil evaporation. Consequently, plastic films significantly slow these processes (film: median = -0.058, no film: median = -0.051), a trend mirrored in firmness changes observed in Figure 54(e). As demonstrated in 55(a), plastic films significantly improve freshness at room or higher temperatures, but their effect is diminished under refrigeration. Nonetheless, the observed results (S1 and S2) still indicate a residual benefit. Therefore, the combination of refrigeration and protective film is the most effective at preserving fruit quality as the variations quantified through the target slope are marginal. The effect of storage practice on SNAKE is evaluated still using



(a) Passion fruit (b) Plum (c) Apple (d) Tomato (e) Mandarin

(f) Passion fruit (g) Plum (h) Apple (i) Tomato (j) Mandarin

Figure 54: Target slope for different conditions. S: Sample; S1 (5°C+no film), S2(5°C + film), S3 (23°C+film), and S4 (23°C+no film).



(a) 1-min touch (b) 10s touch

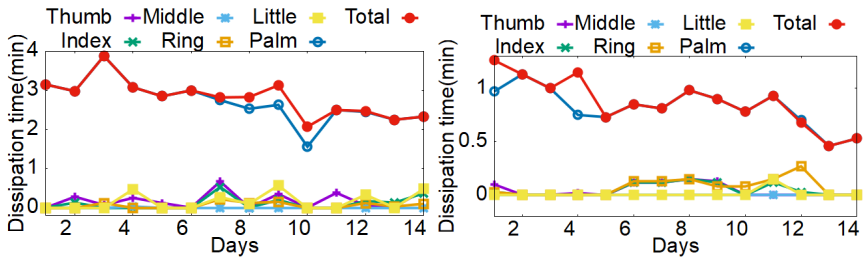
Figure 55: a) Target slope for different conditions. 1 (5°C+no film), 2(5°C + film), 3 (23°C+film), and 4 (23°C+no film). b) Thermal dissipation time in different background.

the same 5-fold cross-validated regression and classification models as shown in Subsection 4.6.2. The input features are target slope (TS), produce type (PU), environment or storage temperature (E) and protective film (F). Results showed that incorporating storage features can incrementally improve average performance: TS+PU (RMSE=0.074, $R^2 = 0.90$, accuracy= 74.7%), TS+PU+E (RMSE=0.065, $R^2 = 0.92$, accuracy=80.4%), TS+PU+E+F (RMSE=0.062, $R^2 = 0.93$, accuracy= 81.2%). Note that the best performance is achieved (RMSE=0.057, $R^2 = 0.95$, accuracy 84.3%) when further adding the palm temperature feature, as depicted in Subsection 4.7. These results are in line with current knowledge and highlight how SNAKE generalizes. Furthermore, this result also suggests that SNAKE can be used to analyze the effectiveness of storage strategies.

Effect of background in thermal footage: The amount of thermal radiation that is captured by a thermal camera depends on the *emissivity* (ε) of the background material which corresponds to the fraction of thermal radiation that the material

transfers back to the environment. Materials with low emissivity only transfer a small amount of thermal radiation to the environment, but they can reflect heat from objects in their vicinity. Our main study considered a black background which has a high emissivity ($\varepsilon \approx 1$), i.e., it eliminates thermal radiation from the environment. In retail shops the background may vary, resulting in differing emissivity patterns. For example, metal surfaces commonly have low emissivity ($\varepsilon < 0.1$), i.e., they reflect thermal radiation from objects in the environment, whereas high emissivity materials mostly are matte surfaces made of other materials than metals [204, 397], e.g., aluminum foil ($\varepsilon \approx 0.04$), concrete($\varepsilon \approx 0.94$), glass ($\varepsilon \approx 0.94$), wood ($\varepsilon \approx 0.90$), plastic ($\varepsilon \approx 0.96$) and paper ($\varepsilon : 0.91 - 0.95$). Most organic produce also have a high emissivity (>0.95) due to water content of the produce [173, 456]. For example, the emissivity of the apple is in the range $\varepsilon : 0.94 - 0.97$. The emissivity value can usually be specified manually in the camera settings, or the camera can perform periodic self-calibration to estimate the emissivity of the background. To assess the effects of differing backgrounds, Figure 55 (b) compares thermal dissipation times from measurements of 6 participants (5 males and 1 female) across five different backgrounds (aluminum, black background as in the main study, glass, wood, and plastic). The dissipation patterns are mostly consistent and in line with our experiments, with the only exception being the aluminum background. This indicates that SNAKE can operate robustly against most backgrounds, but highly polished background materials such as aluminum may cause difficulties, and the background should be considered when deploying SNAKE in retail environments.

Practicality: SNAKE has been designed to aid sustainable retail practices for produce during the retail experience. One way to accomplish this in practice is to integrate SNAKE into a product scale or a self-checkout device, as illustrated in Figure 41. To verify the integration would also be feasible in practice, we collected observations from the field by recording the time the consumers used for weighing produce on a scale. The measurements were done using shadowing and carried out in a local supermarket. Generally, when the consumer places the produce on the weight scale, the produce remains still while the user selects the appropriate label from the scale's screen. We used a time application to measure how much time this takes on average, to assess whether there would be sufficient time to estimate the thermal fingerprint of the produce. 50 observations from consumers' weighing times were recorded (male: 23, female: 27). All produce weighing processes were natural without any interference or interruption from the researchers. One outlier (47.95s) was removed for more robust statistical analysis. The average weighing time was 8.55 ± 4.24s, i.e., there would be $4 - 12$ seconds to capture the thermal footprint. As shown by our experiments, this is sufficient for SNAKE to estimate fruit quality.



(a) 1-min touch (b) 10s touch

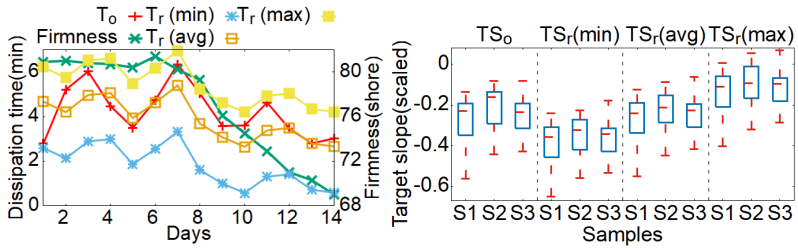
Figure 56: Dissipation time of melon in different parts of the hand. Total: thermal fingerprints of the whole hand, i.e., palm and fingers.

4.7. Reducing palm temperature fluctuations

Thermal transfer from the hand to the produce is influenced by the contact between the hand and the produce. When humans touch objects, the touch patterns vary depending on the type of produce and which parts of the hand are in contact with the produce. Additionally, the skin temperature varies between different parts of the hand, with fingers tending to be colder than the palm. These variations can cause fluctuations in thermal transfer and affect the thermal dissipation process. We next illustrate the extent of these variations and introduce a palm compensation model that can be used to mitigate their effects.

Thermal transfer and touch patterns: Figure 56 depicts the variation in thermal dissipation times alongside the skin temperature between the palm ($32.11 \pm 1.40°C$) and fingers ($31.84 \pm 1.47°C$). Although the temperature variance between the palm and fingers is minimal, the lower pressure applied by the fingers leads to reduced thermal transfer compared to the palm [464]. Therefore, the part of hand that touches the produce influences thermal dissipation, and ultimately produce quality estimation accuracy, and thermal dissipation should be estimated from contact with the palm whenever possible. This information can be obtained by examining the size of the initial thermal footprint (i.e., the size of the region of interest) or using computer vision.

Quantifying effect of palm temperature: Figure 57 illustrates variations in thermal characteristics as a function of palm temperature. On the left-hand side, we compare how variations in palm temperature affect the estimated thermal dissipation and its relationship to produce firmness using data from a single apple sample collected over a 14-day period. On the right-hand side, we present the target slope estimates for thermal characteristics derived from three different melon samples over the same 14-day measurement period. From the left-hand figure we can observe that temperature fluctuations decrease correlations between produce firmness and thermal dissipation, whereas using a reference model (i.e., the averaged measurements) results in a consistently high correlation between thermal dissipation and produce firmness. The right-hand side figure similarly



(a) Long interactions: apple (b) Short interactions: melon

Figure 57: Temperature compensation (max, min, avg). T_o: original dissipation time, T_r: reference dissipation time, TS_o: original target slope, TS_r: reference target slope.

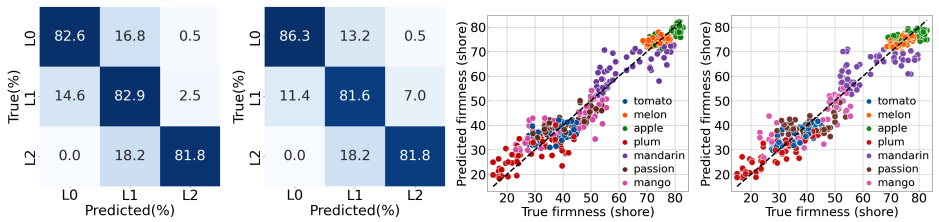
shows that slope estimates obtained from individual interactions can fluctuate more than when a reference model (i.e., $TS_r(avg)$ in the figure) is considered. The idea in our compensation model is to reduce these effects by mapping the thermal dissipation measurements to a reference temperature where consistent estimation of thermal dissipation and other thermal characteristics is possible.

Palm compensation model: To address fluctuations in palm temperature, we employ a calibration model that links the estimated thermal dissipation DP_o to a compensated dissipation value DP_r which approximates the thermal dissipation expected at a specified reference palm temperature P_r. Formally, let P_o be the palm temperature of the user; our compensation model approximates the difference in thermal dissipation times between the observed and reference conditions using differences in palm temperature. Specifically, the compensation model for each produce type is defined as $(DP_r - DP_o) = f(P_o - P_r)$ where $(\cdot)$ is the calibration function. We model the relationship using ordinary least squares (OLS) regression and assume the relationship is linear, i.e., $(DP_r - DP_o) = W_p * (P_o - P_r) + C$ where W_p is a weight parameter and C is a constant. For the purposes of this subsection, we estimate this model from controlled laboratory samples, but in practical deployments, the model can also be learned automatically by using pre-defined palm temperature values as references and comparing thermal dissipation values against this reference. As produce type affects thermal dissipation, we learn the model separately for each type of produce.

Boosting quality estimation: As the final step, we demonstrate that the palm compensation model enhances the performance of SNAKE. We consider the same machine learning models as in Subsection 4.6.2. For classification, the accuracy improves by approximately 9% and is consistently high for both long (average: 81.88%: 79.55% RF, 82.66% SVM, and 83.42% MLPC, 82.81%) and short interactions (average: 82.14% RF, 85.45% SVM and 80.86% MLPC). As with our earlier experiments, the differences between short and long interactions are not statistically significant, demonstrating robustness of the compensation values against variations in touch interaction duration. The results for different produce also are similar and

Table 22: Regression predicting firmness (F) for HIPPO; Features: Thermal dissipation time (T), Target dissipation slope (TS), Palm temperature (P), Produce type (PU).

Sensing modality	Features	Day1/2 RMSE	Day3/4 RMSE	Day5/6 RMSE	Day7/8 RMSE	Day9/10 RMSE	Day11/12 RMSE	Day13/14 RMSE	5-CV RMSE	5-CV R^2
Long interactions	**(T,P,PU)**	0.125	0.073	0.058	0.076	0.074	0.098	0.110	0.076	0.935
Short interactions	**(TS,P,PU)**	0.115	0.106	0.076	0.081	0.072	0.079	0.121	0.081	0.925



(a) Long touch (b) Short touch (c) Long touch (d) Short touch

Figure 58: SNAKE performance boosting by palm temperature, (a)-(b) classification, (c)-(d) regression. Long interactions (1min); Short interactions (10s)

produce with harder epicarp tends to have higher performance than other fruits: passion fruit 84.28%, plum 79.29%, apple 80.35%, tomato 82.92%, mandarin 83.02%, mango 85.07% and melon 87.86%.

Figure 58(a-b) shows the confusion matrices for the SVM classifier, which was the best performing classifier in our experiments. From the matrices we can observe that the accuracy is consistently high across the ripeness classes, demonstrating that the palm compensation also improves robustness of SNAKE. The results of regression experiments, summarized in Table 22, similarly show improvements in performance. Both the average RMSE (0.081 for short interactions) and model fit ($R^2 = 0.92$) improve when the palm temperature is utilized. In terms of measurement day, we observe no statistically significant differences across the 14-day period, and we also found no statistically significant differences between the duration of short and long interaction. Finally, in Figure 58(c-d) we can observe that the compensation model improves the correspondence between the firmness of the product and the thermal dissipation time since the measurements closely approximate a linear trend, whereas our earlier results showed that some types of product result in more significant deviations from a linear trend.

In conclusion, when the thermal camera can be used to estimate palm temperature prior to interaction, the accuracy of produce quality estimation provided by SNAKE can be further enhanced by integrating our palm compensation model into the system. As the experiments show, the palm compensation model improves consistency across produce types, while at the same time improving estimation accuracy.

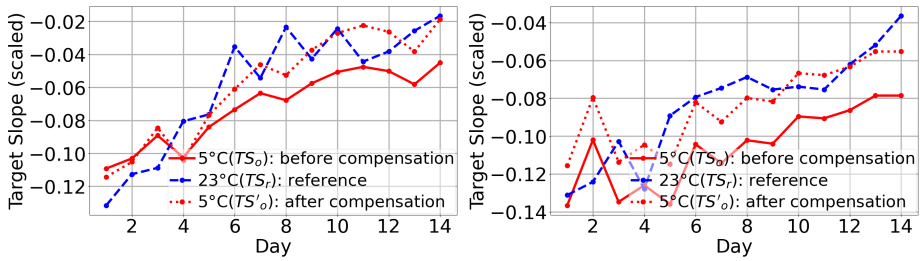
4.8. Reducing environment temperature fluctuations

In a typical retail setting, fresh produce is stored in two primary temperature zones: ambient (room) temperature and refrigerated temperature. The former is maintained by the store's HVAC (heating, ventilation, and air conditioning) system for a stable thermal environment throughout the store. The latter, on the other hand, is regulated by dedicated cooling systems to maintain a consistently lower temperature. Therefore, we can mainly consider two storage temperatures to explore the environmental impact on thermal dissipation. We analyzed SNAKE's performance under refrigerated (5°C) and ambient room temperature (approximately 23°C), as results shown in Subsection 4.6.7. Figure 55 (a) demonstrates that SNAKE effectively distinguishes between these conditions, showing larger average slope amplitudes for all produce at lower temperatures. This observation aligns with Newton's Law of Cooling, which states colder environments accelerate thermal dissipation. Thus, from a physics perspective, the target slope TS_o at one temperature E_o (e.g., 5°C) can be adjusted based on the reference slope TS_r at another temperature E_r (e.g., 23°C).

Environmental compensation model: We develop a nonlinear compensation model to account for environmental variations based on the temperature difference E_{diff}: $TS_r = \frac{TS_o - k*E_{diff}}{1+\beta*E_{diff}}$, where $E_{diff} = E_r - E_o$, and k, β are calibration constants. The numerator offsets the direct effect of temperature shift by subtracting $k * E_{diff}$. However, since linear correction alone may not fully capture the nonlinear behavior of environmental heat exchange, an additional correction factor $(1 + \beta * E_{diff})$ is applied in the denominator to scale the effect of environmental temperature correctly. This term is inspired by Newton's Law of Cooling, which describes how the cooling rate depends on the surrounding environment. Once the compensation equation is applied, we obtain the compensated target slope $TS_o^{'}$. Since our prior results indicate that environmental factors impact the thermal dissipation uniquely for each produce type, we still learn the model separately for each type of produce.

Result: Figure 59 illustrates the environmental temperature compensation for plums and tomatoes as examples, using room temperature (23°C) as the reference. The initial gap between the original TS_o and reference TS_r target slopes highlights the impact of environmental temperature variations. However, after applying the compensation model, the corrected slopes $TS_o^{'}$ closely align with the reference values TS_r, demonstrating that SNAKE maintains consistent performance across different environments. Results in Subsection 4.6.7 also show that adding environment temperature (E) feature improves the classification accuracy (80.5%) compared to using only target slope (TS) and produce type (PU) with 74.7% accuracy. In practical applications, the model's coefficients can be fine-tuned to accommodate variations in retail-specific ambient and refrigerated temperatures.

Currently, we use single compensation models to adjust the target slope effectively based on ambient temperature and palm temperature separately, demonstrating that both factors influence produce quality estimation. However, their



(a) Plum (b) Tomato

Figure 59: Environmental compensation, TS_o: original target slope, TS'_o: compensated target slope, TS_r: reference target slope.

combined effect requires a more sophisticated model for accurate representation. To accurately capture their interaction on produce quality, we still consider the machine learning models, see Subsection 4.6.2. The performance is further improved (RMSE=0.06, $R^2 = 0.937$, accuracy=82.5%) when considering these four parameters: target slope (T) and produce type (PU), environmental temperature (E) and palm temperature (P). This demonstrates that both ambient and hand temperatures jointly influence the target slope in produce quality assessment.

4.9. User study

We finally quantitatively evaluate SNAKE against traditional manual inspections through a comprehensive experiment using short interactions. This study aims to demonstrate how our device can improve consumer purchasing decisions, reduce retail food waste and provide potential economic benefits that justify its adoption in retail.

Application: We developed an Android mobile application on the thermal phone to assess produce quality by analyzing thermal radiation, see Figure 60b. The application is based on the model developed in our main study (short interactions) and we envision integrating the application into the retail weighing scale system. The application workflow involves two steps. When users choose a fruit and place it on the scale, they press "Select a fruit" in the app to capture thermal data and process it. After choosing the produce type (e.g., "apple"), the app classifies its quality into three intuitive levels: Fresh (L0), Not fresh but Edible (L1), and (Near) rotten (L2), helping consumers make informed purchasing decisions. These levels are still coarse-grained to make the content consistent. Note that these labels differ from the technical classification in Subsection 4.6.2—Fresh (L0), Active Decay (L1), and Advanced Decay (L2)—but were adapted for better user comprehension while maintaining equivalence in meaning.

Testbed: Figure 60a illustrates our deployment setup, where the thermal phone is integrated into a 3D-printed design that enhances the standard capabilities of a retail-scale appliance [91]. The scale surface is covered with a black background to

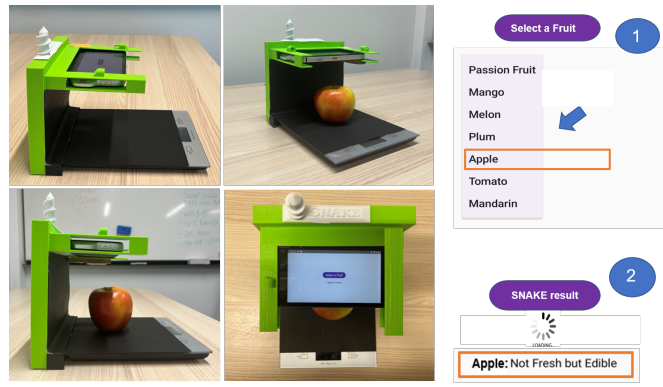


Figure 60: SNAKE augmenting common scale appliances. a) Integration using a 3D-printed design prototype, b) User interface and application usage.

minimize the influence of ambient environments. This setup emulates real-world purchase scenarios: users select a produce, place it on the scale, and receive a quality assessment via the app (similar to receive a price label). The automated nature of the system reduces the reliance on subjective human judgment and helps standardize fruit quality evaluation, which can be beneficial in minimizing food waste and improving overall sales.

Study design: The study was conducted over two weeks in different areas within the same campus building (see Subsection 4.3), where ambient temperature remained consistent with the app model's conditions. We evaluated seven produce types as in Subsection 4.5, with two new samples each labeled S1 and S2. Participants were divided into two groups: Group-1 using sample-1 (S1), and Group-2 using sample-2 (S2). Using two samples for each type could reduce the potential for human-induced variations in produce quality, leading to more reliable results than a single sample.

- Group-1 (App-first): Participants first assessed produce quality using the app and then manually inspected the produce with their own habits. In the manual inspection, they were asked to classify each item into one of the three coarse-grained ripeness levels (Fresh, Not Fresh but Edible, (Near) rotten) for comparison.
- Group-2 (Manual-first): Participants performed manual inspection first, followed by app-based evaluation.

After each item evaluation (app/manual), participants were asked: (1) *"Shall we proceed with purchase?"* (YES/NO); and (2) if NO, *"Would you proceed if a discount was offered?"* (YES/NO), with the option to specify a preferred discount if YES. These questions aimed to evaluate how the app influences consumer behavior and purchasing decisions, which are key factors in determining its economic feasibility. The study was conducted over five measurement days (Days 1, 4, 7, 10, and 14), with produce freshly sourced at the start and stored consistently in the same

room between survey periods. Each measurement day involved 20 new participants (10 per group), leading to a total of 100 participants (59 males, 41 females, ages 26.75 ± 6.74). Participant data was recorded anonymously. Before the study, participants were briefed on the study goal and app usage. After completing the experiment, they participated in a short interview to assess user perceptions. The post-study questionnaire (below) included five closed-ended questions on a five-point Likert scale—Questions 1-4 (Strongly Agree to Strongly Disagree), while Question 5 (Very Likely to Very Unlikely)—along with an open-ended question for additional feedback. Durometer was still used to capture the ground truth (firmness) over the two weeks.

1. *Do you agree with this statement "I often buy fruits"?*
2. *I am familiar with fruit quality testers in supermarkets, like the avocado tester.*
3. *Would this device enhance your fruit-buying experience?*
4. *Do you think this device offers valuable insights into the quality and freshness of fruits?*
5. *Would you use this device if it were available in stores?*
6. *As mentioned, this device uses heat transferred from your hand to estimate fruit quality. Would you have any concerns about how this data is used?*

Results: We first analyzed the agreement rate between app-based and manual classification to determine how often users aligned with the app's labels. The results showed a higher correspondence in group-1 (74.28%) than in group-2 (49.14%), indicating that the app influences human assessments by at least 25%, with most misalignment occurring between adjacent quality levels in group-1. The agreement rate in group-1 was particularly high for fruits that are difficult to evaluate based on visual appearance, such as apple (82.01%), melon (82.04%), and mango (86.03%), whereas group-2 showed significantly lower agreement for these fruits (apple: 58.01%, melon: 48.04%, mango: 62.03%). This suggests that participants in group-1 relied more on the app, prioritizing internal quality over external appearance, as SNAKE captures internal attributes that may not be visually apparent. However, for fruits that undergo visible decomposition, participants tended to trust their own perceptions over the app's assessment. A key example is passion fruit, which wrinkles easily but remains of good quality. Despite this, many participants still perceived it as inedible even on day-1 of purchase, consistent with the findings discussed in Subsection 4.3.1. However, the agreement rate for passion fruit in group-1 (56.05%) was still notably higher than in group-2 (28.05%), highlighting the app's impact on user decision-making in produce quality assessment.

We also assessed the app's impact on purchase decisions by comparing "YES" responses to *"Shall we proceed with purchase?"* across both groups. The app increased the overall purchase rate (73.6%) compared to manual inspection (69.1%), with the most notable increase observed in purchases of "Not Fresh but Edible"

produce (app: 60%, manual: 54%), while almost none occurred for "(Near) rotten" produce. Although the app positively impacts sales, the overall increase remains moderate, as its influence on human perception in group-1 results in similar purchase rates for both methods (app: 72%, manual: 71.71%). However, a significant difference is observed in group-2, where the app leads to a higher purchase rate (app: 75.14%, manual: 66.28%), particularly for produce classified as "Not Fresh but Edible", where the app reduces the rejection rate by at least 10% (app: 60.5%, manual: 50.1%). This suggests that the app helps consumers make more informed choices by encouraging the purchase of produce that is still edible while not fresh.

We further analyzed discount acceptance behavior by examining the percentage of initial “NO” responses to purchasing that changed to “YES” when a discount was offered. The results show that more "Not Fresh" fruits were accepted through discounts in both groups, with a higher promotion rate using the app (42.51%) compared to manual inspection (27.69%), indicating a 15% greater acceptance of discounted produce when using the app. This highlights the app’s role in reducing food waste by encouraging the purchase of still-edible produce. This trend was consistent across groups (group-1: app 45.5%, manual 30.6%; group-2: app 39.8%, manual 24.7%), suggesting that group differences had little impact. Additionally, discount preferences remained similar across methods, with median values (both methods: 30%) and mean values (app 32% and manual 36%), with participants generally favoring discounts between 15% and 50%. Overall, incorporating the app and discounts increased fruit sales by 88%, compared to 77% using manual inspection and discounts alone. This suggests that SNAKE has the potential to reduce produce waste by at least 10%, with the highest reduction reaching 15% (app: 90%, manual: 74%) in group-2, where user perceptions are less influenced by the app.

Finally, we compared both methods against the ground truth. Overall, SNAKE significantly outperforms manual inspection, achieving an accuracy of 81.4% compared to 61.9% for manual assessment. Performance was consistent across groups (group-1 80.3% and group-2 82.5%), while manual inspection in group-1 (68%) outperforms group-2 (55.7%), suggesting that prior app interaction positively influences users’ manual assessment. Note that the app accuracy can be further enhanced by integrating palm temperature measurements, which could be seamlessly automated in retail environments using built-in thermal or temperature sensors. The post-study questionnaire demonstrates that most participants (82%) made independent purchase decisions for reliable assessments. 85% of participants agreed that the device enhances their fruit-buying experience, and 84% found the insights valuable for assessing freshness. Additionally, 92% expressed willingness to use the device in retails, indicating strong potential for adoption. Although only 12% of participants were familiar with existing supermarket fruit testers (e.g., avocado testers), most were open to adopting new technology for produce quality estimation. Importantly, concerns about data usage were minimal, with

90% of respondents stating they had no significant privacy concerns. For example, participant P64 said that *"this technique inspires sustainability and I would love this product"*, and P17 mentioned that *"this technique can help me evaluate the fruits like melon, which cannot be assessed visually"*. However, some concerns remained. P75 mentioned that *"there should be a balance between the data privacy and technology advancements for trustworthiness and transparency"*. P34 worried that *"hand heat data could potentially be misused to infer medical conditions"*, and P62 also said that *"I am concerned about the possibility of fingerprints being captured"*. Overall, these findings highlight SNAKE's practicality and strong consumer acceptance, with the potential to enhance confidence in fruit selection while reducing retail food waste.

4.10. Discussion

Extensions: The presence of fresh produce on supermarket shelves invites interactions from customers, which can potentially accelerate natural decomposition. Integrating SNAKE can assist retailers in maintaining a desired standard level and mitigate the impact of customer handling produce. Repeated or prolonged touching, also referred to as the multiple touch effect, over extended periods (e.g., two weeks) could potentially affect fruit quality due to heat accumulation. We are also interested in exploring how this might affect SNAKE performance. Furthermore, the capabilities of SNAKE can be extended to simultaneously evaluate multiple produce at a time, such as those held in both hands. This extension requires employing additional steps in the analysis, e.g., we can identify centroids of the hottest regions from the thermal footage, as done in previous work [90], and apply SNAKE separately on each region. Another potential extension is to extend SNAKE to outdoor scenarios, e.g., outdoor markets or farms. If the outdoor temperature is higher than that of the hands, using touch interactions may no longer be feasible. In this case we can harness sunlight and temporarily block sunlight to estimate dissipation patterns. Our prior work has demonstrated the potential of this strategy for outdoor litter detection [467], and the same principles could be extended to produce.

Produce with small or uneven surfaces: In our main study, SNAKE can assess the quality of passion fruit accurately (e.g., 84.28% in short interactions), even as its surface wrinkles and becomes irregular during ripening with evolving textures. However, certain produce with highly uneven or hazardous surfaces (e.g. pineapple and cactus fruit) may not be suitable for SNAKE. Similarly, smaller organic produce, such as grapes attached to vines, are not suitable for SNAKE as it requires a sufficiently large surface area to obtain a representative sample for quality analysis. Indeed, as our experiments demonstrated, small contact surfaces (such as from the fingers) do not transfer sufficient heat and this also applies to small produce. Besides fruits, fresh produce also includes a large diversity of vegetables. Unlike fruits, vegetables have additional characteristics that require fine-tuning SNAKE

before it can be used on them. For instance, vegetable can be leafy, thin and have uneven surfaces. When the produce is placed on an even surface, such as a scale or checkout kiosk, a potential way to overcome this is to induce a thermal signature on the produce, e.g., using an infrared light source and then use SNAKE on this fingerprint.

Other produce and storage practices: Our experiments demonstrated accurate and robust produce quality estimation for the main categories of organic produce. However, in practice the same fruit category can have sub-types that vary from the general pattern (e.g., Fuji and Red Delicious for apples), and thus there may be produce for which the results do not directly translate. This may require constructing separate fingerprints for each produce type to be able to use it accurately. Another important consideration for estimating produce quality is storage practices. Different mechanisms have been developed to extend the shelf life of produce in households, e.g., refrigeration, freezing, and canning. Temperature is a key factor that influences any storage mechanism. Moreover, optimal temperature depends on the type of the produce [68]. For instance, non-chilling sensitive fruits (e.g., apple) can tolerate cooler temperatures and can be stored close to 0°C, while chilling sensitive fruits (e.g., passion fruit) are better stored at a higher temperature (7°C-15°C). Thus, we are also interested in exploring various ambient temperatures to determine the best storage practice for each type [68].

Impact of thermal measurements: The performance of SNAKE depends on the quality of the thermal footage, which can be affected, e.g., by atmospheric transmission and the camera resolution [280, 354]. The atmosphere between the thermal cameras and the object can attenuate infrared radiation emitted by the object and is influenced by the distance between the object and the thermal camera, atmospheric temperature and relative humidity [295, 404]. In practice, when the distance between the thermal imager and the produce is small ($< \approx$ one meter), atmospheric effects are negligible. At the same time, the maximum distance depends on the camera resolution (our CAT S61: 80 x 60). Our previous research has show 70cm distance between camera and object to be sufficient with this resolution and higher resolutions can support longer distances without it affecting thermal imaging quality.

Emerging applications and practicability: SNAKE targets assisting end-users (retailers and customers) with quality estimation of produce. Thus, any personal device can deploy our method. New wearable devices like a smart ring can be equipped with a thermal sensor that is the least intrusive, more practical and most intuitive to use [480]. A smartphone (with a thermal camera) can also support quality estimation, but it requires first taking a picture. SNAKE could also be used to identify adulteration of produce, which involves improving the appearance of the produce through chemical substances. Beyond consumer use, grocery retailers are increasingly moving to self-service cashiers. SNAKE could be integrated into these devices and adapt pricing based on produce quality.

Implementation considerations: Integrating thermal sensing technology into retail environments presents challenges related to hardware integration, cost-effectiveness, consumer adoption, and operational efficiency. Deploying thermal cameras or arrays requires an initial investment, with costs ranging from $10 to $500 of each, depending on resolution, and retailers may hesitate without clear financial benefits. Additionally, seamless integration into existing weighing scales and checkout systems is essential to maintain smooth transaction speeds. Consumer concerns about data privacy and the potential complexity of using new technology could also act as barriers to adoption. However, these challenges could be addressed through strategic implementation and automation. For instance, due to their compact size, thermal cameras or arrays can be embedded within existing retail infrastructure (e.g., weighing scales or self-checkout systems) with minimal modifications. Moreover, hand temperature can be opportunistically collected using built-in thermal or temperature sensors, eliminating the need for additional steps from users. The thermal data is processed in real time through retail servers to automate produce quality assessments without slowing down operation efficiency. Results in Subsection 4.6.7 show that the 5-second processing time for thermal dissipation aligns with the average weighing duration, which keeps the process smooth. Furthermore, user studies show that SNAKE helps reduce food waste and build customer trust, which contributes potentially to a strong return on investment and long-term benefits for retailers. While consumer adoption is promising, with 92% of participants willing to use the system, privacy concerns can still be mitigated through transparent policies and regulatory compliance. Importantly, only a short touch is needed before measurement, with minimal interaction naturally occurring as the customer selects the fruit. Overall, adoption barriers remain low, making this system practical, scalable, and cost-effective for modern retail.

Other studies: Given the limited shelf life of produce, our evaluation is based on independent studies conducted over time with the same type items, ensuring the replication and confirmation of our findings. However, while our experiments accounted for a wide range of factors—including different durations, types of produce, touch patterns, and environments—there remains ample opportunity for further research. Our studies aimed to provide various contexts while maintaining a degree of control, which allows for insights into the general applicability of SNAKE. Future research should focus on more uncontrolled studies and extended time spans to encompass a broader array of factors. Retail-specific elements such as store layouts, refrigeration systems, and ventilation, in addition to seasonal variations in ambient temperature and humidity, may significantly affect produce quality over time. Furthermore, handling practices and storage durations could introduce additional variability. Investigating these effects will necessitate longitudinal studies conducted across multiple supermarkets, assessing how environmental fluctuations, seasonal changes, and operational conditions influence the performance of thermal sensing for fruit quality assessment. Understanding these factors could help further refine our method. At the same time, we stress that our results

show that SNAKE already offers significant value to both retailers and consumers. This is particularly evident from the user study results, which indicate that SNAKE can enhance purchase intent while also holding the potential to reduce food waste.

Broader applications: While our work focuses on produce quality estimation using human touch and thermal sensing, the underlying approach has broader applications in food technology and retail. One potential application is in assessing the freshness of other perishable foods, such as bread, dairy, and meat, where human touch can transfer heat and thermal response variations may indicate changes in texture or spoilage levels. In cold storage environments, thermal sensing from human interaction could help detect surface condensation or structural integrity changes in packaged goods. Additionally, thermal-assisted quality assessment could be integrated into self-service kiosks or smart checkout systems, where consumers naturally interact with food items before purchase. This method could enhance food safety monitoring, reduce reliance on subjective visual inspections, and improve consumer confidence in food quality assessments.

4.11. Summary

We contributed SNAKE as an innovative method that harnesses heat from human touch interactions to estimate product quality. The basic principle in SNAKE is to leverage dissipation of thermal radiation transferred from customers to produce to estimate the quality of an item. The main technical challenges are to obtain robust estimates depending on varying interaction patterns with both the size and interaction duration. SNAKE overcomes variations in touch by integrating computer vision techniques that identify a region interest and focus the estimation on the region with the highest thermal transfer. Variations in touch interaction duration, on the other hand, are overcome by using calibration functions that link interactions with a reference duration and enable robust estimation for other duration values. We also extended SNAKE to compensate for palm temperature variations in scenarios where additional palm analysis is possible. SNAKE method can be easily deployed in werables and IoT devices. Rigorous and extensive evaluations demonstrated that SNAKE achieves accurate and robust performance, reaching up to 83% classification accuracy and low error in regression tasks ($RMSE = 0.081$) when compared to a ground truth obtained from a durometer. We also compared SNAKE with two state-of-the-art baselines, optical sensing and wireless sensing, demonstrating that it consistently outperforms them. We also demonstrate the practicality of SNAKE through a 3D-printed prototype and a user study involving 100 participants. Taken together, our work offers a cost-effective and innovative way to harness everyday human interactions. Specifically, the cost of our solution is $\$10 - \$500$ depending on the resolution of the thermal sensor. SNAKE has also potential to enhance environmental sustainability as it can assist in identifying high quality items without relying on misleading visual assessments, potentially helping to reduce food waste and loss in the long term.

5. CONCLUSIONS AND FUTURE DIRECTIONS

5.1. Conclusions

This thesis explored how new sensor designs and data repurposing in smart rings, tailored to natural hand interactions, can support health monitoring, personal safety, and sustainability. Through three core contributions, HIPPO, SpikEy, and SNAKE, I demonstrated the potential of using different hand behavior and natural interactions to develop innovative and unobtrusive sensing solutions for everyday use. All contributions were implemented using existing components, with scientific methods applied to adapt sensor design and data repurposing, enabling new functionalities without additional hardware complexity.

We first designed HIPPO, a light sensing method for estimating hand-grip strength by capturing reflectance changes during common object interactions. By externalizing the sensor design and repurposing the light sensors, we showed that HIPPO can achieve accuracy comparable to clinical baselines, enabling continuous health monitoring in real-life contexts. Building on the new design, we next developed SpikEy for drink spiking detection. SpikEy repurposes the optical sensors to monitor liquid reflectance and incorporates latent modeling and motion calibration to overcome real-world noise. Our results showed that SpikEy not only generalizes across diverse substances and drinks but also significantly outperforms existing baselines in social environments. Finally, we develop SNAKE, a thermal sensing solution for estimating produce quality from human touch. Although implemented using a thermal camera, SNAKE envisions thermal sensing integration in smart rings. By analyzing heat dissipation profiles from natural touch, SNAKE offers a low-cost, accessible alternative to traditional quality inspection methods and has the potential to reduce food waste in retail through informed consumer choices. Together, these systems showcase the power of sensor repurposing and context-aware design in smart rings. By leveraging common hand gestures such as gripping, holding, and touching, we highlight how a single compact wearable can support diverse sensing capabilities without disrupting user routines.

From the thesis, I have learned that innovative functionality in wearable sensing does not always require new hardware. Creative sensor placement and intelligent data repurposing can significantly extend capabilities. However, achieving robust performance in real-world conditions requires careful sensing pipelines that can handle the variability of human interactions and environmental factors.

Beyond the contributions of this thesis, numerous emerging opportunities exist for smart rings, such as drone control, novel interfaces, and new gesture mechanisms. As sensors continue to miniaturize and novel sensing techniques become available, smart rings could integrate an even wider range of sensing capabilities, allowing innovative measurements directly from the hand. This evolution highlights the growing importance of computing and sensing in a smart ring as an integrated field.

5.2. Limitation reflections

While the proposed methods and prototypes in the thesis demonstrate promising results, several common limitations should be addressed for improvement. First, the participant samples were relatively small and demographically narrow, which may limit the generalization of the findings, although from a research perspective the sample size is reasonable for systematic evaluation. Second, for wearables like smart rings, practical applicability is a key consideration. Many experiments were conducted in controlled settings to isolate specific factors of the research problem, with these targeted evaluations combined to address real-world issues, which is a common step in research. Subsequently, simulated real-world deployments were carried out to assess practicality. However, these still do not fully capture the variability and unpredictability of real-world environments, such as the high class imbalance in drink-spiking scenarios where most drinks are not spiked. Additional evaluations in real-life contexts, in collaboration with relevant stakeholders, would help improve model robustness. Third, the current proof-of-concept prototypes remain some distance from fully deployable products, and further commercial collaboration is needed to refine them for everyday use. Finally, for practical usage, a long-term study is necessary, such as smart ring design, robust evaluations across diverse demographics and task-specific environments, user acceptance, and commercial development. Addressing these limitations will help validate the proposed methods on a broader scale and enhance their reliability for real-world deployment.

5.3. Future directions

Smart rings offer promising potential for future innovation due to their discreet design, continuous skin contact, and expanding sensing capabilities. This thesis has demonstrated how smart rings can be repurposed for diverse applications through natural hand interactions. With ongoing advancements in miniaturization, energy efficiency, and intelligent sensing algorithms, smart rings are well-positioned for further evolution. This subsection outlines key opportunities and future directions inspired by the findings of this work, highlighting how next-generation smart ring technologies can extend their impact across broader domains.

Continuous user authentication: Smart rings support continuous authentication by using advanced sensing at finger joints, which reveal user-specific biometric patterns. Sensors capture subtle fingerprint changes during daily use, enabling passive and seamless identity verification. This method enhances spoof resistance and ensures secure and always-on authentication. As sensors become smaller and more efficient, finger-based sensing offers a promising approach for unobtrusive identity management in wearable devices.

Adaptive security and context-aware access: Beyond static authentication, smart rings support adaptive security by adjusting access permissions based on real-time

context. Combining biometric sensing with environmental cues such as motion, location, and proximity to trusted devices, they respond dynamically to different situations. For example, a ring may lock sensitive data if removed or used in an untrusted location. This context-aware approach strengthens data protection while keeping user interaction minimal, making smart rings a strong candidate for intelligent access control in healthcare, finance, and enterprise environments.

Plug and play ecosystem integration: A promising opportunity for smart rings is their role as seamless, cross-device interfaces within connected ecosystems. Using standardized communication protocols, they could automatically connect to smartphones, AR/VR headsets, and smart home platforms, streamlining setup and removing the need for proprietary applications. Beyond initial pairing, smart rings can support fluid, context-aware interaction across multiple devices, such as media control, presentation navigation, or lighting adjustment through proximity cues and intuitive gestures. As personal and professional environments grow increasingly interconnected, smart rings have the potential to act as always-available, personalized controllers that unify digital experiences and enhance everyday interaction.

Bio-sensing: Due to their constant skin contact and unobtrusive form factor, future smart ring designs could move beyond conventional biometrics such as heart rate and skin temperature to include advanced physiological markers like hydration levels, blood oxygen saturation, electrodermal activity, and thermal patterns. Thermal sensing, for instance, can offer insights into circulation, stress levels, and localized inflammation, making it a valuable component for continuous health monitoring. With ongoing miniaturization of biosensors and advances in sensor fusion, smart rings may support real-time and multimodal health tracking in both clinical and everyday settings. This could open new opportunities in preventive care, personalized wellness, and chronic disease management, positioning the smart ring as a discreet yet powerful tool for data-driven health insights.

Multiple rings: Wearing multiple smart rings on different fingers introduces opportunities for richer interaction, advanced sensing, and expanded functionality. While most systems rely on a single ring, emerging research has begun to explore dual-ring setups for capturing bimanual gestures, inter-finger coordination, and finer spatial tracking. For example, two rings can work together to detect complex hand poses or support multi-finger input in sophisticated applications. This configuration also allows for distributed sensing, such as comparing biometric signals across hands, or adds redundancy for more reliable authentication. With ongoing advances in miniaturization and communication efficiency, multi-ring systems may reshape how users engage with digital environments through their hands.

Participatory environmental monitoring: Smart rings equipped with ambient sensors can act as personal environmental monitors, opening new avenues in sustainability and climate resilience. By tracking factors such as air quality, temperature, UV exposure, and humidity, they can provide real-time alerts for personal health risks like heat stress, and contribute to broader environmental

data collection. When linked to citizen science platforms, these rings support community-driven sensing and pollution mapping, offering a scalable, wearable complement to stationary monitoring infrastructure.

Edge AI and on-ring intelligence: Advances in ultra-low-power processors and memory-efficient algorithms allow smart rings to move beyond passive sensing toward real-time and on-device inference. Tasks like gesture recognition, anomaly detection, or biometric classification can be processed directly on the ring, reducing dependence on external devices and improving speed and privacy. With embedded edge AI models that are optimized through techniques such as pruning or quantization, smart rings can deliver fast, personalized responses for health, authentication, and control applications, all without continuous smartphone connectivity.

Modular and reconfigurable ring design: The modular design of smart rings offers a flexible approach by allowing users to customize functionality by adding or swapping small components based on specific needs. For example, users could attach a haptic module for feedback, a temperature sensor for health monitoring, or a gesture module for AR interaction. This adaptability extends the ring's lifespan and broadens its use across different contexts. For developers, modular architecture simplifies prototyping and testing, enabling rapid iteration without redesigning the entire device.

Touchless interaction in public/shared environments: The COVID-19 pandemic has accelerated the demand for hygienic, contact-free interfaces in public and shared environments such as kiosks, elevators, ATMs, or ticket machines. Smart rings enable touchless interaction by replacing physical contact with gestures or proximity-based controls. Smart rings offer a touchless alternative by enabling gesture-based or proximity-driven interaction. For instance, a user could wave or rotate their hand to navigate menus or confirm payments, avoiding direct contact with shared surfaces. With integrated motion sensing, NFC, or Bluetooth, smart rings can securely interact with public systems while supporting private and personalized use. As connected infrastructure expands, smart rings may serve as always-available controllers for safer, more intuitive public interaction.

Retail behavior tracking: In retail environments, smart rings offer a discreet way to capture detailed customer behavior through natural hand interactions with products. They can detect micro-interactions such as hold duration, grip pressure, and browsing movements, providing insights into engagement and purchase intent. This data helps retailers assess product appeal, optimize layouts, and personalize in-store experiences in real time, such as suggesting alternatives or displaying contextual information. With advancements in privacy-preserving analytics, smart rings could support responsive, user-centric retail environments without intrusive surveillance.

Social and emotional cues: As smart rings can support emotion-aware computing by passively monitoring signals like heart rate variability, skin conductance, and temperature to infer states such as stress or relaxation, they can also sense social

cues through touch, handholding, or proximity, offering insight into emotional context during interactions. These capabilities enable applications in digital wellness, relationship tracking, and adaptive interfaces, such as silencing notifications during stressful moments or enhancing feedback in calm states. By capturing subtle emotional signals in real time, smart rings help create more empathetic and personalized user experiences across communication, mental health, and lifestyle domains.

Privacy-preserving machine learning: With the growing use of biometric and behavioral data, smart rings present an opportunity to advance privacy-conscious AI. Techniques like federated learning allow models to train locally without sharing raw data, supporting collaborative insights while protecting user confidentiality. When combined with on-device encryption and differential privacy, smart rings can deliver secure, ethical intelligence, especially in sensitive areas such as hospitals.

Energy autonomy through self-sustaining systems: Self-powered smart rings offer a path toward fully autonomous wearables. By harvesting energy from body heat, finger motion, or ambient RF signals, future rings could reduce or eliminate the need for frequent charging. Paired with low-power processors and event-driven sensing, these systems are well-suited for long-term health monitoring, field use, and operation in remote settings.

Neuromotor and BCI-inspired input: Advances in neuromotor and brain-computer interface (BCI) research open new possibilities for smart rings to detect subtle muscle activity and intention-driven input. By sensing EMG signals or pressure changes at the finger level, rings can move beyond gesture tracking to interpret motor intent and fine finger coordination. This approach supports hands-free interaction in AR/VR, assistive tech, or silent communication in noisy or privacy-sensitive settings. Bringing simplified BCI-like capabilities to smart rings may lead to a new class of intuitive, intention-aware wearables.

BIBLIOGRAPHY

[1] Judith A Abbott. "Quality measurement of fruits and vegetables". In: *Postharvest biology and technology* 15.3 (1999), pp. 207–225.

[2] Khadija AbdulSattar and Alauddin Al-Omary. "Pervasive computing paradigm: A survey". In: *2020 International Conference on Data Analytics for Business and Industry: Way Towards a Sustainable Economy (ICDABI)*. IEEE. 2020, pp. 1–5.

[3] Diane E Adamo, Tara Anderson, Mahtab Koochaki, and Nora E Fritz. "Declines in grip strength may indicate early changes in cognition in healthy middle-aged adults". In: *PloS One* 15.4 (2020), e0232021. DOI: https://doi.org/10.1371/journal.pone.0232021.

[4] Mustafa Elhadi Ahmed, Hongnian Yu, Michael Vassallo, and Pelagia Koufaki. "Enhanced LDA with SVM and Ensemble Learning for Advanced ADL Classification Using Smartwatch Data". In: *2024 29th International Conference on Automation and Computing (ICAC)*. IEEE. 2024, pp. 1–6.

[5] Tousif Ahmed, Md Mahbubur Rahman, Ebrahim Nemati, Mohsin Yusuf Ahmed, Jilong Kuang, and Alex Jun Gao. "Remote breathing rate tracking in stationary position using the motion and acoustic sensors of earables". In: *Proceedings of the 2023 CHI Conference on Human Factors in Computing Systems*. 2023, pp. 1–22.

[6] DaeHan Ahn, Hyerim Chung, Ho-Won Lee, Kyunghun Kang, Pan-Woo Ko, Nam Sung Kim, and Taejoon Park. "Smart gait-aid glasses for Parkinson's disease patients". In: *IEEE Transactions on Biomedical Engineering* 64.10 (2017), pp. 2394–2402.

[7] Mominul Ahsan, Siew Teay Hon, and Alhussein Albarbar. "Development of novel big data analytics framework for smart clothing". In: *IEEE Access* 8 (2020), pp. 146376–146394.

[8] Ali Akbari, Jonathan Martinez, and Roozbeh Jafari. "Facilitating human activity data annotation via context-aware change detection on smartwatches". In: *ACM Transactions on Embedded Computing Systems (TECS)* 20.2 (2021), pp. 1–20.

[9] Sayma Akther, Nazir Saleheen, Shahin Alan Samiei, Vivek Shetty, Emre Ertin, and Santosh Kumar. "mORAL: An mHealth model for inferring oral hygiene behaviors in-the-wild using wrist-worn inertial sensors". In: *Proceedings of the ACM on Interactive, Mobile, Wearable and Ubiquitous Technologies* 3.1 (2019), pp. 1–25.

[10] Md Abdulla Al Mamun and Mehmet Rasit Yuce. "Sensors and systems for wearable environmental monitoring toward IoT-enabled applications: A review". In: *IEEE Sensors Journal* 19.18 (2019), pp. 7771–7788.

[11] Talayeh Aledavood, Ilkka Kivimäki, Sune Lehmann, and Jari Saramäki. "Quantifying daily rhythms with non-negative matrix factorization applied to mobile phone data". In: *Scientific reports* 12.1 (2022), p. 5544.

[12] Maimunah Mohd Ali, Norhashila Hashim, Samsuzana Abd Aziz, and Ola Lasekan. "Emerging non-destructive thermal imaging technique coupled with chemometrics on quality and safety inspection in food and agriculture". In: *Trends in Food Science & Technology* 105 (2020), pp. 176–185.

[13] Shawkat Ali, Saleem Khan, Arshad Khan, and Amine Bermak. "Developing conductive fabric threads for human respiratory rate monitoring". In: *IEEE Sensors Journal* 21.4 (2020), pp. 4350–4356.

[14] Hashem A Almusawi, Christopher M Durugbo, and Afaf M Bugawa. "Wearable technology in education: A systematic review". In: *IEEE Transactions on Learning Technologies* 14.4 (2021), pp. 540–554.

[15] Hanieh Amani et al. "Current progress in the utilization of smartphone-based imaging for quality assessment of food products: a review". In: *Critical reviews in food science and nutrition* (2020), pp. 1–13.

[16] Oliver Amft. "How Wearable Computing Is Shaping Digital Health". In: *IEEE Pervasive Computing* 17.1 (2018), pp. 92–98. DOI: 10.1109/MPRV.2018.011591067.

[17] Akash Anand, Manish Sharma, Rupika Srivastava, Lakshmi Kaligounder, and Divya Prakash. "Wearable motion sensor based analysis of swing sports". In: *2017 16th IEEE international conference on machine learning and applications (ICMLA)*. IEEE. 2017, pp. 261–267.

[18] Jose Anand, J Raja Paul Perinbam, and D Meganathan. "Q-learning-based optimized routing in biomedical wireless sensor networks". In: *IETE Journal of Research* 63.1 (2017), pp. 89–97.

[19] Williams A. Andrews and Richard W Bohannon. "Distribution of muscle strength impairments following stroke". In: *Clinical Rehabilitation* 14.1 (2000), pp. 79–87. DOI: https://doi.org/10.1191/026921500673950113.

[20] Chioma Virginia Anikwe, Henry Friday Nweke, Anayo Chukwu Ikegwu, Chukwunonso Adolphus Egwuonwu, Fergus Uchenna Onu, Uzoma Rita Alo, and Ying Wah Teh. "Mobile and wearable sensors for data-driven health monitoring system: State-of-the-art and future prospect". In: *Expert Systems with Applications* 202 (2022), p. 117362.

[21] Arif Reza Anwary, Hongnian Yu, and Michael Vassallo. "Gait evaluation using procrustes and euclidean distance matrix analysis". In: *IEEE journal of biomedical and health informatics* 23.5 (2018), pp. 2021–2029.

[22] Toru Aonishi, Ryoichi Maruyama, Tsubasa Ito, Hiroyoshi Miyakawa, Masanori Murayama, and Keisuke Ota. "Imaging data analysis using non-negative matrix factorization". In: *Neuroscience Research* 179 (2022), pp. 51–56.

[23] Riku Arakawa, Hiromu Yakura, Vimal Mollyn, Suzanne Nie, Emma Russell, Dustin P DeMeo, Haarika A Reddy, Alexander K Maytin, Bryan T Carroll, Jill Fain Lehman, et al. "Prism-tracker: A framework for multimodal procedure tracking using wearable sensors and state transition information with user-driven handling of errors and uncertainty". In: *Proceedings of the ACM on Interactive, Mobile, Wearable and Ubiquitous Technologies* 6.4 (2023), pp. 1–27.

[24] Erick Javier Argüello Prada and Lina María Santacruz Forero. "A belt-like assistive device for visually impaired people: Toward a more collaborative approach". In: *Cogent Engineering* 9.1 (2022), p. 2048440.

[25] Pablo Arias, Christopher Kelley, Janelle Mason, Kelvin Bryant, and Kaushik Roy. "Classification of user movement data". In: *Proceedings of the International Conference on Digital Signal Processing*. Tokyo, Japan: ACM, 2018, pp. 156–160. DOI: https://doi.org/10.1145/3193025.3193036.

[26] Bert Arnrich, Oscar Mayora, Jakob Bardram, and Gerhard Tröster. "Pervasive healthcare". In: *Methods of Information in Medicine* 49.01 (2010), pp. 67–73. DOI: https://doi.org/10.3414/ME09-02-0044.

[27] Aamir Arsalan and Muhammad Majid. "A study on multi-class anxiety detection using wearable EEG headband". In: *Journal of Ambient Intelligence and Humanized Computing* 13.12 (2022), pp. 5739–5749.

[28] Sahar Aseeri, Kyle Condiff, Maximilian Klein, and Baris Unver. "Freedge: Fighting food insecurity with connected infrastructure". In: *Proceedings of the 2017 CHI Conference Extended Abstracts on Human Factors in Computing Systems*. 2017, pp. 33–38.

[29] Leticia Avellar, Carlos Stefano Filho, Gabriel Delgado, Anselmo Frizera, Eduardo Rocon, and Arnaldo Leal-Junior. "AI-enabled photonic smart garment for movement analysis". In: *Scientific reports* 12.1 (2022), p. 4067.

[30] Md Aashikur Rahman Azim, Adil Rahman, and Seongkook Heo. "UnifiedSense: Enabling Without-Device Gesture Interactions Using Over-the-shoulder Training Between Redundant Wearable Sensors". In: *Proceedings of the ACM on Human-Computer Interaction* 7.MHCI (2023), pp. 1–25.

[31] Emna Baccour, Naram Mhaisen, Alaa Awad Abdellatif, Aiman Erbad, Amr Mohamed, Mounir Hamdi, and Mohsen Guizani. "Pervasive AI for IoT applications: A survey on resource-efficient distributed artificial intelligence". In: *IEEE Communications Surveys & Tutorials* 24.4 (2022), pp. 2366–2418.

[32] Serkan Balli, Ensar Arif Sağbaş, and Musa Peker. "Human activity recognition from smart watch sensor data using a hybrid of principal component analysis and random forest algorithm". In: *Measurement and Control* 52.1-2 (2019), pp. 37–45.

[33] Sandra Bardot, Bradley Rey, Lucas Audette, Kevin Fan, Da-Yuan Huang, Jun Li, Wei Li, and Pourang Irani. “One Ring to Rule Them All: An Empirical Understanding of Day-to-Day Smartring Usage Through In-Situ Diary Study”. In: *Proceedings of the ACM on Interactive, Mobile, Wearable and Ubiquitous Technologies* 6.3 (2022), pp. 1–20.

[34] Alain Barrat, Ciro Cattuto, Alberto Eugenio Tozzi, Philippe Vanhems, and Nicolas Voirin. “Measuring contact patterns with wearable sensors: methods, data characteristics and applications to data-driven simulations of infectious diseases”. In: *Clinical Microbiology and Infection* 20.1 (2014), pp. 10–16.

[35] Durga Prasad Bavirisetti, Gang Xiao, and Gang Liu. “Multi-sensor image fusion based on fourth order partial differential equations”. In: *2017 20th International conference on information fusion (Fusion)*. IEEE. 2017, pp. 1–9.

[36] Abdelkareem Bedri, Yuchen Liang, Sudershan Boovaraghavan, Geoff Kaufman, and Mayank Goel. “FitNibble: A Field Study to Evaluate the Utility and Usability of Automatic Diet Monitoring in Food Journaling Using an Eyeglasses-based Wearable”. In: *27th International Conference on Intelligent User Interfaces*. 2022, pp. 79–92.

[37] AL Behera, SK Sahoo, and SV Patil. “Enhancement of solubility: A pharmaceutical overview”. In: *Der Pharmacia Lettre* 2.2 (2010), pp. 310–318.

[38] Johannes Beller, Alexander Miething, Enrique Regidor, Lourdes Lostao, Jelena Epping, and Siegfried Geyer. “Trends in grip strength: Age, period, and cohort effects on grip strength in older adults from Germany, Sweden, and Spain”. In: *SSM-Population Health* 9 (2019), p. 100456. DOI: https://doi.org/10.1016/j.ssmph.2019.100456.

[39] Shimshon Ben-Yehoshua and Victor Rodov. “Transpiration and water stress”. In: *Postharvest physiology and pathology of vegetables*. CRC Press, 2002, pp. 143–197.

[40] Antonia Bendau, Twyla Michnevich, Moritz B Petzold, Andrea Piest, Rüdiger Schmolke, Daniel Jakobson, Katharin Ahrend, Thale Reitz, Lukas Roediger, and Felix Betzler. “Spiking versus speculation? Perceived prevalence, probability, and fear of drink and needle spiking”. In: *Journal of drug issues* (2023), p. 00220426231197826.

[41] Anuja Bhargava and Atul Bansal. “Fruits and vegetables quality evaluation using computer vision: A review”. In: *Journal of King Saud University-Computer and Information Sciences* (2018).

[42] Anuja Bhargava and Atul Bansal. “Fruits and vegetables quality evaluation using computer vision: A review”. In: *Journal of King Saud University-Computer and Information Sciences* 33.3 (2021), pp. 243–257.

[43] Sarnab Bhattacharya, Rebecca Adaimi, and Edison Thomaz. “Leveraging sound and wrist motion to detect activities of daily living with commod-

ity smartwatches". In: *Proceedings of the ACM on Interactive, Mobile, Wearable and Ubiquitous Technologies* 6.2 (2022), pp. 1–28.

[44] Sourav Bhattacharya, Patrik Floréen, Andreas Forsblom, Samuli Hemminki, Petri Myllymäki, Petteri Nurmi, Teemu Pulkkinen, and Antti Salovaara. "Ma$$iv – An Intelligent Mobile Grocery Assistant". In: *2012 Eighth International Conference on Intelligent Environments*. 2012, pp. 165–172.

[45] Laura-Bianca Bilius and Radu-Daniel Vatavu. ""I Could Wear It All of the Time, Just Like My Wedding Ring:" Insights into Older People's Perceptions of Smart Rings". In: *Extended Abstracts of the 2023 CHI Conference on Human Factors in Computing Systems*. CHI EA '23. Hamburg, Germany: Association for Computing Machinery, 2023. ISBN: 9781450394222.

[46] Athanasios Bimpas, John Violos, Aris Leivadeas, and Iraklis Varlamis. "Leveraging pervasive computing for ambient intelligence: A survey on recent advancements, applications and open challenges". In: *Computer Networks* 239 (2024), p. 110156.

[47] Tess Blandamer, Jo Daniels, James Dear, Fraser Birse, Edward Carlton, Kate Burgess, and Tom Roberts. "Drink and injection spiking: how to approach an increase in presentations?" In: *Emergency Medicine Journal* 40.4 (2023), pp. 308–312.

[48] Jorge Blasco, Thomas M Chen, Juan Tapiador, and Pedro Peris-Lopez. "A survey of wearable biometric recognition systems". In: *ACM Computing Surveys (CSUR)* 49.3 (2016), pp. 1–35.

[49] Richard W Bohannon. "Grip strength: An indispensable biomarker for older adults". In: *Clinical Interventions in Aging* 14 (2019), p. 1681. DOI: https://doi.org/10.2147\%2FCIA.S194543.

[50] Richard W Bohannon and Karen L Schaubert. "Test–retest reliability of grip-strength measures obtained over a 12-week interval from community-dwelling elders". In: *Journal of Hand Therapy* 18.4 (2005), pp. 426–428. URL: https://doi.org/10.1197/j.jht.2005.07.003.

[51] Alexei Botchkarev. "A new typology design of performance metrics to measure errors in machine learning regression algorithms". In: *Interdisciplinary Journal of Information, Knowledge, and Management* 14 (2019), pp. 045–076.

[52] Jean Bourgain, Sjoerd Dirksen, and Jelani Nelson. "Toward a unified theory of sparse dimensionality reduction in euclidean space". In: *Proceedings of the forty-seventh annual ACM symposium on Theory of Computing*. 2015, pp. 499–508.

[53] Adam Burgess et al. "Embodying uncertainty? Understanding heightened risk perception of drink 'spiking'". In: *The British journal of criminology* 49.6 (2009), pp. 848–862.

[54] Oğuz'Oz' Buruk, Mikko Salminen, Nannan Xi, Timo Nummenmaa, and Juho Hamari. "Towards the next generation of gaming wearables". In: *Proceedings of the 2021 CHI Conference on Human Factors in Computing Systems*. 2021, pp. 1–15.

[55] Ruiying Cai, Ao Guo, Jianhua Ma, Runhe Huang, Ruiyun Yu, and Chen Yang. "Correlation analyses between personality traits and personal behaviors under specific emotion states using physiological data from wearable devices". In: *2018 IEEE 16th Intl Conf on Dependable, Autonomic and Secure Computing, 16th Intl Conf on Pervasive Intelligence and Computing, 4th Intl Conf on Big Data Intelligence and Computing and Cyber Science and Technology Congress (DASC/PiCom/DataCom/CyberSciTech)*. IEEE. 2018, pp. 46–53.

[56] Kelly Caine. "Local standards for sample size at CHI". In: *Proceedings of the 2016 CHI conference on human factors in computing systems*. 2016, pp. 981–992.

[57] Manuel Reis Carneiro, Anibal T de Almeida, and Mahmoud Tavakoli. "Wearable and comfortable e-textile headband for long-term acquisition of forehead EEG signals". In: *IEEE Sensors Journal* 20.24 (2020), pp. 15107–15116.

[58] Marta E Cecchinato, Anna L Cox, and Jon Bird. "Smartwatches: the good, the bad and the ugly?" In: *Proceedings of the 33rd Annual ACM Conference extended abstracts on human factors in computing systems*. 2015, pp. 2133–2138.

[59] Carlos A Celis-Morales, Paul Welsh, Donald M. Lyall, Lewis Steell, Fanny Petermann, Jana Anderson, Stamatina Iliodromiti, Anne Sillars, Nicholas Graham, Daniel F. Mackay, Jill P. Pell, Jason M. R. Gill, Naveed Sattar, and Stuart R. Gray. "Associations of grip strength with cardiovascular, respiratory, and cancer outcomes and all cause mortality: Prospective cohort study of half a million UK Biobank participants". In: *theBmj* 361 (2018), pp. 1651–1661. DOI: https://doi.org/10.1136/bmj.k1651.

[60] Doyeli Chakraborty and JB Jeeva. "Detection of Heart Rate Using Reflectance Mode Photoplethysmography". In: *2019 Innovations in Power and Advanced Computing Technologies (i-PACT)*. Vol. 1. IEEE. 2019, pp. 1–3.

[61] David M Chan, Roshan Rao, Forrest Huang, and John F Canny. "t-SNE-CUDA: GPU-Accelerated t-SNE and its Applications to Modern Data". In: *2018 30th International Symposium on Computer Architecture and High Performance Computing (SBAC-PAD)*. IEEE. 2018, pp. 330–338.

[62] Jeremy Chan, Eduardo Veas, and Jörg Simon. "Designing a sensor glove using deep learning". In: *Proceedings of the 26th International Conference on Intelligent User Interfaces*. 2021, pp. 150–160.

[63] Justin Chan et al. “Testing a Drop of Liquid Using Smartphone LiDAR”. In: *Proceedings of the IMWUT 2022* 6.1 (2022), pp. 1–27.

[64] Wan-Jung Chang, Liang-Bi Chen, and Yu-Zung Chiou. “Design and implementation of a drowsiness-fatigue-detection system based on wearable smart glasses to increase road safety”. In: *IEEE Transactions on Consumer Electronics* 64.4 (2018), pp. 461–469.

[65] Wan-Jung Chang, Liang-Bi Chen, Chia-Hao Hsu, Jheng-Hao Chen, Tzu-Chin Yang, and Cheng-Pei Lin. “MedGlasses: A wearable smart-glasses-based drug pill recognition system using deep learning for visually impaired chronic patients”. In: *IEEE Access* 8 (2020), pp. 17013–17024.

[66] Ishan Chatterjee, Maruchi Kim, Vivek Jayaram, Shyamnath Gollakota, Ira Kemelmacher, Shwetak Patel, and Steven M Seitz. “ClearBuds: wireless binaural earbuds for learning-based speech enhancement”. In: *Proceedings of the 20th Annual International Conference on Mobile Systems, Applications and Services*. 2022, pp. 384–396.

[67] KV Chau, RA Romero, CD Baird, and JJ Gaffney. “Transpiration coefficients of fruits and vegetables in refrigerated storage”. In: *ASHRAE Report 370-RP* (1987).

[68] Alicia Chaves and Noemí Zaritzky. “Cooling and freezing of fruits and fruit products”. In: *Fruit Preservation: Novel and Conventional Technologies* (2018), pp. 127–180.

[69] Bo Chen, Wenan Zhang, Guoqiang Hu, and Li Yu. “Networked fusion Kalman filtering with multiple uncertainties”. In: *IEEE transactions on Aerospace and Electronic Systems* 51.3 (2015), pp. 2232–2249.

[70] Ling Chen, Rong Hu, Menghan Wu, and Xin Zhou. “HMGAN: A hierarchical multi-modal generative adversarial network model for wearable human activity recognition”. In: *Proceedings of the ACM on Interactive, Mobile, Wearable and Ubiquitous Technologies* 7.3 (2023), pp. 1–27.

[71] Min Chen, Yujun Ma, Jeungeun Song, Chin-Feng Lai, and Bin Hu. “Smart clothing: Connecting human with clouds and big data for sustainable health monitoring”. In: *Mobile Networks and Applications* 21 (2016), pp. 825–845.

[72] Taizhou Chen, Tianpei Li, Xingyu Yang, and Kening Zhu. “Efring: Enabling thumb-to-index-finger microgesture interaction through electric field sensing using single smart ring”. In: *Proceedings of the ACM on Interactive, Mobile, Wearable and Ubiquitous Technologies* 6.4 (2023), pp. 1–31.

[73] Xiang’Anthony’ Chen, Tovi Grossman, Daniel J Wigdor, and George Fitzmaurice. “Duet: exploring joint interactions on a smart phone and a smart watch”. In: *Proceedings of the SIGCHI Conference on human factors in computing systems*. 2014, pp. 159–168.

[74] Yiqiang Chen, Xin Qin, Jindong Wang, Chaohui Yu, and Wen Gao. “Fedhealth: A federated transfer learning framework for wearable healthcare”. In: *IEEE Intelligent Systems* 35.4 (2020), pp. 83–93.

[75] Pei-Yu Chi and Yang Li. “Weave: Scripting cross-device wearable interaction”. In: *Proceedings of the 33rd annual ACM conference on human factors in computing systems*. 2015, pp. 3923–3932.

[76] Radu Chirila, Abhishek Singh Dahiya, Philippe Schyns, and Ravinder Dahiya. “Self-Powered Multimodal Sensing Using Energy-Generating Solar Skin for Robotics and Smart Wearables”. In: *Advanced Intelligent Systems* (2024), p. 2300824.

[77] Seokmin Choi, Junghwan Yim, Yincheng Jin, Yang Gao, Jiyang Li, and Zhanpeng Jin. “EarPPG: Securing your identity with your ears”. In: *Proceedings of the 28th International Conference on Intelligent User Interfaces*. 2023, pp. 835–849.

[78] Jaewoo Chung, Matt Donahoe, Chris Schmandt, Ig-Jae Kim, Pedram Razavai, and Micaela Wiseman. “Indoor location sensing using geo-magnetism”. In: *Proceedings of the 9th international conference on Mobile systems, applications, and services*. 2011, pp. 141–154.

[79] Frances Cleary, Witawas Srisa-an, Beatriz Gil, Jaideep Kesavan, Tobias Engel, David C Henshall, and Sasitharan Balasubramaniam. “Wearable fabric μ brain enabling on-garment edge-based sensor data processing”. In: *IEEE Sensors Journal* 22.21 (2022), pp. 20839–20854.

[80] Francesco Concas et al. “Low-cost outdoor air quality monitoring and sensor calibration: A survey and critical analysis”. In: *ACM Transactions on Sensor Networks (TOSN)* 17.2 (2021), pp. 1–44.

[81] Francesco Conti, Daniele Palossi, Renzo Andri, Michele Magno, and Luca Benini. “Accelerated visual context classification on a low-power smartwatch”. In: *IEEE Transactions on Human-Machine Systems* 47.1 (2016), pp. 19–30.

[82] Maria Cornacchia, Koray Ozcan, Yu Zheng, and Senem Velipasalar. “A survey on activity detection and classification using wearable sensors”. In: *IEEE Sensors Journal* 17.2 (2016), pp. 386–403.

[83] Gloria Cosoli, Susanna Spinsante, and Lorenzo Scalise. “Wrist-worn and chest-strap wearable devices: Systematic review on accuracy and metrological characteristics”. In: *Measurement* 159 (2020), p. 107789.

[84] Ian Costanzo, Devdip Sen, Lawrence Rhein, and Ulkuhan Guler. “Respiratory monitoring: Current state of the art and future roads”. In: *IEEE Reviews in Biomedical Engineering* 15 (2020), pp. 103–121.

[85] Ulysse Côté-Allard, Cheikh Latyr Fall, Alexandre Drouin, Alexandre Campeau-Lecours, Clément Gosselin, Kyrre Glette, François Laviolette, and Benoit Gosselin. “Deep learning for electromyographic hand gesture

signal classification using transfer learning". In: *IEEE transactions on neural systems and rehabilitation engineering* 27.4 (2019), pp. 760–771.

[86] Hong Cui, Zhiquan Feng, Jinglan Tian, Dehui Kong, Zishuo Xia, and Weina Li. "MAG: a smart gloves system based on multimodal fusion perception". In: *CCF Transactions on Pervasive Computing and Interaction* 5.4 (2023), pp. 411–429.

[87] Alexander Curtiss, Blaine Rothrock, Abu Bakar, Nivedita Arora, Jason Huang, Zachary Englhardt, Aaron-Patrick Empedrado, Chixiang Wang, Saad Ahmed, Yang Zhang, et al. "FaceBit: Smart face masks platform". In: *Proceedings of the ACM on Interactive, Mobile, Wearable and Ubiquitous Technologies* 5.4 (2021), pp. 1–44.

[88] Luigi D'arco, Graham Mccalmont, Haiying Wang, and Huiru Zheng. "Application of smart insoles for recognition of activities of daily living: a systematic review". In: *ACM Transactions on Computing for Healthcare* 5.1 (2024), pp. 1–34.

[89] Gaole Dai, Huatao Xu, Hyungjun Yoon, Mo Li, Rui Tan, and Sung-Ju Lee. "ContrastSense: Domain-invariant Contrastive Learning for In-the-Wild Wearable Sensing". In: *Proceedings of the ACM on Interactive, Mobile, Wearable and Ubiquitous Technologies* 8.4 (2024), pp. 1–32.

[90] Farooq Dar, Hilary Emenike, Zhigang Yin, Mohan Liyanage, Rajesh Sharma, Agustin Zuniga, Mohammad A Hoque, Marko Radeta, Petteri Nurmi, and Huber Flores. "The MIDAS touch: Thermal dissipation resulting from everyday interactions as a sensing modality". In: *Pervasive and Mobile Computing* 84 (2022), pp. 1–18.

[91] Farooq Ayoub Dar, Mayowa Olapade, Abdul-rasheed Ottun, Zhigang Yin, Mohan Liyanage, Ulrich Norbisrath, Marko Radeta, Francisco Silva, Xiang Su, Janick Edinger, et al. "TOAD: Profiling and Evaluating 3D Printed IoT Rapid Prototype Designs". In: *ACM Transactions on Internet of Things* (2025).

[92] Anshuman J Das, Akshat Wahi, Ishan Kothari, and Ramesh Raskar. "Ultra-portable, wireless smartphone spectrometer for rapid, non-destructive testing of fruit ripeness". In: *Scientific reports* 6.1 (2016), pp. 1–8.

[93] Valeria De Laurentiis, Sara Corrado, and Serenella Sala. "Quantifying household waste of fresh fruit and vegetables in the EU". In: *Waste management* 77 (2018), pp. 238–251.

[94] DEA. *Rohypnol Fact Sheet*. `https://www.dea.gov/sites/default/files/2020-06/Rohypnol-2020.pdf` [Accessed: 2024-07-01]. 2020.

[95] Joseph DelPreto, Josie Hughes, Matteo D'Aria, Marco De Fazio, and Daniela Rus. "A wearable smart glove and its application of pose and gesture detection to sign language classification". In: *IEEE Robotics and Automation Letters* 7.4 (2022), pp. 10589–10596.

[96] Berken Utku Demirel, Ting Dang, Khaldoon Al-Naimi, Fahim Kawsar, and Alessandro Montanari. “Unobtrusive air leakage estimation for earables with in-ear microphones”. In: *Proceedings of the ACM on Interactive, Mobile, Wearable and Ubiquitous Technologies* 7.4 (2024), pp. 1–29.

[97] Ramesh Dharavath, G MadhukarRao, Himanshu Khurana, and Damodar Reddy Edla. “t-SNE Manifold Learning Based Visualization: A Human Activity Recognition Approach”. In: *Advances in Data Science and Management: Proceedings of ICDSM 2019*. Springer. 2020, pp. 33–43.

[98] Ashutosh Dhekne et al. “Liquid: A wireless liquid identifier”. In: *Proceedings of ACM MobiSys 2018*. ACM. 2018, pp. 442–454.

[99] Christine Dierk, Scott A Carter, Patrick Chiu, Tony Dunnigan, and Don Kimber. “Use Your Head! Exploring Interaction Modalities for Hat Technologies.” In: *Conference on Designing Interactive Systems*. 2019, pp. 1033–1045.

[100] Aristides Dokoumetzidis and Panos Macheras. “A century of dissolution research: from Noyes and Whitney to the biopharmaceutics classification system”. In: *International journal of pharmaceutics* 321.1-2 (2006), pp. 1–11.

[101] Wentao Dong, Lin Yang, Raffaele Gravina, and Giancarlo Fortino. “Soft wrist-worn multi-functional sensor array for real-time hand gesture recognition”. In: *IEEE Sensors Journal* 22.18 (2021), pp. 17505–17514.

[102] Arockia Selvakumar Arockia Doss, Pavan Kalyan Lingampally, Gia Minh Thao Nguyen, and Daniel Schilberg. “A comprehensive review of wearable assistive robotic devices used for head and neck rehabilitation”. In: *Results in Engineering* 19 (2023), p. 101306.

[103] DrinkSavvy. *DrinkSavvy*. `https://www.theverge.com/2013/8/11/4611018/drinksavvy-glasses-straws-detect-date-rape-drugs` [Accessed: 2024-07-01]. 2013.

[104] Zhenjiao Du, Xiangquan Zeng, Xiangxin Li, Xiaomeng Ding, Jiankang Cao, and Weibo Jiang. “Recent advances in imaging techniques for bruise detection in fruits and vegetables”. In: *Trends in Food Science & Technology* 99 (2020), pp. 133–141.

[105] Don Samitha Elvitigala, Jochen Huber, and Suranga Nanayakkara. “Augmented foot: a comprehensive survey of augmented foot interfaces”. In: *Proceedings of the Augmented Humans International Conference 2021*. 2021, pp. 228–239.

[106] Hilary Emenike, Farooq Dar, Mohan Liyanage, Rajesh Sharma, et al. “Characterizing Everyday Objects using Human Touch: Thermal Dissipation as a Sensing Modality”. In: *2021 IEEE International Conference on Pervasive Computing and Communications (PerCom)*. IEEE. 2021, pp. 1–8.

[107] Hilary Emenike, Farooq Dar, Mohan Liyanage, Rajesh Sharma, Agustin Zuniga, Mohammad A. Hoque, Marko Radeta, Petteri Nurmi, and Huber Flores. "Characterizing everyday objects using human touch: Thermal dissipation as a sensing modality". In: *Proceedings of the IEEE International Conference on Pervasive Computing and Communications*. PerCom'21. Kassel, Germany: IEEE, 2021, pp. 1–8. DOI: https://doi.org/10.1109/PERCOM50583.2021.9439120.

[108] Francisco Espinoza, Pierre Le Blay, Denis Coulon, Sylvain Lieu, Janet Munro, Christian Jorgensen, and Yves-Marie Pers. "Handgrip strength measured by a dynamometer connected to a smartphone: A new applied health technology solution for the self-assessment of rheumatoid arthritis disease activity". In: *Rheumatology* 55.5 (2016), pp. 897–901. DOI: https://doi.org/10.1093/rheumatology/kew006.

[109] Temitayo Matthew Fagbola, Funmilola Ikeolu Fagbola, Oluwasegun Julius Aroba, Ruchi Doshi, Kamal Kant Hiran, and Surendra Colin Thakur. "Smart face masks for Covid-19 pandemic management: A concise review of emerging architectures, challenges and future research directions". In: *IEEE Sensors Journal* 23.2 (2022), pp. 877–888.

[110] Asle Fagerstrøm, Niklas Eriksson, and Valdimar Sigurdsson. "Investigating the impact of Internet of Things services from a smartphone app on grocery shopping". In: *Journal of Retailing and Consumer Services* 52 (2020), p. 101927.

[111] Tarig Faisal, Moath Awawdeh, Daniel Habte, Hala Berhanu, Kibrom Kifle, Lia Misghina, and Anees Bashir. "Smart Cart With Multi-shopping Solutions." In: *International Journal of Interactive Mobile Technologies* 15.24 (2021).

[112] Junjun Fan, Xiangmin Fan, Feng Tian, Yang Li, Zitao Liu, Wei Sun, and Hongan Wang. "What is that in your hand? Recognizing grasped objects via forearm electromyography sensing". In: *Proceedings of the ACM on Interactive, Mobile, Wearable and Ubiquitous Technologies* 2.4 (2018), pp. 1–24. DOI: https://doi.org/10.1145/3287039.

[113] James R Fang, Rajesh Pahwa, Kelly E Lyons, Tobia Zanotto, and Jacob J Sosnoff. "Examining the validity of smart glasses in measuring spatiotemporal parameters of gait among people with Parkinson's disease". In: *Gait & Posture* 113 (2024), pp. 139–144.

[114] Nuruzzaman Faruqui, Mohammad Abu Yousuf, Md Whaiduzzaman, AKM Azad, Alistair Barros, and Mohammad Ali Moni. "LungNet: A hybrid deep-CNN model for lung cancer diagnosis using CT and wearable sensor-based medical IoT data". In: *Computers in Biology and Medicine* 139 (2021), p. 104961.

[115] Chao Feng, Jie Xiong, Liqiong Chang, Ju Wang, Xiaojiang Chen, Dingyi Fang, and Zhanyong Tang. "WiMi: Target material identification with

commodity Wi-Fi devices". In: *2019 IEEE 39th International Conference on Distributed Computing Systems (ICDCS)*. IEEE. 2019, pp. 700–710.

[116] Huber Flores, Agustin Zuniga, Naser Hossein Motlagh, Mohan Liyanage, Monica Passananti, Sasu Tarkoma, Moustafa Youssef, and Petteri Nurmi. "Penguin: Aquatic plastic pollution sensing using AUVs". In: *Proceedings of the ACM Workshop on Micro Aerial Vehicle Networks, Systems, and Applications*. DroNet'20. ACM New York, NY, USA: ACM, 2020, pp. 1–6. DOI: https://doi.org/10.1145/3396864.3399704.

[117] Huber Flores, Agustin Zuniga, Marko Radeta, Zhigang Yin, Mohan Liyanage, Naser Hossein Motlagh, Ngoc Thi Nguyen, Sasu Tarkoma, Moustafa Youssef, and Petteri Nurmi. "SEAGULL: Low-Cost Pervasive Sensing for Monitoring and Analysing Underwater Plastics". In: *2024 IEEE/ACM Ninth International Conference on Internet-of-Things Design and Implementation (IoTDI)*. 2024, pp. 49–60.

[118] Andrea Fois, Filippo Tocco, Antonio Dell'Osa, Laura Melis, Ugo Bertelli, Alberto Concu, Andrea Manuello Bertetto, and Carmen Serra. "Innovative smart face mask to protect workers from COVID-19 infection". In: *2021 IEEE International Symposium on Medical Measurements and Applications (MeMeA)*. IEEE. 2021, pp. 1–6.

[119] Susana C Fonseca, Fernanda AR Oliveira, and Jeffrey K Brecht. "Modelling respiration rate of fresh fruits and vegetables for modified atmosphere packages: a review". In: *Journal of food engineering* 52.2 (2002), pp. 99–119.

[120] Nizan Friedman, Vicky Chan, Andrea N Reinkensmeyer, Ariel Beroukhim, Gregory J Zambrano, Mark Bachman, and David J Reinkensmeyer. "Retraining and assessing hand movement after stroke using the MusicGlove: Comparison with conventional hand therapy and isometric grip training". In: *Journal of NeuroEngineering and Rehabilitation* 11.1 (2014), pp. 1–14. DOI: https://doi.org/10.1186/1743-0003-11-76.

[121] Thomas Fritz, Elaine M Huang, Gail C Murphy, and Thomas Zimmermann. "Persuasive technology in the real world: a study of long-term use of activity sensing devices for fitness". In: *Proceedings of the SIGCHI conference on human factors in computing systems*. 2014, pp. 487–496.

[122] Ana Lúcia Gabas, Wiclef Dymurgo Marra-Júnior, Javier Telis-Romero, and Vânia Regina Nicoletti Telis. "Changes of density, thermal conductivity, thermal diffusivity, and specific heat of plums during drying". In: *International Journal of Food Properties* 8.2 (2005), pp. 233–242.

[123] Eva Ganglbauer, Geraldine Fitzpatrick, and Rob Comber. "Negotiating food waste: Using a practice lens to inform design". In: *ACM Transactions on Computer-Human Interaction (TOCHI)* 20.2 (2013), pp. 1–25.

[124] Eva Ganglbauer, Geraldine Fitzpatrick, and Florian Güldenpfennig. "Why and what did we throw out? Probing on reflection through the food waste

diary". In: *Proceedings of the 33rd Annual ACM Conference on Human Factors in Computing Systems*. 2015, pp. 1105–1114.

[125] Lei Gao, Alan K. Bourke, and John Nelson. "A system for activity recognition using multi-sensor fusion". In: *2011 Annual International Conference of the IEEE Engineering in Medicine and Biology Society*. 2011, pp. 7869–7872.

[126] Xiang Gao, Jennie Si, Yue Wen, Minhan Li, and He Huang. "Reinforcement learning control of robotic knee with human-in-the-loop by flexible policy iteration". In: *IEEE Transactions on Neural Networks and Learning Systems* 33.10 (2021), pp. 5873–5887.

[127] Yang Gao, Wei Wang, Vir V Phoha, Wei Sun, and Zhanpeng Jin. "EarEcho: Using ear canal echo for wearable authentication". In: *Proceedings of the ACM on Interactive, Mobile, Wearable and Ubiquitous Technologies* 3.3 (2019), pp. 1–24.

[128] Zhiyi Gao, Zheng Lou, Shuai Chen, La Li, Kai Jiang, Zuoling Fu, Wei Han, and Guozhen Shen. "Fiber gas sensor-integrated smart face mask for room-temperature distinguishing of target gases". In: *Nano Research* 11 (2018), pp. 511–519.

[129] José A García-Limón, Carlos Alvarado-Serrano, and Ramon Casanella. "A Novel BCG Heart Rate Detection System Using a Piezoelectric Sensor Embedded in a Shoe Insole". In: *IEEE Sensors Journal* (2024).

[130] Shkurta Gashi, Elena Di Lascio, and Silvia Santini. "Using unobtrusive wearable sensors to measure the physiological synchrony between presenters and audience members". In: *Proceedings of the ACM on Interactive, Mobile, Wearable and Ubiquitous Technologies* 3.1 (2019), pp. 1–19.

[131] Lata Gautam, Sarah D Sharratt, and Michael D Cole. "Drug facilitated sexual assault: detection and stability of benzodiazepines in spiked drinks using gas chromatography-mass spectrometry". In: *PloS one* 9.2 (2014), e89031.

[132] Shruti Gedam and Sanchita Paul. "A review on mental stress detection using wearable sensors and machine learning techniques". In: *IEEE Access* 9 (2021), pp. 84045–84066.

[133] Daniel Geißler, Hymalai Bello, Esther Zahn, Emil Woop, Bo Zhou, Paul Lukowicz, and Jakob Karolus. "Head'n Shoulder: Gesture-Driven Biking Through Capacitive Sensing Garments to Innovate Hands-Free Interaction". In: *Proceedings of the ACM on Human-Computer Interaction* 8.MHCI (2024), pp. 1–20.

[134] Bogdan-Florin Gheran, Jean Vanderdonckt, and Radu-Daniel Vatavu. "Gestures for smart rings: Empirical results, insights, and design implications". In: *Proceedings of the 2018 Designing Interactive Systems Conference*. 2018, pp. 623–635.

[135] Kamran Gholizadeh HamlAbadi, Fedwa Laamarti, and Abdulmotaleb El Saddik. “Meta-Review on Brain-Computer Interface (BCI) in the Metaverse”. In: *ACM Transactions on Multimedia Computing, Communications and Applications* 20.12 (2024), pp. 1–42.

[136] Nimisha Ghosh, Rourab Paul, Satyabrata Maity, Krishanu Maity, and Sayantan Saha. “Fault Matters: Sensor data fusion for detection of faults using Dempster–Shafer theory of evidence in IoT-based applications”. In: *Expert Systems with Applications* 162 (2020), p. 113887.

[137] Giada Giorgi, Alessandra Galli, and Claudio Narduzzi. “Smartphone-based IOT systems for personal health monitoring”. In: *IEEE Instrumentation Measurement Magazine* 23.4 (2020), pp. 41–47. DOI: 10.1109/MIM.2020.9126070.

[138] Oliver Glauser, Shihao Wu, Daniele Panozzo, Otmar Hilliges, and Olga Sorkine-Hornung. “Interactive hand pose estimation using a stretch-sensing soft glove”. In: *ACM Transactions on Graphics (ToG)* 38.4 (2019), pp. 1–15.

[139] Mayank Goel et al. “HyperCam: hyperspectral imaging for ubiquitous computing applications”. In: *Proceedings of the 2015 ACM International Joint Conference on Pervasive and Ubiquitous Computing*. 2015, pp. 145–156.

[140] Mayank Goel, Jacob Wobbrock, and Shwetak Patel. “GripSense: Using built-in sensors to detect hand posture and pressure on commodity mobile phones”. In: *ACM Symposium on User Interface Software and Technology*. New York, NY, USA: ACM, 2012, pp. 545–554. DOI: https://doi.org/10.1145/2380116.2380184.

[141] Shantappa G Gollagi, MM Math, and Aruna A Daptardar. “A survey on pervasive computing over context-aware system”. In: *CCF Transactions on Pervasive Computing and Interaction* 2.2 (2020), pp. 79–85.

[142] Walid Gomaa. “Comparative analysis of different approaches to human activity recognition based on accelerometer signals”. In: *Machine Learning and Big Data Analytics Paradigms: Analysis, Applications and Challenges* (2021), pp. 303–322.

[143] Lovedeep Gondara. “Medical image denoising using convolutional denoising autoencoders”. In: *2016 IEEE 16th international conference on data mining workshops (ICDMW)*. IEEE. 2016, pp. 241–246.

[144] GOV.UK. *Spiking factsheet*. https://www.gov.uk/government/publications/spiking-factsheet/spiking-factsheet [Accessed: 2024-07-01]. 2023.

[145] Ella Graham-Rowe, Donna C Jessop, and Paul Sparks. “Identifying motivations and barriers to minimising household food waste”. In: *Resources, conservation and recycling* 84 (2014), pp. 15–23.

[146] Ana Carolina Amaral Gratão et al. “Thermal properties of passion fruit juice as affected by temperature and water content”. In: *Journal of food process engineering* 27.6 (2004), pp. 413–431.

[147] P Greidanus and MA Verhoeven. *Product data of tomatoes*. Tech. rep. Sprenger Instituut, 1986.

[148] Daniel Groeger and Jürgen Steimle. “ObjectSkin: augmenting everyday objects with hydroprinted touch sensors and displays”. In: *Proceedings of the ACM on Interactive, Mobile, Wearable and Ubiquitous Technologies* 1.4 (2018), pp. 1–23.

[149] Weixi Gu, Yuxun Zhou, Zimu Zhou, Xi Liu, Han Zou, Pei Zhang, Costas J Spanos, and Lin Zhang. “SugarMate: Non-intrusive blood glucose monitoring with smartphones”. In: *Proceedings of the ACM on Interactive, Mobile, Wearable and Ubiquitous Technologies* 1.3 (2017), pp. 1–27. DOI: https://doi.org/10.1145/3130919.

[150] Yu Guan and Thomas Plötz. “Ensembles of deep lstm learners for activity recognition using wearables”. In: *Proceedings of the ACM on interactive, mobile, wearable and ubiquitous technologies* 1.2 (2017), pp. 1–28.

[151] RS Guerra, I Fonseca, F Pichel, MT Restivo, and TF Amaral. “Hand length as an alternative measurement of height”. In: *European Journal of Clinical Nutrition* 68.2 (2014), pp. 229–233. DOI: https://doi.org/10.1038/ejcn.2013.220.

[152] Jeremy Gummeson, Bodhi Priyantha, and Jie Liu. “An energy harvesting wearable ring platform for gestureinput on surfaces”. In: *Proceedings of the 12th annual international conference on Mobile systems, applications, and services*. 2014, pp. 162–175.

[153] Esra Gümüs, Jan Christoph Gutzmann, Sebastian Thomas Büttner, and Michael Prilla. “The Impact of Smart-glass-based Video Tutorials on Knowledge Transfer in Practice”. In: *Proceedings of Mensch und Computer 2024*. 2024, pp. 219–230.

[154] Ahmad Anas Nagoor Gunny, Subash CB Gopinath, Asgar Ali, Chalermchai Wongs-Aree, Noor Hasyierah Mohd Salleh, et al. “Challenges of postharvest water loss in fruits: Mechanisms, influencing factors, and effective control strategies–A comprehensive review”. In: *Journal of Agriculture and Food Research* (2024), p. 101249.

[155] Gabriel Guo, Hanbin Zhang, Liuyi Yao, Huining Li, Chenhan Xu, Zhengxiong Li, and Wenyao Xu. “MSLife: digital behavioral phenotyping of multiple sclerosis symptoms in the wild using wearables and graph-based statistical analysis”. In: *Proceedings of the ACM on Interactive, Mobile, Wearable and Ubiquitous Technologies* 5.4 (2021), pp. 1–35.

[156] Tiantian Guo, Tongpo Zhang, Enggee Lim, Miguel Lopez-Benitez, Fei Ma, and Limin Yu. “A review of wavelet analysis and its applications:

Challenges and opportunities". In: *IEEe Access* 10 (2022), pp. 58869–58903.

[157] Xiaonan Guo, Jian Liu, and Yingying Chen. "FitCoach: Virtual fitness coach empowered by wearable mobile devices". In: *IEEE INFOCOM 2017-IEEE Conference on Computer Communications*. IEEE. 2017, pp. 1–9.

[158] Xiaonan Guo, Jian Liu, and Yingying Chen. "When your wearables become your fitness mate". In: *Smart Health* 16 (2020), p. 100114.

[159] Unsoo Ha, Yunfei Ma, Zexuan Zhong, Tzu-Ming Hsu, and Fadel Adib. "Learning Food Quality and Safety from Wireless Stickers." In: *HotNets*. 2018, pp. 106–112.

[160] Juan Haladjian, Daniel Schlabbers, Sajjad Taheri, Max Tharr, and Bernd Bruegge. "Sensor-based detection and classification of soccer goalkeeper training exercises". In: *ACM transactions on Internet of things* 1.2 (2020), pp. 1–20.

[161] Nils Y Hammerla, Reuben Kirkham, Peter Andras, and Thomas Ploetz. "On preserving statistical characteristics of accelerometry data using their empirical cumulative distribution". In: *Proceedings of the 2013 international symposium on wearable computers*. 2013, pp. 65–68.

[162] Jing Han, Chloë Brown, Jagmohan Chauhan, Andreas Grammenos, Apinan Hasthanasombat, Dimitris Spathis, Tong Xia, Pietro Cicuta, and Cecilia Mascolo. "Exploring automatic COVID-19 diagnosis via voice and symptoms from crowdsourced data". In: *Proceedings of IEEE International Conference on Acoustics, Speech and Signal Processing*. ICASSP'21. Toronto, ON, Canada: IEEE, 2021, pp. 8328–8332. DOI: https://doi.org/10.1109/ICASSP39728.2021.9414576.

[163] Jing Han, Tong Xia, Dimitris Spathis, Erika Bondareva, Chloë Brown, Jagmohan Chauhan, Ting Dang, Andreas Grammenos, Apinan Hasthanasombat, Floto Floto Andres, Cicuta Piero, and Mascolo Cecilia. "Sounds of COVID-19: Exploring realistic performance of audio-based digital testing". In: *npj Digital Medicine* 5 (2021), pp. 1–9. DOI: https://doi.org/10.1038/s41746-021-00553-x.

[164] ASHRAE Handbook and Refrigeration Chapter. "Thermal properties of foods". In: *ASHRAE Refrigeration Handbook, ASHRAE, Atlanta, GA* (2018).

[165] Katrin Hänsel, Akram Alomainy, and Hamed Haddadi. "Large scale mood and stress self-assessments on a smartwatch". In: *ACM International Joint Conference on Pervasive and Ubiquitous Computing: Adjunct*. UbiComp '16. New York, NY, USA: ACM, 2016, pp. 1180–1184. DOI: https://doi.org/10.1145/2968219.2968305.

[166] Mahmood Ul Hasan, Zora Singh, Hafiz Muhammad Shoaib Shah, Jashanpreet Kaur, and Andrew Woodward. "Water loss: A postharvest quality

marker in apple storage". In: *Food and Bioprocess Technology* 17.8 (2024), pp. 2155–2180.

[167] Ali Hassani, Amir Iranmanesh, and Najme Mansouri. "Text mining using nonnegative matrix factorization and latent semantic analysis". In: *Neural Computing and Applications* 33 (2021), pp. 13745–13766.

[168] Chunhua He, Jiewen Tan, Xuelei Jian, Guangxiong Zhong, Lianglun Cheng, and Juze Lin. "A smart flexible vital signs and sleep monitoring belt based on MEMS triaxial accelerometer and pressure sensor". In: *IEEE Internet of Things Journal* 9.15 (2022), pp. 14126–14136.

[169] Jibo He, William Choi, Yan Yang, Junshi Lu, Xiaohui Wu, and Kaiping Peng. "Detection of driver drowsiness using wearable devices: A feasibility study of the proximity sensor". In: *Applied ergonomics* 65 (2017), pp. 473–480.

[170] Shan He, Siying Li, Anindya Nag, Shilun Feng, Tao Han, Subhas Chandra Mukhopadhyay, and Warwick Powel. "A comprehensive review of the use of sensors for food intake detection". In: *Sensors and Actuators A: Physical* 315 (2020), p. 112318.

[171] Tongyue He, Junxin Chen, Ben-Guo He, Wei Wang, Zhi-Liang Zhu, and Zhihan Lv. "Toward wearable sensors: advances, trends, and challenges". In: *ACM Computing Surveys* 55.14s (2023), pp. 1–35.

[172] Carolin Helbig, Maximilian Ueberham, Anna Maria Becker, Heike Marquart, and Uwe Schlink. "Wearable sensors for human environmental exposure in urban settings". In: *Current Pollution Reports* 7.3 (2021), pp. 417–433.

[173] Hans J Hellebrand, Horst Beuche, and Manfred Linke. "Determination of thermal emissivity and surface temperature distribution of horticultural products". In: *Sixth international symposium on fruit, nut and vegetable production engineering, Potsdam, Germany*. 2001, pp. 1497–1504.

[174] Javier Hernandez, Daniel McDuff, Christian Infante, Pattie Maes, Karen Quigley, and Rosalind Picard. "Wearable ESM: differences in the experience sampling method across wearable devices". In: *Proceedings of the 18th international conference on human-computer interaction with mobile devices and services*. 2016, pp. 195–205.

[175] Steven M Hernandez and Eyuphan Bulut. "Lightweight and standalone IoT based WiFi sensing for active repositioning and mobility". In: *2020 IEEE 21st International Symposium on" A World of Wireless, Mobile and Multimedia Networks"(WoWMoM)*. IEEE. 2020, pp. 277–286.

[176] Steven M Hernandez, Md Touhiduzzaman, Peter E Pidcoe, and Eyuphan Bulut. "Wi-PT: Wireless sensing based low-cost physical rehabilitation tracking". In: *2022 IEEE International Conference on E-health Networking, Application & Services (HealthCom)*. IEEE. 2022, pp. 113–118.

[177] Maarten LATM Hertog, Ruth Ben-Arie, Erika Róth, and Bart M Nicolaı. "Humidity and temperature effects on invasive and non-invasive firmness measures". In: *Postharvest biology and technology* 33.1 (2004), pp. 79–91.

[178] Christian Holz and Edward J Wang. "Glabella: Continuously sensing blood pressure behavior using an unobtrusive wearable device". In: *Proceedings of the ACM on Interactive, Mobile, Wearable and Ubiquitous Technologies* 1.3 (2017), pp. 1–23. DOI: https://doi.org/10.1145/3132024.

[179] Mohammad Hossin and Md Nasir Sulaiman. "A review on evaluation metrics for data classification evaluations". In: *International journal of data mining & knowledge management process* 5.2 (2015), p. 1.

[180] Xinyu Hou and Jeroen Bergmann. "Pedestrian dead reckoning with wearable sensors: A systematic review". In: *IEEE Sensors Journal* 21.1 (2020), pp. 143–152.

[181] Steven Houben and Nicolai Marquardt. "Watchconnect: A toolkit for prototyping smartwatch-centric cross-device applications". In: *Proceedings of the 33rd annual ACM conference on human factors in computing systems*. 2015, pp. 1247–1256.

[182] Jingyang Hu, Hongbo Jiang, Daibo Liu, Zhu Xiao, Qibo Zhang, Jiangchuan Liu, and Schahram Dustdar. "Combining IMU With Acoustics for Head Motion Tracking Leveraging Wireless Earphone". In: *IEEE Transactions on Mobile Computing* (2023).

[183] Jingyang Hu, Hongbo Jiang, Zhu Xiao, Siyu Chen, Schahram Dustdar, and Jiangchuan Liu. "HeadTrack: Real-time Human-Computer Interaction via Wireless Earphones". In: *IEEE Journal on Selected Areas in Communications* (2023).

[184] Hui Huang, Li Liu, and Michael O Ngadi. "Recent developments in hyperspectral imaging for assessment of food quality and safety". In: *Sensors* 14.4 (2014), pp. 7248–7276.

[185] Wenbo Huang, Lei Zhang, Wenbin Gao, Fuhong Min, and Jun He. "Shallow convolutional neural networks for human activity recognition using wearable sensors". In: *IEEE Transactions on Instrumentation and Measurement* 70 (2021), pp. 1–11.

[186] Yiran Huang, Yexu Zhou, Haibin Zhao, Till Riedel, and Michael Beigl. "A survey on wearable human activity recognition: innovative pipeline development for enhanced research and practice". In: *2024 International Joint Conference on Neural Networks (IJCNN)*. IEEE. 2024, pp. 1–10.

[187] Yongzhi Huang et al. "A Portable and Convenient System for Unknown Liquid Identification with Smartphone Vibration". In: *IEEE TMC* (2021).

[188] Yongzhi Huang et al. "Lili: liquor quality monitoring based on light signals". In: *Proceedings of the MobiCom 2021*. 2021, pp. 256–268.

[189] Yongzhi Huang et al. "Vi-liquid: unknown liquid identification with your smartphone vibration". In: *Proceedings of MobiCom 2021*. 2021.

[190] James M Hunter, Lawrence H Schneider, Evelyn J Mackin, and Anne D Callahan. “Rehabilitation of the hand: Surgery and therapy”. In: *Rehabilitation of the hand: Surgery and therapy*. USA: St. Louis: Mosby, 1990, pp. 1258–1258.

[191] Sinh Huynh, Rajesh Krishna Balan, JeongGil Ko, and Youngki Lee. “VitaMon: Measuring heart rate variability using smartphone front camera”. In: *Proceedings of the ACM Conference on Embedded Networked Sensor Systems*. SenSys’19. New York, NY, United States: ACM, 2019, pp. 1–14. DOI: https://doi.org/10.1145/3356250.3360036.

[192] Jarkko Hyysalo, Sandun Dasanayake, Jari Hannu, Christian Schuss, Mikko Rajanen, Teemu Leppänen, David Doermann, and Jaakko Sauvola. “Smart mask–Wearable IoT solution for improved protection and personal health”. In: *Internet of things* 18 (2022), p. 100511.

[193] Mohamed Ibrahim, Viet Nguyen, Siddharth Rupavatharam, Minitha Jawahar, Marco Gruteser, and Richard Howard. “Visible light based activity sensing using ceiling photosensors”. In: *Proceedings of the 3rd Workshop on Visible Light Communication Systems*. 2016, pp. 43–48.

[194] Anayo Chukwu Ikegwu, Henry Friday Nweke, Chioma Virginia Anikwe, Uzoma Rita Alo, and Obikwelu Raphael Okonkwo. “Big data analytics for data-driven industry: a review of data sources, tools, challenges, solutions, and research directions”. In: *Cluster Computing* 25.5 (2022), pp. 3343–3387.

[195] Nazrul Ismail and Owais A Malik. “Real-time visual inspection system for grading fruits using computer vision and deep learning techniques”. In: *Information Processing in Agriculture* 9.1 (2022), pp. 24–37.

[196] Shunsuke Iwakiri and Kazuya Murao. “User Authentication Method for Wearable Ring Devices using Active Acoustic Sensing”. In: *Proceedings of the 2023 ACM International Symposium on Wearable Computers*. 2023, pp. 17–21.

[197] Sara R Jaeger et al. “Buy, eat or discard? A case study with apples to explore fruit quality perception and food waste”. In: *Food Quality and Preference* 69 (2018), pp. 10–20.

[198] Hayeon Jeong, Heepyung Kim, Rihun Kim, Uichin Lee, and Yong Jeong. “Smartwatch wearing behavior analysis: a longitudinal study”. In: *Proceedings of the ACM on Interactive, Mobile, Wearable and Ubiquitous Technologies* 1.3 (2017), pp. 1–31.

[199] Mingi Jeong, Hyesun Lee, Myungnam Bae, Dong-Beom Shin, Sun-Hwa Lim, and Kang Bok Lee. “Development and application of the smart helmet for disaster and safety”. In: *2018 International conference on information and communication technology convergence (ICTC)*. IEEE. 2018, pp. 1084–1089.

[200] Bowen Ji, Xuanqi Wang, Zekai Liang, Haoyang Zhang, Qianchen Xia, Liang Xie, Huijiong Yan, Fanqi Sun, Huicheng Feng, Kai Tao, et al. "Flexible strain sensor-based data glove for gesture interaction in the metaverse: a review". In: *International Journal of Human–Computer Interaction* (2023), pp. 1–20.

[201] Shuo Jiang, Peiqi Kang, Xinyu Song, Benny PL Lo, and Peter B Shull. "Emerging wearable interfaces and algorithms for hand gesture recognition: A survey". In: *IEEE Reviews in Biomedical Engineering* 15 (2021), pp. 85–102.

[202] Shuo Jiang, Ling Li, Haipeng Xu, Junkai Xu, Guoying Gu, and Peter B Shull. "Stretchable e-skin patch for gesture recognition on the back of the hand". In: *IEEE Transactions on Industrial Electronics* 67.1 (2019), pp. 647–657.

[203] Weiwei Jiang et al. "Probing Sucrose Contents in Everyday Drinks Using Miniaturized Near-Infrared Spectroscopy Scanners". In: *Proceedings of the ACM on Interactive, Mobile, Wearable and Ubiquitous Technologies* 3.4 (2019), pp. 1–25.

[204] Menglin Jin and Shunlin Liang. "An improved land surface emissivity parameter for land surface models using global remote sensing observations". In: *Journal of Climate* 19.12 (2006), pp. 2867–2881.

[205] Yincheng Jin, Seokmin Choi, Yang Gao, Jiyang Li, Zhengxiong Li, and Zhanpeng Jin. "TransASL: A Smart Glass based Comprehensive ASL Recognizer in Daily Life". In: *Proceedings of the 28th International Conference on Intelligent User Interfaces*. 2023, pp. 802–818.

[206] Kevin Jiokeng, Gentian Jakllari, and André-Luc Beylot. "HandRate: Heart rate monitoring while simply holding a smartphone". In: *Proceedings of IEEE International Conference on Pervasive Computing and Communications*. PerCom'21. Kassel, Germany: IEEE, 2021, pp. 1–11. DOI: https://doi.org/10.1109/PERCOM50583.2021.9439134.

[207] Isa John et al. "Determination of thermal conductivity and thermal diffusivity of three varieties of melon". In: *Journal of Emerging Trends in Engineering and Applied Sciences* 5.2 (2014), pp. 123–128.

[208] Pablo Juliano et al. "The need for thermophysical properties in simulating emerging food processing technologies". In: *Innovative food technologies: advances in multiphysics simulation. Wiley-blackwell IFT Press, Ames, USA* (2011), pp. 23–38.

[209] Rohan Reddy Kalavakonda, Naren Vikram Raj Masna, Anamika Bhuniaroy, Soumyajit Mandal, and Swarup Bhunia. "A smart mask for active defense against coronaviruses and other airborne pathogens". In: *IEEE Consumer Electronics Magazine* 10.2 (2020), pp. 72–79.

[210] R Karthickraja, R Kumar, S Kirubakaran, R Manikandan, et al. "COVID-19 prediction and symptom analysis using wearable sensors and IoT". In:

International Journal of Pervasive Computing and Communications 18.5 (2020), pp. 499–507.

[211] Yohei Kawabata, Koichi Wada, Manabu Nakatani, Shizuo Yamada, and Satomi Onoue. "Formulation design for poorly water-soluble drugs based on biopharmaceutics classification system: basic approaches and practical applications". In: *International journal of pharmaceutics* 420.1 (2011), pp. 1–10.

[212] Marike Kellermayr-Scheucher, Laura Hörandner, and Patrick Brandtner. "Digitalization at the point-of-sale in grocery retail-state of the art of smart shelf technology and application scenarios". In: *Procedia Computer Science* 196 (2022), pp. 77–84.

[213] Prakash Khadka, Jieun Ro, Hyeongmin Kim, Iksoo Kim, Jeong Tae Kim, Hyunil Kim, Jae Min Cho, Gyiae Yun, and Jaehwi Lee. "Pharmaceutical particle technologies: An approach to improve drug solubility, dissolution and bioavailability". In: *Asian journal of pharmaceutical sciences* 9.6 (2014), pp. 304–316.

[214] Saad Khan, Simon Parkinson, Liam Grant, Na Liu, and Stephen Mcguire. "Biometric systems utilising health data from wearable devices: applications and future challenges in computer security". In: *ACM Computing Surveys (CSUR)* 53.4 (2020), pp. 1–29.

[215] Shehroz S Khan and Babak Taati. "Detecting unseen falls from wearable devices using channel-wise ensemble of autoencoders". In: *Expert Systems with Applications* 87 (2017), pp. 280–290.

[216] Rushil Khurana, Mayank Goel, and Kent Lyons. "Detachable smartwatch: More than a wearable". In: *Proceedings of the ACM on Interactive, Mobile, Wearable and Ubiquitous Technologies* 3.2 (2019), pp. 1–14.

[217] Ali Kiaghadi, Seyedeh Zohreh Homayounfar, Jeremy Gummeson, Trisha Andrew, and Deepak Ganesan. "Phyjama: Physiological sensing via fiber-enhanced pyjamas". In: *Proceedings of the ACM on Interactive, Mobile, Wearable and Ubiquitous Technologies* 3.3 (2019), pp. 1–29.

[218] Hojoong Kim, Hyuntai Park, Wonhee Lee, Jongwoo Kim, and Yong-Lae Park. "Design of wearable orthopedic devices for treating forward head postures using pneumatic artificial muscles and flex sensors". In: *2017 14th International Conference on Ubiquitous Robots and Ambient Intelligence (URAI)*. IEEE. 2017, pp. 809–814.

[219] Jung-Yoon Kim, Ja Young Hwang, Eunse Park, Hyeon-Uk Nam, and Songhee Cheon. "Flat-feet prediction based on a designed wearable sensing shoe and a PCA-based deep neural network model". In: *IEEE Access* 8 (2020), pp. 199070–199080.

[220] Kee-Eung Kim, Wook Chang, Sung-Jung Cho, Junghyun Shim, Hyunjeong Lee, Joonah Park, Youngbeom Lee, and Sangryoung Kim. "Hand grip pattern recognition for mobile user interfaces". In: *Proceedings of the ACM*

Conference on Innovative Applications of Artificial Intelligence. IAAI'06. Boston Massachusetts, USA: ACM, 2006, pp. 1789–1794. DOI: https://doi.org/10.5555/1597122.1597138.

[221] Yoojung Kim, Hee-Tae Jung, Joonwoo Park, Yangsoo Kim, Nathan Ramasarma, Paolo Bonato, Eun Kyoung Choe, and Sunghoon Ivan Lee. "Towards the design of a ring sensor-based mHealth system to achieve optimal motor function in stroke survivors". In: *Proceedings of the ACM on Interactive, Mobile, Wearable and Ubiquitous Technologies* 3.4 (2019), pp. 1–26. DOI: https://doi.org/10.1145/3369817.

[222] Rachel C King, Emma Villeneuve, Ruth J White, R Simon Sherratt, William Holderbaum, and William S Harwin. "Application of data fusion techniques and technologies for wearable health monitoring". In: *Medical engineering & physics* 42 (2017), pp. 1–12.

[223] Hiroshi Kinoshita, Satoru Kawai, and Komei Ikuta. "Contributions and co-ordination of individual fingers in multiple finger prehension". In: *Ergonomics* 38.6 (1995), pp. 1212–1230. DOI: https://doi.org/10.1080/00140139508925183.

[224] Jyoti A Kodagali and S Balaji. "Computer vision and image analysis based techniques for automatic characterization of fruits-a review". In: *International Journal of Computer Applications* 50.6 (2012).

[225] Mikko Korkiakoski, Paula Alavesa, and Panos Kostakos. "Preference in voice commands and gesture controls with hands-free augmented reality with novel users". In: *IEEE Pervasive Computing* (2024).

[226] Jacob Leon Kröger, Philip Raschke, and Towhidur Rahman Bhuiyan. "Privacy implications of accelerometer data: a review of possible inferences". In: *Proceedings of the 3rd international conference on cryptography, security and privacy*. 2019, pp. 81–87.

[227] Pin-Sung Ku, Md Tahmidul Islam Molla, Kunpeng Huang, Priya Kattappurath, Krithik Ranjan, and Hsin-Liu Cindy Kao. "SkinKit: Construction Kit for On-Skin Interface Prototyping". In: *Proceedings of the ACM on Interactive, Mobile, Wearable and Ubiquitous Technologies* 5.4 (2021), pp. 1–23.

[228] Vishwajit V Kulkarni, Fatjon Seraj, and Jansi Rani Rathikumar. "An embedded wearable device for monitoring diabetic foot ulcer parameters". In: *Proceedings of the 13th ACM International Conference on PErvasive Technologies Related to Assistive Environments*. 2020, pp. 1–7.

[229] Devender Kumar, Steven Jeuris, Jakob E Bardram, and Nicola Dragoni. "Mobile and wearable sensing frameworks for mHealth studies and applications: A systematic review". In: *ACM Transactions on Computing for Healthcare* 2.1 (2020), pp. 1–28.

[230] Korupalli V Rajesh Kumar and Susan Elias. "Smart neck-band for rehabilitation of musculoskeletal disorders". In: *2020 International Conference*

on COMmunication Systems & NETworkS (COMSNETS). IEEE. 2020, pp. 47–52.

[231] Preeti Kumari, Lini Mathew, and Poonam Syal. "Increasing trend of wearables and multimodal interface for human activity monitoring: A review". In: *Biosensors and Bioelectronics* 90 (2017), pp. 298–307.

[232] Setor K Kunutsor, Ari Voutilainen, and Jari A Laukkanen. "Handgrip strength improves prediction of type 2 diabetes: A prospective cohort study". In: *Annals of Medicine* 52.8 (2020), pp. 471–478. DOI: https://doi.org/10.1080/07853890.2020.1815078.

[233] Elina Kuosmanen, Valerii Kan, Aku Visuri, Simo Hosio, and Denzil Ferreira. "Let's Draw: Detecting and measuring parkinson's disease on smartphones". In: *Proceedings of the Conference on Human Factors in Computing Systems*. CHI'20. Honolulu, HI, USA: ACM, 2020, pp. 1–9. DOI: https://doi.org/10.1145/3313831.3376864.

[234] Jonathan Lacanlale, Paruyr Isayan, Katya Mkrtchyan, and Ani Nahapetian. "Look Ma, No Hands: A Wearable Neck-Mounted Interface". In: *Proceedings of the Conference on Information Technology for Social Good*. 2021, pp. 13–18.

[235] Patrick E Lanigan et al. "Trinetra: Assistive Technologies for Grocery Shopping for the Blind." In: *ISWC*. 2006, pp. 147–148.

[236] Gierad Laput and Chris Harrison. "Sensing fine-grained hand activity with smartwatches". In: *Proceedings of the 2019 CHI Conference on Human Factors in Computing Systems*. 2019, pp. 1–13.

[237] Chang-Hung Lee, Cheng-Ru Lin, and Ming-Syan Chen. "Sliding window filtering: an efficient method for incremental mining on a time-variant database". In: *Information systems* 30.3 (2005), pp. 227–244.

[238] Kwangmuk Lee, Hee Young Chae, Kyeonghwan Park, Youngoh Lee, Seungse Cho, Hyunhyub Ko, and Jae Joon Kim. "A multi-functional physiological hybrid-sensing E-skin integrated interface for wearable IoT applications". In: *IEEE transactions on biomedical circuits and systems* 13.6 (2019), pp. 1535–1544.

[239] Lik Hang Lee, Tristan Braud, Farshid Hassani Bijarbooneh, and Pan Hui. "UbiPoint: towards non-intrusive mid-air interaction for hardware constrained smart glasses". In: *Proceedings of the 11th ACM Multimedia Systems Conference*. 2020, pp. 190–201.

[240] Wei-Han Lee and Ruby Lee. "Implicit sensor-based authentication of smartphone users with smartwatch". In: *Proceedings of the Hardware and Architectural Support for Security and Privacy 2016*. 2016, pp. 1–8.

[241] Narara Leesakul et al. "A new screening method for flunitrazepam in vodka and tequila by fluorescence spectroscopy". In: *Luminescence* (2013).

[242] Joanne Leong, Patrick Parzer, Florian Perteneder, Teo Babic, Christian Rendl, Anita Vogl, Hubert Egger, Alex Olwal, and Michael Haller. "pro-

Cover: sensory augmentation of prosthetic limbs using smart textile covers". In: *Proceedings of the 29th Annual Symposium on User Interface Software and Technology*. 2016, pp. 335–346.

[243] Boning Li and Akane Sano. "Extraction and interpretation of deep autoencoder-based temporal features from wearables for forecasting personalized mood, health, and stress". In: *Proceedings of the ACM on Interactive, Mobile, Wearable and Ubiquitous Technologies* 4.2 (2020), pp. 1–26.

[244] Gang Li, Boon-Leng Lee, and Wan-Young Chung. "Smartwatch-based wearable EEG system for driver drowsiness detection". In: *IEEE Sensors Journal* 15.12 (2015), pp. 7169–7180.

[245] Ke Li, Ruidong Zhang, Siyuan Chen, Boao Chen, Mose Sakashita, François Guimbretière, and Cheng Zhang. "EyeEcho: Continuous and Low-power Facial Expression Tracking on Glasses". In: *Proceedings of the CHI Conference on Human Factors in Computing Systems*. 2024, pp. 1–24.

[246] Ping Li, Ramy Meziane, Martin J-D Otis, Hassan Ezzaidi, and Philippe Cardou. "A Smart Safety Helmet using IMU and EEG sensors for worker fatigue detection". In: *2014 IEEE International Symposium on Robotic and Sensors Environments (ROSE) Proceedings*. IEEE. 2014, pp. 55–60.

[247] Ruinian Li, Tianyi Song, Nicholas Capurso, Jiguo Yu, Jason Couture, and Xiuzhen Cheng. "IoT applications on secure smart shopping system". In: *IEEE Internet of Things Journal* 4.6 (2017), pp. 1945–1954.

[248] Tianxing Li, Chuankai An, Zhao Tian, Andrew T Campbell, and Xia Zhou. "Human sensing using visible light communication". In: *Proceedings of the 21st annual international conference on mobile computing and networking*. 2015, pp. 331–344.

[249] Tianxing Li, Qiang Liu, and Xia Zhou. "Practical human sensing in the light". In: *Proceedings of the 14th Annual International Conference on Mobile Systems, Applications, and Services*. 2016, pp. 71–84.

[250] Zhaohui Li, Wei Luo, Yongmin Zhang, Jianxi Chen, Yuanchao Shu, and Yaoxue Zhang. "ASLiquid: Non-Intrusive Liquid Counterfeit Identification with Your Earphones". In: *Proceedings of the 22nd ACM Conference on Embedded Networked Sensor Systems*. 2024, pp. 41–53.

[251] Yongbo Liang, Mohamed Elgendi, Zhencheng Chen, and Rabab Ward. "An optimal filter for short photoplethysmogram signals". In: *Scientific Data* 5.1 (2018), pp. 1–12. DOI: https://doi.org/10.1038/sdata.2018.76.

[252] Yumeng Liang, Anfu Zhou, Huanhuan Zhang, Xinzhe Wen, and Huadong Ma. "FG-LiquID: A contact-less fine-grained liquid identifier by pushing the limits of millimeter-wave sensing". In: *Proceedings of the ACM on Interactive, Mobile, Wearable and Ubiquitous Technologies* 5.3 (2021), pp. 1–27.

[253] Daniyal Liaqat, Mohamed Abdalla, Pegah Abed-Esfahani, Moshe Gabel, Tatiana Son, Robert Wu, Andrea Gershon, Frank Rudzicz, and Eyal De

Lara. “WearBreathing: Real world respiratory rate monitoring using smartwatches”. In: *Proceedings of the ACM on Interactive, Mobile, Wearable and Ubiquitous Technologies* 3.2 (2019), pp. 1–22.

[254] Chi-Wei Lien and Sudip Vhaduri. “Challenges and opportunities of biometric user authentication in the age of iot: A survey”. In: *ACM Computing Surveys* 56.1 (2023), pp. 1–37.

[255] Gabriele Ligorio and Angelo M Sabatini. “A novel Kalman filter for human motion tracking with an inertial-based dynamic inclinometer”. In: *IEEE Transactions on Biomedical Engineering* 62.8 (2015), pp. 2033–2043.

[256] Qi Lin, Shuhua Peng, Yuezhong Wu, Jun Liu, Wen Hu, Mahbub Hassan, Aruna Seneviratne, and Chun H Wang. “E-jacket: Posture detection with loose-fitting garment using a novel strain sensor”. In: *2020 19th ACM/IEEE International Conference on Information Processing in Sensor Networks (IPSN)*. IEEE. 2020, pp. 49–60.

[257] Qi Lin, Shuhua Peng, Yuezhong Wu, Jun Liu, Hong Jia, Wen Hu, Mahbub Hassan, Aruna Seneviratne, and Chun H Wang. “Subject-adaptive loose-fitting smart garment platform for human activity recognition”. In: *ACM Transactions on Sensor Networks* 19.4 (2023), pp. 1–23.

[258] Xinye Lin, Yixin Chen, Xiao-Wen Chang, Xue Liu, and Xiaodong Wang. “Show: Smart handwriting on watches”. In: *Proceedings of the ACM on interactive, mobile, wearable and ubiquitous technologies* 1.4 (2018), pp. 1–23.

[259] Martin Valdemar Anker Lindrup, EunJeong Cheon, Michael B Skov, Dimitrios Raptis, and Rob Comber. “Sustainable Foodtures: Exploring Roles of Future Technology in Sustainable Food Shopping”. In: *Nordic Human-Computer Interaction Conference*. 2022, pp. 1–12.

[260] Gheorghe Lisca, Cristian Prodaniuc, Thomas Grauschopf, and Cristian Axenie. “Less is more: learning insights from a single motion sensor for accurate and explainable soccer goalkeeper kinematics”. In: *IEEE Sensors Journal* 21.18 (2021), pp. 20375–20387.

[261] Aixin Liu, Bei Feng, Bin Wang, Bingxuan Wang, Bo Liu, Chenggang Zhao, Chengqi Dengr, Chong Ruan, Damai Dai, Daya Guo, et al. “Deepseek-v2: A strong, economical, and efficient mixture-of-experts language model”. In: *arXiv preprint arXiv:2405.04434* (2024).

[262] Rongrong Liu, Florent Nageotte, Philippe Zanne, Michel de Mathelin, and Birgitta Dresp-Langley. “Wearable sensor technology for individual grip force profiling”. In: *Automation, Robotics & Communications for Industry 4.0* 1 (2021), pp. 12–13.

[263] Ruibo Liu, Qijia Shao, Siqi Wang, Christina Ru, Devin Balkcom, and Xia Zhou. “Reconstructing human joint motion with computational fabrics”. In: *Proceedings of the ACM on Interactive, Mobile, Wearable and Ubiquitous Technologies* 3.1 (2019), pp. 1–26.

[264] Yang Liu, Chengdong Lin, and Zhenjiang Li. “WR-Hand: Wearable armband can track user’s hand”. In: *Proceedings of the ACM on Interactive, Mobile, Wearable and Ubiquitous Technologies* 5.3 (2021), pp. 1–27.

[265] Yutong Liu et al. “Wi-Fruit: See Through Fruits with Smart Devices”. In: *Proceedings of the ACM on Interactive, Mobile, Wearable and Ubiquitous Technologies* 5.4 (2021), pp. 1–29.

[266] Markus Löchtefeld, Frederik Møller, Lukas Kyster, Anton Nygaard Petersen, Sture Nicolai Jaqué, Anita Larsen, and Hamzah Ziadeh. “FridgeSort-Improving Fridge Sorting behaviour to reduce Food Waste through a Mobile Serious Game”. In: *Proceedings of the 22nd International Conference on Mobile and Ubiquitous Multimedia*. 2023, pp. 420–427.

[267] Darrell Loh, Shaghayegh Zihajehzadeh, Reynald Hoskinson, Hamid Abdollahi, and Edward J Park. “Pedestrian dead reckoning with smartglasses and smartwatch”. In: *IEEE Sensors Journal* 16.22 (2016), pp. 8132–8141.

[268] Jorge E Lozano. “Thermal properties of foods”. In: *Food Engineering-Volume I* (2009), p. 70.

[269] Chris Xiaoxuan Lu, Bowen Du, Hongkai Wen, Sen Wang, Andrew Markham, Ivan Martinovic, Yiran Shen, and Niki Trigoni. “Snoopy: Sniffing your smartwatch passwords via deep sequence learning”. In: *Proceedings of the ACM on Interactive, Mobile, Wearable and Ubiquitous Technologies* 1.4 (2018), pp. 1–29.

[270] Robert Lufu, Alemayehu Ambaw, and Umezuruike Linus Opara. “Water loss of fresh fruit: Influencing pre-harvest, harvest and postharvest factors”. In: *Scientia Horticulturae* 272 (2020), p. 109519.

[271] Pasindu Lugoda, Stephen Clive Hayes, Theodore Hughes-Riley, Alexander Turner, Mariana V Martins, Ashley Cook, Kaivalya Raval, Carlos Oliveira, Philip Breedon, and Tilak Dias. “Classifying gait alterations using an instrumented smart sock and deep learning”. In: *IEEE Sensors Journal* 22.23 (2022), pp. 23232–23242.

[272] Yiyue Luo, Chao Liu, Young Joong Lee, Joseph DelPreto, Kui Wu, Michael Foshey, Daniela Rus, Tomás Palacios, Yunzhu Li, Antonio Torralba, et al. “Adaptive tactile interaction transfer via digitally embroidered smart gloves”. In: *Nature communications* 15.1 (2024), p. 868.

[273] Dong Ma, Ting Dang, Ming Ding, and Rajesh Balan. “ClearSpeech: Improving Voice Quality of Earbuds Using Both In-Ear and Out-Ear Microphones”. In: *Proceedings of the ACM on Interactive, Mobile, Wearable and Ubiquitous Technologies* 7.4 (2024), pp. 1–25.

[274] Michele Magno, Angelo D’Aloia, Tommaso Polonelli, Lorenzo Spadaro, and Luca Benini. “Shelmet: an intelligent self-sustaining multi sensors smart helmet for bikers”. In: *Sensor Systems and Software: 7th International Conference, S-Cube 2016, Sophia Antipolis, Nice, France, December 1-2, 2016, Revised Selected Papers*. Springer. 2017, pp. 55–67.

[275] Michele Magno, Giovanni A Salvatore, Petar Jokic, and Luca Benini. "Self-sustainable smart ring for long-term monitoring of blood oxygenation". In: *IEEE access* 7 (2019), pp. 115400–115408.

[276] Md Shaad Mahmud, Hua Fang, and Honggang Wang. "An integrated wearable sensor for unobtrusive continuous measurement of autonomic nervous system". In: *IEEE Internet of Things Journal* 6.1 (2018), pp. 1104–1113.

[277] Md Shaad Mahmud, Honggang Wang, and Hua Fang. "SensoRing: An integrated wearable system for continuous measurement of physiological biomarkers". In: *2018 IEEE International Conference on Communications (ICC)*. IEEE. 2018, pp. 1–7.

[278] Niko Mäkitalo, Daniel Flores-Martin, Huber Flores, Eemil Lagerspetz, Francois Christophe, Petri Ihantola, Masiar Babazadeh, Pan Hui, Juan Manuel Murillo, Sasu Tarkoma, and Tommi Mikkonen. "Human data model: Improving programmability of health and well-being data for enhanced perception and interaction". In: *ACM Transactions on Computing for Healthcare* 1.4 (2020), pp. 1–39. DOI: https://doi.org/10.1145/3402524.

[279] Kaveh Malek, Keyvan Malek, and Fahimeh Khanmohammadi. "Response of soil thermal conductivity to various soil properties". In: *International Communications in Heat and Mass Transfer* 127 (2021), p. 105516.

[280] Titti Malmivirta, Jonatan Hamberg, Eemil Lagerspetz, Xin Li, Ella Peltonen, Huber Flores, and Petteri Nurmi. "Hot or not? robust and accurate continuous thermal imaging on flir cameras". In: *2019 IEEE International Conference on Pervasive Computing and Communications (PerCom*. IEEE. 2019, pp. 1–9.

[281] Silvia Angela Mansi, Giovanni Barone, Cesare Forzano, Ilaria Pigliautile, Maria Ferrara, Anna Laura Pisello, and Marco Arnesano. "Measuring human physiological indices for thermal comfort assessment through wearable devices: A review". In: *Measurement* 183 (2021), p. 109872.

[282] Maria De Marsico and Alessio Mecca. "A survey on gait recognition via wearable sensors". In: *ACM Computing Surveys (CSUR)* 52.4 (2019), pp. 1–39.

[283] Katsutoshi Masai, Kai Kunze, Daisuke Sakamoto, Yuta Sugiura, and Maki Sugimoto. "Face commands-user-defined facial gestures for smart glasses". In: *2020 IEEE International Symposium on Mixed and Augmented Reality (ISMAR)*. IEEE. 2020, pp. 374–386.

[284] Martina Maselli, Elisa Mussi, Francesca Cecchi, Mariangela Manti, Peppino Tropea, and Cecilia Laschi. "A wearable sensing device for monitoring single planes neck movements: Assessment of its performance". In: *IEEE Sensors Journal* 18.15 (2018), pp. 6327–6336.

[285] Carlo Massaroni, Cecilia Venanzi, Amanda P Silvatti, Daniela Lo Presti, Paola Saccomandi, Domenico Formica, Francesco Giurazza, Michele A Caponero, and Emiliano Schena. "Smart textile for respiratory monitoring and thoraco-abdominal motion pattern evaluation". In: *Journal of biophotonics* 11.5 (2018), e201700263.

[286] Nicola M Massy-Westropp, Tiffany K Gill, Anne W Taylor, Richard W Bohannon, and Catherine L Hill. "Hand grip strength: Age and gender stratified normative data in a population-based study". In: *BMC Research Notes* 4.1 (2011), pp. 1–5. DOI: https://doi.org/10.1186/1756-0500-4-127.

[287] Michel de Mathelin, Florent Nageotte, Philippe Zanne, and Birgitta Dresp-Langley. "Sensors for expert grip force profiling: towards benchmarking manual control of a robotic device for surgical tool movements". In: *Sensors* 19.20 (2019), p. 4575. DOI: https://doi.org/10.3390/s19204575.

[288] Yuki Matsuda, Takashi Hasegaway, Ismail Arai, Yutaka Arakawa, and Keiichi Yasumoto. "Waistonbelt 2: A belt-type wearable device for monitoring abdominal circumference, posture and activity". In: *2016 Ninth International Conference on Mobile Computing and Ubiquitous Networking (ICMU)*. IEEE. 2016, pp. 1–6.

[289] Hidenori Matsui, Takahiro Hashizume, and Koji Yatani. "Al-light: An Alcohol-Sensing Smart Ice Cube". In: *Proc. ACM Interact. Mob. Wearable Ubiquitous Technol.* 2.3 (Sept. 2018). DOI: 10.1145/3264936. URL: https://doi.org/10.1145/3264936.

[290] Hidenori Matsui, Takahiro Hashizume, and Koji Yatani. "Al-light: An alcohol-sensing smart ice cube". In: *Proceedings of the ACM on interactive, mobile, wearable and ubiquitous technologies* 2.3 (2018), pp. 1–20.

[291] Ryan McGrath, Nathaniel Johnson, Lukus Klawitter, Sean Mahoney, Kara Trautman, Caroline Carlson, Ella Rockstad, and Kyle J Hackney. "What are the association patterns between handgrip strength and adverse health conditions? A topical review". In: *SAGE Open Medicine* 8 (2020), pp. 1–12. DOI: https://doi.org/10.1177/2050312120910358.

[292] Ryan McGrath, Sheria G Robinson-Lane, Summer Cook, Brian C Clark, Stephen Herrmann, Melissa Lunsman O'Connor, and Kyle J Hackney. "Handgrip strength is associated with poorer cognitive functioning in aging Americans". In: *Journal of Alzheimer's Disease* 70.4 (2019), pp. 1187–1196. DOI: https://doi.org/10.3233/JAD-190042.

[293] M Mehta. *Biopharmaceutics Classification System (BCS): development, implementation, and growth*. 2016.

[294] Shenghuan Miao, Ling Chen, and Rong Hu. "Spatial-Temporal Masked Autoencoder for Multi-Device Wearable Human Activity Recognition". In:

Proceedings of the ACM on Interactive, Mobile, Wearable and Ubiquitous Technologies 7.4 (2024), pp. 1–25.

[295] Waldemar Minkina and Daniel Klecha. "Atmospheric transmission coefficient modelling in the infrared for thermovision measurements". In: *Journal of Sensors and Sensor Systems* 5.1 (2016), pp. 17–23.

[296] Nuri N Mohsenin. *Thermal properties of food and agricultural materials*. CRC Press, 2020.

[297] Vimal Mollyn, Riku Arakawa, Mayank Goel, Chris Harrison, and Karan Ahuja. "Imuposer: Full-body pose estimation using imus in phones, watches, and earbuds". In: *Proceedings of the 2023 CHI Conference on Human Factors in Computing Systems*. 2023, pp. 1–12.

[298] Shaikat Mondal, Swarup Saha, Himel Mondal, Rajesh De, Rabindranath Majumder, and Koushik Saha. "How to conduct inferential statistics online: A brief hands-on guide for biomedical researchers". In: *Indian Journal of Vascular and Endovascular Surgery* 9.1 (2022), pp. 54–62.

[299] Nathan W Moon, Paul MA Baker, and Kenneth Goughnour. "Designing wearable technologies for users with disabilities: Accessibility, usability, and connectivity factors". In: *Journal of Rehabilitation and Assistive Technologies Engineering* 6 (2019), p. 2055668319862137.

[300] Dan Morris, T Scott Saponas, Andrew Guillory, and Ilya Kelner. "RecoFit: using a wearable sensor to find, recognize, and count repetitive exercises". In: *Proceedings of the SIGCHI Conference on Human Factors in Computing Systems*. 2014, pp. 3225–3234.

[301] Vivian Genaro Motti. "Wearable health: opportunities and challenges". In: *Proceedings of the 13th EAI international conference on pervasive computing technologies for healthcare*. 2019, pp. 356–359.

[302] Vivian Genaro Motti and Kelly Caine. "Smart wearables or dumb wearables? Understanding how context impacts the UX in wrist worn interaction". In: *Proceedings of the 34th ACM International Conference on the Design of Communication*. 2016, pp. 1–10.

[303] Seyed Ahmadreza Mousavi and Rastko Selmic. "Wearable smart rings for multi-finger gesture recognition using supervised learning". In: *IEEE Transactions on Instrumentation and Measurement* (2023).

[304] Matia Mukama, Alemayehu Ambaw, and Umezuruike Linus Opara. "Thermophysical properties of fruit—a review with reference to postharvest handling". In: *Journal of Food Measurement and Characterization* 14 (2020), pp. 2917–2937.

[305] Subhas Chandra Mukhopadhyay. "Wearable sensors for human activity monitoring: A review". In: *IEEE sensors journal* 15.3 (2014), pp. 1321–1330.

[306] Darius Nahavandi, Roohallah Alizadehsani, Abbas Khosravi, and U Rajendra Acharya. "Application of artificial intelligence in wearable devices:

Opportunities and challenges". In: *Computer Methods and Programs in Biomedicine* 213 (2022), p. 106541.

[307] Krisjanis Nesenbergs. "Architecture of smart clothing for standardized wearable sensor systems". In: *IEEE Instrumentation & Measurement Magazine* 19.5 (2016), pp. 36–64.

[308] Ngoc Thi Nguyen, Agustin Zuniga, Marko Radeta, Huber Flores, and Petteri Nurmi. "Life is Plastic? Detecting the Presence of Micro-Plastics in Food and Drink Containers". In: *Proceedings of the 25th International Workshop on Mobile Computing Systems and Applications*. 2024, pp. 93–98.

[309] Naghmeh Niknejad, Waidah Binti Ismail, Abbas Mardani, Huchang Liao, and Imran Ghani. "A comprehensive overview of smart wearables: The state of the art literature, recent advances, and future challenges". In: *Engineering Applications of Artificial Intelligence* 90 (2020), p. 103529.

[310] Shahriar Nirjon, Jeremy Gummeson, Dan Gelb, and Kyu-Han Kim. "Typingring: A wearable ring platform for text input". In: *Proceedings of the 13th Annual International Conference on Mobile Systems, Applications, and Services*. 2015, pp. 227–239.

[311] Aditya Shekhar Nittala and Jürgen Steimle. "Next steps in epidermal computing: Opportunities and challenges for soft on-skin devices". In: *Proceedings of the 2022 CHI Conference on Human Factors in Computing Systems*. 2022, pp. 1–22.

[312] Zhale Nowroozilarki, Bobak J Mortazavi, and Roozbeh Jafari. "Variational autoencoders for biomedical signal morphology clustering and noise detection". In: *IEEE Journal of Biomedical and Health Informatics* (2023).

[313] Cecilia N Nunes and Jean-Pierre Emond. "Relationship between weight loss and visual quality of fruits and vegetables". In: *Proceedings of the Florida State Horticultural Society*. Vol. 120. 2007, pp. 235–245.

[314] Robin Nunkoo, Meetali Bhadain, and Shabanaz Baboo. "Household food waste: attitudes, barriers and motivations". In: *British Food Journal* 123.6 (2021), pp. 2016–2035.

[315] Henry Friday Nweke, Ying Wah Teh, Ghulam Mujtaba, and Mohammed Ali Al-Garadi. "Data fusion and multiple classifier systems for human activity detection and health monitoring: Review and open research directions". In: *Information Fusion* 46 (2019), pp. 147–170.

[316] Ian Oakley, DoYoung Lee, MD Rasel Islam, and Augusto Esteves. "Beats: Tapping gestures for smart watches". In: *Proceedings of the 33rd Annual ACM Conference on Human Factors in Computing Systems*. 2015, pp. 1237–1246.

[317] Mayowa Olapade, Adeyinka Akintola, Zhigang Yin, Reo Kuchida, Marko Radeta, and Huber Flores. "Tiny but Mighty: When Smart Rings Meet Large Language Models". In: *In Adjunct Proceedings of the 2025 ACM*

International Joint Conference on Pervasive and Ubiquitous Computing (ACM UbiComp/ISWC 2025), Workshop on UbiSense: Emerging Techniques in Ubiquitous Sensing and Interaction. 2025.

[318] Mayowa Olapade, Abdul-Rasheed Ottun, Zhigang Yin, Mohan Liyanage, Aleksandr Makarov, and Huber Flores. "Low-cost produce quality monitoring at scale: A practical re-purposing framework for pervasive agriculture". In: *Proceedings of the 13th International Conference on the Internet of Things*. 2023, pp. 129–137.

[319] Aleksandr Ometov, Viktoriia Shubina, Lucie Klus, Justyna Skibińska, Salwa Saafi, Pavel Pascacio, Laura Flueratoru, Darwin Quezada Gaibor, Nadezhda Chukhno, Olga Chukhno, et al. "A survey on wearable technology: History, state-of-the-art and current challenges". In: *Computer Networks* 193 (2021), p. 108074.

[320] Adam Page, Colin Shea, and Tinoosh Mohsenin. "Wearable seizure detection using convolutional neural networks with transfer learning". In: *2016 IEEE international symposium on circuits and systems (ISCAS)*. IEEE. 2016, pp. 1086–1089.

[321] Chao-Yang Pang, Ri-Gui Zhou, Ben-Qiong Hu, WenWen Hu, and Ahmed El-Rafei. "Signal and image compression using quantum discrete cosine transform". In: *Information Sciences* 473 (2019), pp. 121–141.

[322] AC Paniagua, AR East, JP Hindmarsh, and JAa Heyes. "Moisture loss is the major cause of firmness change during postharvest storage of blueberry". In: *Postharvest Biology and Technology* 79 (2013), pp. 13–19.

[323] Luis Paredes, Ananya Ipsita, Juan C Mesa, Ramses V Martinez Garrido, and Karthik Ramani. "StretchAR: Exploiting touch and stretch as a method of interaction for smart glasses using wearable straps". In: *Proceedings of the ACM on Interactive, Mobile, Wearable and Ubiquitous Technologies* 6.3 (2022), pp. 1–26.

[324] Farshid Salemi Parizi, Eric Whitmire, and Shwetak Patel. "Auraring: Precise electromagnetic finger tracking". In: *Proceedings of the ACM on Interactive, Mobile, Wearable and Ubiquitous Technologies* 3.4 (2019), pp. 1–28.

[325] Vishal Patel, Austin Chesmore, Christopher M Legner, and Santosh Pandey. "Trends in workplace wearable technologies and connected-worker solutions for next-generation occupational safety, health, and productivity". In: *Advanced Intelligent Systems* 4.1 (2022), p. 2100099.

[326] Harold E Pattee. *Evaluation of quality of fruits and vegetables*. Springer Science & Business Media, 2012.

[327] Rita Pavasini, Matteo Serenelli, Carlos A Celis-Morales, Stuart R Gray, Kazuhiro P Izawa, Satoshi Watanabe, Eloisa Colin-Ramirez, Lilia Castillo-Martínez, Yasuhiro Izumiya, Shinsuke Hanatani, Yoshiro Onoue, Kenichi Tsujita, Peter S Macdonald, Sunita R Jha, Véronique L Roger, Sheila M

Manemann, Juan Sanchis, Vicente Ruiz, Giulia Bugani, Elisabetta Tonet, Roberto Ferrari, Stefano Volpato, and Gianluca Campo. “Grip strength predicts cardiac adverse events in patients with cardiac disorders: An individual patient pooled meta-analysis”. In: *Heart* 105.11 (2019), pp. 834–841. DOI: http://dx.doi.org/10.1136/heartjnl-2018-313816.

[328] Jennifer Pearson, Simon Robinson, and Matt Jones. “It’s About Time: Smartwatches as public displays”. In: *Proceedings of the 33rd Annual ACM Conference on Human Factors in Computing Systems*. 2015, pp. 1257–1266.

[329] Fang Peng, Wei Peng, Cheng Zhang, and Debao Zhong. “IoT assisted Kernel linear discriminant analysis based gait phase detection algorithm for walking with cognitive tasks”. In: *IEEE access* 7 (2019), pp. 68240–68249.

[330] François Petitjean, Germain Forestier, Geoffrey I Webb, Ann E Nicholson, Yanping Chen, and Eamonn Keogh. “Dynamic time warping averaging of time series allows faster and more accurate classification”. In: *2014 IEEE international conference on data mining*. IEEE. 2014, pp. 470–479.

[331] Thomas PlÖtz. “Applying machine learning for sensor data analysis in interactive systems: Common pitfalls of pragmatic use and ways to avoid them”. In: *ACM Computing Surveys (CSUR)* 54.6 (2021), pp. 1–25.

[332] Godwin Ponraj and Hongliang Ren. “Sensor fusion of leap motion controller and flex sensors using Kalman filter for human finger tracking”. In: *IEEE Sensors Journal* 18.5 (2018), pp. 2042–2049.

[333] Kevin Post, Reo Kuchida, Mayowa Olapade, Zhigang Yin, Petteri Nurmi, and Huber Flores. “ContextLLM: Meaningful Context Reasoning from Multi-Sensor and Multi-Device Data Using LLMs”. In: *Proceedings of ACM HOTMOBILE’25*. Association for Computing Machinery (ACM), 2025.

[334] Kevin Post, Zhigang Yin, Mayowa Olapade, Farid Valiyev, Petteri Nurmi, and Huber Flores. “Sensor Data Co-Pilots: Enabling Human-Centric Pervasive Environments”. In: *Authorea Preprints* (2025).

[335] Parisa Pouladzadeh et al. “Measuring calorie and nutrition from food image”. In: *IEEE Transactions on Instrumentation and Measurement* 63.8 (2014), pp. 1947–1956.

[336] Banu Priya Prathaban, Ramachandran Balasubramanian, and R Kalpana. “A wearable foreseiz headband for forecasting real-time epileptic seizures”. In: *IEEE Sensors Journal* 21.23 (2021), pp. 26892–26901.

[337] United Nations Environment Programme. *Food Waste Index Report 2024. Think Eat Save: Tracking Progress to Halve Global Food Waste*. 2024-03. URL: https://wedocs.unep.org/20.500.11822/45230.

[338] Dov Prusky. “Reduction of the incidence of postharvest quality losses, and future prospects”. In: *Food security* 3 (2011), pp. 463–474.

[339] Philip Quinn, Seungyon Claire Lee, Melissa Barnhart, and Shumin Zhai. "Active edge: Designing squeeze gestures for the google pixel 2". In: *Proceedings of the Conference on Human Factors in Computing Systems*. CHI'19. Glasgow, Scotland UK: ACM, 2019, pp. 1–13. DOI: https://doi.org/10.1145/3290605.3300504.

[340] Mustafa Radha, Pedro Fonseca, Arnaud Moreau, Marco Ross, Andreas Cerny, Peter Anderer, Xi Long, and Ronald M Aarts. "A deep transfer learning approach for wearable sleep stage classification with photoplethysmography". In: *NPJ digital medicine* 4.1 (2021), p. 135.

[341] Peter Ragaert, Wim Verbeke, Frank Devlieghere, and Johan Debevere. "Consumer perception and choice of minimally processed vegetables and packaged fruits". In: *Food quality and preference* 15.3 (2004), pp. 259–270.

[342] Md Mahbubur Rahman, Tousif Ahmed, Mohsin Yusuf Ahmed, Minh Dinh, Ebrahim Nemati, Jilong Kuang, and Jun Alex Gao. "Breathebuddy: Tracking real-time breathing exercises for automated biofeedback using commodity earbuds". In: *Proceedings of the ACM on Human-Computer Interaction* 6.MHCI (2022), pp. 1–18.

[343] Rafiu King Raji, Xuhong Miao, Ailan Wan, Li Niu, Yutian Li, and Andrews Boakye. "Knitted piezoresistive smart chest band and its application for respiration patterns assessment". In: *Journal of Engineered Fibers and Fabrics* 14 (2019), p. 1558925019868474.

[344] Swati Rallapalli, Aishwarya Ganesan, Krishna Chintalapudi, Venkat N Padmanabhan, and Lili Qiu. "Enabling physical analytics in retail stores using smart glasses". In: *Proceedings of the 20th annual international conference on Mobile computing and networking*. 2014, pp. 115–126.

[345] Elangovan Ramanujam, Thinagaran Perumal, and S Padmavathi. "Human activity recognition with smartphone and wearable sensors using deep learning techniques: A review". In: *IEEE Sensors Journal* 21.12 (2021), pp. 13029–13040.

[346] Robinson Ramírez-Vélez, Jorge Enrique Correa-Bautista, Antonio García-Hermoso, Carlos Alberto Cano, and Mikel Izquierdo. "Reference values for handgrip strength and their association with intrinsic capacity domains among older adults". In: *Journal of Cachexia, Sarcopenia and Muscle* 10.2 (2019), pp. 278–286. DOI: https://doi.org/10.1002/jcsm.12373.

[347] Hanae Rateau, Edward Lank, and Zhe Liu. "Leveraging smartwatch and earbuds gesture capture to support wearable interaction". In: *Proceedings of the ACM on Human-Computer Interaction* 6.ISS (2022), pp. 31–50.

[348] Gangireddy Narendra Kumar Reddy, M Sabarimalai Manikandan, and NVL Narasimha Murty. "Lightweight compressed sensing (CS) and partial DCT based compression schemes for energy-efficient wearable PPG monitoring devices". In: *2021 IEEE International Conference on Health,*

Instrumentation & Measurement, and Natural Sciences (InHeNce). IEEE. 2021, pp. 1–6.

[349] Blaine Reeder and Alexandria David. "Health at hand: A systematic review of smart watch uses for health and wellness". In: *Journal of biomedical informatics* 63 (2016), pp. 269–276.

[350] Yili Ren, Sheng Tan, Linghan Zhang, Zi Wang, Zhi Wang, and Jie Yang. "Liquid level sensing using commodity wifi in a smart home environment". In: *Proceedings of the ACM on Interactive, Mobile, Wearable and Ubiquitous Technologies* 4.1 (2020), pp. 1–30.

[351] Yiyi Ren, Xiang Xie, Guolin Li, and Zhihua Wang. "Hand gesture recognition with multiscale weighted histogram of contour direction normalization for wearable applications". In: *IEEE Transactions on Circuits and Systems for Video Technology* 28.2 (2016), pp. 364–377.

[352] Philippe Renevey, Ricard Delgado-Gonzalo, Alia Lemkaddem, Martin Proença, Mathieu Lemay, Josep Solà, Adrian Tarniceriu, and Mattia Bertschi. "Optical wrist-worn device for sleep monitoring". In: *EMBEC & NBC 2017*. Tampere, Finland: Springer, 2017, pp. 615–618. DOI: https://doi.org/10.1007/978-981-10-5122-7_154.

[353] Noorman Rinanto and Chung-Hsien Kuo. "PCA-ANN Contactless Multimodality Sensors for Body Temperature Estimation". In: *IEEE Transactions on Instrumentation and Measurement* 70 (2021), pp. 1–16.

[354] Mikko Rinta-Homi et al. "How low can you go? performance trade-offs in low-resolution thermal sensors for occupancy detection: A systematic evaluation". In: *Proceedings of the ACM on Interactive, Mobile, Wearable and Ubiquitous Technologies* 5.3 (2021), pp. 1–22.

[355] Helen C Roberts, Hayley J Denison, Helen J Martin, Harnish P Patel, Holly Syddall, Cyrus Cooper, and Avan Aihie Sayer. "A review of the measurement of grip strength in clinical and epidemiological studies: Towards a standardised approach". In: *Age and Ageing* 40.4 (2011), pp. 423–429. DOI: https://doi.org/10.1093/ageing/afr051.

[356] Yu Rong and Guoying Gu. "Deep transfer learning-based adaptive gesture recognition of a soft e-skin patch with reduced training data and time". In: *Sensors and Actuators A: Physical* 363 (2023), p. 114693.

[357] Daniel P Rose, Michael E Ratterman, Daniel K Griffin, Linlin Hou, Nancy Kelley-Loughnane, Rajesh R Naik, Joshua A Hagen, Ian Papautsky, and Jason C Heikenfeld. "Adhesive RFID sensor patch for monitoring of sweat electrolytes". In: *IEEE Transactions on Biomedical Engineering* 62.6 (2014), pp. 1457–1465.

[358] Mehran Roshandel, Aarti Munjal, Peyman Moghadam, Shahin Tajik, and Hamed Ketabdar. "Multi-sensor finger ring for authentication based on 3D signatures". In: *Human-Computer Interaction. Advanced Interaction Modalities and Techniques: 16th International Conference, HCI Interna-*

tional 2014, Heraklion, Crete, Greece, June 22-27, 2014, Proceedings, Part II 16. Springer. 2014, pp. 131–138.

[359] Robert Ross, William M Mongan, Patrick O'Neill, Ilhaan Rasheed, Adam Fontecchio, Genevieve Dion, and Kapil R Dandekar. "An adaptively parameterized algorithm estimating respiratory rate from a passive wearable RFID smart garment". In: *2021 IEEE 45th Annual Computers, Software, and Applications Conference (COMPSAC)*. IEEE. 2021, pp. 774–784.

[360] Sajjad Rostami and Martin Maier. "The metaverse and beyond: Implementing advanced multiverse realms with smart wearables". In: *Ieee Access* 10 (2022), pp. 110796–110806.

[361] Soha Rostaminia, Addison Mayberry, Deepak Ganesan, Benjamin Marlin, and Jeremy Gummeson. "Ilid: low-power sensing of fatigue and drowsiness measures on a computational eyeglass". In: *Proceedings of the ACM on interactive, mobile, wearable and ubiquitous technologies* 1.2 (2017), pp. 1–26.

[362] Farida Sabry, Tamer Eltaras, Wadha Labda, Khawla Alzoubi, and Qutaibah Malluhi. "Machine learning for healthcare wearable devices: the big picture". In: *Journal of Healthcare Engineering* 2022.1 (2022), p. 4653923.

[363] Stanisław Saganowski, Bartosz Perz, Adam G Polak, and Przemysław Kazienko. "Emotion recognition for everyday life using physiological signals from wearables: A systematic literature review". In: *IEEE Transactions on Affective Computing* 14.3 (2022), pp. 1876–1897.

[364] Alireza Sahami Shirazi et al. "Exploiting thermal reflection for interactive systems". In: *Proceedings of the SIGCHI Conference on Human Factors in Computing Systems*. 2014, pp. 3483–3492.

[365] Walaa M El-Sais and Walaa S Mohammad. "Influence of different testing postures on hand grip strength". In: *European Scientific Journal* 10.36 (2014), pp. 290–301. URL: `https://eujournal.org/index.php/esj/article/view/4904`.

[366] Jorge Sáiz et al. "Electrophoretic fingerprinting of benzodiazepine tablets in spike drinks". In: *Electrophoresis* 35.21-22 (2014).

[367] Mahadev Satyanarayanan. "Pervasive computing: Vision and challenges". In: *IEEE Personal communications* 8.4 (2001), pp. 10–17.

[368] Stefan Schneegass and Alexandra Voit. "GestureSleeve: using touch sensitive fabrics for gestural input on the forearm for controlling smartwatches". In: *Proceedings of the 2016 ACM International Symposium on Wearable Computers*. 2016, pp. 108–115.

[369] Lisa Schrader, Agustín Vargas Toro, Sebastian Konietzny, Stefan Rüping, Barbara Schäpers, Martina Steinböck, Carmen Krewer, Friedemann Müller, Jörg Güttler, and Thomas Bock. "Advanced sensing and human activity recognition in early intervention and rehabilitation of elderly people".

In: *Journal of Population Ageing* 13 (2020), pp. 139–165. DOI: https://doi.org/10.1007/s12062-020-09260-z.

[370] Dominik Schürmann, Sergej Dechand, and Lars Wolf. "Openkeychain: an architecture for cryptography with smart cards and nfc rings on android". In: *Proceedings of the ACM on Interactive, Mobile, Wearable and Ubiquitous Technologies* 1.3 (2017), pp. 1–24.

[371] Andrea Sciarrone, Igor Bisio, Chiara Garibotto, Fabio Lavagetto, Gerhard H Staude, and Andreas Knopp. "Leveraging IoT wearable technology towards early diagnosis of neurological diseases". In: *IEEE Journal on Selected Areas in Communications* 39.2 (2020), pp. 582–592.

[372] Katie Seaborn, Johanna Mähönen, and Yvonne Rogers. "Scaling up to tackle low levels of urban food waste recycling". In: *Proceedings of the 2020 ACM Designing Interactive Systems Conference*. 2020, pp. 1327–1340.

[373] Juliane R Sempionatto, Rupesh K Mishra, Aida Martín, Guangda Tang, Tatsuo Nakagawa, Xiaolong Lu, Alan S Campbell, Kay Mengjia Lyu, and Joseph Wang. "Wearable ring-based sensing platform for detecting chemical threats". In: *ACS sensors* 2.10 (2017), pp. 1531–1538.

[374] Suranga Seneviratne, Yining Hu, Tham Nguyen, Guohao Lan, Sara Khalifa, Kanchana Thilakarathna, Mahbub Hassan, and Aruna Seneviratne. "A survey of wearable devices and challenges". In: *IEEE Communications Surveys & Tutorials* 19.4 (2017), pp. 2573–2620.

[375] Farhad Shahmohammadi, Anahita Hosseini, Christine E King, and Majid Sarrafzadeh. "Smartwatch based activity recognition using active learning". In: *2017 IEEE/ACM International Conference on Connected Health: Applications, Systems and Engineering Technologies (CHASE)*. IEEE. 2017, pp. 321–329.

[376] Celia Shahnaz, Md Julker Neyen Sampad, Dimitri Adhikary, Sajid Mahfuz Uchayash, Marjana Mahdia, Sayeed Shafayet Chowdhury, and Shaikh Anowarul Fattah. "Smart-hat: Safe and smooth walking assistant for elderly people". In: *2017 IEEE International Symposium on Technology and Society (ISTAS)*. IEEE. 2017, pp. 1–7.

[377] Mobeen Shahroz, Muhammad Faheem Mushtaq, Maqsood Ahmad, Saleem Ullah, Arif Mehmood, and Gyu Sang Choi. "IoT-based smart shopping cart using radio frequency identification". In: *IEEE Access* 8 (2020), pp. 68426–68438.

[378] Gözel Shakeri and Claire H McCallum. "Envirofy your shop: Development of a real-time tool to support eco-friendly food purchases online". In: *Extended abstracts of the 2021 CHI conference on human factors in computing systems*. 2021, pp. 1–10.

[379] Fei Shang et al. "LiqRay: non-invasive and fine-grained liquid recognition system". In: *Proceedings of MobiCom 2022*. 2022, pp. 296–309.

[380] Fei Shang, Panlong Yang, Dawei Yan, Sijia Zhang, and Xiang-Yang Li. "LiquImager: Fine-grained Liquid Identification and Container Imaging System with COTS WiFi Devices". In: *Proceedings of the ACM on Interactive, Mobile, Wearable and Ubiquitous Technologies* 8.1 (2024), pp. 1–29.

[381] Fei Shang, Panlong Yang, Yubo Yan, and Xiang-Yang Li. "PackquID: In-packet liquid identification using RF signals". In: *Proceedings of the ACM on Interactive, Mobile, Wearable and Ubiquitous Technologies* 6.4 (2023), pp. 1–27.

[382] Adwait Sharma, Michael A Hedderich, Divyanshu Bhardwaj, Bruno Fruchard, Jess McIntosh, Aditya Shekhar Nittala, Dietrich Klakow, Daniel Ashbrook, and Jürgen Steimle. "SoloFinger: Robust microgestures while grasping everyday objects". In: *Proceedings of Conference on Human Factors in Computing Systems*. CHI'21. Yokohama, Japan: ACM, 2021, pp. 1–15. DOI: https://doi.org/10.1145/3411764.3445197.

[383] Garima Sharma, Kartikeyan Umapathy, and Sridhar Krishnan. "Trends in audio signal feature extraction methods". In: *Applied Acoustics* 158 (2020), p. 107020.

[384] Pradip Kumar Sharma, Jisun Park, Jong Hyuk Park, and Kyungeun Cho. "Wearable computing for defence automation: Opportunities and challenges in 5G network". In: *IEEE Access* 8 (2020), pp. 65993–66002.

[385] Laura Sheard. "'Anything could have happened': Women, the night-time economy, alcohol and drink spiking". In: *Sociology* 45.4 (2011).

[386] Sheng Shen, He Wang, and Romit Roy Choudhury. "I am a smartwatch and i can track my user's arm". In: *Proceedings of the 14th annual international conference on Mobile systems, applications, and services*. 2016, pp. 85–96.

[387] Kiichi Shirai, Kyosuke Futami, and Kazuya Murao. "A method to manipulate subjective time by using tactile stimuli of wearable device". In: *Proceedings of the 2021 ACM International Symposium on Wearable Computers*. 2021, pp. 63–67.

[388] Joseph Shor. "Compact thermal sensors for dense cpu thermal monitoring and regulation: A review". In: *IEEE Sensors Journal* 21.11 (2020), pp. 12774–12788.

[389] Prakash Shrestha and Nitesh Saxena. "An offensive and defensive exposition of wearable computing". In: *ACM Computing Surveys (CSUR)* 50.6 (2017), pp. 1–39.

[390] Alexandru-Ionut Siean and Radu-Daniel Vatavu. "Wearable interactions for users with motor impairments: systematic review, inventory, and research implications". In: *Proceedings of the 23rd International ACM SIGACCESS Conference on Computers and Accessibility*. 2021, pp. 1–15.

[391] Dorian Sinclear, Linda Birch Flensborg, Ask Lindblad Fogsgaard, and Markus Lochtefeld. "Face-the-Waste-Learning about Food Waste through

a Serious Game". In: *Proceedings of the 20th International Conference on Mobile and Ubiquitous Multimedia*. 2021, pp. 67–72.

[392] Dilpreet Singh, Neena Bedi, and Ashok K Tiwary. "Enhancing solubility of poorly aqueous soluble drugs: Critical appraisal of techniques". In: *Journal of pharmaceutical investigation* 48 (2018), pp. 509–526.

[393] Sophie Skach, Rebecca Stewart, and Patrick GT Healey. "Smart arse: posture classification with textile sensors in trousers". In: *Proceedings of the 20th ACM International Conference on Multimodal Interaction*. 2018, pp. 116–124.

[394] Kwangsub Song, Ku-young Chung, and Joon-Hyuk Chang. "Cuffless deep learning-based blood pressure estimation for smart wristwatches". In: *IEEE Transactions on Instrumentation and Measurement* 69.7 (2019), pp. 4292–4302.

[395] M Sornalakshmi, S Balamurali, M Venkatesulu, M Navaneetha Krishnan, Lakshmana Kumar Ramasamy, Seifedine Kadry, Gunasekaran Manogaran, Ching-Hsien Hsu, and Bala Anand Muthu. "Hybrid method for mining rules based on enhanced Apriori algorithm with sequential minimal optimization in healthcare industry". In: *Neural Computing and Applications* (2020), pp. 1–14.

[396] Vasilis Stavrou and Dimitris Papakyriakopoulos. "Smart Retail: Efficient in-store localization using ensemble classifiers". In: *Proceedings of the 24th Pan-Hellenic Conference on Informatics*. 2020, pp. 301–304.

[397] F Steiner, F Bleicher, and M Klingenbrunner. "Emissivity Factor of Thermoplastic Materials for a Robot Bending Process". In: *Proceedings of the 27th DAAAM International Symposium*. 2016, pp. 0664–0670.

[398] Sari Stenholm, Janne Sallinen, Annemarie Koster, Taina Rantanen, Päivi Sainio, Markku Heliövaara, and Seppo Koskinen. "Association between obesity history and hand grip strength in older adults—exploring the roles of inflammation and insulin resistance as mediating factors". In: *Journals of Gerontology Series A: Biomedical Sciences and Medical Sciences* 66.3 (2011), pp. 341–348. DOI: https://doi.org/10.1093/gerona/glq226.

[399] Tao Sun, Yankai Zhao, Wentao Xie, Jiao Li, Yongyu Ma, and Jin Zhang. "EyeGesener: Eye Gesture Listener for Smart Glasses Interaction Using Acoustic Sensing". In: *Proceedings of the ACM on Interactive, Mobile, Wearable and Ubiquitous Technologies* 8.3 (2024), pp. 1–28.

[400] Xue Sun, Wenwen Deng, Xudong Wei, Dingyi Fang, Baochun Li, and Xiaojiang Chen. "Akte-liquid: Acoustic-based liquid identification with smartphones". In: *ACM Transactions on Sensor Networks* 19.1 (2023), pp. 1–24.

[401] Suzanne C Swan et al. “Just a dare or unaware? Outcomes and motives of drugging (“drink spiking”) among students at three college campuses.” In: *Psychology of violence* 7.2 (2017), p. 253.

[402] Benjamin Tag, Andrew W Vargo, Aman Gupta, George Chernyshov, Kai Kunze, and Tilman Dingler. “Continuous alertness assessments: Using EOG glasses to unobtrusively monitor fatigue levels In-The-Wild”. In: *Proceedings of the 2019 CHI Conference on Human Factors in Computing Systems*. 2019, pp. 1–12.

[403] Jason Tallis, Rob S James, and Frank Seebacher. “The effects of obesity on skeletal muscle contractile function”. In: *Journal of Experimental Biology* 221.13 (2018), pp. 1–14. DOI: https://doi.org/10.1242/jeb.163840.

[404] Milda Tamošiunaite, Stasys Tamošiunas, Mindaugas Žilinskas, and Milda Tamošiuniene. “Atmospheric attenuation due to humidity”. In: *Electromagnetic Waves*. IntechOpen, 2011.

[405] Sheng Tan, Linghan Zhang, and Jie Yang. “Sensing fruit ripeness using wireless signals”. In: *2018 27th international conference on computer communication and networks (ICCCN)*. IEEE. 2018, pp. 1–9.

[406] Chi Ian Tang, Ignacio Perez-Pozuelo, Dimitris Spathis, Soren Brage, Nick Wareham, and Cecilia Mascolo. “Selfhar: Improving human activity recognition through self-training with unlabeled data”. In: *Proceedings of the ACM on interactive, mobile, wearable and ubiquitous technologies* 5.1 (2021), pp. 1–30.

[407] Arvin Tashakori, Zenan Jiang, Amir Servati, Saeid Soltanian, Harishkumar Narayana, Katherine Le, Caroline Nakayama, Chieh-ling Yang, Z Jane Wang, Janice J Eng, et al. “Capturing complex hand movements and object interactions using machine learning-powered stretchable smart textile gloves”. In: *Nature Machine Intelligence* 6.1 (2024), pp. 106–118.

[408] Cátia Tavares, Cátia Leitão, Daniela Lo Presti, MF Domingues, Nélia Alberto, Hugo Silva, and Paulo Antunes. “Respiratory and heart rate monitoring using an FBG 3D-printed wearable system”. In: *Biomedical Optics Express* 13.4 (2022), pp. 2299–2311.

[409] Caitlin N Teague, Sinan Hersek, Hakan Töreyin, Mindy L Millard-Stafford, Michael L Jones, Géza F Kogler, Michael N Sawka, and Omer T Inan. “Novel methods for sensing acoustical emissions from the knee for wearable joint health assessment”. In: *IEEE Transactions on Biomedical Engineering* 63.8 (2016), pp. 1581–1590.

[410] P Thamarai and K Adalarasu. “Denoising of EEG, ECG and PPG signals using wavelet transform”. In: *Journal of Pharmaceutical Sciences and Research* 10.1 (2018), pp. 156–161.

[411] D Trosclair, D Bellar, LW Judge, J Smith, N Mazerat, and A Brignac. “Hand-grip strength as a predictor of muscular strength and endurance”.

In: *The Journal of Strength & Conditioning Research* 25 (2011), S99. DOI: https://doi.org/10.1097/01.JSC.0000395736.42557.bc.

[412] Tran Quang Trung, Subramaniyan Ramasundaram, Byeong-Ung Hwang, and Nae-Eung Lee. "An all-elastomeric transparent and stretchable temperature sensor for body-attachable wearable electronics". In: *Advanced materials* 28.3 (2016), pp. 502–509.

[413] Hoang Truong, Shuo Zhang, Ufuk Muncuk, Phuc Nguyen, Nam Bui, Anh Nguyen, Qin Lv, Kaushik Chowdhury, Thang Dinh, and Tam Vu. "Capband: Battery-free successive capacitance sensing wristband for hand gesture recognition". In: *Proceedings of the 16th ACM Conference on Embedded Networked Sensor Systems*. 2018, pp. 54–67.

[414] Ying-Chao Tung, Chun-Yen Hsu, Han-Yu Wang, Silvia Chyou, Jhe-Wei Lin, Pei-Jung Wu, Andries Valstar, and Mike Y Chen. "User-defined game input for smart glasses in public space". In: *Proceedings of the 33rd Annual ACM conference on human factors in computing systems*. 2015, pp. 3327–3336.

[415] Ihsan Ullah, Joosang Youn, and Youn-Hee Han. "Multisensor data fusion based on modified belief entropy in Dempster–Shafer theory for smart environment". In: *IEEE Access* 9 (2021), pp. 37813–37822.

[416] R Vadivambal and Digvir S Jayas. "Applications of thermal imaging in agriculture and food industry—a review". In: *Food and bioprocess technology* 4 (2011), pp. 186–199.

[417] Logan R Vallandingham, Quan Yu, Nakul Sharma, Jo W Strandhagen, and Jan Ola Strandhagen. "Grocery retail supply chain planning and control: Impact of consumer trends and enabling technologies". In: *IFAC-PapersOnLine* 51.11 (2018), pp. 612–617.

[418] Ramachandran Varatharajan, Gunasekaran Manogaran, Malarvizhi Kumar Priyan, and Revathi Sundarasekar. "Wearable sensor devices for early detection of Alzheimer disease using dynamic time warping algorithm". In: *Cluster Computing* 21 (2018), pp. 681–690.

[419] Radu-Daniel Vatavu and Laura-Bianca Bilius. "GestuRING: A web-based tool for designing gesture input with rings, ring-like, and ring-ready devices". In: *The 34th Annual ACM Symposium on User Interface Software and Technology*. 2021, pp. 710–723.

[420] Peter M Visscher. "Sizing up human height variation". In: *Nature genetics* 40.5 (2008), pp. 489–490. DOI: https://doi.org/10.1038/ng0508-489.

[421] Wilhelm Von Rosenberg, Theerasak Chanwimalueang, Valentin Goverdovsky, David Looney, David Sharp, and Danilo P Mandic. "Smart helmet: Wearable multichannel ECG and EEG". In: *IEEE journal of translational engineering in health and medicine* 4 (2016).

[422] Gideon Vos, Kelly Trinh, Zoltan Sarnyai, and Mostafa Rahimi Azghadi. "Generalizable machine learning for stress monitoring from wearable devices: A systematic literature review". In: *International Journal of Medical Informatics* 173 (2023), p. 105026.

[423] Anandghan Waghmare, Youssef Ben Taleb, Ishan Chatterjee, Arjun Narendra, and Shwetak Patel. "Z-ring: Single-point bio-impedance sensing for gesture, touch, object and user recognition". In: *Proceedings of the 2023 CHI Conference on Human Factors in Computing Systems*. 2023, pp. 1–18.

[424] Dongran Wang, Ji Ouyang, Peiru Zhou, Junlan Yan, Lin Shu, and Xiangmin Xu. "A novel low-cost wireless footwear system for monitoring diabetic foot patients". In: *IEEE Transactions on Biomedical Circuits and Systems* 15.1 (2020), pp. 43–54.

[425] Hailong Wang, Jiyu Peng, Chuanqi Xie, Yidan Bao, and Yong He. "Fruit quality evaluation using spectroscopy technology: a review". In: *Sensors* 15.5 (2015), pp. 11889–11927.

[426] Ju Wang et al. "TagScan: Simultaneous target imaging and material identification with commodity RFID devices". In: *Proceedings of the 23rd Annual International Conference on Mobile Computing and Networking (MobiCom 2017)*. 2017, pp. 288–300.

[427] Lefan Wang, Dominic Jones, Graham J Chapman, Heidi J Siddle, David A Russell, Ali Alazmani, and Peter Culmer. "A review of wearable sensor systems to monitor plantar loading in the assessment of diabetic foot ulcers". In: *IEEE transactions on biomedical engineering* 67.7 (2019), pp. 1989–2004.

[428] Nan-Nan Wang, Da-Wen Sun, Yi-Chao Yang, Hongbin Pu, and Zhiwei Zhu. "Recent advances in the application of hyperspectral imaging for evaluating fruit quality". In: *Food analytical methods* 9.1 (2016), pp. 178–191.

[429] Qi Wang, Panos Markopoulos, Bin Yu, Wei Chen, and Annick Timmermans. "Interactive wearable systems for upper body rehabilitation: a systematic review". In: *Journal of neuroengineering and rehabilitation* 14 (2017), pp. 1–21.

[430] Wei Wang, Yan Huang, Yizhou Wang, and Liang Wang. "Generalized autoencoder: A neural network framework for dimensionality reduction". In: *Proceedings of the IEEE conference on computer vision and pattern recognition workshops*. 2014, pp. 490–497.

[431] Yan Wang, Shuang Cang, and Hongnian Yu. "A survey on wearable sensor modality centred human activity recognition in health care". In: *Expert Systems with Applications* 137 (2019), pp. 167–190.

[432] Yasi Wang, Hongxun Yao, and Sicheng Zhao. "Auto-encoder based dimensionality reduction". In: *Neurocomputing* 184 (2016), pp. 232–242.

[433] Yiming Wang, Bin Zhang, and Lamei Di. “Research Progress of EEG-Based Emotion Recognition: A Survey”. In: *ACM Computing Surveys* 56.11 (2024), pp. 1–49.

[434] Zeyu Wang, Ruotong Yu, Xiangyang Wang, Jiexin Ding, Jiankai Tang, Jun Fang, Zhe He, Zhuojun Li, Tobias Röddiger, Weiye Xu, et al. “Computing with Smart Rings: A Systematic Literature Review”. In: *arXiv preprint arXiv:2502.02459* (2025).

[435] Zhu Wang, Yifan Guo, Zhihui Ren, Wenchao Song, Zhuo Sun, Chao Chen, Bin Guo, and Zhiwen Yu. “LiqDetector: Enabling Container-Independent Liquid Detection with mmWave Signals Based on a Dual-Reflection Model”. In: *Proceedings of the ACM on Interactive, Mobile, Wearable and Ubiquitous Technologies* 7.4 (2024), pp. 1–24.

[436] Zi Wang, Sheng Tan, Linghan Zhang, Yili Ren, Zhi Wang, and Jie Yang. “EarDynamic: An ear canal deformation based continuous user authentication using in-ear wearables”. In: *Proceedings of the ACM on Interactive, Mobile, Wearable and Ubiquitous Technologies* 5.1 (2021), pp. 1–27.

[437] Johan Wannenburg and Reza Malekian. “Body Sensor Network for Mobile Health Monitoring, a Diagnosis and Anticipating System”. In: *IEEE Sensors Journal* 15.12 (2015), pp. 6839–6852. DOI: 10.1109/JSEN.2015.2464773.

[438] Rebecca Webb et al. “A rapid CZE method for the analysis of benzodiazepines in spiked beverages”. In: *Electrophoresis* 28.19 (2007).

[439] Martin Weigel, Tong Lu, Gilles Bailly, Antti Oulasvirta, Carmel Majidi, and Jürgen Steimle. “Iskin: flexible, stretchable and visually customizable on-body touch sensors for mobile computing”. In: *Proceedings of the 33rd Annual ACM Conference on Human Factors in Computing Systems*. 2015, pp. 2991–3000.

[440] Karl Weiss, Taghi M Khoshgoftaar, and DingDing Wang. “A survey of transfer learning”. In: *Journal of Big data* 3 (2016), pp. 1–40.

[441] WeSipSafe. *Drug Test Kits for Scopolamine, Benzodiazepines, Roofies GHB*. https://wesipsafe.com/ [Accessed: 2024-07-01]. 2024.

[442] Asanga Wickramasinghe and Damith C Ranasinghe. “Recognising activities in real time using body worn passive sensors with sparse data streams: To interpolate or not to interpolate?” In: *Proceedings of the 12th EAI international conference on mobile and ubiquitous systems: computing, networking and services on 12th EAI international conference on mobile and ubiquitous systems: computing, networking and services*. 2016, pp. 21–30.

[443] Chanphot Wongtaweesup, Kristina Thapa, Chutiporn Anutariya, Aekavute Sujarae, and James Tisyakorn. “Using Consumer-Graded Wearable Devices for Sleep Apnea Pre-Diagnosis: A Survey and Recommendations”. In: *2023*

20th International Joint Conference on Computer Science and Software Engineering (JCSSE). IEEE. 2023, pp. 517–522.

[444] Taiyang Wu, Fan Wu, Chunkai Qiu, Jean-Michel Redouté, and Mehmet Rasit Yuce. "A rigid-flex wearable health monitoring sensor patch for IoT-connected healthcare applications". In: *IEEE Internet of Things Journal* 7.8 (2020), pp. 6932–6945.

[445] Tony Wu, Shiho Fukuhara, Nicholas Gillian, Kishore Sundara-Rajan, and Ivan Poupyrev. "ZebraSense: A double-sided textile touch sensor for smart clothing". In: *Proceedings of the 33rd Annual ACM Symposium on User Interface Software and Technology*. 2020, pp. 662–674.

[446] Yu Wu, Dai Jiang, Andy Bardill, Richard Bayford, and Andreas Demosthenous. "A 122 fps, 1 MHz bandwidth multi-frequency wearable EIT belt featuring novel active electrode architecture for neonatal thorax vital sign monitoring". In: *IEEE transactions on biomedical circuits and systems* 13.5 (2019), pp. 927–937.

[447] Yujin Wu, Mohamed Daoudi, and Ali Amad. "Transformer-based self-supervised multimodal representation learning for wearable emotion recognition". In: *IEEE Transactions on Affective Computing* 15.1 (2023), pp. 157–172.

[448] Xantus. *Xantus - Drinksafe*. `https://www.xantus-drinksafe.de/` [Accessed: 2024-07-01]. 2024.

[449] Fuyuan Xiao. "Multi-sensor data fusion based on the belief divergence measure of evidences and the belief entropy". In: *Information Fusion* 46 (2019), pp. 23–32.

[450] Yanze Xie, Mengzhen Gao, Xiaoning Liu, Shuo Huana, Helei Cui, Zhiwen Yu, and Bin Guo. "EarPass: Unlock When Wearing Your Earphones". In: *2024 IEEE 44th International Conference on Distributed Computing Systems (ICDCS)*. IEEE. 2024, pp. 1283–1293.

[451] Dezhen Xiong, Daohui Zhang, Xingang Zhao, and Yiwen Zhao. "Deep learning for EMG-based human-machine interaction: A review". In: *IEEE/CAA Journal of Automatica Sinica* 8.3 (2021), pp. 512–533.

[452] Weitao Xu, Yiran Shen, Chengwen Luo, Jianqiang Li, Wei Li, and Albert Y Zomaya. "Gait-Watch: A Gait-based context-aware authentication system for smart watch via sparse coding". In: *Ad Hoc Networks* 107 (2020), p. 102218.

[453] Weitao Xu, Huanqi Yang, Jiongzhang Chen, Chengwen Luo, Jia Zhang, Yuliang Zhao, and Wen Jung Li. "Washring: An energy-efficient and highly accurate handwashing monitoring system via smart ring". In: *IEEE Transactions on Mobile Computing* 23.1 (2022), pp. 971–984.

[454] Xuhai Xu, Haitian Shi, Xin Yi, WenJia Liu, Yukang Yan, Yuanchun Shi, Alex Mariakakis, Jennifer Mankoff, and Anind K Dey. "Earbuddy: Enabling on-face interaction via wireless earbuds". In: *Proceedings of the*

2020 CHI Conference on Human Factors in Computing Systems. 2020, pp. 1–14.

[455] Zihan Yan, Jiayi Zhou, Yufei Wu, Guanhong Liu, Danli Luo, Zihong Zhou, Haipeng Mi, Lingyun Sun, Xiang'Anthony' Chen, Ye Tao, et al. "Shoes++ A smart detachable sole for social foot-to-foot interaction". In: *Proceedings of the ACM on Interactive, Mobile, Wearable and Ubiquitous Technologies* 6.2 (2022), pp. 1–29.

[456] Boran Yang, Govindaraj Dev Kumar, and Kevin Mis Solval. "Evaluation of Low-Cost Smartphone-Based Infrared Cameras to Assess the Cooling and Refrigerated Storage Temperatures of Fresh Produce". In: *Foods* 11.21 (2022), p. 3440.

[457] Dong Yang, Yongqiang Cheng, Jin Zhu, Dongfei Xue, Grant Abt, Hangyang Ye, and Yonghong Peng. "A novel adaptive spectrum noise cancellation approach for enhancing heartbeat rate monitoring in a wearable device". In: *IEEE Access* 6 (2018), pp. 8364–8375.

[458] Haixia Yang, Yixian Shen, Wei Zhuang, Chunming Gao, Dong Dai, and Weigong Zhang. "A smart wearable ring device for sensing hand tremor of Parkinson's Patients". In: *Computer Modeling in Engineering & Sciences* 126.3 (2021), pp. 1217–1238.

[459] Luyao Yang, Osama Amin, and Basem Shihada. "Intelligent Wearable Systems: Opportunities and Challenges in Health and Sports". In: *ACM Comput. Surv.* 56.7 (Apr. 2024). ISSN: 0360-0300. DOI: 10.1145/3648469. URL: https://doi.org/10.1145/3648469.

[460] Yanni Yang et al. "HearLiquid: Non-intrusive Liquid Fraud Detection Using Commodity Acoustic Devices". In: *IEEE IoT Journal* (2022).

[461] Zhijian Yang, Yu-Lin Wei, Sheng Shen, and Romit Roy Choudhury. "Ear-ar: indoor acoustic augmented reality on earphones". In: *Proceedings of the 26th Annual International Conference on Mobile Computing and Networking*. 2020, pp. 1–14.

[462] Zhilu Ye, Yun Ling, Minye Yang, Yadong Xu, Liang Zhu, Zheng Yan, and Pai-Yen Chen. "A breathable, reusable, and zero-power smart face mask for wireless cough and mask-wearing monitoring". In: *ACS nano* 16.4 (2022), pp. 5874–5884.

[463] Hui-Shyong Yeo, Juyoung Lee, Hyung-il Kim, Aakar Gupta, Andrea Bianchi, Daniel Vogel, Hideki Koike, Woontack Woo, and Aaron Quigley. "Wrist: Watch-ring interaction and sensing technique for wrist gestures and macro-micro pointing". In: *Proceedings of the 21st international conference on human-computer interaction with mobile devices and services*. 2019, pp. 1–15.

[464] Zhigang Yin et al. "HIPPO: Pervasive Hand-Grip Estimation from Everyday Interactions". In: vol. 6. 4. 2023, pp. 1–30.

[465] Zhigang Yin, Mohan Liyanage, Abdul-Rasheed Ottun, Farooq Dar, Mayowa Olapade, and Huber Flores. “Demo Abstract: A Smart Ring Monitoring Your Health using Hand-grip Strength”. In: *Proceedings of the 21st ACM Conference on Embedded Networked Sensor Systems*. 2023, pp. 486–487.

[466] Zhigang Yin, Mohan Liyanage, Agustin Zuniga, Petteri Nurmi, and Huber Flores. “Hedgehog: Detecting Drink Spiking on Wearables”. In: *Proceedings of the 24th International Workshop on Mobile Computing Systems and Applications*. 2023, pp. 61–67.

[467] Zhigang Yin, Mayowa Olapade, Mohan Liyanage, Farooq Dar, Agustin Zuniga, Naser Hossein Motlagh, Xiang Su, Sasu Tarkoma, Pan Hui, Petteri Nurmi, et al. “Toward city-scale litter monitoring using autonomous ground vehicles”. In: *IEEE Pervasive Computing* 21.3 (2022), pp. 74–83.

[468] Han Yu and Akane Sano. “Semi-supervised learning for wearable-based momentary stress detection in the wild”. In: *Proceedings of the ACM on Interactive, Mobile, Wearable and Ubiquitous Technologies* 7.2 (2023), pp. 1–23.

[469] Hongnian Yu, Shuang Cang, and Yan Wang. “A review of sensor selection, sensor devices and sensor deployment for wearable sensor-based human activity recognition systems”. In: *2016 10th international conference on software, knowledge, information management & applications (skima)*. IEEE. 2016, pp. 250–257.

[470] Tianhong Catherine Yu, Manru Mary Zhang, Peter He, Chi-Jung Lee, Cassidy Cheesman, Saif Mahmud, Ruidong Zhang, Francois Guimbretiere, and Cheng Zhang. “SeamPose: Repurposing Seams as Capacitive Sensors in a Shirt for Upper-Body Pose Tracking”. In: *Proceedings of the 37th Annual ACM Symposium on User Interface Software and Technology*. 2024, pp. 1–13.

[471] Xinyang Yu et al. “Development of a handheld spectrometer based on a linear variable filter and a complementary metal-oxide-semiconductor detector for measuring the internal quality of fruit”. In: *Journal of Near Infrared Spectroscopy* 24.1 (2016), pp. 69–76.

[472] Yue Yu, Sophia Yi, Xi Nan, Leo Yu-Ho Lo, Kento Shigyo, Liwenhan Xie, Jeffry Wicaksana, Kwang-Ting Cheng, and Huamin Qu. “FoodWise: Food Waste Reduction and Behavior Change on Campus with Data Visualization and Gamification”. In: *Proceedings of the 6th ACM SIGCAS/SIGCHI Conference on Computing and Sustainable Societies*. 2023, pp. 76–83.

[473] Shichao Yue and Dina Katabi. “Liquid Testing with Your Smartphone”. In: *Proceedings of ACM MobiSys 2019*. ACM. 2019, pp. 275–286.

[474] Chi Zhang, Josh Tabor, Jialiang Zhang, and Xinyu Zhang. “Extending mobile interaction through near-field visible light sensing”. In: *Proceedings*

of the 21st Annual International Conference on Mobile Computing and Networking. 2015, pp. 345–357.

[475] Hechuan Zhang, Zhiyong Chen, Shihui Guo, Juncong Lin, Yating Shi, Xiangyang Liu, and Yong Ma. "Sensock: 3D foot reconstruction with flexible sensors". In: *Proceedings of the 2020 CHI conference on human factors in computing systems*. 2020, pp. 1–13.

[476] Jingwen Zhang, Dingwen Li, Ruixuan Dai, Heidy Cos, Gregory A Williams, Lacey Raper, Chet W Hammill, and Chenyang Lu. "Predicting postoperative complications with wearables: a case study with patients undergoing pancreatic surgery". In: *Proceedings of the ACM on Interactive, Mobile, Wearable and Ubiquitous Technologies* 6.2 (2022), pp. 1–27.

[477] Panyu Zhang, Gyuwon Jung, Jumabek Alikhanov, Uzair Ahmed, and Uichin Lee. "A Reproducible Stress Prediction Pipeline with Mobile Sensor Data". In: *Proceedings of the ACM on Interactive, Mobile, Wearable and Ubiquitous Technologies* 8.3 (2024), pp. 1–35.

[478] Shibo Zhang, Yuqi Zhao, Dzung Tri Nguyen, Runsheng Xu, Sougata Sen, Josiah Hester, and Nabil Alshurafa. "NeckSense: A multi-sensor necklace for detecting eating activities in free-living conditions". In: *Proceedings of the ACM on Interactive, Mobile, Wearable and Ubiquitous Technologies* 4.2 (2020), pp. 1–26. DOI: https://doi.org/10.1145/3397313.

[479] Shijia Zhang, Taiting Lu, Hao Zhou, Yilin Liu, Runze Liu, and Mahanth Gowda. "I Am an Earphone and I Can Hear My User's Face: Facial Landmark Tracking Using Smart Earphones". In: *ACM Transactions on Internet of Things* 5.1 (2023), pp. 1–29.

[480] Tengxiang Zhang et al. "Thermalring: Gesture and tag inputs enabled by a thermal imaging smart ring". In: *Proceedings of the 2020 CHI Conference on Human Factors in Computing Systems*. 2020, pp. 1–13.

[481] Xiaoliang Zhang, Ziqi Yang, Taiyu Chen, Diliang Chen, and Ming-Chun Huang. "Cooperative sensing and wearable computing for sequential hand gesture recognition". In: *IEEE Sensors Journal* 19.14 (2019), pp. 5775–5783.

[482] Yiwei Zhang, Bin Gao, Daili Yang, Wai Lok Woo, and Houlai Wen. "Online learning of wearable sensing for human activity recognition". In: *IEEE Internet of Things Journal* 9.23 (2022), pp. 24315–24327.

[483] Kaiyi Zhao, Li Li, Zeqiu Chen, Ruizhi Sun, Gang Yuan, and Jiayao Li. "A survey: Optimization and applications of evidence fusion algorithm based on Dempster–Shafer theory". In: *Applied Soft Computing* 124 (2022), p. 109075.

[484] Yingying Zhao, Yuhu Chang, Yutian Lu, Yujiang Wang, Mingzhi Dong, Qin Lv, Robert P Dick, Fan Yang, Tun Lu, Ning Gu, et al. "Do smart glasses dream of sentimental visions? Deep emotionship analysis for eyewear

devices". In: *Proceedings of the ACM on Interactive, Mobile, Wearable and Ubiquitous Technologies* 6.1 (2022), pp. 1–29.

[485] Ya-Li Zheng, Xiao-Rong Ding, Carmen Chung Yan Poon, Benny Ping Lai Lo, Heye Zhang, Xiao-Lin Zhou, Guang-Zhong Yang, Ni Zhao, and Yuan-Ting Zhang. "Unobtrusive sensing and wearable devices for health informatics". In: *IEEE transactions on biomedical engineering* 61.5 (2014), pp. 1538–1554.

[486] Bo Zhou, Daniel Geissler, Marc Faulhaber, Clara Elisabeth Gleiss, Esther Friederike Zahn, Lala Shakti Swarup Ray, David Gamarra, Vitor Fortes Rey, Sungho Suh, Sizhen Bian, et al. "Mocapose: Motion capturing with textile-integrated capacitive sensors in loose-fitting smart garments". In: *Proceedings of the ACM on Interactive, Mobile, Wearable and Ubiquitous Technologies* 7.1 (2023), pp. 1–40.

[487] Chen Zhou, Zihan Yan, Ashwin Ram, Yue Gu, Yan Xiang, Can Liu, Yun Huang, Wei Tsang Ooi, and Shengdong Zhao. "GlassMail: Towards Personalised Wearable Assistant for On-the-Go Email Creation on Smart Glasses". In: *Proceedings of the 2024 ACM Designing Interactive Systems Conference*. 2024, pp. 372–390.

[488] Chong Zhou and Randy C Paffenroth. "Anomaly detection with robust deep autoencoders". In: *Proceedings of the 23rd ACM SIGKDD international conference on knowledge discovery and data mining*. 2017, pp. 665–674.

[489] Han Zhou, Yi Gao, Wenxin Liu, Yuefang Jiang, and Wei Dong. "Posture tracking meets fitness coaching: A two-phase optimization approach with wearable devices". In: *2020 IEEE 17th International Conference on Mobile Ad Hoc and Sensor Systems (MASS)*. IEEE. 2020, pp. 524–532.

[490] Han Zhou, Yi Gao, Xinyi Song, Wenxin Liu, and Wei Dong. "Limbmotion: Decimeter-level limb tracking for wearable-based human-computer interaction". In: *Proceedings of the ACM on Interactive, Mobile, Wearable and Ubiquitous Technologies* 3.4 (2019), pp. 1–24.

[491] Hao Zhou, Taiting Lu, Yilin Liu, Shijia Zhang, and Mahanth Gowda. "Learning on the rings: Self-supervised 3d finger motion tracking using wearable sensors". In: *Proceedings of the ACM on Interactive, Mobile, Wearable and Ubiquitous Technologies* 6.2 (2022), pp. 1–31.

[492] Hao Zhou, Taiting Lu, Yilin Liu, Shijia Zhang, Runze Liu, and Mahanth Gowda. "One ring to rule them all: An open source smartring platform for finger motion analytics and healthcare applications". In: *Proceedings of the 8th ACM/IEEE Conference on Internet of Things Design and Implementation*. 2023, pp. 27–38.

[493] Liyong Zhou, Vikram Chalana, and Yongmin Kim. "PC-based machine vision system for real-time computer-aided potato inspection". In: *International journal of imaging systems and technology* 9.6 (1998), pp. 423–433.

[494] Yangda Zhu, Changhai Wang, Jianzhong Zhang, and Jingdong Xu. “Human activity recognition based on similarity”. In: *2014 ieee 17th international conference on computational science and engineering*. IEEE. 2014, pp. 1382–1387.

[495] Yongpan Zou, Haibo Lei, and Kaishun Wu. “Beyond legitimacy, also with identity: Your smart earphones know who you are quietly”. In: *IEEE Transactions on Mobile Computing* 22.6 (2021), pp. 3179–3192.

[496] Yongpan Zou, Dan Wang, Shicong Hong, Rukhsana Ruby, Dian Zhang, and Kaishun Wu. “A low-cost smart glove system for real-time fitness coaching”. In: *IEEE Internet of Things Journal* 7.8 (2020), pp. 7377–7391.

[497] Paula Zuccotti. *Every thing we touch: A 24-hour inventory of our lives*. UK: Penguin UK, 2015.

[498] Agustin Zuniga, Huber Flores, and Petteri Nurmi. “Ripe or rotten? Low-cost produce quality estimation using reflective green light sensing”. In: *IEEE Pervasive Computing* 20.3 (2021), pp. 60–67. DOI: https://doi.org/10.1109/MPRV.2021.3074474.

Appendix A. THE EVOLUTION OF WEARABLES: A SURVEY ON TRENDS, CHALLENGES, AND THE EMERGING IMPACT OF SMART RINGS

Wearable computing and sensing technologies have revolutionized various domains by providing real-time data collection and analysis. These wearables (e.g., smartwatches, glasses and patches) integrate advanced sensors and techniques to offer applications ranging from health monitoring and activity recognition to environmental sensing. Despite small sizes, the expectations of continuous working drive the need to reduce power consumption and increase data security. The survey first examines the sensing pipeline of wearables in detail, including common sensors, data collection, processing, and modeling. It explores the innovations in sensor fusion, multimodal data processing and machine learning to enhance wearable functionality. The study also highlights common challenges such as data privacy, power efficiency and user comfort while identifying opportunities for future research to address these issues and expand wearable applications further.

A.1. Introduction

As smartphone adoption plateaus due to functionality limitations, users are increasingly turning to wearable devices for enhanced capabilities and seamless integration into daily life. Wearables act as natural extensions of personal devices, designed for specific body parts to enhance usability and interaction. For instance, earpods not only provide audio playback but also enable biometric authentication [127, 495]. A broad range of wearable devices supports applications such as health monitoring, fitness tracking, and muscle growth [374, 171]. Despite the abundance of options, user adoption and long-term retention depend on factors like ease of use, transparency, and battery longevity. The evolution of wearable technology underscores the importance of prioritizing user-centric design [302]. Identifying key preferences and usability challenges can inform the refinement of existing wearables and inspire innovative applications, ensuring future devices align more effectively with user needs and behaviors.

Among existing wearable devices, smart rings are emerging as powerful wearable devices that seamlessly integrate into everyday interactions while offering a wide range of functionalities. Smart rings offer greater benefits whe compared with other wearables devices [20, 16, 306], such as smartwatches or necklaces, smart rings provide a more discreet, comfortable, and ergonomic experience [45, 443]. For example, while both smart rings and smartwatches can track sleep patterns, users often find it more convenient to wear a lightweight ring overnight rather than a smartwatch, which can feel intrusive. This usability advantage contributes to the increasing adoption of smart rings over other wearables offering similar features. Beyond convenience, smart rings also leverage their unique placement

on the hands to enable novel interactions and functionalities. Their proximity to fingers allows for intuitive gesture control, biometric authentication, and enhanced haptic feedback, making them particularly valuable for applications such as secure transactions, touch-based interactions, and continuous health monitoring [419, 423, 463, 196, 358, 370, 453, 277]. Additionally, their compact form factor enables efficient energy consumption, contributing to extended battery life compared to larger wearables.

In this survey, we first review the current state of wearable device technologies, exploring the diverse range of available wearable devices. We then reflect on various wearable designs and developments, highlighting how different devices are integrated into various parts of the human body to enhance functionality and usability. Since wearable devices are commonly used alongside smartphones, we analyze the benefits of this integration and explore how wearable sensing pipelines are structured to process and interpret the vast amounts of data collected from these devices. With this information, we then compare the functionalities of different wearable devices against the emerging smart ring. We illustrate how smart rings not only offer the same capabilities as most common wearable devices but also provide unique advantages in terms of usability, discretion, and efficiency. Additionally, we explore novel applications that can be uniquely enabled by smart rings, leveraging their compact form factor and proximity to the fingers for enhanced biometric sensing, gesture recognition, and seamless authentication. We then outline a roadmap of open technical challenges that could drive further advancements in smart ring technology. These challenges are identified by examining the general wearable sensing pipeline and determining areas where improvements are needed, such as power efficiency, data privacy, and real-time analytics. Finally, we conclude our survey with a discussion on future research directions and opportunities, emphasizing the potential of smart rings to redefine the next generation of wearable technology.

A.2. Survey scope

Wearable computing and sensing technologies have advanced significantly over the years [171]. This progress is also evident in the growing number of research publications, with a query for *wearable* returning approximately 473,000 results on Google Scholar from 2014 to 2024. These publications span a wide range of topics, including health monitoring, user interaction, human activity recognition, fitness and sports, workplace and industrial applications, education, and entertainment. The growing interest in wearable technologies is driven by the increasing demand for personalized and context-aware functionalities in everyday life. When narrowing the query to focus specifically on computation (*wearable computing*), the total number of publications is significantly smaller, returning approximately 16,200 results. Nevertheless, the field has experienced steady growth in recent years, with around 2,000 publications appearing annually. Despite this surge,

Table 23: Comparison between related surveys and this survey, focusing on sensing pipeline, sensor details, wearable device coverage, and depth in smart rings.

Survey	Focus	Sensing pipeline	Sensor details	Device coverage	Depth in smart rings
[82]	human activity recognition HAR	no	no	median	no
[305]	human activity recognition HAR	no	no	median	no
[431]	HAR in health care	yes	no	median	no
[282]	gait recognition	yes	yes	large	no
[186]	human activity recognition HAR	partial	no	median	no
[459]	health and sports	partial	yes	large	few
[20]	healthcare	yes	yes	large	no
[390]	interactions for users with motor impairments	no	no	large	few
[201]	interfaces for hand gesture recognition	yes	no	large	few
[429]	interactive systems for upper body rehabilitation	no	no	median	no
[254]	biometric authentication	partial	no	median	no
[48]	biometric recognition	yes	yes	median	no
[14]	education	no	no	large	no
[10]	environmental monitoring	no	no	large	few
[325]	workplace and occupational safety, health, and productivity	no	no	large	few
[384]	defence automation	no	no	large	no
[389]	privacy and safety by advanced authentication and risk detection systems	no	no	large	no
[132]	mental stress detection	partial	no	large	no
[363]	emotion recognition using physiological signals	yes	no	median	no
[306]	artificial intelligence	yes	no	large	no
[319]	systematic review	partial	no	large	few
[309]	systematic review	no	no	large	no
[374]	systematic review	no	no	large	few
[171]	systematic review	no	yes	large	few
[434]	systematic review	no	yes	only ring	yes
Our survey	systematic review	yes	yes	large	yes

critical surveys that evaluate the current state of wearable computing are limited. Existing reviews often focus on specific applications or isolated components of the processing pipeline, lacking an in-depth examination of the end-to-end wearable sensing systems. This survey aims to address that gap by providing an in-depth analysis of recent advancements in wearable technologies, with particular emphasis on emerging trends, system-level integration, and the unique challenges presented by smart rings.

A.2.1. Related surveys

Existing surveys on wearable computing predominantly concentrate on specific applications or device categories—such as health monitoring, human activity

recognition, or interactive systems. However, they often lack a comprehensive perspective that spans the full sensing pipeline, diverse sensor modalities, and comparative analysis across wearable form factors. Table 23 summarizes the most relevant surveys in this area, categorizing them according to five critical dimensions: breadth of application domains (focus), sensing pipeline coverage, sensor-level detail, device diversity, and depth of analysis on smart rings.

- **Focus:** how comprehensively the survey spans different application domains (e.g., healthcare, fitness, accessibility, AR/VR, workplace, etc.). *Systematic review: covers broad application areas in a structured and organized manner.*.
- **Sensing pipeline coverage:** whether the survey discusses the full end-to-end sensing process, including data acquisition, processing, modeling, and evaluation. *Partial: covers only certain stages or lacks detail in the pipeline.*
- **Sensor-level detail:** whether the paper explores specific sensor types, usage and signal modalities.
- **Device coverage scope:** the breadth of wearable form factors considered, ranging from head-mounted displays to foot-worn devices. *Median: covers only some wearable types*; *Large: includes most major wearable device categories.*
- **Smart ring depth:** the extent to which smart rings are examined or emphasized within the survey. *Few: mentions limited use cases with no in-depth analysis.*

Most existing surveys either focus narrowly on specific sensing domains or only provide surface-level mentions of the sensing process. For instance, works on human activity recognition (HAR) [82, 305, 186] typically examine only the recognition stage, such as activities of daily living (ADLs), without detailing upstream aspects like sensor configuration or data preprocessing. Similarly, while some surveys describe the sensing pipeline, their focus is confined to health monitoring [20, 431] or gait recognition [282]. These surveys focus on domain-specific applications and overlook system-level challenges in designing and deploying complete wearable sensing systems.

Several systematic reviews have explored a variety of sensor types, but they often lack deeper analysis of sensor operation, placement strategies, signal quality considerations, or integration constraints [171]. Other works focus on providing high-level system overviews while overlooking the low-level sensing mechanisms that directly impact performance and usability [374, 319, 309]. These limitations reduce their practical value for system designers and researchers who require a more structured understanding of sensing modalities and configurations. In addition, surveys focused on specific application domains often limit the scope of wearable technologies, concentrating on areas such as human activity recognition (HAR) [82, 186], interactive systems [429], and biometric authentication [254, 48]. For instance, surveys on biometric authentication typically emphasize upper-

body wearables like earphones and smartwatches, without addressing the broader spectrum of wearable form factors. While broader reviews do exist, many treat wearables as a general category and overlook the impact of body placement on sensing performance, as well as the need for a high-level processing pipeline that can generalize across diverse wearable applications.

Smart rings are rarely analyzed in depth in prior surveys. They are often omitted or briefly mentioned as niche devices, even in comprehensive surveys with limited coverage [374, 171, 319]. One survey focused specifically on smart rings [434]. However, it lacked a technical discussion of sensing modalities, data processing, system architecture, emerging applications and the challenges associated with integrating multiple functions within such a compact form factor. In contrast, our survey builds the discussion of smart rings upon a comprehensive examination of various wearable devices across different application domains, providing both context and depth to the emergence of smart rings.

In summary, while many existing surveys explore specific wearable applications, sensing modalities, or system components, there remains a significant gap in research that considers wearable systems from an end-to-end perspective. Most prior works are either domain-specific or focus narrowly on individual pipeline stages, lacking a holistic view of how sensing, data processing, and placement interact across diverse use cases. Smart rings, in particular, are often overlooked as niche devices, with limited technical analysis in the literature. Our survey addresses this critical gap by providing a comprehensive examination of wearable sensing systems, spanning multiple application domains and emphasizing the emergence of smart rings. We systematically discuss sensing modalities, system design, and hardware constraints, and identify open challenges in integrating functionality within compact form factors. By offering a structured and in-depth discussion, this survey contributes to both foundational understanding and practical guidance for researchers and developers working on the next generation of wearable technologies, especially smart rings.

A.2.2. Selection of articles

A systematic literature search was conducted across four major academic databases: IEEE Xplore, ACM Digital Library, Elsevier, and Springer. To keep the review focused and relevant, we primarily considered articles from the past decade (2014–2024). To comprehensively cover the wearable computing landscape, we constructed search queries based on a four-part keyword taxonomy: fundamental, category, technique, and application. These groups are summarized in Table 24. The fundamental group included core descriptors such as *wearable*, *wearables*, *wearable sensing*, and *wearable computing*, forming the basis of each search query. The category group captured device types and body placement diversity using keywords such as *watch*, *glass*, *ring*, *patch*, *wristband*, *shoe*, and *textile*, which reflect wearable locations across the head, neck, trunk, upper and lower limbs, as

Table 24: Keyword descriptions

Group	Keywords
Fundamental	wearable, wearables, wearable sensing, wearable computing
Category	head, hat, headband, glass, headphone, earbud, mask, neck, collar, trunk, T-shirt, belt, watch, glove, ring, wristband, shoe, insole, sock, leg, textile, patch
Technique	data processing, data analysis, machine learning, artificial intelligence
Application	human activity, user interaction, user interface, healthcare, fitness, sport, assistance, safety, workplace, industry, VR, AR, authentication, defense, entertainment

shown in Figure 61. The technique group focused on sensing and computational components by including terms like *data processing*, *data analysis*, *machine learning*, and *artificial intelligence*. This can allow us to distinguish and filter out work that solely focuses on engineering and technical advancements, such as enhanced signal processing, alternative algorithm designs, or the development of new sensors. Finally, the application group targeted practical domains such as *human activity*, *healthcare*, *user interaction*, *authentication*, *fitness*, *safety*, *workplace*, *AR/VR*, and *entertainment*. These queries were combined and iteratively refined to ensure both breadth and depth of coverage. Citation chaining was also used to identify influential papers missed by initial searches.

We applied several filters to ensure the quality and relevance of the articles. Only full-length, peer-reviewed journal or conference papers written in English were included. Articles such as demonstration, book chapters, short papers, posters, workshop papers, interviews, opinions, editorials, invited talks, and demo descriptions were excluded. Titles and abstracts were reviewed to verify that the article involved wearable devices with embedded sensing capabilities and addressed data-driven analysis or real-world application scenarios. Articles focused solely on industrial design, fabrication, or aesthetic elements without analytical components were excluded. In cases where multiple papers reported incremental improvements on similar topics, we selected either the most recent or most cited version. This filtering process resulted in 264 core articles. Each article in the final corpus was reviewed in detail to extract technical and contextual features related to wearable sensing. We recorded key elements such as the sensing pipeline, sensor types, device form factors, user interaction strategies, and application areas.

A.3. Wearable computing and applications areas

Wearable computing refers to the integration of computing technology into clothing or accessories that can be comfortably worn on the body, allowing users to perform computing tasks continuously and seamlessly in daily life [20, 16, 306]. It combines Internet of Things (IoT) and Artificial Intelligence (AI) technologies to integrate diverse data sources for a better understanding of body conditions and surrounding contexts [319]. Many wearable devices incorporate *haptic* technology, using vibrations, pressure, or skin deformation to convey information through touch. Haptics provides non-visual feedback for alerts, guidance, or confirmation,

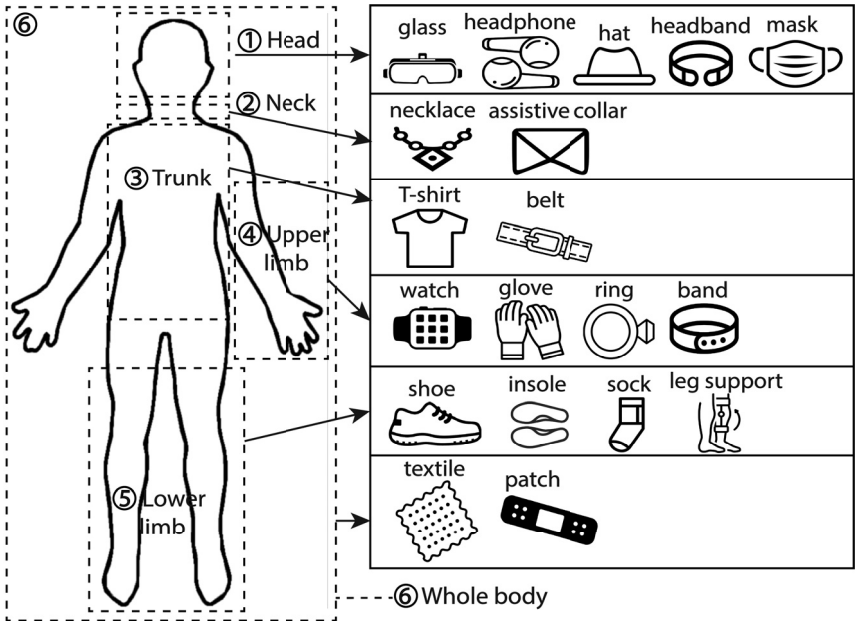


Figure 61: Wearable applications on different body parts

particularly in contexts where visual or auditory cues are limited or disruptive. Common devices, such as smartwatches, smart rings, smart glasses, and sensor-embedded garments, are designed to be always on, always accessible, and capable of sensing, processing, and communicating information in real-time. The main goal of wearable computing is to enhance human capabilities by seamlessly blending digital functionality into physical experiences. Its core areas include human activity recognition (HAR), user interfaces and interactions (e.g., authentication and gesture control), physiological (health) monitoring, assistance and safety for individuals with special needs.

A.3.1. Core functional areas

Human activity recognition (HAR): Human Activity Recognition (HAR) involves recognizing and interpreting the physical activities of individuals using data collected from wearables. It has gained significant attention due to its strong relevance in diverse fields such as healthcare, assisted living, rehabilitation, elderly fall detection, fitness tracking, human-computer interaction, and surveillance [82]. Wearable computing provides continuous and mobile monitoring of activities in real-world settings, in contrast to fixed-location sensors that offer limited coverage and flexibility. These wearables can detect motion, orientation, and environmental context to recognize activities of daily living (ADLs), such as walking, running, sitting, or more complex tasks like eating and house cleaning. Moreover, they can achieve subtle and fine-grained motion detection, such as head gestures via smart glasses or headphones, arm and hand postures via smartwatches or gloves,

and finger gestures with smart rings. Activity recognition performance can be further enhanced by integrating both physical movement data and contextual cues for context-aware applications.

User interfaces and interactions: User interactions offer alternative input modalities that enhance accessibility and usability across diverse contexts [390]. Gesture-based activation and control are increasingly common, allowing users to interact with devices through natural hand, head, or body movements. These capabilities are especially valuable in situations where traditional inputs like keyboards or touchscreens are impractical, such as during meetings, physical activities, or formal settings. To support varied user needs, user-centered studies have informed the development of diverse wearable prototypes and interaction techniques. Wearable devices now incorporate multiple input modalities: smart glasses utilize head movements, eye gaze, and voice commands for immersive, hands-free control; smartwatches support taps, swipes, and voice-based interactions for navigating interfaces; smart gloves and rings detect hand gestures like grasping, pointing, or stretching to control external devices; smart shoes enable foot-based inputs, particularly aiding users with limited hand mobility. Additionally, voice control is gaining popularity for its intuitiveness, especially in scenarios requiring hands-free interaction, such as while driving or exercising [225]. Some wearables also integrate proximity sensing, skin contact recognition, or brain-computer interfaces (BCIs) to offer touchless or thought-based control [135]. Furthermore, wearables support secure authentication using unique biometrics, including the ear canal, body sound, blood vessels, fingerprints, and behavioral patterns like gait or head motion. These diverse interaction approaches make wearable devices more inclusive, adaptable, and practical for everyday use.

Physiological (health) monitoring: Wearable computing can enhance physiological monitoring by continuously capturing vital signals that reflect an individual's health status [20]. Devices measure key biomarkers including heart rate, heart rate variability, respiration rate, body temperature, skin conductance, muscle activity, blood oxygen saturation (SpO_2), and sleep patterns. These signals provide critical insights into cardiovascular function, respiratory health, metabolic activity, stress levels, and neuromuscular performance. By detecting abnormal patterns or trends in physiological data, wearables support early identification of health risks such as arrhythmias, sleep apnea, dehydration, and fatigue. Advanced wearables also integrate multi-sensor data to offer comprehensive real-time feedback for both clinical use and personal wellness tracking. As a result, physiological monitoring through wearables contributes to preventive healthcare, rehabilitation, and informed lifestyle management, bridging the gap between everyday health tracking and clinical diagnostics.

Assistance and safety: Wearable computing offers significant support in assistive technologies for individuals with physical, sensory, or cognitive limitations, as well as in enhancing safety and efficiency across various environments, including

industrial and outdoor settings. For example, wearable glasses improve communication for the deaf by recognizing American Sign Language (ASL) and assist the visually impaired with object detection and spatial awareness [205, 65]. Smart belts and obstacle detection systems aid navigation and improve mobility safety for visually impaired users [24], while smart headwear enhances navigation and situational awareness for motorcyclists and workers in hazardous areas [274]. For cognitive support, wearables provide memory cues, task reminders, and guided navigation for users with neurological conditions. In industrial and occupational settings, wearables such as smart hats, badges, and vests improve worker safety by tracking physiological metrics and environmental hazards, including exposure to harmful gases, excessive noise, UV radiation, or extreme temperatures. Environmental monitoring wearables collect geo-tagged data on air quality, heat exposure, and toxic substances, delivering immediate alerts and informing risk mitigation. These systems not only assist individuals with disabilities but also support worker protection, emergency preparedness, and proactive interventions in dynamic and high-risk environments.

In summary, wearable computing utilizes these four core functional areas that form the foundation for various applications. Human Activity Recognition focuses on recognizing physical activities and movement patterns through motion and orientation sensing in dynamic and real-world environments. User interfaces and interactions center on alternative input modalities such as gestures, voice, proximity, and brain-computer interfaces that enhance accessibility, hands free control, and personalized engagement. Physiological monitoring involves continuous tracking of vital signs and biomarkers to assess cardiovascular, respiratory, metabolic, and neuromuscular health. Assistance and safety extend wearable capabilities into both assistive and high risk contexts, supporting users with disabilities and improving situational awareness and hazard detection in industrial or outdoor environments. These functional pillars provide the technical backbone for diverse real world applications, which are explored in the following domain specific sections.

A.3.2. Domain-specific applications

Gaming and entertainment: Gaming wearables allow players to interact with digital environments through body movements, biometric signals, and brain computer interfaces (BCIs), supporting more immersive, expressive, and socially engaging experiences[54]. Devices like AR/VR headsets and haptic costumes provide real-time interaction based on gestures, proximity, and physiological signals such as heart rate or brain activity. For example, wearables can translate stress levels into gameplay mechanics, activating special abilities when a player is calm or adjusting game difficulty based on heart rate. BCI headbands advance interactivity by translating neural signals into in-game commands, allowing thought-controlled gameplay. Social interaction is enhanced through wearables that respond to proximity or facilitate non-verbal communication, such as vibration cues or visual

signals. Moreover, wearables double as performative artifacts like wigs, rings, or bracelets that visually and physically connect players to their avatars, enhancing role play and character immersion. Additionally, VR headsets and smart earbuds integrate 3D spatial audio to create lifelike directional sound, enhancing immersion in gaming and virtual concerts. These innovations make entertainment more engaging and interactive while also improving accessibility for users with mobility limitations.

Metaverse and augmented reality: Immersive experiences of AR can be driven by enabling hands-free, gesture-based, and voice-controlled interactions in wearables [360]. Devices such as smart glasses with eye tracking allow users to navigate virtual spaces naturally, while haptic gloves and motion-capture suits enable realistic object manipulation by simulating tactile sensations like texture or resistance when interacting with digital elements. As AR and Metaverse applications expand, wearables are redefining how users engage with digital content, seamlessly bridging the physical and virtual worlds. For instance, companies like Sony are advancing Head-Mounted Displays (HMDs) by adapting content based on user pose and position to enhance AR experiences. Additionally, voice assistants integrated into wearable devices allow real-time control of digital overlays, spatial navigation, and contextual information retrieval. In the Metaverse, they function as personal guides, managing tasks, customizing environments, and supporting collaboration all through simple voice commands.

Military and defense: Wearable computing can improve military operations by enhancing situational awareness, biometric monitoring, communication, and tactical effectiveness across the land, air, and naval forces [384]. Smart helmets and glasses with AR heads-up displays deliver real-time battlefield data, including enemy positions, navigation cues, and threat alerts. Biometric sensors embedded in smartwatches, vests, and patches continuously monitor vital signs, ensuring soldiers maintain peak performance under stress. In the air force, smart clothing tracks pilots' physiological status during high-speed missions, while the navy leverages AR/VR technologies for immersive, cost-effective training in simulated maritime environments. Vision and surveillance capabilities are strengthened using smart helmets, AR glasses, and wearable cameras, offering extended views, hands-free communication, and real-time intelligence sharing, which can reduce reliance on traditional radios during covert operations. Exoskeletons and adaptive wearables enhance mobility and physical endurance, supporting soldiers in demanding missions. Together, these innovations increase operational efficiency, situational safety, and rapid decision-making in dynamic combat environments.

Education and training: Educational applications can be reshaped by wearable technologies potentially, including physical education, STEM learning, technical skill development, and inclusive education for learners with disabilities [14, 153]. These technologies enable real-time feedback, physiological monitoring, and increased engagement through gamified and context-aware learning environ-

ments. For example, AR/VR wearables offer immersive simulations for complex training scenarios, while smart clothing tracks students' physical activity and motivation. Smart glasses further enhance knowledge transfer in workplace training by allowing experienced professionals to record and share tasks on site, providing just-in-time learning without the constraints of time or location. Wearables also foster collaborative learning and provide instructors with valuable data on student behavior and engagement. These innovations enhance motivation and equip learners with practical skills for both classroom and remote educational settings.

Health and medical: As the demand for continuous monitoring and personalized healthcare increases, wearable technologies are being applied many use cases, including chronic disease management, rehabilitation, mental health monitoring, and elderly care [20]. These wearables track vital signs such as heart rate, physical activity, blood oxygen levels, glucose, sleep patterns, and stress, which help patients and healthcare providers make informed decisions. In both clinical and home settings, wearables facilitate early detection of health anomalies, support recovery through remote monitoring, and reduce hospital visits by empowering individuals to manage their conditions independently. For instance, they assist in monitoring cardiac health, detecting falls in older adults, and delivering haptic or vibration-based feedback during physiotherapy. Wearables also contribute to mental health management by tracking mood-related indicators and supporting behavioral interventions. By integrating with mobile health platforms and AI-driven analytics, wearable computing enhances the efficiency, accessibility, and personalization of modern healthcare systems.

Fitness and sports: In recent years, wearable devices have been increasingly used to support performance analysis, injury prevention, and personalized training [459]. These devices can monitor athletes' activity, biomechanics, and physiology in real time, enabling precise sports activity recognition, posture analysis, and motion tracking to help coaches optimize techniques and reduce injury risks. For example, devices like the WHOOP Strap and OPTIMEYE S5 provide continuous feedback on athlete readiness and fatigue levels. Wearables also support injury prevention by identifying early signs of overtraining, muscle fatigue, or improper form. Moreover, they allow for the prediction of key physiological metrics like oxygen uptake (VO2), tidal volume and running variability, which are critical for tailoring endurance training. By combining multi-sensor data with advanced insights, wearable computing can help athletes and trainers make data-informed decisions, improve performance, and create safer, more efficient training environments.

Workplace and industry: In industrial environments such as construction, manufacturing, warehousing, and logistics, wearables provide critical support for workers exposed to physical, environmental, and ergonomic risks [325]. For example, safety helmets monitor environmental hazards such as gas leaks, noise levels, or proximity to dangerous zones for protection in high-risk settings. Devices like smart belts detect unsafe postures and deliver haptic feedback to correct lifting

techniques, while exoskeletons reduce physical strain during repetitive or overhead tasks. AR headsets and smart glasses offer hands-free guidance by overlaying step-by-step instructions, maintenance procedures, or system alerts directly into the worker's field of view, which can boost task accuracy and reduce cognitive load. Smart head-mounted displays also integrate location tracking, environmental sensing, and communication tools to increase situational awareness and enable remote supervision. In terms of productivity tasks, smart gloves allow hands-free barcode scanning, while AR smart glasses assist with training, inventory management, and field service. Additionally, cognitive and stress monitoring wearables such as headbands and wristbands support mental well-being and biometric security in high-demand work environments.

Environmental and sustainability monitoring: Wearable Environmental Monitoring Systems (WEMS) allow individuals to collect geo-tagged environmental data such as temperature, humidity, air quality, noise, UV radiation, and even chemical threats and pollution like micro-plastics [308]. These systems provide continuous, high-resolution insights into individual exposure to pollutants and surrounding microclimates [10]. They facilitate a variety of sustainability-focused applications, including air pollution mapping, urban planning, microclimate analysis, and energy efficiency assessment. For instance, smart wristbands and helmets allow individuals to track their exposure to pollutants such as particulate matter (PM), carbon monoxide (CO), nitrogen dioxide (NO_2), and volatile organic compounds (VOCs). Smart badges can detect radiation levels or the presence of hazardous gases in both environmental and industrial safety contexts. Some wearable systems are powered by solar energy, improving sustainability and reducing reliance on batteries, particularly in long-term outdoor monitoring scenarios. Through mobile connectivity and cloud integration, these systems facilitate large-scale environmental data collection and visualization, which promote citizen science, informed urban decision-making, and proactive environmental protection.

Accessibility and assistive technology: For those with physical, sensory, and cognitive impairments, wearables can provide alternative interaction modes such as voice commands, haptic feedback, gesture control, and brain-computer interfaces They can help individuals with disabilities, mobility impairments, and the elderly by improving independence, safety, and connectivity [299]. For example, smart glasses can convert text to speech for visually impaired users, while wrist-worn devices deliver tactile alerts to those who are deaf or hard of hearing. For elderly or mobility-impaired users, wearables like smart belts and insoles facilitate real-time monitoring of gait, posture, and movement patterns to detect falls, track activity levels, and dispatch emergency alerts. Integration with smart home and telehealth platforms further supports autonomy, allowing users to safely navigate their surroundings and access timely assistance.

Biometric authentication: Traditional authentication methods such as fingerprints, facial recognition, iris scans, and passwords, often pose security and usability

concerns. In contrast, wearable computing offers continuous and user-friendly alternatives for identity verification [254]. Devices like smartwatches and rings support passive identity verification through physiological and behavioral traits, including heart rate, gait, blood vessel patterns, voice, and signature dynamics. Unlike traditional systems that rely on active user input at fixed access points and often raise privacy and security concerns, wearable biometrics operate discreetly and maintain authentication throughout use. Data is typically stored locally on the device, which strengthens user privacy and reduces exposure to centralized breaches. When paired with IoT ecosystems such as mobile payments, smart home control, or health platforms, wearables offer a more personalized and secure approach to identity verification in dynamic and connected environments.

A.4. Wearable usage and sensors

The diverse applications are supported through specific usage patterns and embedded sensing technologies. While wearables are worn on the body, they often rely on smartphones for processing, visualizing, storage, and connectivity. This section examines how such systems are typically used and highlights the core sensors such as motion, physiological, electromechanical, and environmental sensors, that support real-time monitoring across these domains.

A.4.1. Wearable usage

Wearable devices are typically designed to operate in coordination with smartphones due to their limited resources in terms of processing power, energy capacity, and interface capabilities. To maintain a compact and lightweight form factor, most wearables prioritize efficient data acquisition while offloading complex tasks, such as signal processing and analytics, to more capable external systems. Among these, smartphones play a central role in managing wearable devices by serving as a hub for data transmission, analysis, visualization, and user interaction.

In a typical usage scenario, a wearable device continuously captures data, such as physical activity, physiological signals, or environmental context, and transmits it to the smartphone via short range wireless protocols like Bluetooth or WiFi. The smartphone then performs data processing, displays results through a dedicated companion application (or its on small screen), and may sync data with cloud services for long-term storage or further analysis. This architecture extends the functionality of wearables while minimizing their hardware demands. In more advanced systems, cloud infrastructure complements the wearable–smartphone pair by providing large-scale data analysis, personalized feedback through machine learning models, and seamless access to historical data across devices. This distributed approach allows the wearable to deliver real-time feedback through the smartphone while supporting more complex processing in the cloud. Although modern smartwatches and other advanced wearables are beginning to incorporate onboard processors and operating systems capable of partial or full on-device

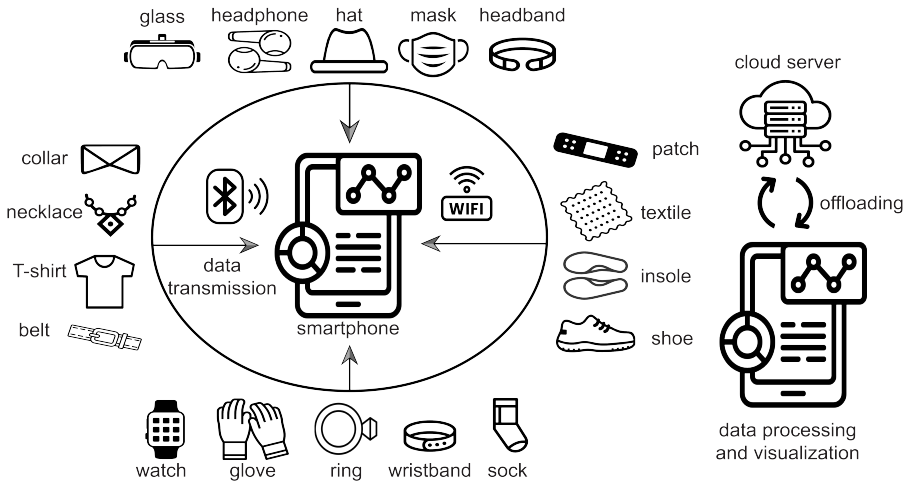


Figure 62: Wearable usage with smartphones

processing, smartphones remain essential for managing connectivity, heavy computation tasks, and user-facing applications. Smartphone apps play a crucial role in managing and interacting with wearable devices; and latest work has explored how LLMs enhance interaction and centralize wearable data [333, 334]. Figure 62 further illustrates the typical interaction between wearable devices, smartphones, and cloud services, showing the data flow and distribution of processing across the system.

A.4.2. Sensors

Different sensing configurations impact sensor performance and are suited to specific applications. Prior works have categorized wearable sensors based on their sensing principles and described their advantages and limitations [229, 180, 171]. Instead of examining the internal mechanisms of each sensor, our work focuses on the characteristics of sample data, sensor data types, sensing units, and functions. We emphasize the nature of sensor data, as it directly influences downstream processing in the wearable sensing pipeline. We focus sensor commonly available in different wearable devices. Table 25 summarizes all type of sensors that can be found in wearable devices. We can observe that all wearable sensors generate data that varies over time and can be treated as time series. Inertial signals, for example, are collected continuously and contain both temporal and spatial features through multi-axis motion data. Physiological and audio signals are also captured over time and reflect dynamic patterns. Even image data, when captured as a sequence over time, forms a time series with spatial structure.

Motion sensors. These sensors monitor physical activity and provide real-time data on movement. **Accelerometer (ACC)** measures linear acceleration (meters per second squared, m/s^2) along the x, y, and z axes, capturing speed and direction for activity recognition, such as body gestures, step counting and velocity changes

Table 25: Common sensor in wearables: unit, data type and functionality

Category	Sensors	Unit	Data type	Functionality
Motion sensors	**Accelerometer**	meters per second squared m/s^2	spatio-temporal	direction
	Gyroscope	radians per second rad/s	spatio-temporal	rotation
	Magnetometer	Tesla T	spatio-temporal	magnetic field change
	IMUs	combination of above three sensors		
Physiological sensors	**ECG**	millivolts mV	time-series	cardiovascular system
	EEG	microvolts uV	time-series	brain activity
	EMG	millivolts mV	time-series	muscle activity
	EOG	millivolts mV	time-series	eye movement
	EDA	microsiemens uS	time-series	skin conductance
	Respiration	breaths per minute BPM	time-series	chest/abdomen movement
	PPG (Optical)	Arbitrary Units AU	time-series	blood volume change
	Pulse oximetry (Optical)	BPM, SpO2 %	time-series	blood oxygen SpO2 and pluse rate
Electromechanical sensors	**Capacitive (touch)**	farads F	time-series	capacitance change
	Piezoresistive (pressure, force, strain , flex)	ohms Ω, force N Pascal Pa, strain $\mu\varepsilon$, volts V	time-series	resistance change
	Piezoelectric (pressure, force)	volts V, force N, Pascal Pa	time-series	electrical charge generation
Other sensors	**Camera**	pixels px, frames per second eps	image, video	image data
	Thermal	degrees celsius °C	time-series, image	infrared radiation
	Ambient (Temperature, Humidity, Light, Gas)	degrees celsius °C, humidity % light intensity LUX, air quality PPM	time-series	environment condition
	Microphone	hertz Hz, volts V	audio	sound waves
	Electromagnetic (Wi-Fi, RFID, ...)	hertz Hz, Tesla T, decibel-milliwatts dBm	time-series	wireless transmission
	GPS	degree °, speed km/h altitude m	time-series	navigation
	Proximity	Millimeters (mm)	time-series	object distance

[282, 226, 20]. **Gyroscope (GYRO)** detects angular velocity (radians per second rad/s), aiding in motion differentiation and orientation tracking, e.g., fall detection. It is commonly used alongside accelerometers to distinguish dynamic motions or similar activity patterns [315]. Integrated inertial measurement units (**IMUs**) combine ACC and GYRO for precise motion tracking, while some extend to **Magnetometer (MAG)** to measure magnetic field strength (Tesla T or Gauss G) and direction (Degrees) for enhanced orientation and heading [459]. Compared to standalone sensors, IMUs are preferred for comprehensive motion analysis.

Physiological sensors. Physiological sensors monitor various body functions, including brain, heart, eyes, muscles, and respiration, supporting applications in stress monitoring, sleep analysis, and chronic disease management [363]. Most detect electrical signals generated by the body. For instance, **ECG (Electrocardiogram)** sensors record the electrical activity of the cardiovascular system (millivolts mV), which track heart rate, rhythm, and waveforms to diagnose arrhythmias, heart attacks, and other conditions [229, 437]. **EEG (Electroencephalogram)** measures brain electrical activity (microvolts uV), analyzing amplitude (strength) and frequency (speed) in waveforms to study sleep, cognitive functions, epilepsy, and brain-computer interfaces (BCIs) [433]. **EMG (Electromyography)** detects muscle electrical activity (millivolts mV or microvolts uV) produced by muscle contraction and relaxation in regular and pathological circumstances [451]. It can assess contraction strength, fatigue, and neuromuscular disorders for sports and rehabilitation applications. **EOG (Electrooculography)** tracks eye movement by measuring cornea-retina potential (mV), useful in drowsiness detection and human-computer interaction [231]. **EDA (Electrodermal Activity)** monitors skin conductance (microsiemens uS or micromhos $umho$), which reflects sweat gland activity and sympathetic nervous system response for stress and emotional state assessments [422]. **Respiration (Resp)** sensors measure breathing rate (breaths per minute BPM) and volume by inductance changes in chest and abdomen expansion, mainly used in respiratory health monitoring and smart belts [84].

Optical sensors can also track physiological signals. They generally use a light source (LED or laser) and a photodetector to measure changes in light properties, e.g., reflectivity, intensity, phase, wavelength and polarization, caused by interactions with the body. For instance, **PPG (photoplethysmography)** detects blood volume changes of each heartbeat via light absorption or reflection (arbitrary units AU), which can be used on wrists for heart rate variability (HRV), blood pressure (BP), and respiration rate monitoring [214]. PPG is non-invasive but prone to motion artifacts, often requiring ECG integration for improved accuracy. **Pulse oximetry** measures blood oxygen saturation (SpO2, %) and pulse rate (BPM) by using red and infrared light absorption through the skin [485]. It is widely used in respiratory health monitoring, exercise oxygenation and altitude adaptation.

Electromechanical sensors. Electromechanical sensors convert physical changes (e.g., force, deformation or other mechanical phenomena) into electrical signals and are primarily categorized as capacitive, piezoresistive, and piezoelectric sen-

sors, widely used for pressure monitoring in wearables [171]. **Capacitive** sensors detect capacitance changes (farads F) caused by object proximity, position shifts, or material properties. They are commonly used in **touch** sensors, which respond to physical contact or the close presence of an object (e.g., a finger). **Piezoresistive** sensors detect changes in resistance (ohms Ω), commonly used for pressure (Pascal Pa or pounds per square inch psi), force (N), strain ($\mu\varepsilon$) detection. **Pressure** sensors measure force exerted on a surface while **force** sensors quantify applied force. **Strain** sensors measure the deformation per unit length based on resistance changes. **Flex** sensors also primarily operate on piezoresistive principles, detecting bending or angular displacement by measuring changes in resistance (ohms Ω) or voltage (V). **Piezoelectric** sensors generate electrical charge signals from stress, pressure, or vibration, making them suitable for dynamic force or pressure measurements, unlike piezoresistive sensors, which are better suited for static measurements.

Other sensors. Wearable devices utilize various sensors beyond motion, physiological and electromechanical monitoring. **Cameras** capture visual data, depth information, motion behavior, and light intensity, commonly used in augmented reality and user authentication. **Thermal (infrared)** sensors measure infrared radiation emitted by objects and convert it into electrical signals to estimate skin or environment temperature (°C) [388]. **Ambient** sensors monitor temperature, humidity, light intensity levels LUX, air quality PPM. For instance, **humidity** sensors measure relative humidity %, absolute humidity g/m^3 and dew point °C. **Temperature** $TEMP$ sensors track heat or cold changes and often integrate humidity sensing [412]. **Gas** sensors measure the concentration of environmental gases (e.g., CO, CO_2, O_2, CH_4 and NOx) and alcohol vapors. **Acoustic (microphone)** sensors convert the sound waves into electrical signals (V, hertz Hz, decibels $dB\ SPL$) for voice recognition, audio recording and call handling [409]. **GPS** sensors provide positioning and navigation data, including coordinates (degree °), altitude (m), speed (km/h), distance, and timestamps. **Electromagnetic** sensors measure electric and magnetic field waves (Hz, Tesla T) that travel through space and carry information. RF (Radio Frequency) communication sensing (decibel-milliwatts dBm) is a subset of electromagnetic waves, e.g., Wi-Fi, Bluetooth, and RFID. **Proximity** sensors detect object presence and distance (millimeters mm) for motion sensing, screen activation, and gesture control by electromagnetic fields, sound waves, light, or capacitance. [169]. **Flexible** sensors are are stretchable and conformable, which pertains to physical adaptability rather than the specific functions or data types they handle [459].

A.5. Wearable devices

Building on the large spectrum of available sensing technologies, wearable devices can be designed to support diverse applications through strategic placement on the body (as shown in Figure 61). Advances in sensor technology have improved per-

formance and allowed devices to monitor both physiological and contextual signals [281, 172]. This section introduces wearable devices categorized by body placement, drawing from both commercial products and research prototypes. Devices are grouped by location, including the head, neck, chest, hands, arms, and legs. Many sensor types can be used in multiple locations depending on the application. We provide an overview of sensor functions, placement strategies, and performance characteristics. Table 26 summarizes current research by main application areas, body locations, purposes, and sensor types.

A.5.1. Head-mounted wearables

The head serves as the body's control center for monitoring vital signs and activities. Head-mounted wearables capture rich physiological and contextual data, enabling hands-free interaction and enhancing user experience across various industries. Their proximity to the brain, eyes, and ears makes them valuable for augmented cognition and immersive technologies like AR and VR. These sensors are seamlessly integrated into smart hats, headbands, glasses, headphones, and masks, which can provide comfort and usability without disrupting daily activities [171].

Common commercial products are smart glasses and headphones. Smart glasses, such as Microsoft HoloLens 2, Apple Vision Pro, and Google Glass Enterprise 2, enhance augmented reality (AR) and virtual reality (AR) applications by providing hands-free access to real-time data. They incorporate RGB cameras for video streaming, depth sensors for spatial mapping, GPS for navigation, infrared sensors for gaze tracking, IMUs for head motion detection, and microphones for voice commands. Smart headphones and earbuds now integrate motion tracking, biometrics, and adaptive audio techniques. Noise-canceling models (e.g., AirPods Pro, Sony WH-1000XM5) use microphones for active noise cancellation (ANC), while Powerbeats Pro employs motion sensors for workout tracking and auto-pause. AirPods feature optical and proximity sensors for automatic playback control, and Jabra Elite Sport includes a heart rate monitor for real-time fitness tracking. Head-mounted products also include hats, headbands and masks for safety, health monitoring, and environmental tracking. The Lumos Helmet enhances cyclist visibility with LED lights and accelerometers, while BrainBit and Muse headbands use EEG sensors for cognitive training and stress monitoring. The LG PuriCare Mask features filters and fans for airflow regulation and respiratory protection, and the AirPop Active+ Mask tracks breathing patterns and environmental air quality via a connected app. Beyond these commercial wearables, academic research explores new sensing technologies and experimental features to further enhance functionality and expand potential use cases.

Smart glass. Smart glasses primarily serve functions in human activity recognition, user experience enhancement, healthcare, and assistive technology, with existing works and commercial products in development. For instance, GlassMail

Table 26: Existing works of wearables: main areas, body parts, purposes and sensors

Main area	Body	Wearables	Purposes	Sensors
human activity recognition HAR	1	glasses, headphones	head/face/eye gesture detection [283, 245, 399, 183, 182, 479]	IMU, Optical, Microphone
	1, 4	glasses, watches, wristbands, gloves	hand/arm gesture or posture detection [239, 236, 386, 264, 101, 413], [95, 62, 263, 202, 356]	Camera, IMU, ACC, GYRO, EMG, Strain, Pressure, Flex
	4, 5, 6	watches, patches insoles, e-textile, wristbands,	activities of daily living ADLs and body posture detection [43, 8, 23, 29, 257, 256, 486, 470, 393, 88]	ACC,GYRO, Microphone, Optical, Capacitive, Pressure,IMU
	4	rings	finger gesture detection [303, 492, 491, 324, 480, 72]	IMU, ACC, GYRO, Electromagnetic, Thermal
user interaction enhancement	1	glasses, headphones	on-the-go email composition [487], speech and noise separation [66, 273]	Microphone
	1, 4, 6	glasses, headphones, watches, rings, e-textile, patches	touch/stretch/tapping/sliding/beating gesture detection for device interactions [323, 454, 258, 73, 316, 272, 138], [310, 152, 484, 368, 445, 439]	Touch, Microphone, ACC, GYRO, Capacitive, Force, Optical, Proximity, Pressure, IMU
	1, 4, 5	glasses, shoes wristbands	emotional/physiological state monitoring, foot gesture detection for social interaction [484, 130, 455]	Camera, EDA, IMU
	1	headphones	indoor location and gazing orientation [461]	IMU
user authentication	1, 4	headphones, watches, rings	unique property: ear canal, body sound, blood vessel, activity patterns, finger [127, 436, 495, 450, 77, 452, 240, 196]	Microphone, ACC, GYRO, PPG
healthcare	1, 4	glasses, hats, watches	drowsiness and fatigue [64, 361, 402, 246, 244]	Optical, Camera, EOG, IMU, EEG
	1, 3	glasses, hats, headbands, belts rings	neurological health: brain activity, anxiety epileptic seizure, sleep [371, 113, 6, 421, 57, 336, 27, 168, 394]	EOG, ACC, GYRO, ECG, EEG, Pressure, PPG
	4, 5, 6	rings, insoles, patches	cardiovascular health: heart rate and blood [275, 129, 238, 444]	Pulse oximetry, Pressure, ECG, PPG, Temperature
	1, 3, 6	headphones, belts,e-textile, masks	respiratory health [342, 285, 13, 343, 253, 217, 462]	ACC, Optical, Respiration, Piezoresistive, GYRO, Wireless,
	2	collars	neck rehabilitation [102, 230, 284, 218, 234]	ACC, GYRO, EMG, FLex
	4	rings	hand-related detection: handwashing [453], tremors [458], hand-grip strength [464]	ACC, GYRO, Optical
	5	insoles,shoes, socks	diabete monitoring [424, 228], flat feet detection [219]	Pressure, Optical, ACC, PPG, Temperature, Flex, Force
	1, 3, 4, 6	belts, wristbands, masks, patches	others: chest parameter [408, 168], oral health [9], harmful gas [128], sweat [357]	Optical, ACC, Pressure, GYRO, Gas, Wireless
fitness/sport	4	wristbands, gloves watches	exercise/training, sport activity monitoring [300, 496, 17, 160, 260, 157, 158, 121, 489]	ACC, IMU, GYRO, Microphone
assistance/ safety	1, 3	glasses, belts,	recognition for disabled: ASL, pill, obstacle [205, 65, 24]	Microphone, Camera, Optical
	1, 4	hats, rings	disaster, motorcycle and navigation safety [199, 274, 376], drink spiking [466]	Camera, IMU, GPS, ACC, Temperature, Optical, Proximity, Gas

facilitates hands-free email composition by leveraging voice input and large language models LLMs to understand user intent and generate appropriate content [487]. Users can then dictate, receive suggestions, and review emails seamlessly. TransASL improves communication for the deaf and hard-of-hearing by recognizing American Sign Language (ASL) through dual acoustic sensing modalities (outward-facing and inward-facing microphones and speakers) [205] . For seamless interaction, UbiPoint leverages a monocular camera to enable marker-free mid-air hand gestures (fingertip) detection [239], which studies show are preferred over handheld devices [414]. To further minimize reliance on mid-air gestures or handheld controllers, StretchAR introduces wearable straps that support stretching, tapping, and swiping interactions, providing a more discreet and comfortable alternative for augmented reality (AR) [323]. Beyond hand gestures, IMU and optical sensors facilitate facial, eye, and head movements for AR, addressing input limitations when voice or hands are unavailable [283]. Similarly, EyeGesensr emits ultrasonic sound waves and measures the reflected signals to detect eye gestures, such as looking left, right, up, or down [399]. EyeEcho also continuously monitors facial expressions by emitting encoded inaudible signals and capturing subtle skin deformations [245]. Additionally, smart glasses can process visual cues (cameras) from facial expressions and surroundings to infer the emotional state of users and those nearby, enhancing social communication and mental health applications [484].

Smart glasses also play a vital role in health monitoring and assistive technology. They can detect drowsiness and fatigue in real-time using infrared sensors, cameras, and physiological sensors (EOG) by analyzing eye movements, blink patterns, and head positions to provide timely safety alerts [64, 361, 402]. Similar sensors (EOG, ACC, and GYRO) help track physiological and behavioral data, such as eye blinks and gait, for early detection of neurological conditions like Parkinson's and Alzheimer's [371, 113, 6]. These systems can facilitate timely interventions and improve patient outcomes. Additionally, smart glasses assist visually impaired individuals by recognizing medication pills through AI-powered image processing models [65].

Smart headphones/earbuds. Acoustic sensing is widely used in smart headphones for motion and gesture tracking, device interactions. For example, HeadTrack utilizes this technology to capture head motion by calculating the time-of-flight of sound signals between a smartphone and earphones, determining the user's face orientation and distance [183]. Similarly, EarBuddy detects tapping and sliding gestures near the face and ears for seamless device interactions [454]. In-ear sound reflections are captured for 3D facial reconstruction, supporting applications like facial expression tracking and user interfaces [479]. ClearBuds and ClearSpeech enhance voice communication by using dual microphones to separate speech from background noise [66, 273]. Additionally, earbuds can analyze distortions, reflections, and external noise within the ear canal to estimate air leakage, improving audio quality and noise isolation [96]. Beyond acoustic sensing, Ear-ar

employs IMUs to estimate indoor location and gaze orientation for acoustic augmented reality (AAR) [461], while the combination of IMU and acoustic sensing enhances head motion tracking accuracy [182]. Lastly, BreatheBuddy utilizes an earbud's low-power accelerometer to track breathing biomarkers in real time for stress reduction [342].

Acoustic sensing is also widely used for biometric authentication and security, leveraging the unique physical and physiological properties of the ear. EarEcho authenticates users by analyzing in-ear sound wave reflections, which are shaped by the ear canal's unique structure [127]. EarID captures passive body sounds transmitted through the canal for identity verification [495]. EarDynamic enhances authentication by incorporating both the static geometry and dynamic deformations of the ear canal during speech [436]. Beyond acoustic methods, EarPass utilizes ACC and GYRO sensors to recognize unique head motion patterns for secure device unlocking [450]. Since microphones and motion sensors can be vulnerable to environmental factors such as loud noise or occlusions, EarPPG utilizes in-ear photoplethysmography (PPG) signals to verify identity based on changes in blood vessel geometry during speech [77].

Smart hats. Smart hats and helmets incorporate various sensing technologies for safety and healthcare. Head gestures serve as intuitive input methods to control applications such as audio playback, and notifications [99]. For elderly assistance, motion and sonar (acoustic) sensors monitor movement and detect obstacles to enhance safety [376]. In health monitoring, ECG and EEG sensors track heart and brain activity for early stroke detection, particularly in high-risk environments like industrial workplaces and athletic training [421]. IMU and EEG sensors also detect worker fatigue in hazardous environments [246]. Smart helmets also use cameras, GPS, and IMU sensors for disaster response and risk assessment [199]. Additionally, Shelmet enhances motorcycle safety with a dense sensor network (ACC, TEMP, light, proximity, alcohol gas) while leveraging solar and kinetic modules for energy sustainability [274].

Smart headbands. EEG sensors still remain essential for continuous brain signal and sleep monitoring [57]. The Foreseiz headband can predict epileptic seizures in real-time by integrating with mobile phones to alert users [336]. EEG headbands also classify anxiety levels (non-anxiety, low, or high) through multi-class analysis [27].

Smart masks. Smart masks integrate multiple sensors, including temperature, humidity, pressure, air quality, and gas sensors, for respiratory health monitoring and protection against harmful substances, particularly during respiratory disease outbreaks-COVID [109, 192, 209, 118]. FaceBit offers an open-source smart mask platform with sensors for heart rate, respiration rate, and mask fit, utilizing ballistocardiography, temperature, and pressure signals, along with energy harvesting capabilities [87]. Wireless (RF) sensing monitors cough activity and mask compliance [462], while fiber gas sensor-integrated masks help detect harmful gases at room temperature [128].

A.5.2. Neck wearables

The neck serves as a vital interface for transmitting human signals between head and torso. Commercial smart necklaces, such as the Bellabeat Leaf Urban, use motion sensors and vibrating reminders to track physical activity, sleep, and stress levels via a mobile app. In academic research, neck wearables, such as collars, are primarily used in head and neck rehabilitation to restore movement and manage pain in musculoskeletal or neurological conditions [102]. These devices incorporate accelerometers, gyroscopes, and EMG sensors to track movement and muscle activity, aiding therapy while ensuring comfort and adaptability. For example, accelerometers and gyroscopes monitor neck posture to support rehabilitation for cervical spine disorders [230, 284], while flex sensors in orthopedic devices help correct forward head posture [218]. Additionally, a neck-mounted wearable interface using e-textiles and flex sensors enables software interaction via subtle head movements, offering an alternative to touchscreens for users with mobility constraints [234].

A.5.3. Trunk-worn wearables

Wearable sensors on the trunk, including the chest, abdomen, and back, are primarily used for respiratory and cardiovascular monitoring in clinical and healthcare settings. Commercial smart wearables, such as smart belts Polar H10 and T-shirts Hexoskin, utilize ECG, respiration and ACC sensors to monitor heart rate, breathing rate, and movement. In academic research, advanced smart textiles incorporate stretchable and flexible sensors, such as Fiber Bragg Grating (FBG) optical and respiration sensors, to detect respiratory changes for patients with respiratory conditions [285, 13]. Belts are mainly used in trunk wearables. For instance, flexible belts with MEMS accelerometers and pressure sensors monitor vital signs, snoring, and sleep stages [168], while piezoresistive chest bands assess respiration through embedded yarns [343]. A 3D-printed wearable with an FBG sensor detects chest wall deformations [408], and a multi-frequency electrical impedance tomography (EIT) belt tracks vital signs in neonates with a remarkable 122 fps and 1 MHz bandwidth [446]. Additionally, smart belts like Waistonbelt 2 monitor abdominal circumference and posture for obesity management [288], while others assist visually impaired users through ultrasonic and infrared sensors providing obstacle detection via audio and vibration feedback [24].

A.5.4. Upper-limb wearables

Limbs are essential for human functions, and various smart wearables such as gloves, rings, watches, and wristbands, have been developed for health monitoring, rehabilitation, and interactive applications. Commercial devices like Oura Ring and Motiv Ring use accelerometers and PPG sensors to track sleep and activity, while the Padrone Ring enables remote control, and the FinchRing supports gesture recognition for augmented reality. Apple Watch and Fitbit watches integrate

GPS, heart rate (PPG/ECG), and motion sensors for fitness and health tracking. SensoGlove uses pressure sensors to analyze and improve a golfer's grip, while the WHOOP Strap provides continuous monitoring of recovery, strain, and sleep using PPG, accelerometers, skin temperature, and pulse oximetry. Researchers continue to enhance these wearables for improved activity detection, authentication, user experience, and health monitoring through innovative sensor designs.

Smart watches. Smartwatches are widely used for daily activity recognition due to their built-in IMUs (accelerometer and gyroscope), which achieve high-granularity detection of hand and arm movements [305, 236, 386]. This offers a practical and non-intrusive alternative to camera- or glove-based methods for activity recognition, gesture control, and context-aware interactions. Integrating smartwatch microphone data with motion sensors further enhances activity recognition [43]. Additionally, motion data combined with context-aware change detection can reduce annotation workload by prompting users only during significant activity changes [8]. Additionally, an active learning framework improves accuracy by selectively querying users on uncertain data points, minimizing labeling effort while adapting to individual variations [375].

Smartwatches support both identification and interaction purposes. For authentication, Gait-Watch captures gait patterns (step length, speed, and body sway) using accelerometers and sparse coding, providing security without active user input [452]. A smartwatch-smartphone collaboration continuously monitors motion-based behavioral patterns for implicit authentication [240]. However, security risks still exist, as shown by Snoopy, which exploits motion data to predict user passwords [269]. Beyond authentication, smartwatches improve user interactions. Duet facilitates seamless cross-device workflows through synchronized touch and motion interactions [73], while detachable smartwatch designs offer greater adaptability [216]. A handwriting recognition system allows text input on smartwatches through fingertip gestures, using gyroscope and accelerometer data to identify letters and words despite limited screen space [258]. Tapping gestures offer an alternative control method by detecting different beats on the watch face [316]. Additionally, optimized algorithms support fast, low-power visual context classification using sensors like cameras, temperature, accelerometers, and microphones [81].

Smartwatches monitor health metrics, promote physical activity, and support chronic disease management through interactive features and clinical integration [349]. WearBreathing tracks respiratory rates using accelerometers and gyroscopes with a random forest filter and CNN extractor [253], while EEG signals help detect driver drowsiness and provide timely fatigue alerts [244]. Blood pressure can be estimated without traditional cuffs by combining physiological signals like PPG and ECG [394]. In sports, motion sensors are commonly used to recognize sports activities such as swings [17], and WearCoach uses IMU and acoustic sensing for real-time fitness feedback [489]. WatchConnect facilitates smartwatch-centric cross-device prototyping with modular hardware and flexible software

[181]. As users rely on smartwatches for fitness tracking, notifications, and quick information access, contextual factors influence long-term usage [198]. However, visible notifications and screens may inadvertently expose user information, raising privacy concerns in social settings [328].

Smart wristbands/armbands. Wristbands and armbands, similar to smartwatches, use sensors (EMG, gyroscope, strain, and pressure) and machine learning to track and recognize hand gestures, enhancing interactions in virtual reality, human-robot interfaces, and assistive devices [264, 101]. Capband, a battery-free wristband, recognizes hand gestures through capacitive sensing by detecting skin deformations from muscle and tendon movements [413]. PrISM-Tracker enhances human activity recognition (HAR) by integrating sound, motion, and state transition models for real-time procedural task tracking in medical and industrial settings [23]. Empatica E4 measures electrodermal activity (EDA) to analyze physiological synchrony between presenters and audiences for better engagement [130]. Wrist-worn sensors also support health monitoring, as seen in mORAL, which detects brushing and flossing behaviors using accelerometers and gyroscopes [9]. RecoFit, FitCoach, and similar wristbands use motion sensors to track exercises, recognize movements, and assess postures for improved fitness and health [300, 121, 157, 158].

Smart gloves. Smart gloves recognize hand movements and gestures for applications in human-computer interaction, virtual reality, robotics, physical therapy, and the metaverse. They feature fabric-flexible, stretch-sensing designs with pressure (capacitive or piezoresistive) or strain sensors [138, 272, 200]. IMUs combined with pressure sensors capture complex hand motions and object interactions [407], while accelerometers and strain sensors enhance hand pose and gesture recognition for American Sign Language classification [95]. Deep learning models along with IMUs, flex, and pressure sensors, further refine gesture recognition [62]. Additionally, multimodal fusion integrating motion, audio, and camera data also enhances user intention detection at the decision-making level [86]. Beyond gesture recognition, iCoach recognizes training programs for real-time strength training monitoring by motion data [496]. IMUs also classify goalkeeper exercises like dives, catches, and throws [160, 260].

Smart rings. Research on smart rings explores their potential to enhance daily life and user interaction [33]. GestuRING supports ring-based gesture design with a searchable gesture-to-function dictionary [419], while empirical studies provide guidelines for designing intuitive gesture sets despite low user consensus [134]. Several smart ring platforms have been developed to improve interaction and tracking capabilities. OmniRing offers an open-source solution equipped with IMU and PPG sensors to monitor finger motion and heart rate [492], while two-ring setups improve finger gesture recognition with accelerometers and gyroscopes[303]. Auraring achieves millimeter-level 3D finger-movement tracking via electromagnetic sensing, overcoming optical limitations in low-light or obstructed conditions [324]. Advancements in self-supervised learning improve tracking accuracy, as seen in ssLOTR, which refines 3D motion tracking with minimal labeled data [491]. Efring

detects thumb-to-index-finger (T2I) microgestures using electric-field sensing for smartphone, VR, and AR control [72]. Additionally, ThermalRing enables gesture recognition through thermal imaging, detecting temperature variations from finger movements [480].

Smart rings can enhance user interaction and authentication. TypingRing converts finger movements into text input using accelerometers, proximity, and optical sensors, providing an alternative to traditional keyboards or touch screens [310]. IMUs combined with edge computing allow real-time keystroke recognition [484]. An energy-harvesting ring platform identifies gestures like tapping, swiping, and handwriting through pressure, audio, and motion sensors [152]. Additionally, acoustic sensing enables user authentication by analyzing unique finger acoustic characteristics between the current wearer and the pre-registered individual [196]. In healthcare and safety, WashRing tracks handwashing gestures via accelerometers to promote hygiene [453], while HIPPO estimates hand-grip strength using light sensors for continuous health monitoring without specialized equipment [464]. Pulse oximetry enables non-intrusive blood oxygen monitoring with minimal energy needs [275], and IMU sensors detect hand tremors for early Parkinson's detection and intervention [458]. Smart rings also improve personal safety in social contexts by detecting drink spiking through detecting light reflectivity changes [466].

A.5.5. Lower-limb wearables

Industrial wearable products leverage advanced sensing technologies to monitor mobility, prevent injuries, and enhance lower-limb performance. Accelerometers and gyroscopes track posture and movement (e.g., Xsens Moven, Ottobock C-Brace), while advanced systems like the ReWalk Exoskeleton and Wandercraft Atalante integrate force sensors and IMUs for mobility assistance and rehabilitation. These technologies drive research in wearable sensing, fostering more precise and adaptable systems, with smart shoes and insoles, particularly augmented foot interfaces (AFIs), as key areas of focus [105]. Pressure sensors and IMUs are the primary input modalities in AFI, often combined with temperature and humidity sensing. A review highlights their effectiveness in smart insoles for recognizing activities of daily living (ADLs) and emphasizes optimizing sensor configurations and data processing for improved health monitoring [88]. IMU-embedded detachable soles also enable foot-to-foot gestures for social interaction and team collaboration [455]. In healthcare, smart insoles and socks use pressure, optical, and physiological sensors to assess and continuously monitor diabetic foot ulcers (DFUs) by tracking temperature, pressure, acceleration, and heart rate (PPG) [427, 424, 228]. Additionally, piezoelectric sensors in insoles track heart rate via ballistocardiogram (BCG) signals [129]. Deep neural network models analyze gait to predict flat feet using force and flex sensors [219] and classify movement disorders through accelerometers in smart socks [271]. Sensock further integrates

pressure sensors and machine learning to reconstruct 3D foot models for custom footwear and clubfoot orthotics [475].

A.5.6. Wearables across whole body

Smart clothing and patches play a vital role in wearable innovation, integrating sensors into garments or adhesive designs for seamless health monitoring, athletic performance tracking, and personalized care. Smart apparel like the OMSignal Smart Bra (ECG, accelerometer) monitors heart activity during workouts, while Athos Training Wear (EMG sensors) and Lumo Run Shorts (IMUs) track muscle activity and running metrics. The Polar Team Pro Shirt combines heart rate, MEMS motion sensors, and GPS for professional sports training. In healthcare, smart patches such as VitalPatch (ECG) and MC10 BioStamp (EMG, IMUs) enable remote health monitoring and muscle recording for patients. TempTraq tracks body temperature, Abbott's FreeStyle Libre monitors glucose levels, and the Epicore Biosystems Sweat Patch analyzes hydration from sweat rate. G-Tech GutTracker detects myoelectric signals for GI motility assessment. As wearable technology advances, research continues to enhance the sensing capabilities and applications of smart clothing and patches.

Smart clothing/textile. A standardized smart clothing architecture should include wires, layout, connections, sensors, software, and updates for optimal performance [307]. Innovations like ZebraSense, a dual-sided woven capacitive sensor, can differentiate interactions on both surfaces [445]. Some garments use polymer optical fiber (POF) and piezo-resistive strain sensors for human activity recognition (ADLs) [29, 257, 256], while others incorporate capacitive sensors for upper-body motion and pose tracking [486, 470]. Capacitive sensing also facilitates hands-free bike interaction through gesture control [133], and strain-pressure fabrics monitor elbow joint movement by detecting skin deformation [263]. Wearable textiles further enhance interaction and health monitoring. Smart trousers with textile pressure sensors track posture changes to assess attention and engagement levels [393], while GestureSleeve extends smartwatch controls through forearm touch gestures like swipes and taps [368]. Fiber-enhanced pajamas use resistive and triboelectric sensors to monitor cardiac and respiratory rhythms [217], and a smart textile cover enhances prosthetic limbs with piezoresistive sensors for tactile feedback [242]. Smart clothing can also integrate with cloud-based platforms for real-time data processing, analytics, and user feedback, advancing health monitoring and activity tracking [71, 7, 79].

Smart patches. Smart patches are ultra-thin, non-invasive epidermal computing devices that integrate with the skin for human-computer interaction in healthcare, augmented reality, and communication [311]. The SkinKit modular system supports rapid prototyping of interactive on-skin interfaces with flexible electronic components [227]. Stretchable e-skin patches recognize ASL hand gestures by estimating skin strain with soft resistance sensors, offering a privacy-friendly alter-

native to camera-based systems, while transfer learning reduces training data and time for improved gesture recognition [202, 356]. iSkin incorporates capacitive and resistive touch sensing, such as stretch and bend, for mobile input in finger-worn and on-body devices [439]. Smart patches also support multi-functional physiological monitoring by measuring ECG, PPG, blood pressure, temperature, and pressure [238, 444]. Additionally, e-skin integrates solar cells for energy generation and multimodal sensing, while adhesive RFID patches track sweat electrolyte levels to monitor hydration and electrolyte balance [76, 357].

A.5.7. Wearable fusion

Coordinating multiple wearable devices creates a seamless, context-aware ecosystem for richer insights and intuitive interactions, but variations in measurement reliability highlight the need for standardized protocols [83]. Weave provides a JavaScript-based framework with high-level APIs for cross-device interactions, simplifying UI distribution and sensor integration [75]. UnifiedSense leverages sensor data from smartwatches, rings, headphones, and glasses for gesture recognition, allowing interactions even when the primary device is absent [30]. A cooperative sensing framework combines data from smart armbands and gloves using sensor fusion (IMU, EMG, pressure) to improve sequential gesture recognition [481]. IMUs in smartwatches and earbuds facilitate gesture-based interactions, such as head swipes to dismiss calls or in-air pinches for notifications [347]. Real-time body pose tracking is achieved through inertial sensors in smartphones, smartwatches, and earbuds, with an adaptive pipeline that processes available IMU data for a best-guess pose [297]. WRIST integrates smartwatch and ring IMU data for wrist gesture recognition and macro-micro pointing [463], while smartglasses and smartwatches improve pedestrian dead reckoning by analyzing the relative angles of arm swing and head direction, enhancing movement tracking in GPS-limited environments [267].

A.6. Wearable sensing pipeline

While wearable devices differ in form and function, they all follow a common structure for collecting, processing, and interpreting sensor data. To better understand how wearables transform raw signals into meaningful outputs, this section presents the typical sensing pipeline from data acquisition to application-level inference.

A.6.1. Overview

The general structure of the wearable sensing pipeline remains similar, even if the specifics can be different for each [186, 477]. While some operations are applied to data from individual sensors, others involve integrating data from multiple sources. This distinction focuses on whether an operation is performed on individual or aggregated data. For example, analyzing complex movements might involve

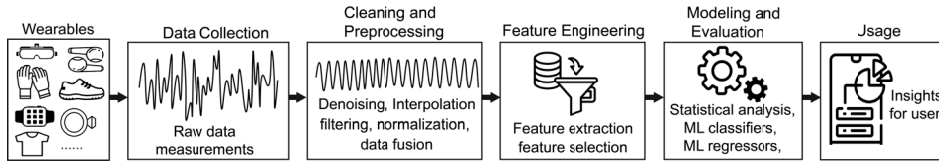


Figure 63: Wearable sensing pipeline

integrating data from accelerometers and gyroscopes. Therefore, we consider a general processing pipeline applicable to both single and multiple-sensor wearables, as the fundamental steps are largely consistent. The key difference arises in the processing stage, specifically the data fusion required for multi-source systems. Figure 63 depicts a brief overview of the five steps involved in the wearable sensing pipeline: (1) data collection, (2) data cleaning and preprocessing, (3) feature engineering, (4) modeling and performance evaluation, and (5) insight delivery through user-facing interfaces. The details are shown in the following sections.

- **Data collection (Section A.6.2):** This step focuses on acquiring high-quality sensor data from wearables. Accurate data collection depends on user compliance, time constraints, and the availability of reliable ground truth [301].
- **Data cleaning and preprocessing (Section A.6.3):** Raw data is cleaned and structured to reduce noise and motion artifacts. Common tasks include filtering, outlier removal, interpolation for missing values, normalization, and alignment. If multiple sensors are used, this step may also include data fusion to combine and synchronize inputs from different sources [194].
- **Feature engineering (Section A.6.4):** It aims to further reduce errors and computational complexity while improving model performance [315]. Feature extraction derives numerical representations of data using methods from the time and frequency domains, such as statistical metrics or Fourier transforms. Feature selection identifies the most informative variables, often using machine learning techniques like deep learning.
- **Modeling and evaluation (Section A.6.5):** In this stage, machine learning models are built and assessed. Both traditional algorithms and deep learning approaches are applied depending on the task [132, 331, 362]. Model performance is typically evaluated using metrics such as accuracy and F1 score for classification, or root mean square error and mean absolute error for regression. Statistical and structural tools like analysis of variance and Pearson correlation are also used to identify patterns and validate model reliability [34].
- **Usage (Section A.6.6):** The final step involves presenting processed insights to the user through smartphones, wearable screens, or other interfaces. This stage supports real-time feedback, trend visualization, and actionable guidance based on the analyzed data.

A.6.2. Data collection

Effective data collection is essential for wearable applications but often complex, involving user comfort, time management, environmental constraints, recruitment costs, and data annotation. While some domains offer benchmark datasets, many applications still require data and ground truth labels from diverse populations over extended periods. Studies aim for diversity in age, gender, weight, height, and health conditions, though participant numbers are typically limited to around 20, with even fewer for elderly or patient groups [56].

The data collection protocol is shaped by factors such as participant numbers, task types, activity execution (natural vs. constrained), and study environments (controlled vs. real-world). Many studies should follow predefined protocols in controlled settings, such as labs, to generate consistent and accurate data, which is later generalized to real-world environments like homes, parks and hospitals. Similarly, users perform guided tasks for cleaner data to extract meaningful insights that can be then applied to natural behaviors. Ground truth is essential for datasets, requiring careful annotation to minimize mislabeling. This can be achieved through manual supervision, video recording, semi-automated techniques, and custom applications [469]. Despite wearable technology's broad applications beyond activity recognition and health monitoring, data collection methods share challenges, and careful planning promises reliable and representative datasets. Finally, ethical considerations play a vital role in safegurading participant rights, privacy, and data security. Studies typically require IRB approval and informed consent, which outlines the study purpose, data usage and personal information protection measures.

A.6.3. Data cleaning and preprocessing

Basic preprocessing techniques. Sensor measurements are affected by noise and physical variations, impacting data accuracy and reliability. Preprocessing techniques, such as normalization, denoising, interpolation, and segmentation, enhance data quality [48, 194].

Smoothing and de-noising: Smoothing reduces noise and fluctuations to enhance reliability, especially in wearable sensors affected by movement or environmental factors. For instance, moving average computes an average within a sliding window to reduce short-term irregularities, while median filtering replaces each data point with the median of neighboring values, preserving edges and reducing outliers. The advance method Savitzky-Golay filter smooths data while retaining critical features like peaks and trends. It can help breathing detection in RFID-based smart garments even when respiratory frequencies change sharply [359]. Other filtering techniques target specific noise types: low-pass filters remove high-frequency noise for applications such as motion recognition, band-pass filters isolate relevant frequency bands for application such as eye movement tracking [399], and Fast Fourier Transform (FFT) converts data to the frequency domain to

filter out noise before transforming it back for a cleaner signal, as seen in wearables for human breathing rate extraction [5]. A wrist-wearable device improves heart rate monitoring by applying both band-pass and low-pass IIR filters to eliminate noise and motion artifacts [457]. In addition, convolutional filtering applies a kernel (filter matrix) over the input data, performing element-wise multiplication with each segment and summing the results to extract features and reduce noise.

Interpolation: Interpolation maintains dataset continuity by estimating missing values, often caused by signal loss, sensor malfunctions, or communication issues [282]. Linear interpolation uses a straight-line trend between adjacent points, while cosine and cubic interpolation create smoother curves for complex datasets. In human activity recognition by accelerometers, cosine interpolation produces a smoother signal than linear methods [442]. Additionally, machine learning-based methods, such as K-nearest neighbors (KNN), impute missing values by identifying patterns in neighboring points. For instance, KNN reconstructs short-term missing heart rate (PPG) data in Fitbit wristbands by analyzing heart rate and step count trends within a sliding time window, as higher step counts often indicate increased physical activity [476].

Segmentation: Segmentation breaks continuous data into smaller units or windows, often with overlap (e.g., 1-second windows with 50% overlap), to simplify analysis and improve computational efficiency for tasks like activity recognition and gesture analysis [399]. Fixed-size windowing divides data into equal-length segments based on time (e.g., 5s or 10s) or sample count, while activity-based segmentation detects boundaries dynamically by identifying transitions, such as shifting from walking to running. More advanced techniques, like dynamic time warping (DTW), align segments of varying lengths to detect patterns and similarities [330, 418]. In addition, segmentation is applied using thresholding, edge detection, and clustering to distinguish objects, backgrounds, and regions of interest, especially in images.

Normalization and synchronization: Normalization standardizes data to a comparable scale, reducing disparities caused by varying measurement units. Min-max normalization rescales data to a fixed range (e.g., [0,1]), while z-score standardization adjusts data to have a mean of 0 and a standard deviation of 1. In hand gesture recognition, direction normalization aligns hand contour features to a common reference, reducing variations in orientation and positioning [351]. Synchronization aligns sensor timestamps so that data from different sources corresponds to the same time period, such as in studies analyzing interactions between presenters and audiences [130]. This process supports the correlation of movement patterns from accelerometers with physiological data like heart rate monitors. When sensors operate at different sampling frequencies, data can be aggregated using mean values within a defined window or interpolated to align timestamps, with linear interpolation often being sufficient for short synchronization windows [80].

Data fusion across multiple sources. Data fusion combines information from multiple sensors, to improve data reliability and reduce the impact of sensor

displacement and misalignment [315]. The following are common methods.

Statistical approaches: Common methods, such as weighted averaging and least squares, help refine sensor data by reducing errors and noise caused by time delays, incorrect sensor placement, misalignment, and malfunctions. Weighted averaging calculates an average of all sensor readings while reducing the influence of outliers or erroneous sensors in the final estimate [449]. Least squares minimize the sum of squared differences across multiple measurements to produce a more reliable estimate [35].

Probabilistic methods: Common methods, such as Kalman filtering, Bayesian networks, and particle filters, integrate sensor data by modeling uncertainty and system dynamics. Kalman filtering, a predict-update fusion approach, estimates covariance and confidence between past and current sensor readings to reduce posterior estimation errors [69]. For example, it combines position and velocity data within a linear state-space model to reduce errors from self-occlusion, improving finger position tracking accuracy [332]. It also fuses accelerometer and gyroscope data in human motion tracking [255]. However, its reliance on linearity and Gaussian assumptions limits its use in real-world applications like mobile and wearable systems. As a stochastic approach, particle filtering (PF) estimates target probability distributions when analytical solutions are not feasible [222]. It generates random particles from a sampled importance distribution, assigning weights to correct mismatches between the target and importance distributions. In Bayesian terms, PF approximates posterior distributions even in nonlinear and non-Gaussian systems, where traditional methods like Kalman filtering struggle.

Evidential theory: Dempster-Shafer Theory (DST) handles uncertainty and combines evidence when dealing with incomplete or conflicting information, such as calibration drifts and missing values [483]. Unlike traditional probabilistic models, DST does not require prior probabilities, allowing it to merge multiple degrees of belief. However, its flexibility comes with high computational complexity for large-scale problems. DST integrates evidence from different sources and redistributes conflicting information based on their support, giving greater weight to sensors with higher reliability and confidence in decision-making. It can achieve high fault detection accuracy and surpassing traditional machine learning methods [136]. Additionally, DST improves uncertainty measures through modified belief entropy techniques in smart environments [415].

Machine learning-based fusion: These methods integrate data from multiple sensors to improve predictions and system accuracy. Common approaches include k-Nearest Neighbor (k-NN), Decision Trees (DT), Support Vector Machines (SVM), Random Forest (RF), Artificial Neural Networks (ANN), Gaussian Mixture Models (GMM), and K-means clustering [222]. These algorithms analyze data patterns to determine optimal ways to combine sensor inputs. Unlike traditional fusion methods that rely on fixed rules, machine learning models adapt based on training data and capture complex relationships between sensor modalities. Deep learning

models, such as Convolutional Neural Networks (CNNs), are also widely applied for data fusion. While these methods effectively detect non-linear patterns and handle large datasets, they require substantial computational resources and labeled training data, which can pose challenges in resource-constrained applications.

A.6.4. Feature engineering

After preprocessing, feature engineering further refines sensor data by reducing noise and dimensionality, focusing on extracting significant information. Techniques span time and frequency domains, as well as image processing, all designed to improve the performance of classification and regression models.

Feature extraction. The majority is time domain and frequency domain-based features [20].

Time-domain features: These capture the raw behavior of signals over time and are widely used due to their computational efficiency. Common statistical metrics include mean, median, standard deviation, variance, root mean square (RMS), kurtosis, and skewness, which summarize central tendency, dispersion, and distribution shape [125]. Signal magnitude area (SMA) reflects activity intensity by summing absolute signal values, while peak detection identifies counts, amplitudes, and inter-peak intervals, often relevant for IMU-based motion analysis [30]. Time delay measures synchronization, phase shifts, or system dynamics by analyzing the lag between related signals, with cross-correlation identifying the delay at which signals exhibit maximum similarity and reaction delays assessing response times to stimuli. Small variations in time echo can help identify unique ear canal features [127], while changes in signal amplitude due to eye movements influence reflection intensity, aiding in eye position and motion detection [399].

Frequency-domain features: These features depict the distribution of energy in a signal and are widely used in audio and radio signal processing [383, 156]. Common spectral features include Fast Fourier Transform (FFT), Discrete Cosine Transform (DCT), spectral energy, entropy, power spectral density (PSD), Fourier coefficients, and wavelet transform [137]. FFT reveals periodic components, while DCT represents signals as a sum of cosine functions, concentrating most energy into a few frequency coefficients, which is effective for data compression (e.g., JPEG) [321]. A partial DCT-based method applied to PPG data achieves higher compression ratios with minimal distortion and reduced reconstruction time for energy-efficient wearables [348]. Spectral energy measures power across frequency bands, while entropy quantifies signal randomness. PSD shows power distribution over frequencies, and Fourier coefficients capture amplitude and phase. The wavelet transform combines time-frequency analysis to detect transient and non-stationary patterns in signals like PPG, ECG, and EEG [410]. Its multi-resolution capability provides detailed insights at different scales. Additionally, Mel-Frequency Cepstral Coefficients (MFCCs) are widely used in acoustic sensing, representing a sound's short-term power spectrum, which is well-suited for machine

learning applications [127].

Feature selection. Feature selection techniques often leverage dimensionality reduction to simplify data while retaining critical information. Principal Component Analysis (PCA) projects high-dimensional data onto orthogonal components that capture maximum variance, minimizing noise. It improves model performance in human activity recognition (HAR) using multimodal sensors like accelerometers and gyroscopes [32, 353]. Linear Discriminant Analysis (LDA) enhances classification tasks such as activities of daily living (ADLs) and gait phase detection by maximizing class separability, optimizing between-class and within-class variance [4, 329]. t-SNE (t-Distributed Stochastic Neighbor Embedding) maps high-dimensional data into 2D or 3D while preserving local and global structures. It captures the relative distances and clusters similar points using a probability distribution over pairwise distances in high-dimensional space. t-SNE outperforms PCA for visualizing non-linear patterns, though its high computational cost limits its real-time applications [97, 61]. Non-Negative Matrix Factorization (NMF) decomposes data into non-negative components for applications where negative values lack meaning, such as word frequencies in text or pixel values in images [22, 167]. It can segment daily activity data into temporal components (morning, noon, evening, and night) with corresponding weights that indicate an individual's activity distribution for behavioral analysis [11].

Autoencoders are neural networks designed to learn compressed data representations by reducing dimensionality through an encoder, which minimizes reconstruction error, and a decoder, which reconstructs the original data from this lower-dimensional space [430, 432]. Their versatility from non-linearity and unsupervised learning allows adaptation to various data types such as images, time series, and text. For instance, a hierarchical recurrent autoencoder can automatically extract temporal features from wearable sensor data (e.g., skin temperature, conductance, acceleration) and be fine-tuned for personalized feature enhancement [243]. Sparse learning constructs a dictionary of fundamental elements, representing data as sparse combinations where most coefficients are zero or near zero and fewer components efficiently capture essential structures while reducing computational complexity [52]. This technique enhances classification in fields like signal processing, computer vision, natural language processing, and audio analysis [117]. In smartwatches, sparse coding extracts discriminative gait features from inertial sensor data for context-aware authentication by representing signals as sparse combinations of basis vectors while suppressing noise [452].

A.6.5. Modeling and evaluation

After data collection and processing, modeling and evaluation play a crucial role in extracting insights and assessing system accuracy in wearable applications. Modeling involves representing sensor data to capture specific events and situations. It also enables sensor data repurposing, allowing a single sensor to support

multiple applications based on contextual conditions and factors. Modeling involves analyzing sensor data through two main approaches: statistical analysis and machine learning (ML). Statistical methods, such as t-tests, ANOVA, and visualizations, establish baseline insights into data distributions and relationships. With advancements in AI, traditional statistics are increasingly complemented by ML techniques, which optimize systems and uncover hidden patterns for improved decision-making.

Statistical and structural analysis. Before applying machine learning techniques, it is essential to understand and interpret the underlying characteristics of sensor data. Statistical and structural analysis provides the foundation for this process by offering tools to summarize distributions, test hypotheses, examine variable relationships, and compare data patterns. These approaches support early-stage data interpretation, model validation, and insight generation in wearable sensing systems.

Descriptive statistics: These methods provide a foundation for understanding data distributions and variability. Measures such as mean and median represent central tendencies, while standard deviation, variance, and interquartile range (IQR) describe data spread and help detect potential outliers. Often used as a first step in analysis, these techniques highlight patterns or anomalies in data and support further modeling. Visualizations also play a key role in data interpretation. Plots such as histograms, box plots, scatter plots, and line graphs offer intuitive insights into distribution, variability, relationships, and temporal trends. Together, statistical summaries and visual tools enhance the overall understanding of sensor data.

Inferential statistics: Inferential statistics allow generalization from sample data to a broader population by testing hypotheses and estimating population parameters. When data does not meet the assumptions of normality, often assessed using the Shapiro-Wilk test, non-parametric tests are preferred. These tests do not rely on specific data distributions and include the Mann-Whitney U test for comparing two independent groups, the Wilcoxon Signed-Rank test for paired samples, the Kruskal-Wallis test for multiple independent groups, and the Friedman test for repeated measures [298]. Effect size measures complement significance testing by quantifying the magnitude of differences, such as eta-squared (η^2) for Kruskal-Wallis and Kendall's W for Friedman. Post-hoc analysis commonly uses Dunn's test (for Kruskal-Wallis) and Wilcoxon rank-sum tests (for Friedman), often with Bonferroni correction. Parametric tests, which assume normally distributed data, include the t-test for comparing means of two groups, and one-way ANOVA or repeated measures ANOVA for comparing more than two. Their effect size is typically reported using partial eta-squared (η_p^2). These inferential methods are widely applied in wearable research. For instance, Kruskal-Wallis tests have been used to assess differences in self-reported answers across phones, watches, and glasses [174], while Friedman tests with Bonferroni-corrected Wilcoxon Signed-Rank tests have been applied to examine variations in subjective time perception

based on tactile stimuli in wrist-worn devices [387]. Repeated measures ANOVA has also been used to analyze smartwatch-wearing behavior by context, including location and time of day [198].

Correlation analysis: Correlation analysis measures the strength and direction of relationships between two or more variables. Common methods include Pearson correlation r , which assesses linear relationships between continuous variables, and Spearman's rank correlation ρ and Kendall τ, which are suitable for monotonic relationships in ordinal or non-normally distributed data. For example, Kendall correlation has been used to evaluate the relationship between light reflectivity and baseline signals in smart gloves to optimize finger positioning for hand grip estimation [464]. Similarly, Spearman's rank correlation has been applied to examine the association between participants' personality traits and physiological responses under various emotional states using wearable devices such as an EEG headset (Emotiv Insight), a smartwatch (Huawei), and a smart tracker (Spire Stone) [55].

Similarity analysis: Similarity analysis evaluates how closely two datasets, patterns, or distributions resemble each other. Common techniques include cosine similarity and Euclidean distance. Cosine similarity measures the directional alignment between vectors, while Euclidean distance calculates the straight-line difference in multidimensional space. In human activity recognition, feature vectors from sensors are compared to predefined templates or clusters using cosine similarity for activity classification [494], whereas Euclidean distance can assess deviations in gait features from a standardized model to identify abnormalities, especially in older adults [21]. Common distribution comparison methods include the Kolmogorov–Smirnov (KS) test, Anderson–Darling test, chi-square test, Cramer–von Mises test, Earth Mover's Distance (EMD), and Jensen–Shannon Divergence (JSD). These techniques evaluate differences in distribution characteristics such as location, shape, and variability. For instance, the KS test examines the maximum difference in cumulative distribution functions, while Anderson–Darling gives more weight to tail behavior. The chi-square test analyzes binned frequencies, EMD quantifies the effort to morph one distribution into another, and JSD measures probabilistic similarity based on information theory. In wearable sensing, the KS test has been used to compare smart ring measurements to baseline values for hand grip estimation, where no significant difference ($p > 0.05$) indicates similar distributions [464]. The Cramer–von Mises test has been applied to evaluate how closely accelerometer data matches a reference distribution for human activity modeling [142], and the chi-square test has been used to assess the impact of demographic factors on COVID-19 symptoms using physiological signals [210]. In addition, cross-correlation is used to measure time-lagged similarity, such as estimating the time difference of arrival (TDoA) between acoustic signals for limb posture tracking with smartwatches [490], or analyzing predictive synchrony between physiological signals from presenters and their audiences [130].

Machine learning. While statistical and structural analysis provides foundational insights into data patterns and relationships, more advanced tasks such as classification, prediction, and anomaly detection often rely on machine learning techniques. In this section, we discuss four primary categories of machine learning: supervised, unsupervised, semi-supervised, and reinforcement learning (RL) [459]. Building on these, we also explore emerging paradigms such as hybrid learning and transfer learning.

Supervised learning: Supervised learning is the most widely used machine learning approach, where models are trained on labeled data to learn mappings between inputs and outputs by minimizing a cost function [80]. It is typically divided into classification, which predicts discrete categories such as hand gestures, and regression, which estimates continuous values like heart rate. A range of traditional algorithms has been applied in wearable systems, including support vector machines (SVM), decision trees (DT), k-nearest neighbors (k-NN), Naive Bayes (NB), logistic regression, linear regression, random forests (RF), gradient boosting (GB), and artificial neural networks (ANN) [80, 306, 132, 48, 20]. As these classical techniques have been extensively discussed in prior reviews, including their strengths and limitations, we do not cover them in further details.

As part of machine learning, deep learning has shown superior performance over classical approaches in handling large-scale and complex data through effective parameter tuning. Deep learning models use neural networks to learn mappings from input data to labeled outputs in wearable tasks such as image recognition, natural language processing, and time-series prediction. Common architectures include convolutional neural networks (CNNs), recurrent neural networks (RNNs) like long short-term memory (LSTM), fully connected networks (FCNs), and transformers. Unlike traditional methods that rely on manual feature extraction, deep learning models automatically learn hierarchical features from raw data. Training involves minimizing a loss function that quantifies the difference between predictions and ground truth, typically using optimization methods such as stochastic gradient descent. CNNs extract spatial features from grid-like data (e.g., images or multichannel sensor inputs) through convolutional and pooling layers. RNNs, including LSTMs and GRUs, model temporal dependencies in sequential data such as time series or speech. FCNs are suited for tasks with independent input features, while transformers apply self-attention mechanisms to model long-range dependencies without sequential processing. These models support a variety of wearable applications. For example, shallow CNNs with encoder-decoder structures have been used for human activity recognition (HAR) by enabling cross-channel communication and reducing redundancy in multiaxial sensor inputs [185]. CNNs have also been applied in emotion recognition tasks [484]. An ensemble of deep LSTM models, trained with random sampling and combined through score-level fusion, improves HAR performance in noisy and imbalanced datasets [150]. Additionally, transformer-based models with shared encoders have been proposed to capture both intra-modal and inter-modal correlations for effective multimodal fusion in

wearable systems [447].

Unsupervised learning: Unsupervised learning analyzes unlabeled data to uncover hidden patterns by mapping inputs to observations, which is especially useful when labeling is time-consuming or when datasets lack clear categories. Common techniques include clustering, dimensionality reduction, and association analysis [459]. Clustering groups similar data points using algorithms such as K-means, DBSCAN, and Gaussian Mixture Models (GMM). Dimensionality reduction methods like principal component analysis (PCA), singular value decomposition (SVD), t-distributed stochastic neighbor embedding (t-SNE), and linear discriminant analysis (LDA) reduce feature space while preserving essential information. Association techniques, such as the Apriori algorithm, identify relationships between variables by mining frequent item sets and generating association rules based on support and confidence. For example, in the healthcare domain, an enhanced Apriori algorithm (EAA) has been developed that incorporates context ontology to efficiently discover frequent patterns while reducing unnecessary candidate generation [395].

In deep learning, autoencoders (AEs) are commonly used for tasks such as dimensionality reduction, data denoising, and anomaly detection, with variations like sparse and denoising autoencoders. AEs are typically trained on normal data to learn compact representations and reconstruct input patterns; when presented with anomalous or unseen data, they often produce high reconstruction errors due to the absence of such patterns in training. For instance, a channel-wise ensemble of autoencoders has been proposed where each AE learns features from a specific sensor channel, and reconstruction errors are used to detect falls from normal data [215]. Another powerful deep learning framework is the Generative Adversarial Network (GAN), which consists of a generator that synthesizes data and a discriminator that distinguishes between real and generated instances. Through adversarial training, GANs can learn data distributions without labeled input and are applied in areas such as image generation, style transfer, anomaly detection, and data augmentation. For example, a hierarchical multimodal GAN has been proposed in wearable human activity recognition (WHAR), where individual generators capture features from specific sensor modalities, and a hierarchical discriminator ensures both modality-specific fidelity and global consistency. This approach addresses challenges related to limited labeled data and the complexity of multi-sensor fusion [70].

Semi-supervised learning: Semi-supervised learning bridges supervised and unsupervised approaches by using a small amount of labeled data alongside a large volume of unlabeled data to enhance model performance. Traditional methods include self-training (or pseudo-labeling) and graph-based models. In self-training, a model is initially trained on labeled data and then used to assign pseudo-labels to unlabeled samples. High-confidence pseudo-labeled instances are added to the labeled set for iterative retraining, which can gradually improve performance, though label noise can accumulate over iterations. Graph-based methods represent

data as a graph, where nodes correspond to data points and edges reflect similarity, allowing labels to propagate from labeled to unlabeled nodes through the graph structure. In wearable applications, a teacher-student self-training approach has been used to transfer knowledge from both labeled and unlabeled data for human activity recognition, with added data augmentation [406]. Similarly, graph-based analysis on smartwatch data has been applied to monitor symptoms of multiple sclerosis by modeling daily activities and symptom severity as interconnected nodes [155].

Consistency regularization in semi-supervised learning is based on the assumption that small perturbations to input data should not alter the model's predictions. Popular techniques such as MixMatch and FixMatch apply data augmentations, including noise, shifting, cropping, and flipping—to unlabeled data, encouraging the model to produce consistent outputs for both the original and transformed versions. MixMatch generates pseudo-labels for unlabeled data, applies augmentations, and blends labeled and pseudo-labeled data to optimize a consistent loss during training. FixMatch first applies weak augmentation (e.g., flipping or cropping) to create confident pseudo-labels using a threshold, then trains the model with strong augmentations (e.g., RandAugment) to align predictions with those pseudo-labels. This sequential process improves label reliability while increasing robustness to variations. These approaches have been effectively applied in wearable scenarios, such as stress detection using wrist-worn and chest devices with multimodal data like skin conductance, temperature, accelerometer, and ECG signals [468]. Additionally, tri-training uses three classifiers that iteratively update one another based on consensus from the other two, allowing reliable expansion of the labeled set with high-confidence pseudo-labels and improving performance in wearable HAR tasks [482].

Self-supervised learning (SSL) trains on unlabeled data using pretext tasks to learn useful representations, often serving as a pretraining step in semi-supervised learning. These representations are later fine-tuned with a small labeled dataset for downstream prediction tasks. For example, an SSL framework pre-trained on large-scale wearable data (e.g., EDA, BVP, and temperature) learned generalized representations to address overfitting on small physiological datasets, which were later fine-tuned for motion recognition [447]. Common SSL techniques include contrastive learning, masked prediction (e.g., MAE), and generative methods (e.g., variational autoencoders, VAEs). Contrastive learning distinguishes between similar and dissimilar samples using a contrastive loss, while masked prediction recovers masked input elements. Generative approaches aim to reconstruct input data, often capturing robust latent features. In wearable sensing, a domain-invariant contrastive learning method refines negative sampling and integrates temporal information to improve generalization in HAR and gesture recognition across different environments and devices [89]. A spatial-temporal masked autoencoder (MAE) improves HAR performance from multi-device data, particularly under missing device scenarios, by masking spatial and temporal segments using an asymmetric

encoder-decoder architecture [294]. Additionally, VAEs learn a probabilistic latent space to model biomedical signal morphology and effectively separate clean from noisy signals [312].

Reinforcement learning: Reinforcement learning (RL) trains agents to interact with an environment by maximizing cumulative rewards through trial and error. The agent takes actions and receives feedback in the form of rewards or penalties, gradually improving its policy or strategy. Common approaches include value-based RL (e.g., Q-Learning), policy-based RL, and model-based RL (e.g., AlphaGo) [459]. Value-based methods estimate the value of states or state-action pairs to find optimal strategies, while policy-based methods directly optimize the policy without relying on value estimation. Model-based approaches build an internal model of the environment to predict outcomes and guide decision-making. However, RL is rarely used in wearable computing due to practical challenges such as the absence of clear reward signals, difficulty in simulating real-time interactions, and the high data and computational demands, which are unsuitable for resource-constrained devices. Nonetheless, it has shown promise in control-oriented applications. For instance, Q-learning has been used to optimize communication between on-body sensors for reliable and energy-efficient data transmission [18], and flexible policy iteration (FPI) has been applied to wearable robotic knees, incorporating experience replay and prior knowledge to improve learning with limited data [126].

Hybrid learning: Hybrid learning models integrate multiple architectures to utilize the strengths of different techniques and improve performance. For example, combining convolutional neural networks (CNNs) for spatial data (e.g., joint angles) with recurrent neural networks (RNNs) for temporal sequences (e.g., finger movements) enables accurate 3D finger motion tracking [491]. In the context of human activity recognition (HAR), various hybrid approaches such as adjusted CNN-LSTM and deep learning–symbolic models have been explored to address complex sensing challenges effectively [345]. Hybrid models have also been applied in health monitoring, including a deep CNN-based framework for lung cancer diagnosis [114].

Transfer learning: Transfer learning addresses the challenge of reduced model accuracy across different contexts such as varying users, locations, or time periods, by leveraging shared patterns between them. It improves efficiency by adapting a pre-trained model to a new task using only a small amount of new data, typically through fine-tuning [440]. In wearable computing, transfer learning is widely applied to handle user variability. For example, gesture recognition models trained on one user often struggle with generalization due to differences in hand anatomy and gesture styles; transfer learning mitigates this without requiring extensive retraining [30, 85]. It is also used in personalized federated learning, where a global model trained on public data is fine-tuned locally on private user data for tasks such as activity recognition and Parkinson's disease diagnosis [74]. In other health applications, transfer learning generalizes features from pooled EEG data

to detect epileptic seizures in unseen patients and environments [320], and adapts a deep recurrent neural network trained on a large ECG dataset to classify sleep stages from a smaller PPG dataset [340].

Evaluation metrics. Evaluation metrics in machine learning assess model performance based on the specific task, with classification and regression being the most commonly used in wearable computing. For classification, commonly used metrics include accuracy, precision, recall, F1-score, sensitivity, specificity, true positive rate (TPR), false positive rate (FPR), and error rate. All these metrics can be calculated from the confusion metrics. Additionally, ROC-AUC evaluates the trade-off between TPR and FPR across different thresholds, with higher AUC values indicating better overall classification performance for binary classification. As these metrics are widely used and well-documented, we do not elaborate further here [20, 179]. For regression tasks, metrics such as mean absolute error (MAE), mean squared error (MSE), root mean squared error (RMSE), mean bias error (MBE), mean relative error (MRE), mean absolute percentage error (MAPE), and R-squared (R^2) are commonly applied. These metrics have also been thoroughly analyzed in prior works, with clear discussions on their strengths and limitations [80, 51].

A.6.6. End-user usage and perception

The final step of the wearable sensing pipeline involves presenting model outputs to users, with the smartphone serving as the main interface. Depending on the task, outputs may be classification results (such as activity type, stress level, or health status) or regression values (such as heart rate, temperature, or motion intensity). These insights are typically delivered through smartphone applications that visualize trends, provide alerts, or offer personalized feedback. Graphs, color-coded indicators, and summaries make the information easy to understand and act upon. While wearables like smartwatches may display basic results for quick access, the smartphone app typically handles detailed feedback, interaction history, and configuration settings. Web applications can also be used for broader access and cross-platform usability, although smartphones remain the primary means for real-time interaction. This centralized delivery approach supports real-time awareness, long-term tracking, and user engagement by translating sensor data into meaningful, context-aware information.

A.7. Wearable smart ring: emerging applications and challenges

Building on the understanding of general wearable usage, sensor configurations, and system pipelines, this section focuses on smart rings, an increasingly popular form factor known for their compact size and discreet design. Compared to other wearables, smart rings offer unique opportunities for continuous sensing and natural

hand-based interaction. We explore their emergence, hand-driven interfaces, new application areas, and key challenges in design and development.

A.7.1. Smart ring wearable emergence

Table 27 highlights the comparative strengths and limitations of widely used wearable devices, each designed to meet specific application needs. Among them, smart rings have emerged as a particularly promising category due to their unique combination of low obtrusiveness, very small form factor, and long battery life. Unlike bulkier devices such as smartwatches, smart glasses, or gloves, smart rings offer a discreet and seamless user experience, making them exceptionally well-suited for continuous activity and biometric monitoring in both daily and research contexts.

Smart glasses excel in augmented reality and real-time information overlay, but they are hindered by high power consumption, short usage time, and privacy concerns. Smart earphones and watches provide health tracking and rich user interaction features but often suffer from comfort issues in the long term, or the need for frequent recharging [58, 198]. Wristbands, while lightweight and power-efficient, offer limited sensing and computational capabilities similar to smart rings, but tend to be bulkier and less discreet for continuous wear. Smart gloves offer precise motion capture and haptic feedback for VR applications and rehabilitation studies but are too bulky for daily use. Smart textiles and patches provide unobtrusive physiological monitoring, especially in medical applications, but face issues with durability, cost, and usage lifespan. Smart shoes (e.g., socks and insoles) support posture correction and gait analysis but may not be comfortable or broadly applicable for long-term or casual use.

In contrast, smart rings provide a highly wearable, culturally acceptable, and ergonomically natural solution for long-term use [443]. Their very low energy consumption and long usage time allow for continuous data collection without user interruption. Positioned on the finger, a site rich in nerve endings and blood vessels, smart rings are ideally suited for capturing physiological signals such as heart rate, blood oxygen levels, or even blood vessel imaging. Despite their small size and limited onboard computing power, smart rings can integrate with external processing systems like smartphones, edge devices, or cloud platforms to support advanced applications. Smart rings also support intuitive interaction and secure, low-friction authentication for everyday use across health, fitness, and security domains. Recent advancements in sensor miniaturization, wireless connectivity, and energy-efficient design have expanded the potential of smart rings far beyond simple gesture control. Today, they represent a powerful, minimally invasive alternative to more obtrusive wearables, combining practicality with technical sophistication.

Table 27: Comparison of common wearables: advantages and disadvanges. Number means body parts. Energy consumption/ Computing power: *High* means intensive processing needs. Usage time: *Long* means suitability for all-day monitoring. Obtrusiveness: *High* means a greater level of user disturbance or visibility.

Wearables	Energy Consumption	Computing Power	Usage Time	Size	Obtrusiveness	Advantages	Disadvantages
Glasses[1]	High	High	Short	Medium	Medium	Hands-free interaction, real-time overlay, AR support	Privacy concerns, short battery life, high cost
Earphones[1]	Low to Moderate	Low	Medium	Small	Low	biometric sensing, continuous health tracking	Limited by small form factor, discomfort over long use
Watches[4]	Moderate	Moderate	Medium	Small	Medium	Multi-functionality, fitness tracking, strong research support	Frequent charging, may be bulky for some users
Wristbands[4]	Low	Low	Long	Small	Low	Lightweight, long battery life, cost-effective	Limited sensing capabilities, may be bulky for some users
Gloves[4]	High	High	Short	Large	High	Precise motion capture, useful for hand-based research	Bulky, restrictive for daily wear
Shoes (Socks/Insoles)[5]	Moderate	Low to Moderate	Medium	Small to Medium	Low	Gait analysis, posture correction, activity monitoring	Limited use cases, may not be comfortable for all users
Textiles[6]	Low to Moderate	Low	Long	Variable	Very Low	Comfortable, washable, unobtrusive	Expensive, durability concerns
Patches[6]	Low to Moderate	Low	Short to Medium	Small	Very Low	Non-intrusive, high accuracy, ideal for medical applications	Disposable or short lifespan, can be costly
Rings[4]	Very Low	Low	Long	Very Small	Very Low	Discreet, long battery life	Small size limits sensor capabilities

A.7.2. Hand-driven interfaces for smart rings

The human hand is an inherently expressive and information-rich medium, combining dexterity, sensory richness, and mobility in a compact form [434]. With its high degree of motor control, tactile sensitivity, and complex anatomical structure, the hand serves as a natural and versatile interface for wearable computing. It supports a wide spectrum of inputs from subtle gestures to intricate movements for intuitive and expressive interaction. Furthermore, its dense network of nerve endings, blood vessels, and musculature makes the hand a valuable site not only for interaction but also for capturing rich physiological and behavioral data [419, 492].

In this context, smart rings, worn on the finger, are uniquely positioned to harness the hand's full potential with minimal intrusiveness. Compared to wrist-worn or head-mounted wearables, smart rings capture input directly at the source of action, allowing fine-grained gesture recognition, continuous biometric sensing, and seamless integration into everyday hand movements. They maintain constant contact with the finger phalanges while remaining socially acceptable and comfortable for all-day wear. Their proximity to tendons, skin, and blood vessels allows for passive detection of physiological signals, while also supporting rich interaction techniques such as tapping, swiping, rotating, and mid-air gestures. Recent work has demonstrated how smart rings facilitate various input methods such as tap, swipe, on-skin, mid-air, and around-device interactions, which are low-effort and well-suited to mobile or ambient contexts where traditional devices like mice or keyboards are impractical [419]. Gesture inputs mapped to natural hand movements (e.g., thumb-to-index tap to confirm, finger rotation to scroll) enhance both usability and learnability.

Figure 64 illustrates hand-driven interfaces for smart rings. A smart ring typically consists of four key components: sensing, battery, communication, and microcontroller (MCU). The sensing module integrates various sensors, such as PPG and IMU, tailored for specific tasks [492]. The battery powers the device and requires efficient energy management to maximize usage time in the compact form. Communication is achieved through wireless technologies like Bluetooth Low Energy (BLE) for data transfer between the smart ring and other devices, such as smartphones. The microcontroller (MCU) serves as the central unit, managing data processing, power consumption, and device control, ensuring optimal performance with minimal energy usage. In cases where processing power and battery life are limited, the MCU can offload data processing to external devices like smartphones. Smart rings can be worn on different fingers, although most research has focused on the index finger, with the little finger being less explored [434]. The hand's dual role in active interaction and passive sensing enhances the value of smart rings, offering greater flexibility in sensor data repurposing. This allows data from a single sensor to support diverse applications through strategic sampling and adaptive design. Moreover, their active interaction capabilities allow them to replace conventional input devices in contexts requiring subtle and hands-free control. Simultaneously,

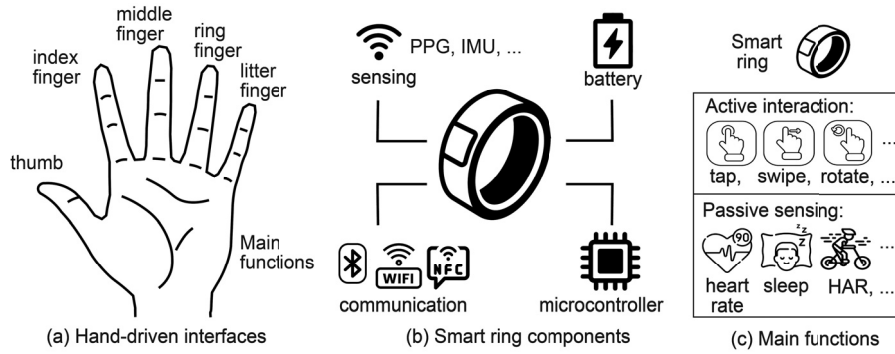


Figure 64: Hand-driven interfaces for smart rings. two main functions: active interaction and passive sensing

they support passive sensing by continuously monitoring physiological indicators such as heart rate, blood oxygen saturation, and body impedance, as well as contextual signals like activity levels (HAR) and environmental conditions. This seamless integration of interaction and sensing underscores the versatility of smart rings for both real-time control and unobtrusive wellness tracking. The synergy between hand-based expressiveness and ring-based computing ultimately paves the way for the next generation of compact, context-aware, and user-centric wearable experiences.

A.7.3. New emerging applications with smart rings

Beyond their compact design, smart rings offer unique opportunities for sensor data repurposing. By leveraging hand and finger movements, gestures, and specific positions, sensor data can be adapted to support a wide range of applications. This section explores these emerging applications.

Sleep monitoring: The presence of capillaries and rich blood flow in the fingers, allow smart rings to continuously collect physiological signals such as heart rate variability (HRV), peripheral skin temperature, blood oxygen saturation (SpO_2), and movement patterns for assessing sleep stages and quality [443]. Smart rings are minimally obtrusive and can remain comfortably worn throughout the night. Many modern smart rings like Oura Ring integrate advanced algorithms to estimate sleep onset, duration, REM cycles, and recovery trends, delivering personalized insights into sleep health. Their passive sensing capabilities and long battery life make them suitable for long-term sleep tracking at home, supporting both consumer wellness and clinical research in sleep medicine.

Mental stress and emotion recognition: Smart rings can offer continuous insight into a user's stress levels and emotional fluctuations by capturing physiological signals such as heart rate variability (HRV), electrodermal activity EDA, peripheral temperature, and subtle changes in skin tone or pulse amplitude [276]. These indicators can be processed using on-device algorithms or edge/cloud computing to detect signs of sympathetic nervous system activation, a physiological marker of

stress. Smart rings maintain tighter and more stable skin contact on the finger than wrist-worn devices, which improves signal quality and reduces motion artifacts. Their discreet design allows comfortable use without drawing attention in various settings such as professional, social, and high-stress environments, making smart rings useful for mental health awareness, stress management, and emotion-aware computing.

Hand-grip strength: Hand-grip strength is a key indicator of physical and cognitive health, widely used for early frailty detection and rehabilitation monitoring [464]. Despite its clinical significance, conventional assessment tools like handheld dynamometers are often bulky, require supervision, and are unsuitable for continuous or everyday use. To address this limitation, smart rings can estimate grip strength unobtrusively during natural, daily interactions such as squeezing a plastic cup or household items. By incorporating advanced sensing techniques, smart rings can detect subtle variations in finger pressure, skin deformation, and joint movement to infer grip intensity without requiring dedicated user effort or equipment. This passive and always-worn form of monitoring enables continuous strength assessment in both clinical and everyday contexts for rehabilitation tracking and muscular fatigue monitoring.

Drink spiking: Drink spiking is an increasing public safety concern in nightlife and social environments, where individuals may unknowingly consume beverages contaminated with sedatives or illicit substances [466]. Traditional methods for detecting such tampering are limited, often requiring external tools or active testing, which may not be discreet or readily available. In response, smart rings are being explored as subtle, always-worn tools for passive drink spiking detection. By repurposing or developing new sensing modalities, these rings can assess changes in a liquid's composition when in contact with a beverage, identifying abnormal chemical signatures or the presence of common spiking agents. This supports natural and unobtrusive interactions for real-time safety checks, such as simply touching a container with the ring. Smart ring–based solutions require no specialized materials like external testing kits and function passively during daily use. This offers a scalable and socially acceptable method to enhance personal security in public spaces.

Food quality estimation: Food spoilage and waste are critical global challenges, impacting environmental sustainability, food security, and consumer health [93]. Accurate and accessible methods for assessing food quality can reduce unnecessary waste and promote informed decision-making. In this context, smart rings are increasingly being explored as compact tools for evaluating food freshness through thermal, tactile, or chemical sensing during natural interactions with food items. Smart rings can capture subtle temperature variations caused by heat transfer, surface moisture, or pressure distribution when users touch or hold fresh produce or packaged goods. These interactions can reveal indicators of spoilage, ripeness, or contamination such as unexpected cold spots, texture inconsistencies, or degraded

surface properties. When combined with machine learning, data from smart rings can estimate freshness or classify food quality in real time. This supports waste reduction, informed consumer choices, and greater accessibility for visually impaired individuals. Compared to larger handheld scanners or specialized tools, smart rings offer a hands-free and discreet solution for food inspection in everyday settings, particularly within retail environments.

Activity recognition and motion tracking: Smart rings are increasingly recognized for fine-grained activity recognition and motion tracking, particularly in tasks involving the fingers and hands [419]. Compared to wrist-worn devices that capture broad arm or wrist movements, smart rings provide higher spatial resolution for detecting fine finger gestures like tapping, swiping, or pinching. This supports applications like handwriting recognition, sign language interpretation, and monitoring of hand-based rehabilitation exercises. Although smart gloves also offer high precision, smart rings provide a lightweight and unobtrusive alternative that maintains natural hand dexterity. Their small form factor, combined with embedded motion sensors and gesture recognition algorithms, supports continuous and seamless motion capture in everyday contexts.

Secure authentication and identity-based applications: With their proximity to the hand and support for intuitive gestures, smart rings are emerging as seamless tools for secure access, authentication, and identity-driven interactions [196]. They can perform continuous, passive, or gesture-based authentication that is less intrusive and more resistant to spoofing than traditional PIN codes or biometric scans such as face and fingerprints. Equipped with sensors, touch interfaces, and wireless protocols like NFC and Bluetooth, smart rings can unlock smartphones, laptops, smart locks, or vehicles with simple hand gestures or advanced biometric inputs. They also support contactless payment and access control by linking to digital wallets and identification credentials, allowing users to make purchases, board transit, or open doors with minimal effort. This dual functionality (secure authentication and transaction) makes smart rings a practical and hygienic alternative to smartphones and cards, reducing contact with shared surfaces and lowering the risk of loss or theft. As digital identity becomes more integrated into daily routines, smart rings are well-positioned as wearable tokens for seamless and secure interaction.

Ubiquitous and gesture-based interaction: In ubiquitous computing environments, smart rings provide a discreet, low-effort way to interact with digital systems through gestures such as swipes, finger rotations, and thumb-to-finger taps. These interactions are especially useful when touchscreens or voice commands are impractical such as during presentations, commuting, or hands-busy tasks. Smart rings can function as wearable controllers for smartphones, smart home devices, AR/VR platforms, and even robotic systems like delivery drones. Their support for context-aware, low-latency, and private interactions makes them a strong fit for advanced ubiquitous interfaces. Smart ring can provide activation via gesture

identification or bio-sensing indicators from humans, like temperature [480].

Environmental awareness and alerts: Environmental factors such as extreme heat, poor air quality, and UV exposure can greatly impact health and well-being, particularly for vulnerable populations and high-risk environments. As real-time awareness of these conditions grows in importance, smart rings are emerging as discreet and practical tools for continuous environmental monitoring [373]. By integrating sensors for temperature, humidity, light, and air quality, smart rings can track a user's immediate surroundings throughout the day. This supports applications like heat-stress prevention, UV overexposure alerts, and indoor comfort monitoring. For example, workers in outdoor or industrial settings may receive vibrations or app notifications when environmental thresholds are exceeded, such as high heat indicating dehydration risk or nighttime light exposure affecting sleep. Smart rings offer a more elegant, body-worn alternative to larger or clip-on devices, supporting continuous tracking without disrupting daily routines.

Assistance and accessibility: Assistive technologies support independence for individuals with disabilities, and smart rings are emerging as inclusive and socially acceptable tools in accessibility-focused design. Their ability to detect fine finger movements supports alternative input methods for users with limited mobility or speech impairments. For example, smart rings could track gestures to translate sign language into speech, facilitating communication between deaf and hearing individuals. When integrated with voice assistants, smart home systems, or wearable displays, they can offer intuitive environmental control, hands-free communication, and personalized assistance. Bulkier or stigmatizing devices can hinder everyday use, whereas smart rings offer a culturally familiar form factor. This blend of functionality and subtle design makes them a compelling interface for inclusive interaction and ambient assistive computing.

Productivity and focus monitoring: Smart rings are being used to support personal productivity and cognitive performance by tracking indicators such as focus, fatigue, and work patterns. Through continuous monitoring of heart rate variability, movement, and skin temperature, they can infer cognitive states like alertness or distraction. These insights are valuable for knowledge workers, students, and others engaged in high-focus tasks. While many tools rely on manual input or screen-time tracking, smart rings offer passive and objective sensing with context-aware feedback. Some systems provide real-time nudges or session summaries to promote healthier work habits, better sleep, and overall digital well-being, highlighting a growing role for wearables in both health and performance enhancement.

Mixed reality in metaverse: As mixed reality MR grows within the Metaverse, smart rings are emerging as compact interfaces that support natural gestures and precise hand tracking for intuitive and low-latency interaction. Smart rings can detect fine-grained interactions like swipes, taps, and 3D hand movements, enabling users to manipulate virtual objects and navigate spatial interfaces without bulky controllers. When paired with AR/VR headsets or smart glasses, they create seam-

less cross-device experiences by bridging physical gestures and digital responses. Their support for multimodal interaction, combining motion sensing with tactile or haptic feedback, positions smart rings as key tools for embodied interaction in the Metaverse.

Habit formation and behavior nudging: To support habit formation and deliver subtle behavioral nudges, smart rings provide real-time feedback without disrupting the user's environment. Using physiological and contextual sensing such as activity level, movement patterns, or time-of-day routines, smart rings can detect behavior gaps and prompt timely actions. For instance, gentle vibrations or thermal pulses can serve as subtle reminders to drink water, monitoring smoking patterns, stand after prolonged sitting, take medication, or engage in breathing exercises during stressful moments. While smartphone apps or other wearable alarms may be obtrusive or easily dismissed, smart rings offer ambient, personalized feedback that integrates naturally into daily routines. This seamless interaction supports self-regulation and encourages long-term behavior change in areas such as wellness, productivity, and mindfulness.

A.7.4. Challenges for smart ring design and development

While new applications continue to expand the potential of smart rings across various domains, their practical adoption still faces several challenges, which should be addressed to support reliable performance, user acceptance, and long-term scalability.

Sensor data re-purposing: Current smart ring systems like the Oura Ring and OmniRing typically follow a one-to-one mapping between sensor types and specific applications, such as using PPG sensors for heart rate and sleep monitoring, IMUs for activity tracking, and wireless sensing for communication. While effective, this approach limits the versatility of onboard sensors, especially given the tight space and power constraints of smart rings. Recent studies have explored repurposing sensors to extract additional insights for broader applications, for example, using optical sensors to estimate hand grip strength or wireless signals to identify beverages [464, 250]. However, utilizing sensor data for secondary or more functions introduces challenges such as signal ambiguity, increased noise, and interference with the primary sensing task. A key challenge, therefore, lies in extending sensor functionality without adding hardware complexity. Addressing this may require context-aware modeling or multi-task learning techniques that can distinguish between concurrent sensing objectives. Successfully repurposing sensor data not only improves system efficiency but also opens new application areas in behavioral sensing, object interaction, and daily activity analysis.

Design constraints: Recent progress in smart ring platforms has demonstrated the feasibility of integrating components such as IMUs, PPG sensors, batteries, and Bluetooth modules onto compact, flexible circuit boards suitable for long-term wear [492]. However, the small and curved structure of the ring significantly

limits internal volume, surface area, and component arrangement. These constraints make it difficult to incorporate more advanced sensing technologies or higher-performance processors, such as multi-modal biosensors or haptic feedback systems. In addition, limited battery capacity restricts energy available for sensing and on-ring computation, while daily exposure to mechanical stress, moisture, and dust poses challenges to durability and signal reliability. A key challenge, therefore, is to integrate more capable and diverse sensing elements within the constrained physical and thermal budget of a finger-worn device. Progress in materials science and electronics fabrication may offer viable solutions. For instance, stretchable or layered circuit designs could optimize space usage without increasing bulk. Furthermore, advances in sensor miniaturization and ultra-low-power electronics may support more advanced sensing functions without exceeding energy limits.

Interaction limitations: Due to the limited space for touchscreens, displays, or physical buttons, smart rings currently support only simple input methods for device interaction and control, such as tapping, swiping, and rotational gestures. These gestures typically rely on discrete and predefined motion patterns that are easy to detect using embedded sensors like inertial measurement units (IMUs) or capacitive touch surfaces. Feedback is generally limited to haptic vibrations, offering subtle confirmation of user input without requiring visual or auditory output. However, this interaction pattern remains mostly static and restricted to short, intentional gestures. It lacks the flexibility needed for more sophisticated or high-speed input tasks, such as text entry, real-time navigation in AR environments, or precise control in gaming or smart home systems. Gesture recognition accuracy can also degrade in dynamic conditions, such as during walking or multitasking, due to interference from finger orientation, hand movement, or ambient noise. Additionally, the absence of visual or audio feedback reduces user awareness and responsiveness in real-world settings. The key challenge, therefore, is to advance gesture recognition algorithms toward dynamic, context-aware interaction that adapts to movement and environment. The integration with external systems such as smartphones and other wearables could also improve contextual awareness, where the ring serves as a lightweight control interface within a larger ecosystem.

Data collection challenges: The small size of smart rings limits space for sensors, batteries, and memory, restricting both the quality and quantity of data that can be collected over time. As a result, smart rings often offload raw data to companion smartphones or external servers, which introduces issues such as synchronization errors, and reliance on stable wireless connectivity. Continuous sensing further strains energy and sensor resources, as miniature batteries cannot sustain high-frequency sampling, reducing data granularity and resolution. Signal quality is also affected by user-related factors such as movement artifacts and hand orientation. Moreover, individual differences in finger size, skin tone, muscle tension, and interaction pressure lead to divergent sensor readings, even during identical activities or gestures. These variations complicate the goal of maintaining uniform sensing

conditions across diverse users and real-world contexts. The key challenge, therefore, lies in collecting consistent, high-quality data despite the physical, energy, and user variability constraints of smart rings. This suggests developing adaptive sampling or event-triggered sensing strategies to preserve signal fidelity, along with personalized calibration or user-specific tuning to account for anatomical and behavioral differences.

Data processing and computing power: The processing capability of smart rings is severely limited by constrained energy resources and minimal hardware space. They cannot accommodate high-performance processors or large memory units and instead rely on low-power microcontrollers suitable only for basic signal processing. This restricts the execution of adaptive or context-aware computing tasks such as real-time classification, sensor fusion, or dynamic feature extraction. While offloading computation to external devices can partially address these gaps, it compromises autonomy and introduces delays that may not suit scenarios requiring immediate, on-ring decision-making or continuous offline operation. The key challenge, therefore, lies in supporting meaningful computation directly on the ring without dependence on external devices. Innovations of energy-efficient algorithms and ultra-compact model architectures could be tailored to embedded processors. Another potential is to explore task-specific hardware acceleration and algorithm-architecture co-design, such as application-specific integrated circuits (ASICs), to support selective local processing of critical tasks.

Energy harvesting and power management: Although low-power sensors and microcontrollers have advanced many real-time applications such as health monitoring, fall detection, and gesture recognition, they still generate intermittent spikes in energy demand for smart rings. Sustaining continuous operation without frequent recharging limits long-term usability, particularly in scenarios where users expect seamless and hands-free functionality over extended periods, such as daily health tracking. To extend battery life, dynamic power management strategies, such as sleep modes, voltage scaling, and event-driven activation, are commonly applied to reduce energy consumption during idle periods. In parallel, energy harvesting (EH) technologies are gaining attention as a means to supplement battery power and reduce reliance on frequent charging. Methods such as kinetic, solar, and thermoelectric harvesting particularly from body heat, offer supplementary energy without increasing device size or weight [374]. However, the core challenge lies in meeting variable energy demands using sources that are inherently limited, unstable, and dependent on environmental or physiological factors. Harvested energy typically delivers low output and cannot reliably support peak sensing or processing loads. Moreover, integrating energy harvesting components within the compact ring enclosure adds complexity to the hardware design and may compromise overall performance. Thus, it is important to improve the efficiency of energy harvesting systems through better materials, miniaturized converters, and multi-source integration to smooth power input. Adaptive workload management can

also be applied, where computational tasks and sensing activities are dynamically scheduled based on real-time energy availability.

User acceptance and perception: User acceptance of smart rings is shaped by factors such as comfort, aesthetics, ease of use, perceived intrusiveness, and cost. While smart rings offer advantages such as compact form, discretion, and alignment with familiar jewelry formats, current designs tend to address only a subset of these factors in isolation. For example, some works focus on improving comfort through lighter and more flexible materials, while others emphasize affordability by minimizing hardware features. However, discomfort from prolonged wear, such as tightness, skin irritation, or heat buildup, remains a common issue, particularly for users with sensitive skin or varying finger sizes. A one-size-fits-all approach rarely accommodates these differences, and daily mechanical stress from handwashing or gripping can further degrade comfort and durability. In parallel, social and cultural considerations such as appearance, context of use, and visibility are often overlooked, affecting how smart rings are perceived in public or professional settings. Cost also remains a barrier when advanced sensing capabilities require expensive components. Therefore, a key challenge lies in designing smart rings that holistically address physical, social, and contextual factors to support broader user acceptance without compromising core functionality or robustness. Failure to address these aspects can limit adoption, especially in populations that require special consideration, such as the elderly or individuals with disabilities. This suggests users early in the design process through participatory methods that reflect diverse preferences, cultural norms, and accessibility requirements.

Privacy and security: Smart rings, like other wearable technologies, collect highly sensitive personal data. Their discreet form and constant contact with the body make them effective for continuous monitoring, but also raise concerns about user awareness, data transparency, and informed consent. While advanced biometric authentication methods have been explored, current implementations are often inconsistent across devices and depend heavily on external platforms such as smartphones or cloud services. Many users remain unaware of what data is being collected, how it is processed, or who has access, particularly in public or shared environments. The key challenge, therefore, is to protect user privacy and data integrity throughout the sensing, transmission, and storage pipeline, without compromising usability or device performance. To address the issue, lightweight and context-aware encryption protocols could be implemented for securing data transmission between the smart ring and connected devices. These protocols should be optimized for low-power environments while preserving confidentiality. On the policy side, clear data governance frameworks and privacy regulations are needed to guide the use of smart rings in public or sensitive spaces. Manufacturers can also integrate visible indicators, such as visual and haptic alerts, to notify users when sensitive sensing is active. Finally, user education and social norms around acceptable wearable use are essential to support responsible adoption.

A.8. Conclusion

In conclusion, this survey has examined the landscape of wearable technologies, tracing their evolution across diverse device types, body placements, and application domains. By analyzing the wearable sensing pipeline and the integration of wearables with smartphones, we established a foundation for understanding how data is collected, processed, and applied in real-world contexts. Building on this, we highlighted the emerging role of smart rings, showcasing their ability to match and in some cases surpass the capabilities of traditional wearables through their discreet design, constant skin contact, and finger-based sensing. We explored unique applications made possible by smart rings, such as seamless authentication, gesture-based interaction, and fine-grained biometric monitoring. Finally, we identified key technical challenges in areas like power efficiency, privacy, modularity, and real-time analytics. Together, these insights position smart rings as a promising frontier in wearable computing, with the potential to shape more intelligent, responsive, and user-friendly systems in the years ahead.

ACKNOWLEDGEMENTS

I would like to express my sincere gratitude to my supervisor, Associate Prof. Huber Flores, for his continuous guidance, support, and encouragement throughout my doctoral studies. His insightful advice, thoughtful feedback, and dedication to research have been invaluable in shaping this thesis and my growth as a researcher. I have greatly benefited from his disciplined approach to academia, his sharp academic taste, and his high standards for scholarly rigor. His pursuit of excellence has pushed me to improve the quality of my work, which contributed to having my research published at top-tier conferences ultimately. I am truly fortunate to have learned under his mentorship.

I am also deeply thankful to Prof. Petteri Nurmi, with whom I closely collaborated throughout my doctoral journey. His attention to structure and clarity significantly influenced my academic writing. I also thank Dr. Thi Ngoc Nguyen and Dr. Agustin Zuniga from the same research group at the University of Helsinki for their valuable insights and collaborative support. I am especially grateful for the opportunity to visit Helsinki, where I was inspired by the academic atmosphere of a world-class institution. In addition, I would like to thank Assistant Prof. Marko Radeta for his constructive feedback and collaborative spirit, which helped address several key challenges in my research.

I extend my sincere thanks to all the reviewers and opponents for their valuable comments that helped me improve my dissertation: Prof. Marlon Dumas, Associate Prof. Marco Zuñiga, and Prof. Stephan Sigg. My thanks also go to my labmates from the Distributed and Pervasive Systems Group: Dr. Mohan Liyanage, Farooq Ayoub Dar, Abdul-Rasheed Ottun, Mayowa Olapade, Akintola Adeyinka, Kevin Post, and Reo Kuchida. I am deeply grateful for their encouragement, friendship, and support over the years. Their presence made this journey both academically enriching and personally meaningful.

I would also like to thank the University of Tartu and all its academic staff, especially those from the Institute of Computer Science, for providing an excellent academic environment and continuous support throughout my doctoral studies. I am sincerely grateful for the financial support that allowed me to participate in academic conferences, which helped broaden the reach of my research within the scholarly community.

Finally, I thank my friends for their companionship and encouragement, and my parents for their unwavering love, patience, and support. Their belief in me has been a constant source of strength throughout this journey.

This research has been financed by European Social Fund via “ICT programme” measure and by the Estonian Research Council grant (PRG 2725).

All content in the thesis is original, and generative AI tools were used solely to help polish the text for improved readability.

SISUKOKKUVÕTE

Arvutused ja andurite integreerimine nutisõrmustesse

Lausandmetöötluse eesmärgiks on arvutusvõimekuse sujuv põimimine igapäevakeskkondadesse, võimaldades pidevaid ja kohanduvaid teenuseid, mis arvestavad kasutaja olukorda ja asukohta. Selle visiooni saavutamiseks toob lausandmetöötlus kantavate seadmete kaudu andurtehnoloogiad ja andmete analüüsi kasutaja kehale lähemale. Kantavate seadmete hulgas on nutisõrmused esile kerkinud paljutõotava platvormina tänu kompaktsele ja diskreetsele kujule, pidevale kontaktile nahaga kui mõõtepinnaga ja arenevatele andurtehnoloogiatele. Doktoritöö uurib kuidas käelisi igapäevatoimingud saab nutisõrmuste abil ära kasutada mitmes valdkonnas, keskendudes tervishoiule, isikuohutuse tagamisele ja keskkonna jätkusuutlikusele.

Lähtudes vajadusest kasutada igapäevaelus eeskätt mittehäirivaid ja märkamatuid andurtehnoloogiaid, uurime kuidas nutisõrmustega ära kasutada tavapäraseid käeliigutusi (nagu pigistamine, haaramine ja puudutamine) eri füsioloogiliste näitajate, olukorrateabe ja keskkonnaandmete tuvastamiseks. Kuna tänapäevaste nutisõrmuste võimekus piirdub üksnes põhifunktsioonidega, on antud väitekirja keskseks uurimisküsimuseks: *Kuidas kohandada praeguste nutisõrmuste piiratud võimalusi, et need sobiksid eri rakendusteks?* Selle uurimiseks käsitletakse kahte peamist väljakutset: andurite disaini ja paigutust ning anduriandmete rakendamist uuel otstarbel. Sellele küsimusele vastamisel esitame kolm anduripõhist süsteemi, millest igaüks käsitleb erinevaid tehnilisi väljakutseid ja rakendusvaldkondi.

HIPPO võimaldab mõõta käte pigistusjõudu igapäevaste tegevuste käigus. Süsteem kasutab nutisõrmusesse integreeritud optilist andurit, mis tuvastab ja analüüsib eseme (näiteks plasttopsi) pigistamisel tekkivaid pinddeformatsioone, võimaldades pigistusjõu määramist kuni 86%-se täpsusega, olles võrreldav kliiniliste seadmetega. SpikEy näitab nutisõrmuste potentsiaali diskreetse isikliku turvalisuse vahendina. Süsteem aitab kaitsa kasutajat sotsiaalsetes olukordades, tuvastades uimastavate ainete olemasolu joogis. Kui kasutaja hoiab käes jooki, analüüsib SpikEy valguse peegeldumist vedelikus. Varjatud esitlusel põhineva masinõppe ja liigutuste kalibreerimise abil loodud valgusprofiilide alusel tuvastab SpikEy mürgitatud jooke 86%-se täpsusega eri vedelikes ja tingimustes. SNAKE hindab puuviljade kvaliteeti, jälgides ja analüüsides soojuse hajumist puuvilja pinnalt pärast inimese puudutust. Kuigi süsteem tugineb hetkel termokaamerale, loob antud töö võimaluse kasutada nutisõrmuseid puuviljade kvaliteedi hindamiseks miniatuursete termoandurite abil. SNAKE saavutab puuvilja kvaliteedi hindamisel 83%-se täpsuse, pakkudes praktilist ja väheste kuludega lahendust toidujäätmete vähendamiseks tavapäraste interaktsioonide kaudu.

Kokkuvõttes laiendavad need panused nutisõrmuste kasutusvõimalusi läbi andurite kasutuse ja inimkäitumist arvestav disaini. Käesolev töö näitab nutisõrmuste potentsiaali mitmekülgse ja praktilise platvormina lausandmetöötluses, võimaldades luua ressursisäästlikke ja igapäevaeluga sujuvalt ühilduvaid lahendusi.

CURRICULUM VITAE

Personal data

Name:	Zhigang Yin
Date of birth:	02/04/1994
Citizenship:	China
E-mail:	yinzhigang1994@gmail.com, zhigang.yin@ut.ee

Education

2013–2017	Hubei University, Bachelor studies, Specialty: Communication Engineering
2017–2020	University of Chinese Academy of Sciences, Master studies, Specialty: Electronics and Communication Engineering
2021–2025	University of Tartu, Doctoral studies, Specialty: Computer Science University of Helsinki, Doctoral exchange internship (2023.03–2023.06)

Research awards

Year 2023	SIGMOBILE student travel grant award (ACM HotMobile)
Year 2023	Best Demo Runner-up Award (ACM HotMobile)
Year 2025	Best Paper Award Nomination (ACM ICMI)

Teaching experience

Spring 2022	Teaching assistant in LTAT.06.007 Distributed Systems
Spring 2023	Co-supervision of master thesis – "Quantifying the impact of human touch to estimate quality of fresh fruits using light sensing" by Ayodeji Pelumi Odetoyinbo

Academic community service

Year 2023	Video Chair (ACM MobiSys)
2022–2024	Reviewer (IEEE Percom)
Year 2025	Reviewer (ACM ISS)
Year 2025	Volunteer (IEEE SERVICES)

ELULOOKIRJELDUS

Isikuandmed

Nimi:	Zhigang Yin
Sünniaeg:	02/04/1994
Kodakondsus:	Hiina
Meil:	yinzhigang1994@gmail.com, zhigang.yin@ut.ee

Haridus

2013–2017	Hubei Ülikool, Bakalaureuseõpe, Eriala: Kommunikatsiooni inseneeria
2017–2020	Hiina Teaduste Akadeemia Ülikool, Magistriõpe, Eriala: Elektroonika ja sidetehnika
2021–2025	Tartu Ülikool, Doktoriõpe, Eriala: Arvutiteadus Helsingi Ülikool, Välispraktika (2023.03–2023.06)

Teaduspreemiad

Aasta 2023	SIGMOBILE üliõpilaste reisitoetuse auhind (ACM HotMobile)
Aasta 2023	Teise koha auhind demo eest (ACM HotMobile)
Aasta 2025	Nomineeritud parima artikli auhinnale (ACM ICMI)

Õpetamiskogemus

Kevad 2022	Õppeassistent aines LTAT.06.007 Hajussüsteemid
Kevad 2023	Ayodeji Pelumi Odetoyinbo magistritöö kaasjuhendaja "Valgusandurite kasutamine värskete puuviljade kvaliteedi määramiseks ja inimese puudutuse mõju hindamiseks"

Akadeemiline ühiskondlikult kasulik töö

Aasta 2023	Videomaterjalide esimees (ACM MobiSys)
2022–2024	Retsensent (IEEE Percom)
Aasta 2025	Retsensent (ACM ISS)
Aasta 2025	Vabatahtlik (IEEE SERVICES)

DISSERTATIONES INFORMATICAE PREVIOUSLY PUBLISHED IN DISSERTATIONES MATHEMATICAE UNIVERSITATIS TARTUENSIS

19. **Helger Lipmaa.** Secure and efficient time-stamping systems. Tartu, 1999, 56 p.
22. **Kaili Müürisep.** Eesti keele arvutigrammatika: süntaks. Tartu, 2000, 107 lk.
23. **Varmo Vene.** Categorical programming with inductive and coinductive types. Tartu, 2000, 116 p.
24. **Olga Sokratova.** Ω-rings, their flat and projective acts with some applications. Tartu, 2000, 120 p.
27. **Tiina Puolakainen.** Eesti keele arvutigrammatika: morfoloogiline ühestamine. Tartu, 2001, 138 lk.
29. **Jan Villemson.** Size-efficient interval time stamps. Tartu, 2002, 82 p.
45. **Kristo Heero.** Path planning and learning strategies for mobile robots in dynamic partially unknown environments. Tartu 2006, 123 p.
49. **Härmel Nestra.** Iteratively defined transfinite trace semantics and program slicing with respect to them. Tartu 2006, 116 p.
53. **Marina Issakova.** Solving of linear equations, linear inequalities and systems of linear equations in interactive learning environment. Tartu 2007, 170 p.
55. **Kaarel Kaljurand.** Attempto controlled English as a Semantic Web language. Tartu 2007, 162 p.
56. **Mart Anton.** Mechanical modeling of IPMC actuators at large deformations. Tartu 2008, 123 p.
59. **Reimo Palm.** Numerical Comparison of Regularization Algorithms for Solving Ill-Posed Problems. Tartu 2010, 105 p.
61. **Jüri Reimand.** Functional analysis of gene lists, networks and regulatory systems. Tartu 2010, 153 p.
62. **Ahti Peder.** Superpositional Graphs and Finding the Description of Structure by Counting Method. Tartu 2010, 87 p.
64. **Vesal Vojdani.** Static Data Race Analysis of Heap-Manipulating C Programs. Tartu 2010, 137 p.
66. **Mark Fišel.** Optimizing Statistical Machine Translation via Input Modification. Tartu 2011, 104 p.
67. **Margus Niitsoo**. Black-box Oracle Separation Techniques with Applications in Time-stamping. Tartu 2011, 174 p.
71. **Siim Karus.** Maintainability of XML Transformations. Tartu 2011, 142 p.
72. **Margus Treumuth.** A Framework for Asynchronous Dialogue Systems: Concepts, Issues and Design Aspects. Tartu 2011, 95 p.
73. **Dmitri Lepp.** Solving simplification problems in the domain of exponents, monomials and polynomials in interactive learning environment T-algebra. Tartu 2011, 202 p.

74. **Meelis Kull.** Statistical enrichment analysis in algorithms for studying gene regulation. Tartu 2011, 151 p.
77. **Bingsheng Zhang.** Efficient cryptographic protocols for secure and private remote databases. Tartu 2011, 206 p.
78. **Reina Uba.** Merging business process models. Tartu 2011, 166 p.
79. **Uuno Puus.** Structural performance as a success factor in software development projects – Estonian experience. Tartu 2012, 106 p.
81. **Georg Singer.** Web search engines and complex information needs. Tartu 2012, 218 p.
83. **Dan Bogdanov.** Sharemind: programmable secure computations with practical applications. Tartu 2013, 191 p.
84. **Jevgeni Kabanov.** Towards a more productive Java EE ecosystem. Tartu 2013, 151 p.
87. **Margus Freudenthal.** Simpl: A toolkit for Domain-Specific Language development in enterprise information systems. Tartu, 2013, 151 p.
90. **Raivo Kolde.** Methods for re-using public gene expression data. Tartu, 2014, 121 p.
91. **Vladimir Šor.** Statistical Approach for Memory Leak Detection in Java Applications. Tartu, 2014, 155 p.
92. **Naved Ahmed.** Deriving Security Requirements from Business Process Models. Tartu, 2014, 171 p.
94. **Liina Kamm.** Privacy-preserving statistical analysis using secure multi-party computation. Tartu, 2015, 201 p.
100. **Abel Armas Cervantes.** Diagnosing Behavioral Differences between Business Process Models. Tartu, 2015, 193 p.
101. **Fredrik Milani.** On Sub-Processes, Process Variation and their Interplay: An Integrated Divide-and-Conquer Method for Modeling Business Processes with Variation. Tartu, 2015, 164 p.
102. **Huber Raul Flores Macario.** Service-Oriented and Evidence-aware Mobile Cloud Computing. Tartu, 2015, 163 p.
103. **Tauno Metsalu.** Statistical analysis of multivariate data in bioinformatics. Tartu, 2016, 197 p.
104. **Riivo Talviste.** Applying Secure Multi-party Computation in Practice. Tartu, 2016, 144 p.
108. **Siim Orasmaa.** Explorations of the Problem of Broad-coverage and General Domain Event Analysis: The Estonian Experience. Tartu, 2016, 186 p.
109. **Prastudy Mungkas Fauzi.** Efficient Non-interactive Zero-knowledge Protocols in the CRS Model. Tartu, 2017, 193 p.
110. **Pelle Jakovits.** Adapting Scientific Computing Algorithms to Distributed Computing Frameworks. Tartu, 2017, 168 p.
111. **Anna Leontjeva.** Using Generative Models to Combine Static and Sequential Features for Classification. Tartu, 2017, 167 p.
112. **Mozhgan Pourmoradnasseri.** Some Problems Related to Extensions of Polytopes. Tartu, 2017, 168 p.

113. **Jaak Randmets.** Programming Languages for Secure Multi-party Computation Application Development. Tartu, 2017, 172 p.
114. **Alisa Pankova.** Efficient Multiparty Computation Secure against Covert and Active Adversaries. Tartu, 2017, 316 p.
116. **Toomas Saarsen.** On the Structure and Use of Process Models and Their Interplay. Tartu, 2017, 123 p.
121. **Kristjan Korjus.** Analyzing EEG Data and Improving Data Partitioning for Machine Learning Algorithms. Tartu, 2017, 106 p.
122. **Eno Tõnisson.** Differences between Expected Answers and the Answers Offered by Computer Algebra Systems to School Mathematics Equations. Tartu, 2017, 195 p.

DISSERTATIONES INFORMATICAE UNIVERSITATIS TARTUENSIS

1. **Abdullah Makkeh**. Applications of Optimization in Some Complex Systems. Tartu 2018, 179 p.
2. **Riivo Kikas**. Analysis of Issue and Dependency Management in Open-Source Software Projects. Tartu 2018, 115 p.
3. **Ehsan Ebrahimi**. Post-Quantum Security in the Presence of Superposition Queries. Tartu 2018, 200 p.
4. **Ilya Verenich**. Explainable Predictive Monitoring of Temporal Measures of Business Processes. Tartu 2019, 151 p.
5. **Yauhen Yakimenka**. Failure Structures of Message-Passing Algorithms in Erasure Decoding and Compressed Sensing. Tartu 2019, 134 p.
6. **Irene Teinemaa**. Predictive and Prescriptive Monitoring of Business Process Outcomes. Tartu 2019, 196 p.
7. **Mohan Liyanage.** A Framework for Mobile Web of Things. Tartu 2019, 131 p.
8. **Toomas Krips.** Improving performance of secure real-number operations. Tartu 2019, 146 p.
9. **Vijayachitra Modhukur.** Profiling of DNA methylation patterns as biomarkers of human disease. Tartu 2019, 134 p.
10. **Elena Sügis.** Integration Methods for Heterogeneous Biological Data. Tartu 2019, 250 p.
11. **Tõnis Tasa.** Bioinformatics Approaches in Personalised Pharmacotherapy. Tartu 2019, 150 p.
12. **Sulev Reisberg.** Developing Computational Solutions for Personalized Medicine. Tartu 2019, 126 p.
13. **Huishi Yin.** Using a Kano-like Model to Facilitate Open Innovation in Requirements Engineering. Tartu 2019, 129 p.
14. **Faiz Ali Shah.** Extracting Information from App Reviews to Facilitate Software Development Activities. Tartu 2020, 149 p.
15. **Adriano Augusto**. Accurate and Efficient Discovery of Process Models from Event Logs. Tartu 2020, 194 p.
16. **Karim Baghery.** Reducing Trust and Improving Security in zk-SNARKs and Commitments. Tartu 2020, 245 p.
17. **Behzad Abdolmaleki.** On Succinct Non-Interactive Zero-Knowledge Protocols Under Weaker Trust Assumptions. Tartu 2020, 209 p.
18. **Janno Siim.** Non-Interactive Shuffle Arguments. Tartu 2020, 154 p.
19. **Ilya Kuzovkin.** Understanding Information Processing in Human Brain by Interpreting Machine Learning Models. Tartu 2020, 149 p.
20. **Orlenys López Pintado.** Collaborative Business Process Execution on the Blockchain: The Caterpillar System. Tartu 2020, 170 p.
21. **Ardi Tampuu.** Neural Networks for Analyzing Biological Data. Tartu 2020, 152 p.

22. **Madis Vasser.** Testing a Computational Theory of Brain Functioning with Virtual Reality. Tartu 2020, 106 p.
23. **Ljubov Jaanuska.** Haar Wavelet Method for Vibration Analysis of Beams and Parameter Quantification. Tartu 2021, 192 p.
24. **Arnis Parsovs.** Estonian Electronic Identity Card and its Security Challenges. Tartu 2021, 214 p.
25. **Kaido Lepik.** Inferring causality between transcriptome and complex traits. Tartu 2021, 224 p.
26. **Tauno Palts.** A Model for Assessing Computational Thinking Skills. Tartu 2021, 134 p.
27. **Liis Kolberg.** Developing and applying bioinformatics tools for gene expression data interpretation. Tartu 2021, 195 p.
28. **Dmytro Fishman.** Developing a data analysis pipeline for automated protein profiling in immunology. Tartu 2021, 155 p.
29. **Ivo Kubjas.** Algebraic Approaches to Problems Arising in Decentralized Systems. Tartu 2021, 120 p.
30. **Hina Anwar.** Towards Greener Software Engineering Using Software Analytics. Tartu 2021, 186 p.
31. **Veronika Plotnikova.** FIN-DM: A Data Mining Process for the Financial Services. Tartu 2021, 197 p.
32. **Manuel Camargo.** Automated Discovery of Business Process Simulation Models From Event Logs: A Hybrid Process Mining and Deep Learning Approach. Tartu 2021, 130 p.
33. **Volodymyr Leno.** Robotic Process Mining: Accelerating the Adoption of Robotic Process Automation. Tartu 2021, 119 p.
34. **Kristjan Krips.** Privacy and Coercion-Resistance in Voting. Tartu 2022, 173 p.
35. **Elizaveta Yankovskaya.** Quality Estimation through Attention. Tartu 2022, 115 p.
36. **Mubashar Iqbal.** Reference Framework for Managing Security Risks Using Blockchain. Tartu 2022, 203 p.
37. **Jakob Mass.** Process Management for Internet of Mobile Things. Tartu 2022, 151 p.
38. **Gamal Elkoumy.** Privacy-Enhancing Technologies for Business Process Mining. Tartu 2022, 135 p.
39. **Lidia Feklistova.** Learners of an Introductory Programming MOOC: Background Variables, Engagement Patterns and Performance. Tartu 2022, 151 p.
40. **Mohamed Ragab.** Bench-Ranking: A Prescriptive Analysis Approach for Large Knowledge Graphs Query Workloads. Tartu 2022, 158 p.
41. **Mohammad Anagreh.** Privacy-Preserving Parallel Computations for Graph Problems. Tartu 2023, 181 p.
42. **Rahul Goel.** Mining Social Well-being Using Mobile Data. Tartu 2023, 104 p.

43. **Anti Ingel.** Algorithms using information theory: classification in brain-computer interfaces and characterising reinforcement-learning agents. Tartu 2023, 142 p.
44. **Shakshi Sharma.** Fighting Misinformation in the Digital Age: A Comprehensive Strategy for Characterizing, Identifying, and Mitigating Misinformation on Online Social Media Platforms. Tartu 2023, 158 p.
45. **Kristiina Rahkema.** Quality Analysis of iOS Applications with Focus on Maintainability and Security Aspects. Tartu 2023, 182 p.
46. **Ivan Slobozhan.** Studying Online Social Media Engagement in CIS Countries during Protests, Mass Demonstrations and War. Tartu 2023, 81 p.
47. **Nurlan Kerimov.** Building a catalogue of molecular quantitative trait loci to interpret complex trait associations. Tartu 2023, 248 p.
48. **Pavlo Tertychnyi.** Machine Learning Methods for Anti-Money Laundering Monitoring. Tartu 2023, 117 p.
49. **Abasi-amefon Obot Affia.** A Framework and Teaching Approach for IoT Security Risk Management. Tartu 2023, 180 p.
50. **Raimond-Hendrik Tunnel.** Video Game Design and Development Bachelor's Curriculum for Estonia. Tartu 2024, 137 p.
51. **Ahto Salumets.** Bioinformatics analysis of various aspects in immunology. Tartu 2024, 198 p.
52. **Mohammed Abdulhameed Shaif Ali.** Deep Learning Methods for Cell Microscopy Image Analysis. Tartu 2024, 143 p.
53. **Pille Pullonen-Raudvere**. Foundations of Efficient and Secure Algorithm Development for Secure Multiparty Computation. Tartu 2024, 265 p.
54. **Marili Rõõm.** Multiple approaches to learners' success and factors affecting it in computer programming MOOCs. Tartu 2024, 170 p.
55. **Shivananda Rangappa Poojara.** Design and Orchestration of Scalable, Event-Driven Serverless Data Pipelines for Internet of Things (IoT) Applications. Tartu 2024, 172 p.
56. **Hassan Abdulgaleel Hassan Salim Eldeeb.** Empowering Machine Learning Pipelines with Automated Feature Engineering. Tartu 2024, 121 p.
57. **Muhammad Uzair.** Soft decision making for agri-food 4.0. Tartu 2024, 158 p.
58. **Kirill Milintsevich.** Estimation of Depression Level from Text: Symptom-Based Approach, External Knowledge, Dataset Validity. Tartu 2024, 130 p.
59. **Maksym Del.** Multilingual and Multi-Domain Representational Patterns Across Trpansformer-Based Models. Tartu 2024, 131 p.
60. **Kristo Raun.** Adaptive Out-of-order Handling in Streaming Conformance Checking. Tartu 2024, 118 p.
61. **Toivo Vajakas.** Towards integration of mobile network data into analyzing human mobility. Tartu 2024, 103 p.
62. **Katsiaryna Lashkevich.** Data-Driven Analysis and Optimization of Waiting Times in Business Processes. Tartu 2024, 169 p.
63. **Alejandra Duque-Torres.** Classifying, Constraining and Ranking Metamorphic Relations. Tartu 2025, 159 p.

64. **Mariia Bakhtina.** A Method for Information Security and Privacy Management in Smart Solutions. Tartu 2025, 199 p.
65. **Andre Tättar.** Multilingual Machine Translation for Under-Resourced Languages. Tartu 2025, 170 p.
66. **Mahmoud Shoush.** Prescriptive Process Monitoring Under Uncertainty and Resource Constraints. Tartu 2025, 178 p.
67. **Alireza Akhavi Zadegan.** A Multimodal approach for refining Mapping and Localization by Integrating Generative AI and Pedestrian-Centric Data. Tartu 2025, 147 p.
68. **Eerik Muuli.** Automating the assessment and feedback processes in IT teaching – improving creation and maintenance from the teaching staff perspective. Tartu 2025, 196 p.
69. **Kateryna Kubrak.** Towards User-Centered Prescriptive Process Monitoring Systems. Tartu 2025, 151 p.